Alma Mater Studiorum – Università di Bologna

DOTTORATO DI RICERCA IN

SCIENZE DELLA TERRA, DELLA VITA E DELL'AMBIENTE

Ciclo XXXI

Settore Concorsuale: 04/A2

Settore Scientifico Disciplinare: GEO/01

LATE QUATERNARY MEIOFAUNAL ASSEMBLAGES AS A KEY TO DECIPHER COASTAL AND DELTA DYNAMICS FROM THE NORTH ADRIATIC RECORD

Presentata da: Giulia Barbieri

Coordinatore Dottorato

Prof. Giulio Viola

Supervisore

Dott. Stefano Claudio Vaiani

Co-supervisore

Dott.ssa Veronica Rossi

Esame finale anno 2019

ABSTRACT

Benthic foraminifera and ostracoda represent excellent proxies to characterize modern and fossil settings, since composition and structure of assemblages reflect a suite of environmental parameters. Nevertheless, the response of each group to coastal dynamics on river-influenced shelves and their record beneath modern coastal plains are poorly investigated.

This Ph.D. thesis presents six study cases where modern and fossil assemblages of benthic foraminifera and ostracoda are compared and integrated to obtain a high-resolution palaeoecological characterization of the Po coastal plain late Quaternary sediment succession. Multivariate statistical techniques allowed to discern most of the (palaeo)environmental information inherited by meiofauna. The first study case combines benthic foraminifera and ostracoda from the shallow river-influenced North Adriatic shelf to define depositional environments dependent on the position from the Po Delta. The resulting biofacies are applied to the second study case to test how meiofauna record delta dynamics within a Holocene shallow marine succession of the Po Delta. In the third study case, paleontological, sedimentological and geochemical data reveals distinct facies associations within a three-stage progradation model for the Holocene high-stand succession of the Po Plain along a 70-km stretch of coast. Then, focusing on the last phase of high-stand progradation, benthic foraminifera are tested as tracers of short time-scale autogenic deltaic processes within an expanded prodelta succession. The high resolution obtained inspired the fifth study case, where the palaeoecological record provided by benthic foraminifera and ostracoda within a Pleistocene back-barrier succession of the Po coastal plain is compared. The last study aims to identify biotopes and ecological zones of the Bellocchio Lagoon in order to define environmental drivers on meiofaunal assemblages of the North Adriatic back-barrier settings.

This research work emphasizes the importance of integrating benthic foraminifera and ostracoda, since exclusively their combination allows to extract complete (palaeo)environmental information from modern and fossil settings.

INDEX

“There are only two ways to live your life:
as though nothing is a miracle, or as though everything is a miracle”

Albert Einstein

1. INTRODUCTION

Meiofauna is a term commonly employed in biology and ecology to indicate benthic organisms with dimension generally <1 mm (Mare, 1942). It includes a wide number of phyletic groups, such as nematodes, harpacticoid copepods, polychaetes, oliochaetes and turbellarians (Ellison, 1984). In this Ph.D. thesis, the word “meiofauna”, will be specifically referred to benthic foraminifera (unicellular protistans) and Ostracoda (crustaceans), since they are also included within this group (Sherman and Coull, 1980; Ellison, 1984; Moodley et al., 1997; Murray, 2006). With the exception of soft-shelled benthic foraminifera, these organisms share the characteristic of being enclosed within a hard test that can be preserved within sediments, which is an essential feature for the study of fossil assemblages. Tested benthic foraminifera are distributed from transitional brackish-water settings to the deep ocean, whereas ostracoda also live in continental freshwater bodies, but they are usually far more scarce than benthic foraminifera in the marine realm (Athersuch et al., 1989; Murray, 2006). Due to their high preservation potential, complementary distribution, and short life cycle that allow them to rapidly modify the structure and composition of assemblages, benthic foraminifera and ostracoda are considered excellent palaeoenvironmental and palaeoecological indicators (Alve, 1995; Scott et al., 2001; Boomer et al., 2003; Frenzel and Boomer, 2005; Murray, 2006; Rodriguez-Lazaro and Ruiz-Muñoz, 2012; Horton et al., 2013). They have been commonly employed for the characterization of late Quaternary sediment successions of the major Mediterranean coastal areas (e.g., Amorosi et al., 1999b, 2004, 2016b; Carboni et al., 2002; Fanget et al., 2013a, 2016; Cearreta et al., 2016; Rossi et al., 2017).

An essential requirement for palaeoenvironmental studies is the availability of modern databases that can be compared with the fossil record. Classically, modern benthic foraminifera and ostracoda were studied to define biotopes or biofacies, i.e. assemblages formed in response to a series of specific environmental conditions and defined by a similar faunal content. This is also the case of river-influenced shelves, areas of peculiar interest due to the high amount of organic carbon that is transported, stored and remineralized within their sediments (McKee et al., 2004 and references therein). Analyzing the existing bibliography about the modern meiofauna of the Mediterranean shallow marine areas, two main problems can be detected:

1. Benthic foraminiferal and ostracod databases have been treated separately, even if they were represented by the same set of samples. This is the case, for example, of the Po prodelta databases of Colalongo (1969) and D’Onofrio (1969) and the Adriatic databases for ostracoda and benthic foraminifera created by Breman (1975) and Jorissen (1988), respectively. First attempts were made by Frezza and Di Bella (2015), who briefly described the composition of the benthic foraminiferal fauna (Frezza and Carboni, 2009) associated to each ostracod assemblage identified near the modern Ombrone River mouth.

2. The correlation between the distribution of the benthic fauna and selected, significant, environmental factors is not always clear. Benthic foraminifera are known to be strongly dependent on quantity and quality of organic matter inputs, but they are also influenced by possibly stressful conditions like high deposition rates and hydrodynamic conditions (Mojtahid et al., 2009; Goineau et al., 2011, 2012). Other studies identified bathymetry and grain-size of the bottom sediment as the controlling factors on benthic foraminifera (Frezza and Carboni, 2009) or even did not define the most significant environmental drivers on the fauna (Donnici and Serandrei Barbero, 2002). Far more scarce are the studies about the distribution of ostracoda, and they usually identify a series of environmental drivers that determine the structure and composition of assemblages, such as organic matter, sediment grain-size, depth and distance from river mouths (Angue Minto'o et al., 2013; Frezza and Di Bella, 2015; Salel et al., 2016).

From a palaeoecological perspective, the combined application of benthic foraminifera and ostracoda could represent a useful tool to reconstruct changes in palaeoenvironmental conditions. Benthic foraminifera were applied to quantify past environmental changes from tidal marshes (e.g. Horton and Edwards, 2006) to the deep ocean (e.g. Rasmussen and Thomsen, 2017). Studies performed from coastal plains to continental shelves of the Mediterranean are mostly focused on the palaeobathymetric oscillations in relationship with glacial-interglacial cycles (Carboni et al., 2002, 2010; Morigi et al., 2005; Milker et al., 2011, 2017; Di Bella et al., 2013, 2014). The same purpose was accomplished by means of the ostracod fauna, which was even considered indicative of phases of increasing fluvial discharge (Mazzini et al., 1999; Bassetti et al., 2010; Marco-Barba et al., 2013; Angue Minto'o et al., 2015; Fanget et al., 2016).

In the last decades, it was demonstrated that the Po Plain late Quaternary sediment succession was formed as well in response to the eustatic oscillations connected to climatic changes at the Milankovitch time scale (100 ky) (Amorosi et al., 1999a, 2016a) and quantitative relative sea-level variations were locally reconstructed by means of benthic foraminifera (Rossi and Horton, 2009). However, the high-stand succession was formed under a strong autogenic control related to the development of the Po Delta, and delta dynamics such as river avulsions and delta lobe switching prevailed over the allogenic control of the glacio-eustatic cyclicity (Amorosi et al., 2017). In this context, the application of benthic foraminifera and ostracoda as palaeobathymetric proxies could not be sufficient anymore. In fact, the evolution of a river delta depends on the geomorphological setting of the coast, as well as on the relative influence of three key features that are at the base of the classical classification of deltas: tides, waves and river inputs (Galloway, 1975). Changes of these parameters are reflected not only on the subaerial morphology of the deltas, but also on their submerged portion and on the facing shelf (i.e., prodelta) in terms of bottom grain-size, sediment accumulation, organic matter content, and a plethora of other variables that contribute to the creation of peculiar biogeochemical conditions at the bottom (McKee et al., 2004). Bathymetry is considered an indirect parameter in the sense that it includes itself a lot of environmental variables that co-vary with water depth, therefore it defines a point in the space associated with specific environmental conditions (Rossi and Horton, 2009). However, in spatially restricted geographical areas the bathymetric control on the benthic communities is barely detectable and other factors, secondary at larger spatial scales, prevail (Tyler and Kowalewski, 2014). In front of the Po Delta and coastal plain, the North Adriatic shelf is characterized by low depths (maximum of ca. 45 m water depth) and assemblages of benthic foraminifera and ostracoda greatly change in a relatively restricted space (Breman, 1975; Jorissen, 1988; Donnici and Serandrei Barbero, 2002).

In this case it is required to investigate if bathymetry still represents an important driving factor on the distribution of the benthic fauna, but it is also necessary to take into consideration additional environmental parameters. In order to achieve these objectives, part of this work will focus on the analysis of the modern meiofauna of the North Adriatic Sea (Chapter 5). Specifically, through the multivariate analysis of selected test sets from the modern Adriatic databases of benthic foraminifera (Jorissen, 1988) and ostracoda (Breman, 1975), the objectives of this part of the work are:

- to recognize the main environmental drivers on the distribution of each faunal group in a shallow marine, river-influenced setting;
- to build a model for the distribution of benthic foraminifera and ostracoda in areas subject to different degrees of riverine inputs;
- to evaluate the combined application of benthic foraminifera and ostracoda as a proxy for specific ecological and palaeoecological conditions in shallow marine settings subject to deltaic progradation.

After the definition of the environmental drivers that control the benthic community turnover on the modern North Adriatic shelf, it will be possible to obtain a comprehensive and detailed interpretation of the mud-dominated, shallow marine sediment succession of the Po Plain. In order to achieve this aim, the record of benthic foraminifera and ostracoda was integrated:

- at a local scale, within the shallow marine succession of the reference core EM13 (Chapter 6); the micropalaeontological record was analyzed and directly compared to the modern North Adriatic dataset by means of statistical techniques, in order to select the benthic group that provides the best palaeoenvironmental resolution potential in river-influenced sediment successions.

- at a larger scale, on a series of cores analyzed during the Ph.D. project (EM13, Core 7 and Core 1) including the Holocene shallow marine succession (Chapter 7); here, palaeontological (benthic foraminifera, ostracoda and mollusks) and geochemical data were integrated to test the applicability of these proxies for the interpretation of the mud-dominated prograding succession of the Po Delta, which can be difficult to characterize by means of sedimentological data alone.

Marine ostracod fauna can be very scarce, especially in sediment successions recovered in areas subject to strong riverine sedimentation (Fanget et al., 2013b), preventing the application of quantitative statistic to detect faunistic changes. Therefore, we performed a study exclusively on benthic foraminifera, to test them as indicators of short palaeoenvironmental variations induced by short-term autogenic deltaic processes within the Holocene shallow marine succession of Core 7 (Chapter 8).

Even though shallow marine sediments represent a high portion of the late Quaternary Po Delta and coastal plain subsurface succession, also back barrier deposits are well developed, especially in proximity to the innermost palaeoshoreline position reached during the maximum marine ingressions (Amorosi et al., 1999a; Campo et al., 2017). Benthic foraminifera and ostracoda were applied in conjunction to qualitatively characterize these deposits in terms of degree of confinement (*sensu* Guélorget and Perthuisot, 1983), and assemblages indicative of outer, central and inner lagoonal/estuary conditions were recorded (Amorosi et al., 2004, 2017). The degree of confinement within a back-barrier setting is defined as the time required for the complete renewal of marine waters in terms of dissolved elements (Guélorget and Perthuisot, 1983). It is a complex parameter that combines several environmental variables which greatly change in time and space in response to the physiographic setting of the coast and climate conditions (Debenay and Guillou, 2002). Benthic foraminifera represent a tool to define not exclusively the degree of isolation from the sea, but the environmental stress as well (Armynot du Châtelet and Debenay, 2010; Frontalini and Coccioni, 2011). On the other hand, composition and structure of ostracod assemblages in transitional environments are known to be strongly controlled by salinity, followed by a series of additional environmental parameters, such as characteristics of the substrate (e.g. grain-size, vegetation), water depth and environmental stability (Frenzel and Boomer, 2005 and references therein). Therefore, benthic foraminifera and ostracoda have been always applied as comprehensive proxies in transitional environments, since their distribution is influenced by multiple parameters (Murray, 2006; Mesquita-Joanes et al., 2012). A similar approach was adopted for the late Quaternary back-barrier sediments of the Po Plain (Amorosi et al., 2003, 2004), but the palaeoecological information provided by single meiofaunal groups have never been compared.

In contrast to the previous studies, we applied a new approach to a peculiar back-barrier sediment succession attributed to the Middle Pleistocene (MIS 7; Amorosi et al., 1999a) within core 223-S12 recovered in the Po coastal plain (Chapter 9). In analogy with the studies performed within this Ph.D. project on the Holocene shallow marine succession, the record of benthic foraminifera and ostracoda was compared in a back-barrier succession as well, in order to:

- understand the palaeoecological information provided by single benthic groups;
- assess which benthic group shows the highest palaeoenvironmental resolution in back-barrier settings.

However, in order to understand in detail the response of benthic foraminifera and ostracoda to changes induced by global (sea-level) and local (fluvial and wave regime, sediment transport, trophic conditions, etc.) factors on transitional settings, it is necessary to disentangle the contribution of the most significant environmental drivers on each meiofaunal group. This can be performed through the analysis of modern databases composed by biotic and abiotic variables, that represent the “modern analogues” of late Quaternary successions, with an approach similar to the one undertaken for the shallow marine setting. In order to obtain a reliable comparison with fossil assemblages, it is necessary to produce modern training sets from the area close to the recovered sediment successions, due to site-specific assemblages (Gehrels, 2007). Even though several ecological studies were performed on transitional environments in the Mediterranean, the quantification of the most important influencing factors on biota is difficult to obtain (Ruiz et al., 2006; Carboni et al., 2009; Frontalini et al., 2013; Melis and Covelli, 2013; Ferraro et al., 2016; Salel et al., 2016) and only few works achieved this aim (Armynot du Châtelet et al., 2016). Few studies were performed on the lagoons of the Po Delta close to the cored successions of the Po Plain, but they lack of a detailed dataset (D’Onofrio et al., 1976) or are focused on the application of living benthic foraminifera as bioindicators of heavy metal pollution (Coccioni, 2000). Therefore, the characterization of the “Sacca di Bellocchio”, a coastal lagoon located south of the Po Delta, is currently being performed (Chapter 10) with the following aims:

- to obtain a modern training set from a transitional environment of the Po coastal plain;
- to understand the environmental drivers on modern benthic foraminifera and ostracoda within a back-barrier setting of the study area.

The data included within the present Ph.D. thesis are preliminary, but the meiofaunal characterization of the lagoon of Bellocchio is work in progress and future perspectives include:

- the definition of biotopes for living benthic foraminifera in relationship with environmental conditions;

- the analysis of dead benthic foraminiferal assemblages to obtain the response of benthic foraminifera to general environmental conditions, since this type of assemblage is not affected by seasonal fluctuations (Horton and Edwards, 2006 and references therein).
- the comparison between living and dead foraminiferal assemblages in order to assess the degree of taphonomic alteration on assemblages and, possibly, differences in the composition and structure of assemblages due to population dynamics;
- the comparison between the meiofaunal assemblages of the Sacca di Bellocchio and the late Quaternary microfossil fauna in order to shed light on the evolution of the back-barrier environments of the Po coastal plain.

2. GEOLOGICAL AND MEIOFAUNAL SETTING

2.1 The North Adriatic

2.1.2 Physiographic and oceanographic setting of the North Adriatic Sea

The Adriatic Sea is an epicontinental basing elongated in NW-SE direction, approximately 800 km long and 200 km wide that represents the northernmost portion of the Mediterranean Sea (Fig. 2.1). The northern sector of the Adriatic Sea is characterized by a low-gradient platform (ca. 0.02°) gently dipping towards SE (Cattaneo et al., 2003). It is interrupted in proximity of Pescara by the Meso-Adriatic Depression, a remnant slope basin that reaches a maximum depth of 260 m. The southern Adriatic Sea is a deep basin, bordered by steep slopes, and reaches ca. 1200 m of water depth.

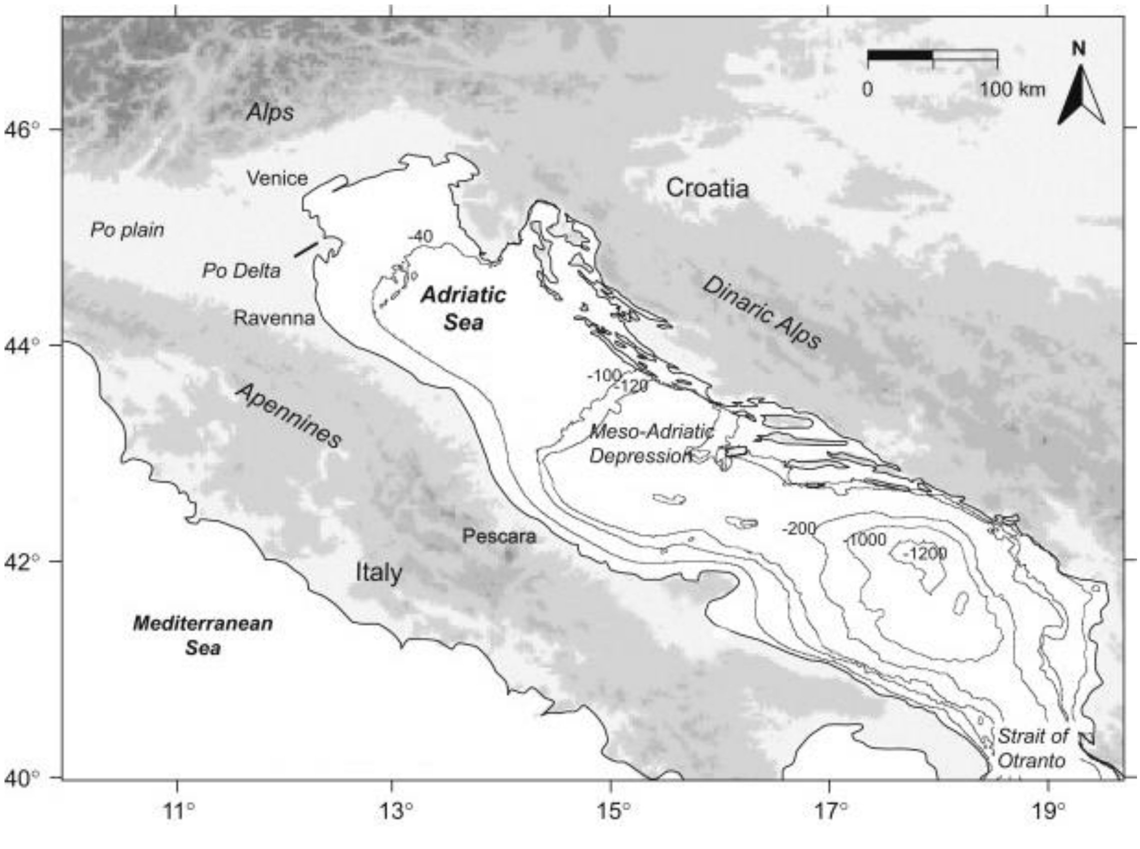

Fig. 2.1 Location, bathymetry and main morphological features of the Adriatic Sea (modified from Storms et al., 2008).

The Adriatic Sea is characterized by a microtidal regime and is strongly influenced by the thermohaline circulation of surficial waters (0-30 m) (Paschini et al., 1993). The interaction between freshwater inputs from the NW side of the basin and the Mediterranean saltwater from the south determines the general circulation pattern characterized by the northward current on the eastern Adriatic and the southward Western Adriatic Current (WAC in Fig. 2.2; Poulain, 2001). This anti-clockwise circulation pattern greatly affects the distribution of river-supplied sediments on the shallow Adriatic shelf. Sediments are predominantly supplied by the rivers located along the northern and western Adriatic coasts, whereas sediment inputs from the Croatian margin are limited and confined in proximity to the coastline due to the karstic nature of the drainage basins (Milliman et al., 2016).

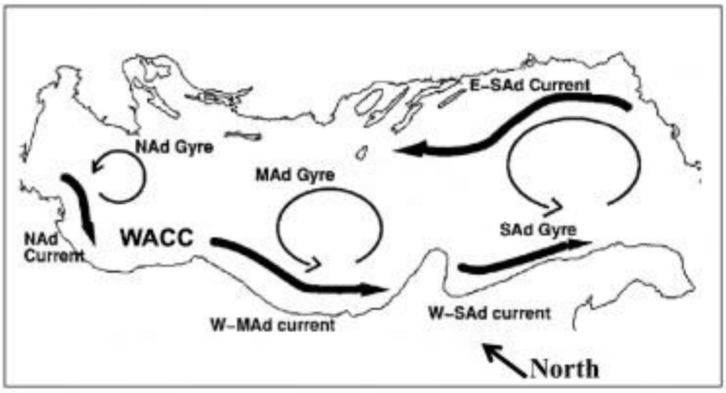

Fig. 2.2 Main circulation pattern of surface currents in the Adriatic Sea (modified from Spagnoli et al., 2014).

The North Adriatic Sea, extended from the northern Italian coasts to the Conero promontory in proximity of Ancona (Fig. 2.3), can be distinguished from the southern sector of the basin on the basis of the main depositional regimes (Frignani et al., 2005):

- in the North Adriatic, the sediment supply is prevalent: the amount of riverine inputs is higher than the amount of sediment accumulated on the seafloor, determining an excess of sediment which is transported in a southward direction by the WAC;
- in the South Adriatic, the sediment accumulation is prevalent: sediments exported from the North Adriatic are deposited in this sector, where the accumulation of sediment exceeds the low sediment inputs provided by the southern Apennine rivers.

In the North Adriatic, sediment inputs are provided by Alpine rivers (mean sediment load of 3.2 $Tg \cdot yr^{-1}$), the Po River (that represents itself the major sediment source of the whole Adriatic Sea, with ca. 12.2 $Tg \cdot yr^{-1}$) and Apennine rivers down to Ancona (16.9 $Tg \cdot yr^{-1}$) (Frignani et al., 2005).

As a consequence of the interplay between sediment inputs and water currents, the North Adriatic sediments are distributed according to their grain-size along belts parallel to the coast (Brambati et al., 1983). The substrate is sandy in proximity to the coastline, followed by the “Adriatic mud belt”, a fine-grained zone enriched in organic matter at ca. 20-40 m water depth (van der Zwaan and Jorissen, 1991) and finally by offshore sands.

North of the Adige River, the relatively low suspended load provided by other Alpine rivers prevents the formation of a continuous mud belt, which consists of scattered mud patches in front of river mouths (Frignani et al., 2005). In contrast, sedimentation rates increase from the Adige River towards the south. The extremely high sediment accumulation rates near the Po Delta mouths (Fig. 2.3) are largely related to episodic flood sedimentation (Palinkas and Nittrouer, 2007). After major flood events, sediments can be deposited down to >20 m water depth, and their thickness progressively increase towards the Po outlets, reaching values even >35 cm (Wheatcroft et al., 2006). The shallow (<20 m water depth) shelf from the Po Delta to Ravenna and the Adriatic mud belt (20-40 m water depth) are characterized by the occurrence of episodic hypoxic events due to the deposition and remineralization of high amounts of riverine organic matter, and by seasonal water stratification (Van der Zwaan and Jorissen, 1991; Alvisi et al., 2013).

On the sediment-starved Adriatic shelf, offshore sands consist of a thin layer of marine sands deposited in response to the shift of a barrier-lagoon-estuary system during the Holocene transgression (Trincardi et al., 1994).

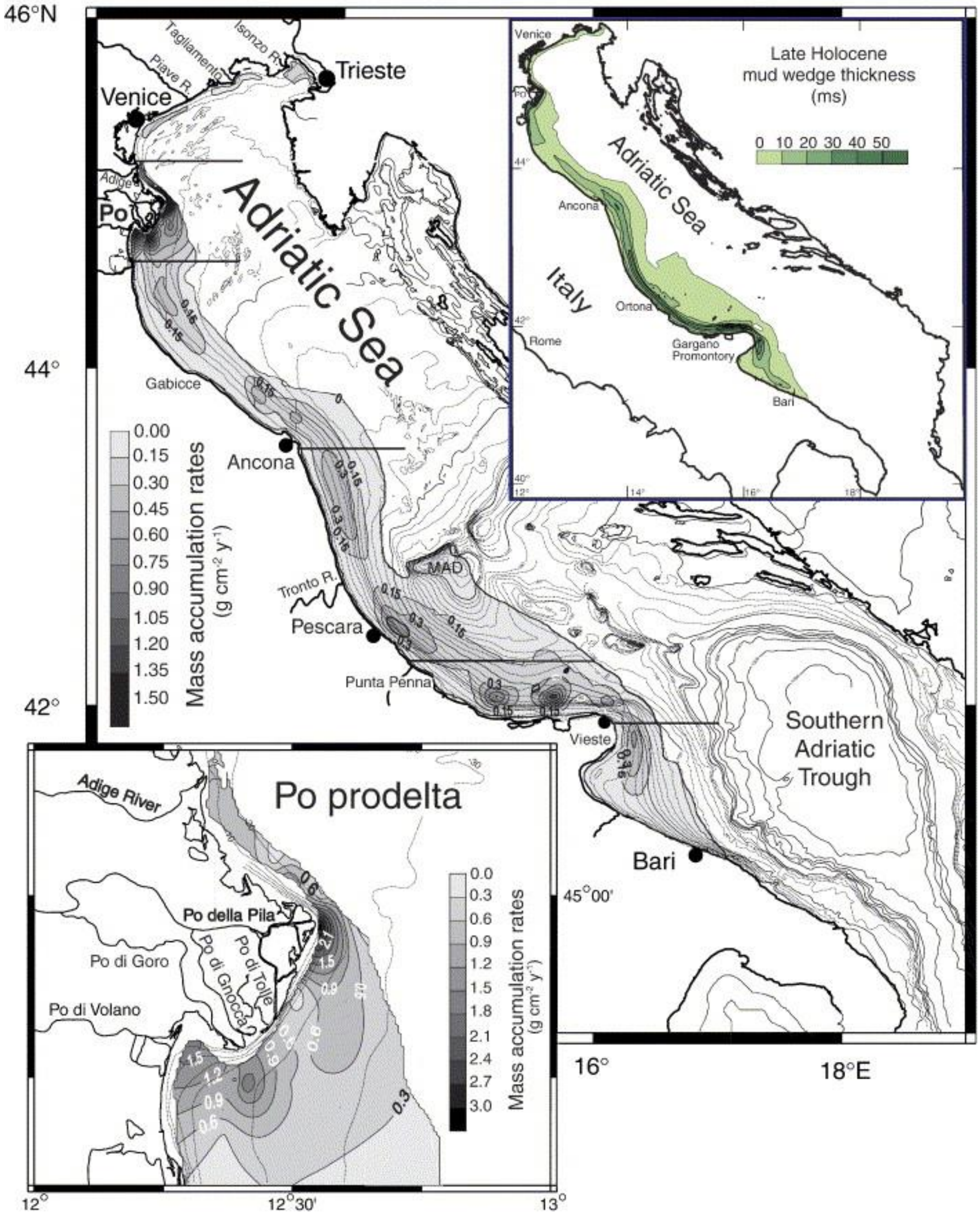

Fig. 2.3 Mass accumulation rates for the six depositional compartments identified by Frignani et al. (2005). The Po Delta area is shown in detail in the lower-left box. The upper-right box show the thickness of the HST wedge calculated by Correggiari et al. (2001) (from Frignani et al., 2005).

2.1.2 Transitional environments of the Po Delta and coastal plain

Several wetlands are developed along the Po Delta and coastal plain (Fig. 2.4) and are included in the Po Delta Regional Park. All of them are distributed on a lowland coastal area <2 m above the sea level with a large portion below the mean sea level due to the intense natural and anthropogenic subsidence (Antonellini et al., 2019). The coastal wetlands of the Po Plain originated from the interaction between the eastward progradation of the coastline and the high subsidence rate, that promoted the formation of wide lagoons and marshes behind the prograding sand ridges (Bondesan and Simeoni, 1983; Bondesan et al., 1995). Wetlands and lagoons of the Po Delta plain were formed in response to the rapid progradation of the deltaic lobes during the last centuries (Correggiari et al., 2005; Verza and Cattozzo, 2015). South of the Po Delta, wide portions of the submerged coastal plain were reclaimed for agro-pastoral activities from the XIX to the first half of the XX century (Stefani and Vincenzi, 2005) and the present-day wetlands along the coastal plain represent the remnants of these activities.

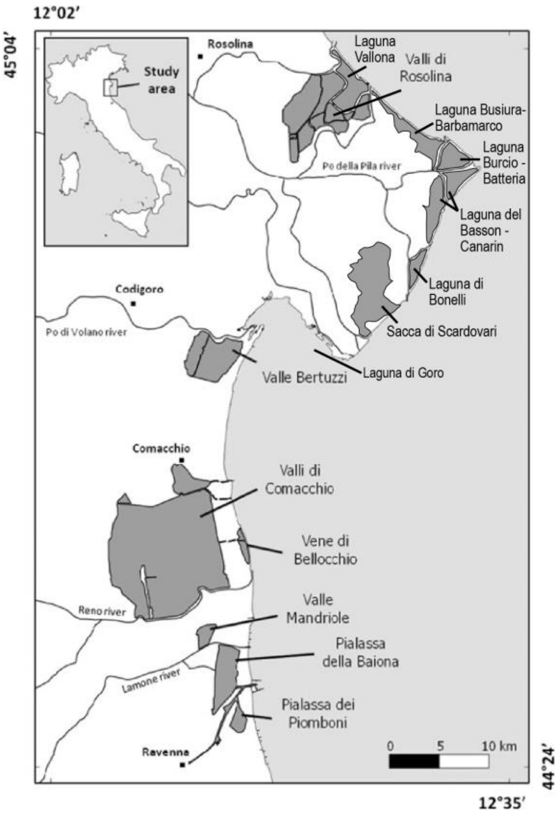

Fig. 2.4 Location of the wetlands along the Po Delta and coastal plain (modified from Migani et al., 2015).

The widest extension is shown by “Valli di Comacchio” (112.3 km^2), followed by the complex of the lagoons and weatlands located on the Po Delta (110 km^2). The coastal wetlands “Valle Bertuzzi”, “Piallassa Baiona” and the minor wetlands “Piallassa Piomboni”, “Valle Mandriole” and “Vene di Bellocchio” are characterized by a much lower extension (Migani et al., 2015; Verza and Cattozzo, 2015). These deltaic lagoons and coastal wetlands are connected to the Adriatic Sea, whereas two of them (Valle Mandriole and Valle Bertuzzi) are completely isolated from the sea and their brackish water results from saltwater intrusion (Antonellini et al., 2006). Almost all these humid areas are impacted by anthropogenic activities, since they host industrial settlements or they are artificially regulated for fishing activities, with the exception of Valle Mandriole and the coastal system of Vene di Bellocchio, which are natural and protected areas.

2.1.3 Modern meiofauna of the North Adriatic area

The historical importance of the Adriatic area for the study of benthic foraminifera and ostracoda is testified by abundant literature sources. The first attempts to study the meiofauna of the North Adriatic are dated back to the XVIII century, with the works of Linnaeus (1758), d'Orbigny (1826) and Fornasini (1904) about the descriptions of benthic foraminifera recovered from the shoreface sands of Rimini (southern Po coastal plain). In the second half of the XX century, the first researches about ostracod and benthic foraminiferal assemblages of the modern Po prodelta were performed by Colalongo (1969) and D'Onofrio (1969). At a basin scale, the reference studies about the distribution of the meiofauna on the whole Adriatic Sea were performed by Bonaduce (1975) and Breman (1975) for ostracoda, and by Jorissen (1987, 1988) for benthic foraminifera.

An abundant literature is available for the distribution of the meiofauna of the North Adriatic lagoons, even though studies concerning ostracoda are far more scarce than those about benthic foraminifera. This fact can be related to the widespread application of benthic foraminifera as bio-indicators of the environmental quality, since these lagoons are classically polluted areas due to the developed anthropogenic activities on the nearby coastal plains. The Lagoon of Venice is certainly the most studied, with a great number of researches about both benthic foraminifera (Albani and Serandrei Barbero, 1982, 1990; Albani et al., 2007; Coccioni et al., 2009) and ostracoda (Ruiz et al., 1999, 2000). Reference studies for ostracoda and benthic foraminifera were also carried out in the Marano and Grado Lagoons (Montenegro and Pugliese, 1996; Melis and Covelli, 2013), whereas only benthic foraminifera were investigated in the lagoons of the Po Delta (D'Onofrio et al., 1976; Coccioni, 2000).

Lagoons – The lagoons of the North Adriatic are generally characterized by oligotypic meiofaunal assemblages, especially in the innermost and central portions (Fig. 2.5). Inner lagoonal areas influenced by the fluvial runoff are characterized by benthic foraminiferal assemblages with a strong dominance of *Ammonia tepida*, usually accompanied by locally abundant *Haynesina germanica* and *Cribroelphidium oceanense*, species tolerant to salinity and organic matter fluctuations (D'Onofrio et al., 1976; Albani and Serandrei Barbero, 1982; Debenay and Guillou, 2002; Melis and Covelli, 2013). In the same areas, the ostracod fauna is mainly represented by the eurihalyne, opportunistic *Cyprideis torosa* and the freshwater-tolerant taxon *Loxoconcha elliptica*, but low frequencies of *Leptocythere bacescoi, Leptocythere lagunae* and *Loxoconcha stellifera* are also recorded (Montenegro and Pugliese, 1996; Ruiz et al., 2000; Fig. 2.6). Central lagoonal areas are dominated by the foraminifera *A. tepida* and *A. parkinsoniana* (Melis and Covelli, 2013) and the ostracod taxon *Cyprideis torosa*, locally associated to *Xestoleberis* spp. in areas with vegetated bottoms (Ruiz et al., 2000). *Ammonia tepida, A. parkinsoniana* and *C. torosa* are still common in outer lagoons, but the meiofaunal assemblages are more diversified and include marine taxa locally transported from the nearby marine areas. Among benthic foraminifera, *Miliolinella* spp., *Triloculina* spp. and *Quinqueloculina seminula* are recorded, whereas ostracoda are represented by *Semicytherura* spp., *Pontocythere turbida* and *L. bacescoi* (Albani and Serandrei Barbero, 1990; Ruiz et al., 2000; Debenay and Guillou, 2002; Melis and Covelli, 2013). Agglutinated benthic foraminifera, mainly represented by *Trochammina inflata,* are recorded in salt marsh environments highly influenced by tidal oscillations (Debenay and Guillou, 2002; Serandrei Barbero et al., 2004).

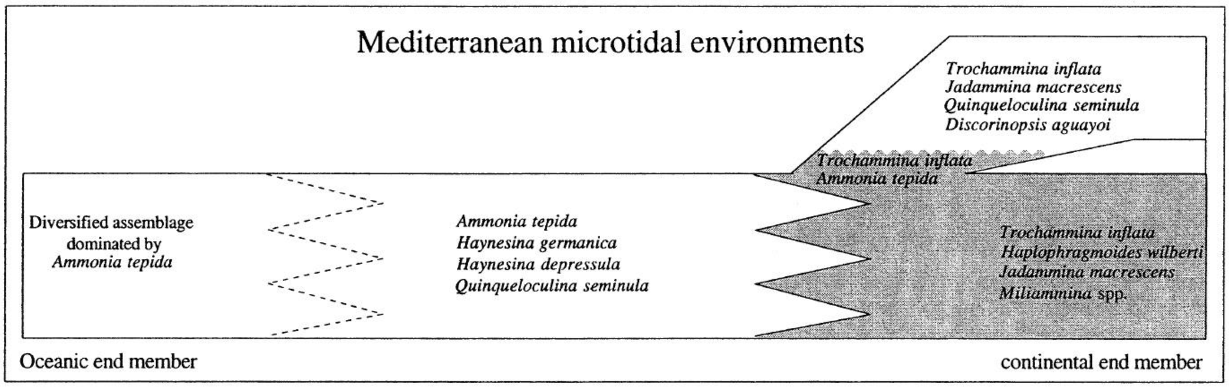

Fig. 2.5 Distribution of the most characteristic benthic foraminiferal species in Mediterranean microtidal environments (modified from Debenay and Guillou, 2002).

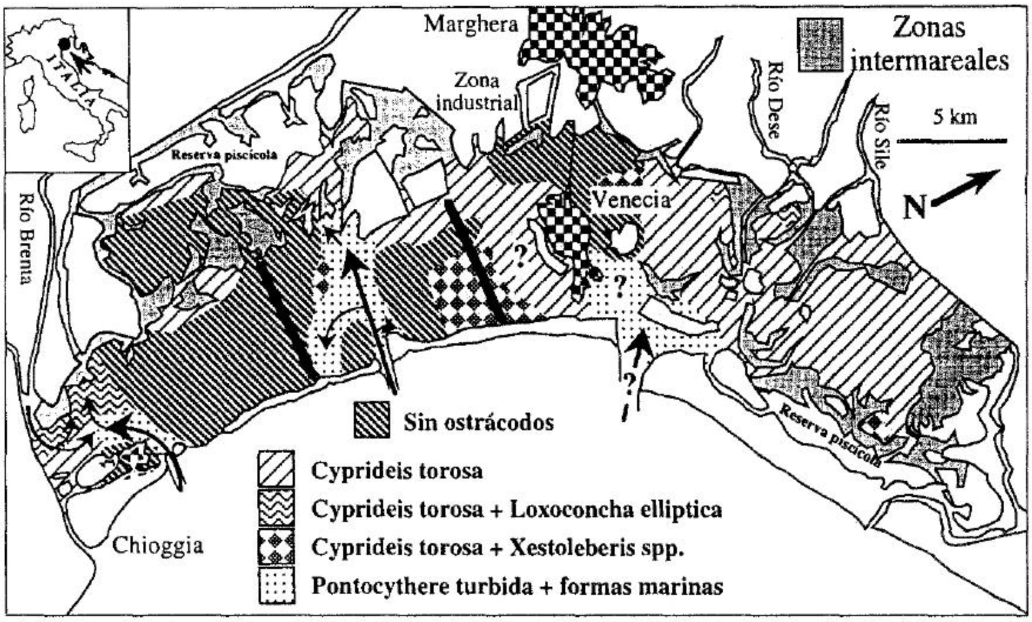

Fig. 2.6 Distribution of ostracod assemblages in the Lagoon of Venice (from Ruiz et al., 2000).

Nearshore and prodelta areas – The meiofauna is extremely scarce along the whole coastline of the Po Delta between 0-10 m water depth (Colalongo, 1969; D'Onofrio, 1969; Fig. 2.7). Here, foraminifera are represented by a very low number of specimens and are absent in front of the main Po River outlets ("Zone A" of D'Onofrio, 1969). Faunas include different species of benthic foraminifera (both shallow-water and deep-water taxa) and reworked plaktonic taxa from older units. Ostracoda are absent, or represented by extremely low number of valves ("Zone A" of Colalongo, 1969) of mixed marine and brackish/freshwater taxa, with predominant *Pontocythere* *turbida* and *C. torosa* and subordinately *Cytheromorpha fuscata, Heterocypris salinus* and *Leptocythere rarepunctata*. Authors considered this assemblage the result of the high fluvial inputs of the Po River, that (i) prevent the development of an abundant meiofauna, due to the turbidity of the water and salinity oscillations, and (ii) transport valves of brackish and freshwater ostracoda from the humid areas on the delta plain and reworked foraminifera from older rock units.

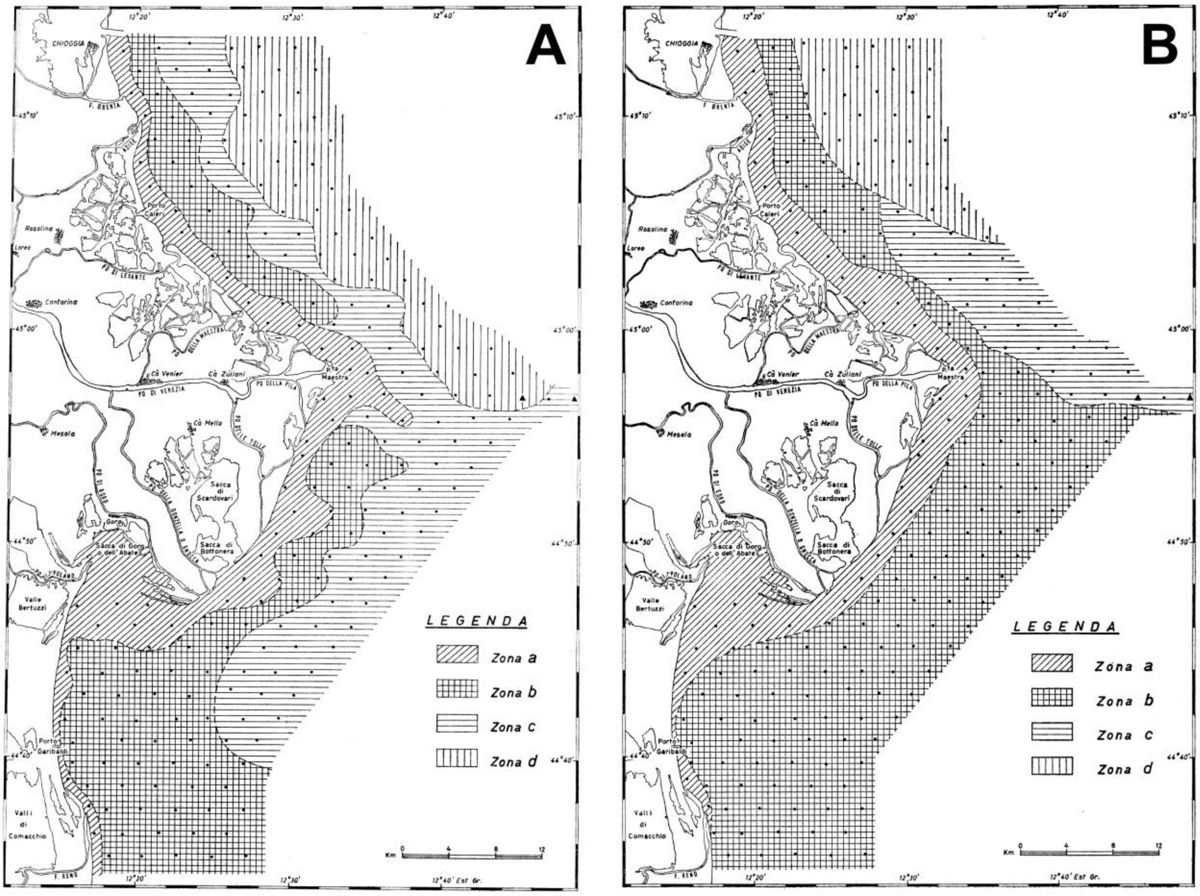

Fig. 2.7 Distribution of the meiofaunal zones in the bottom sediments in front of the Po Delta: A) benthic foraminifera (from D'Onofrio, 1969); B) ostracoda (from Colalongo, 1969).

In the nearshore zone of the North Adriatic Sea, between ca. 7-25 m of water depth, benthic foraminiferal assemblages are mainly composed by *A. parkinsoniana, A. tepida, Ammonia beccarii, Aubignyna perlucida, Textularia agglutinans, Cribroelphidium* spp. and Miliolidae ("biofacial unit II" of Jorissen, 1987; "biotope I" of Donnici and Serandrei Barbero, 2002; Fig. 2.8). This group includes both taxa tolerant to organic matter inputs (*A. parkinsoniana, A. tepida, A. perlucida, Porosononion granosum, Cribroelphidium poeyanum, T. agglutinans*) and species related to sandy substrates with relatively low organic matter concentrations (*A. beccarii, Porosononion lidoense, C. decipiens, Adelosina* spp., *Miliolinella* spp., *Quinqueloculina* spp., *Triloculina* spp.). Overall, this assemblage is indicative of variable stressed conditions in terms of riverine inputs, with local high concentrations of species tolerant to fluctuating salinities and organic matter inputs (e.g., in front of the Po outlets and at 10-15 m water depth along the Italian coastline). More or less in the same zone, at 5-20 m water depth, Breman (1975) identify the “shallow infrallitoral assemblage” (biofacies I).The areal distribution and the composition of this ostracod assemblage is in accordance with the “Zone B” identified by Colalongo (1969) at ca. 10-25 m water depth in proximity of the Po Delta. The most abundant species are the widespread opportunistic taxa *Palmoconcha turbida, Semicytherura incongruens* and *Pontocythere turbida*, also recorded by Bonaduce et al. (1975). These species are associated to lower frequencies of taxa commonly found on sandy substrates, such as *Carinocythereis whitei, Loxoconcha tumida*, *Cytheretta adriatica, Cytheretta judaea,* and *Xestoleberis fuscomaculata.*

At 20-40 m water depth along the so called “Adriatic mud-belt”, an area characterized by the accumulation of abundant riverine organic matter provided by the Po River (Van der Zwaan and Jorissen, 1991), Jorissen (1987) recorded the “biofacial unit IV” and Donnici and Serandrei Barbero (2002) the “biotope 2”. From lower to higher depths, the most abundant benthic foraminiferal taxa are *Nonionella turgida, Bulimina marginata* and *Valvulineria bradyana*, which tolerate high organic matter inputs and oxygen deficiency (Jorissen, 1988; Fig. 2. 9). Within the same area, ostracoda are characterized by the “biofacies IIa” of Breman (1975), with the dominance of the mud-lovers *Cytheridea neapolitana* and *Palmoconcha turbida*, associated to species distributed on every type of substrate such as *S. incongruens, Hiltermannicythere turbida, Pontocythere turbida* and *C. whitei* (Fig. 2. 10). Low frequencies of *Loxoconcha tumida* and *Loxoconcha versicolor* are recorded as well. Within the same area, Bonaduce et al. (1975) recorded a relatively scarce ostracod fauna, mostly represented by *Pontocythere turbida, L. ramosa, Palmoconcha turbida, S. incongruens* and *Semicytherura* spp.

Sand platform – Out of the fluvial influence of the Po and Apennine rivers, benthic foraminiferal and ostracod assemblages of the North Adriatic sand platform at >20 m water depth are extremely diversified. Benthic foraminifera are represented by the “biofacial unit III” of Jorissen (1987) and the “biotope 3” of Donnici and Serandrei Barbero (2002), which mainly include sandy-related taxa with a low tolerance for organic matter inputs such as *Asterigerinata* spp. (*A. mamilla* and *A. adriatica*), *Cibicides lobatulus, Neoconorbina terquemi, Rosalina bradyi, Buccella granulata, Elphidium crispum, Reussella spinulosa* and Miliolidae (*Quinqueloculina* spp. and *Triloculina trigonula*). The ostracod biofacies IId of Breman (1975) is typical of this area, which includes high percentages of taxa adapted to bottoms with different grain size, mainly *S. incongruens, Pontocythere turbida, L. tumida, H. turbida* (Breman, 1975; Bonaduce et al., 1975). They are associated to species that prefer sandy substrates such as *C. whitei, C. adriatica, Aurila* spp. and a variety of *Semicytherura* (e.g., *S. inversa, S. tergestina, S. ruggierii, S. robusta*) and *Callistocythere* (*C. flavidofusca, C. intricadoides* and *C. rastrifera*) species. Within a mixed sand-mud substrate at 25-30 m water depth slightly north of the main Po River outlet, Colalongo (1969) recorded the presence of very rich assemblages in terms of abundance of valves and number of species (“Zone C”). The composition of this assemblage is rather similar to the previously cited biofacies IIb of Breman (1975). The most abundant species are *S. incongruens* and *Pontocythere turbida*, with the subordinate occurrence of a large number of taxa belonging to the genera *Aurila, Callistocythere, Leptocythere, Loxoconcha, Semicytherura* and *Xestoleberis* and also the species *C. whitei* and *C. neapolitana*. However, at the same water depth but in a northernmost position within sediments mostly made of fine sands, Colalongo (1969) distinguished an additional assemblage (“Zone D”). The number of valves and the species richness is drastically lower compared to the “Zone C”, valves are usually thick and poorly preserved, suggesting a taphonomic control on the ostracod assemblage. *Pontocythere turbida, S. incongruens, L. tumida* and *C. adriatica* are the most common species.

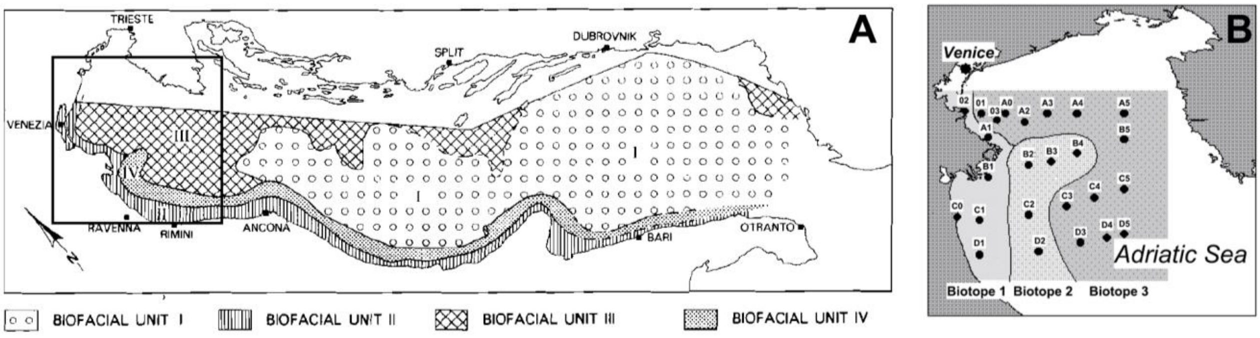

Fig. 2.8 A) Distribution of benthic foraminiferal biofacial units identified by Jorissen (1987) on the Adriatic Sea. The square indicates the area represented in panel B. B) Biotopes identified by Donnici and Serandrei Barbero (2002) on the North Adriatic shelf, east of the Po Delta.

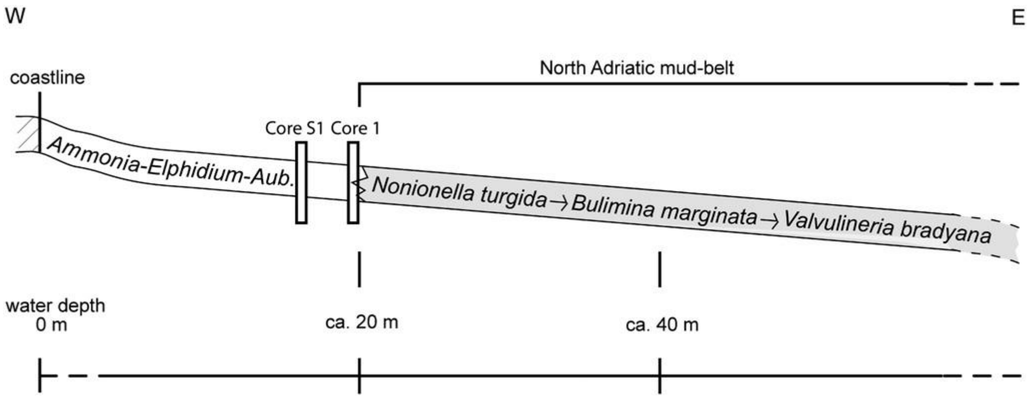

Fig. 2. 9 Distribution pattern of benthic foraminifera from shallower to deeper waters along a generic E-W transect of the Adriatic Sea (from Rossi and Vaiani, 2008).

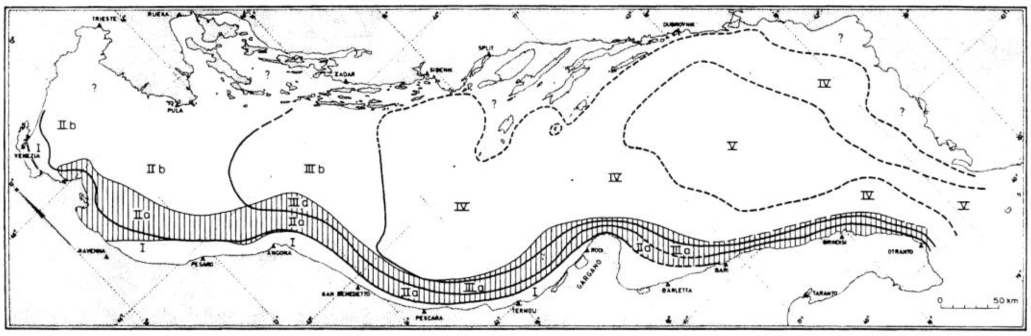

Fig. 2. 10 Distribution of the ostracod biofacies in the Adriatic Sea (from Breman, 1975).

2.2 The Po coastal plain

2.2.1 Stratigraphic architecture

The Po coastal plain represents the easternmost sector of the Po Plain, the surficial expression of a foreland basin bounded by the southern Alps to the north and the northern Apennines to the south (Castellarin et al., 1985; Doglioni, 1993). The Po Basin is filled by Pliocene-Quaternary sediments, up to 7 km thick in the major depocenters (Pieri and Groppi, 1981), that cover the south-verging Alpine and north-verging Apennine thrusts. Geophysical investigation revealed that the lower portion of this sediment succession is affected by the deformation induced by the buried thrusts, but the late Quaternary deposits are relatively undisturbed (Regione Emilia-Romagna and Eni-Agip, 1998). Six depositional sequences were recognized and classified as unconformity bounded stratigraphic units (UBSU) within the Plio-Quaternary infilling of the Po Basin (Fig. 2.11), which shows an overall regressive trend, from open marine to alluvial deposits (Ricci Lucchi et al., 1982; Regione Emilia-Romagna and Eni-Agip, 1998).

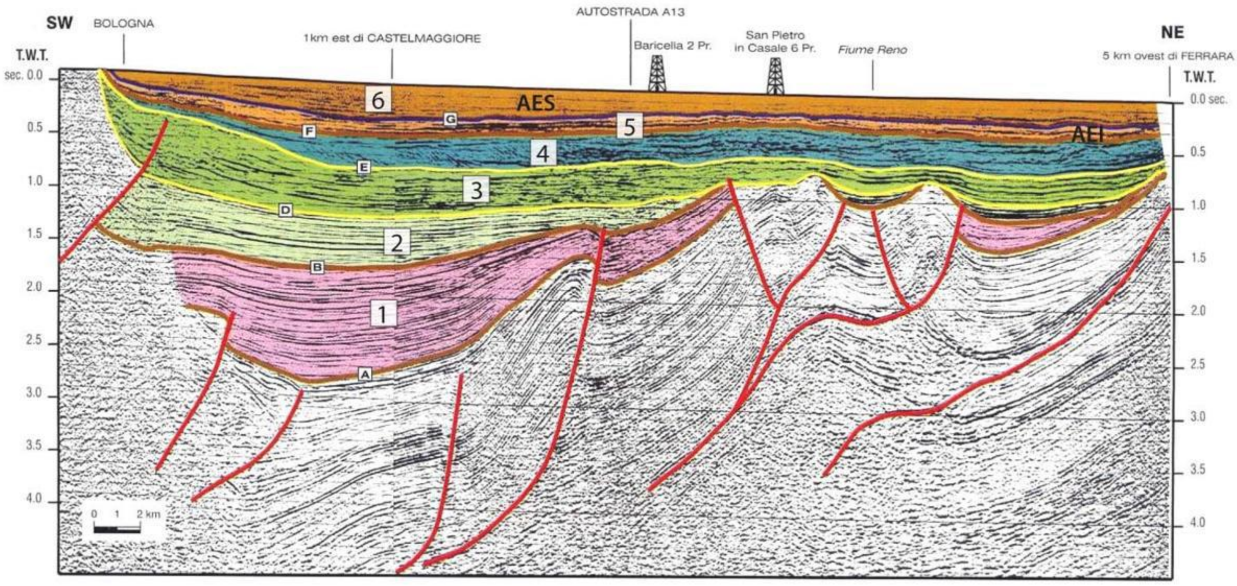

Fig. 2.11 Seismic profile interpretation showing the subdivision of the Plio-Quaternary Po Plain sediments into six depositional sequences identified as UBSU (from Regione Emilia-Romagna and Eni-Agip, 1998).

The uppermost UBSU (Emilia-Romagna Supersynthem; Regione Emilia-Romagna and Eni-Agip, 1998) was deposited after ca. 0.87 Ma and it is subdivided in the “lower Emilia-Romagna synthem” (AEI) and “upper Emilia-Romagna synthem” (AES), separated by an unconformity with an estimated age of ca. 0.45 Ma (Molinari et al., 2007). Beneath the modern Po coastal plain, five subsynthems with a thickness of ca. 50-100 m were identified (Fig. 2.12) within the upper Emilia-Romagna synthem (AES 4-8 of the CARG Project – Geological Mapping of Italy at scale 1:50.000). Each one corresponds to a transgressive-regressive (T-R) sequence formed under a major glacio-eustatic control at the Milankovitch-scale cyclicity of 100 ky (Amorosi et al., 1999a, 2004, 2005).

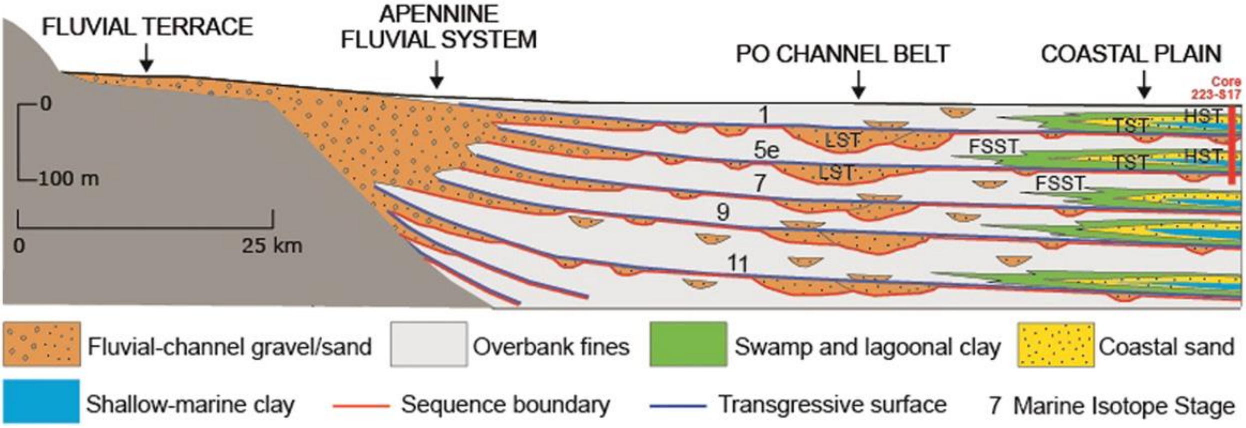

Fig. 2.12 Schematic cross-section from the Apennines to the Po coastal plain that shows the transgressive-regressive sequences within the “upper Emilia-Romagna synthem” (AES) and their subdivision into systems tract (modified from Amorosi et al., 2016a).

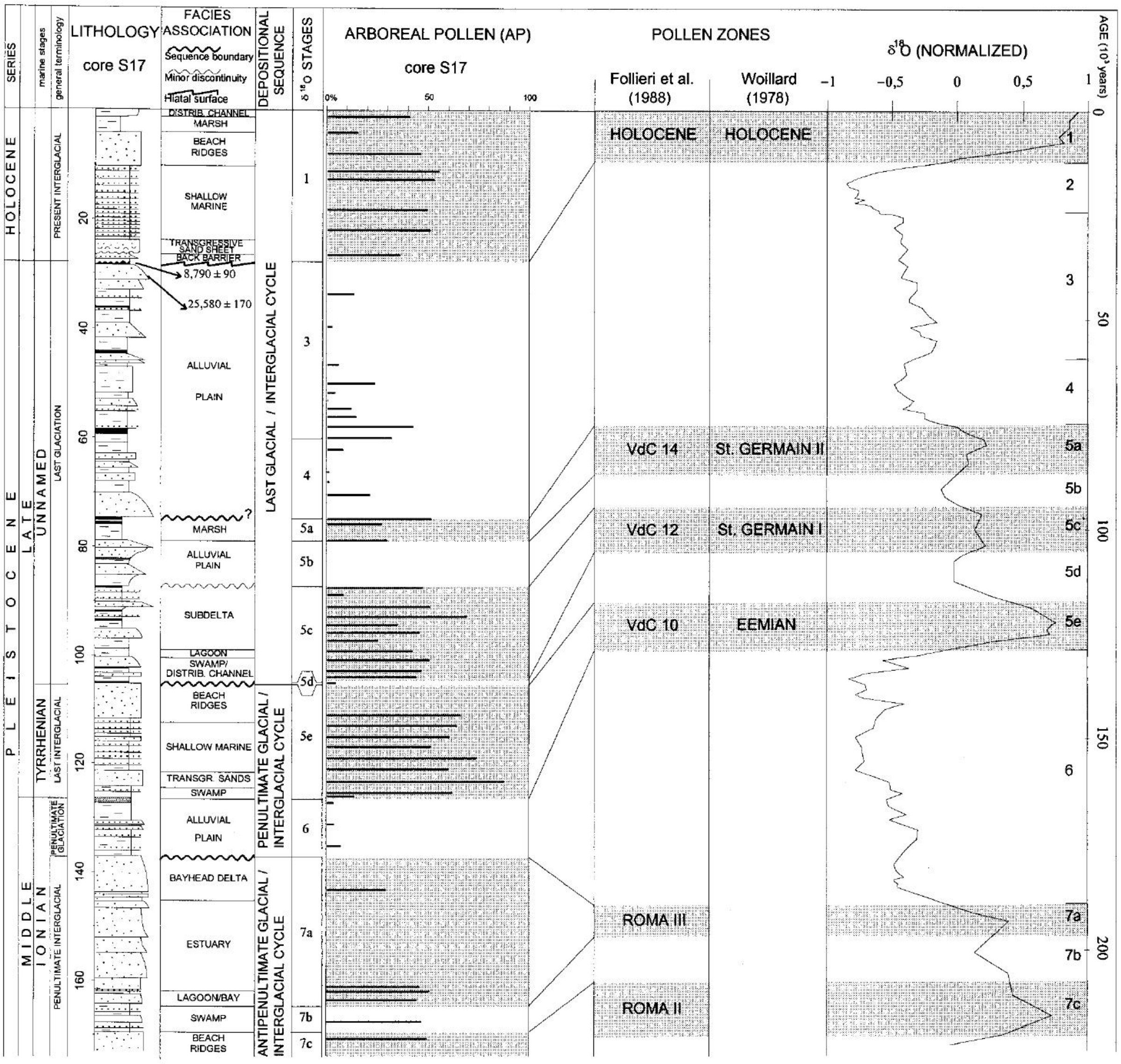

Fig. 2.13 Stratigraphy, interpreted facies association and frequencies of arboreal pollens from core 223-S17 (location in Fig. 2.12), correlation with pollen zones from European series and the oxygen-isotope curve of Martinson et al. (1987) (from Amorosi et al., 1999a).

Detailed chronostratigraphic and pollen analyses allowed to correlate the three uppermost T-R cycles with the oxygen isotope curve (Amorosi et al., 1999a). Specifically, pollen assemblages of the lower portion of each T-R sequence mainly include termophilous taxa indicative of relatively warm, interglacial conditions (Fig. 2.13). Conversely, the high concentrations of non-arboreal pollens recorded within the upper portion of the T-R sequences suggest that they formed during cold, glacial intervals. Therefore, transgressive deposits were attributed to the Marine Isotope Stages (MIS) 1, 5 and 7, and low-stand sediments were ascribed to MIS 3-4 and 6 (Amorosi et al., 2004).

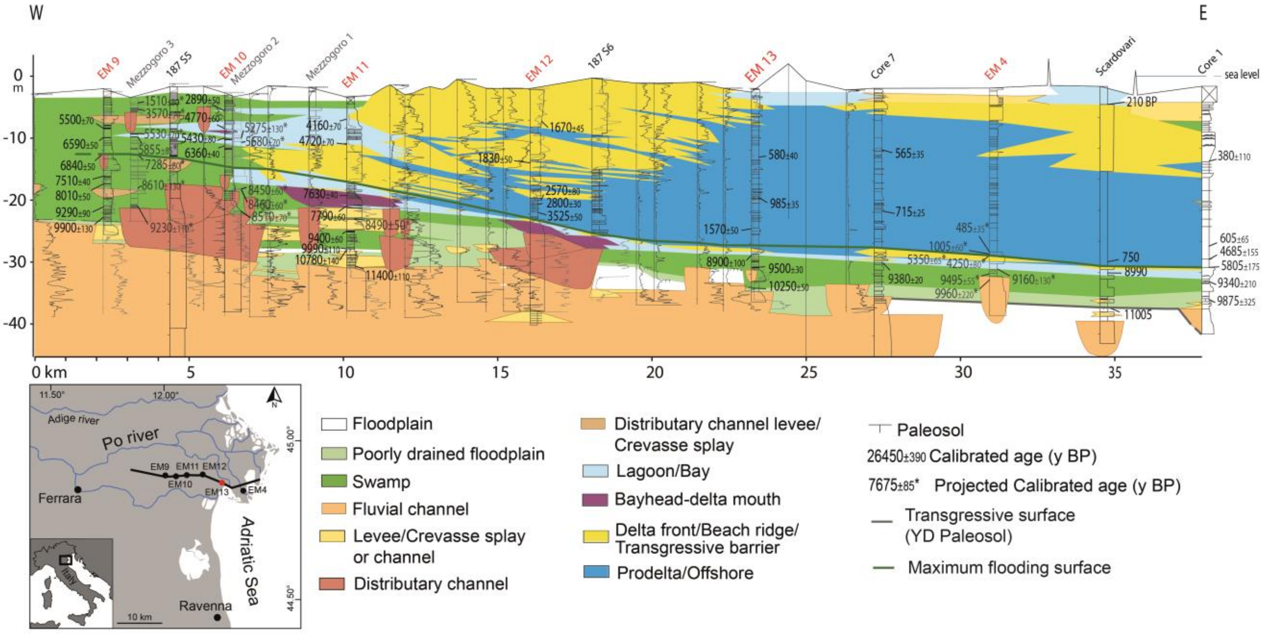

Fig. 2.14 Cross-section illustrating the stratigraphic architecture of the Holocene succession beneath the modern Po delta plain (modified from Amorosi et al., 2017).

Due to the availability of high amounts of data, the youngest T-R cycle (which corresponds to AES8, Ravenna subsynthem) has been extensively studied in the last years (Amorosi et al., 1999b, 2017; Campo et al., 2017). It was formed in response to the Holocene transgression and it was subdivided into the classical sequence-stratigraphic units that show the following features on the coastal portion of the Po Plain (Fig. 2.14):

1. The sequence boundary is represented by a major paleosol formed at the onset of the Last Glacial Maximum (30-26 ky BP). The overlying alluvial deposits are interpreted to represent the Low-stand Systems Tract (LST).

2. Above the transgressive surface (TS) locally marked by the Younger Dryas paleosol (12.5-10 ky BP; Campo et al., 2017), the Transgressive Systems Tract (TST) is characterized by a thin, deepening-upward succession of paludal to shallow-marine deposits, formed in

response to the development of a wide wave-dominated estuary in the area (Amorosi et al., 2017).

3. The High-stand Systems Tract (HST) is developed above the Maximum Flooding Surface (MFS), which marks the switch from deepening-upward to shallowing-upward trends. The HST includes shallow-marine to coastal plain sediments deposited after ca. 7 cal. ky BP under a major autogenic component (Amorosi et al., 2017). Sediment deposition was mainly influenced by local factors, such as river avulsions and delta lobe switching occurred during the Holocene progradation of the Po Delta system.

2.2.2 Holocene evolution of the Po Delta

The morphology of the modern Po Delta was determined by the combined influence of natural and anthropogenic processes occurred in the last millennia. The main branches on the modern Po Delta plain are Levante, Maestra, Pila, Tolle, Gnocca and Goro, from north to south. Volano and Primaro represent two additional distributary channels located south of the modern Po Delta, but the latter is nowadays occupied by the artificially diverted Reno River. At present, the Po Delta is classified as a wave-influenced delta (Pranzini, 2013), since after the middle of the XX century the strong human intervention (with processes such as fluvial regimentation, damming, water-methane extraction, etc.) produced a noticeable reduction of the solid transport to the delta (Simeoni and Corbau, 2009). However, conditions were different in the past, since the Po Delta experienced several evolutionary phases, as reconstructed by a series of comprehensive reviews (e.g., Ciabatti, 1967; Veggiani, 1990; Bondesan et al., 1995; Correggiari et al., 2005; Stefani and Vincenzi, 2005; Amorosi et al., 2017).

During the LGM, the Po Delta was located several hundred km south from its current position (Maselli et al., 2011), when the sea level was 120-130 m lower than today (Fairbanks, 1989), and a wide alluvial plain was developed in the modern Po Plain and North Adriatic Sea. At the beginning of transgression (19 cal. ky BP), the Po River flowed within its incised valley in a NW-SE direction through the modern Po Plain (Fig. 2.15a). During the YD climate instability phase (14.8-11.3 cal. ky BP), a minor sea-level fall possibly occurred and channel incision was promoted (Maselli et al., 2011), whereas interfluve areas were sediment-starved and a YD paleosol developed (Amorosi et al., 2014b). In response to the rapid sea-level rise that started with Meltwater Pulse 1B (MWP-1B between 11.6-11.3 cal. ky BP; Fairbanks, 1989), a backstepping wave-dominated estuary developed with wide freshwater and low-brackish water areas in its inner portions (Fig. 2.15b-c; Amorosi et al., 2017).

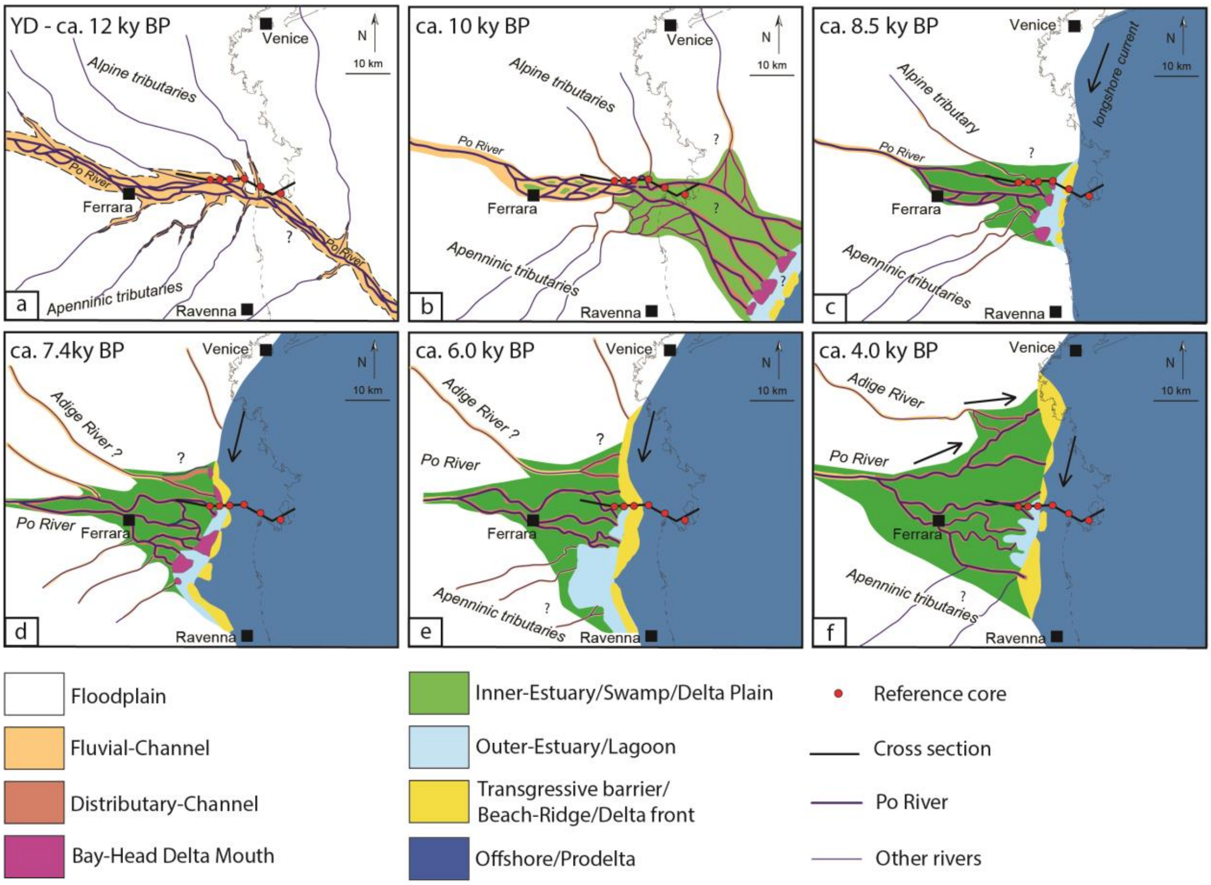

Fig. 2.15 Palaeogeographic evolution of the Po coastal plain from the Younger Dryas (YD) to ca. 4 ky BP, when the earlier deltaic system started to prograde after the infilling of the estuary (modified from Amorosi et al., 2017).

At the maximum marine transgression, dated at 7.7-7 cal. ky BP, the shoreline was located up to 20 km inland from its present position (Fig. 2.15d; Amorosi et al., 2017). The following formation of the high-stand shallow marine to coastal succession of the Po coastal plain was subject to a strong autogenic control operated by the Po Delta (Amorosi et al., 2016a). The shelf was sediment-starved until the wave-dominated estuary was filled (Fig. 2.15e-f; Amorosi et al., 2017). Coastal progradation started after 7.0 cal. ky BP, when the Po River branches evolved through a series of natural avulsions under a dominant wave activity, occupying a broad coastal area (Correggiari et al., 2005; Stefani and Vincenzi, 2005; Amorosi et al., 2017). At ca. 5 cal. ky BP, the most active Po outlet was located ca. 30 km north of the present-day position near the Venice region (Saline-Cona branch, Piovan et al., 2012), whereas the rest of the shoreline was relatively starved due to the modest sediment supply provided by the southern river branches (Amorosi et al., 2017). From ca. 3.0 cal. ky BP, the main Po river branches was located between Adria and Ravenna and formed a series of cuspate deltas testified by a series of sand ridges parallel to the modern coastline (Ciabatti, 1967; Bondesan et al., 1995).

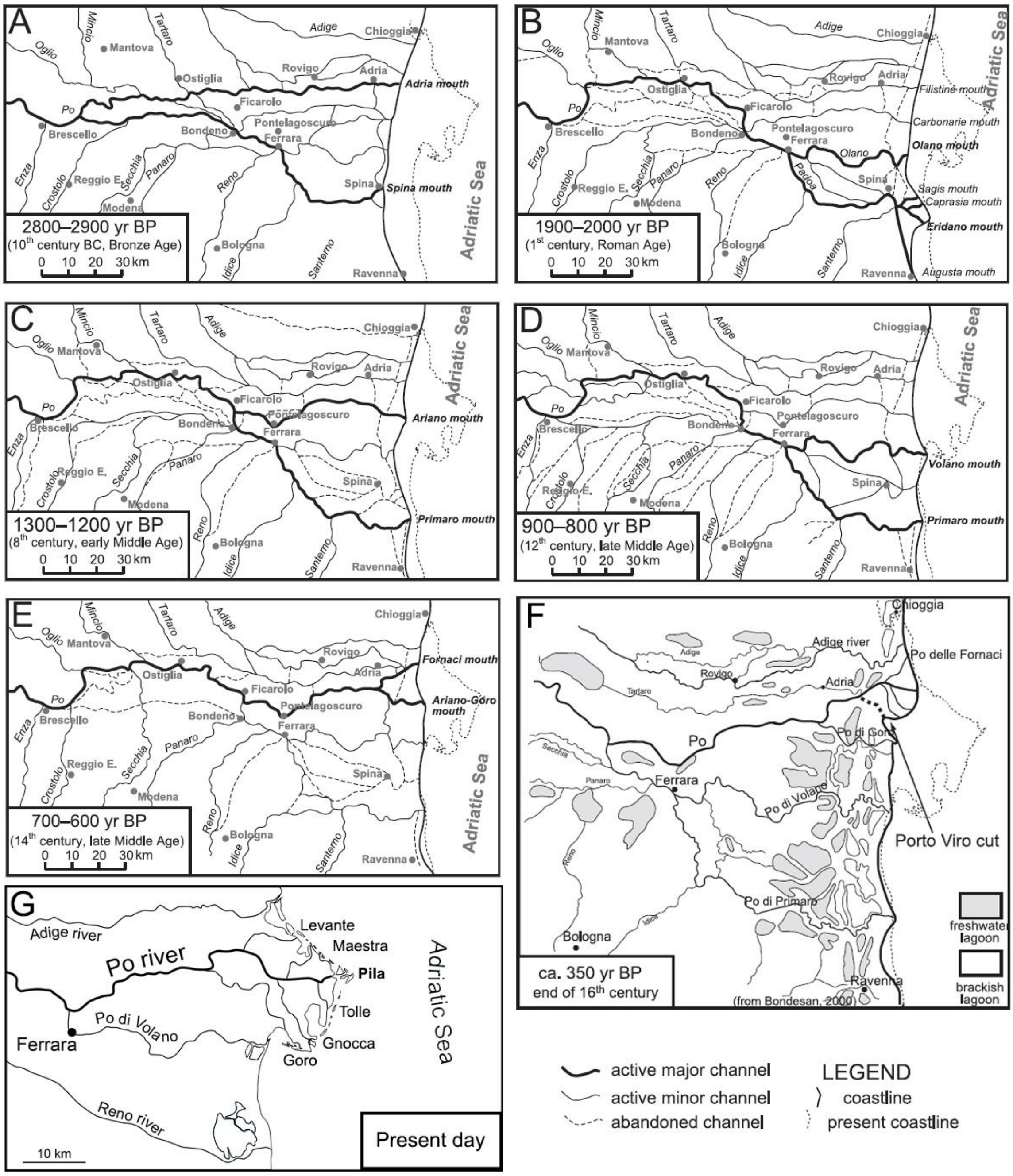

Fig. 2.16 Palaeogeographic reconstruction of the Po Delta evolution from the Bronze Age to present, derived from geomorphologic and historical data (modified from Correggiari et al., 2005).

Geomorphologic and stratigraphic analyses allowed to reconstruct the activation of the main fluvial channels that led to the construction of several wave-dominated deltas along the Po coastal plain (Fig. 2.16a-e). Specifically, Po di Adria to the north and Po di Spina to the south were the most active channels during the late Bronze Age (Correggiari et al., 2005). During the Roman Age (ca. 2500-1500 yr BP) the Olano and Eridano were the southernmost and the most important Po river branches. At ca. 1500 yr BP, a natural avulsion determined the formation of the Po di Primaro which significantly prograded during the Middle Ages (ca. 1500-500 yr BP). At the same time, in the northern sector of the coastal plain, the most active channels were Po di Ariano first, followed by Po di Volano. In the middle of XII century, a major natural avulsion called “Rotta di Ficarolo” greatly reshaped the evolution of the Po River, shifting the entire fluvial system in a northernmost position and determining the definitive abandonment of the Po di Primaro. In this new position, Po di Ariano-Goro firstly prograded, followed by Po delle Fornaci (the modern Po di Levante), which created the first lobate delta of the Po River (Ciabatti, 1967). The rapid progradation of this delta is ascribed to an increased solid transport, due to a phase of climate change after the Little Ice Age and the human intervention with the deforestation of the drainage basin (Veggiani, 1990; Correggiari et al., 2005). The risk of the infilling of the nearby Venice Lagoon by the high sediment supply provided by Po delle Fornaci led to the Porto Viro cut, a forced diversion operated ca. 350 yr BP (1599-1604 A.D.; Fig. 2.16f). The formation of the supply-dominated modern Po Delta system started after this event, which deviated the entire drainage system towards a southern position. A very rapid progradation started, influenced by delta lobe shifting, advancement and abandonment, that determined the peculiar shape of the present-day Po Delta (Fig. 2.16g).

2.2.3 Microfossil assemblages of the late Quaternary succession of the Po coastal plain

Benthic foraminifera and ostracoda included in the late Quaternary sediment succession of the Po coastal plain have been extensively studied in the recent years mainly for palaeoenvironmental purposes (Amorosi et al., 1999a, 2003, 2004, 2017). Identification of facies associations was performed on the basis of stratigraphic and sedimentological characteristics, as well as through the analysis of benthic foraminiferal and ostracod assemblages. Moreover, within lithologically homogeneous sediment successions, benthic foraminifera and ostracoda were able to track significant changes even at the scale of the sub-environment (e.g. Rossi and Vaiani, 2008). These microfossils have been proved to be useful indicators, providing information about past ecological conditions in terms of depth, salinity, degree of confinement, hydrodynamic conditions, food and oxygen availability (Rossi and Vaiani, 2008; Amorosi et al., 2008, 2017; Rossi and Horton, 2009).

Microfossil assemblages with peculiar palaeoenvironmental significance, related to different facies associations, were recognized in the uppermost 140 m of the Po coastal plain sediment succession, that include the two most recent T-R cycles attributed to MIS 1 and 5e (Amorosi et al., 2003, 2004).

Freshwater microfossil assemblage (F) – This assemblage is exclusively composed of freshwater to mesohaline ostracod taxa, with dominant *Pseudocandona albicans* and *Candona neglecta*. It was recorded within soft, organic-rich clays attributed to swamp facies association.

Back-barrier microfossil assemblages (B) – The late Quaternary brackish-water microfossil assemblages of the Po Plain sediment succession are mainly characterized by the opportunistic benthic foraminifera *Ammonia tepida* and *Ammonia parkinsoniana* and the ostracod *Cyprideis* *torosa*. However, changes in the relative proportions of these taxa and the occurrence of a variety of subordinate species, led to the differentiation between different associations. Specifically, outer lagoonal/estuarine deposits (association Bd) include scarce frequencies of *Cribroelphidium* spp., *Aubignyna perlucida,* Miliolidae, *Loxoconcha elliptica, Leptocythere* spp. and *Loxoconcha stellifera*. The central lagoonal/estuarine fauna is still dominated by *A. tepida, A. parkinsoniana* and *C. torosa*, but it is more oligotypic (association Bc). Inner lagoonal/estuarine sediments include almost exclusively the euryhaline ostracod *C. torosa*, with scattered tests of the benthic foraminifera *A. tepida* and *A. parkinsoniana* (association Bb). Ostracoda are absent within the marsh assemblage (association Ba), dominated by extremely high frequencies of *Trochammina inflata*.

Reworked microfossil assemblages (R) – Microfossil assemblages with large-size tests of benthic foraminifera and thick ostracod valves with evident traces of abrasion were commonly found in sandy deposits and are considered indicative of a high-energy depositional environment. Beach ridge and upper shoreface sands usually include coastal taxa such as *Ammonia beccarii, Elphidium crispum, Elphidium macellum* and Miliolidae along with reworked planktonic and benthic foraminifera from older units, whereas ostracoda are rare and mainly represented by *Pontocythere turbida* (association Rm). Conversely, washover sands are characterized by brackish-water taxa, likely transported from nearby lagoonal environments, mainly *A. tepida, A. parkinsoniana, Elphidium* spp. and *C. torosa* (association Rb).

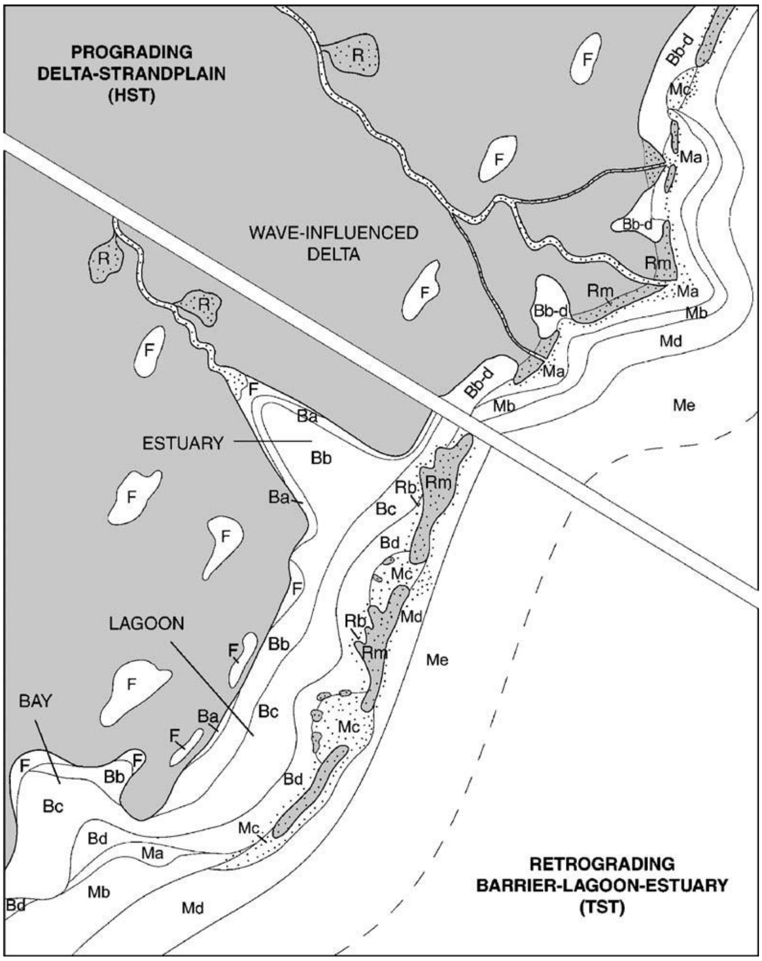

Fig. 2. 17 Model for the palaeoecologic distribution of the microfossil assemblages identified in the late Quaternary sediment successions of the Po Plain (from Amorosi et al., 2004).

Marine microfossil assemblages (M) – These assemblages are found from offshore transition to prodelta and transgressive barrier deposits. Specifically, microfossil assemblages within transgressive barrier sands and offshore transition sediments are composed by abundant and well-diversified marine species (associations Me-Md). The most common benthic foraminiferal taxa are *Texularia* spp. (mainly *T. agglutinans* and *T. bocky*, subordinately *T. sagittula, T. candeiana* and *T. aciculata*) and Miliolidae (*Adelosina, Quinqueloculina, Triloculina, Cycloforina, Sigmoilinita, Siphonaperta, Spiroloculina, Miliolinella* and *Pseudotriloculina*), associated to lower frequencies of *P. granosum* and *P. lidoense* (listed as *Cribroelphidium granosum* and *Cribroelphidium lidoense* in the cited works but nowadays gathered into the single species *P. granosum*; in this thesis, the genus is updated in accordance with the standard references, but I retain the differentiation of the two species due to their distinct ecological distribution recorded in the reference works of Jorissen for the Adriatic Sea), *Elphidium* spp., *Nonionella turgida, Asterigerinata* spp., *Lagena* spp. and *Buccella granulata*. Ostracoda are diversified as well as foraminifera, represented by *Pontocythere turbida, Leptocythere* spp. (mostly *L.* cf. *L. multipunctata*, *L. bacescoi* and *L. laevis*), *Callistocythere* spp. (mostly *C. adriatica, C.* cf. *flavidofusca* and *C. intricadoides*), *Semicytherura* spp., *Loxoconcha* spp. and *Carinocythereis whitei*. Prodelta facies association is characterized by abundant opportunistic species, like the benthic foraminifera *A. tepida* and *A. parkinsoniana*, associated to locally high frequencies of *Semicytherura incongruens* or *Pontocythere turbida* (associations Mb-Ma). Subordinate benthic foraminiferal taxa are *P. granosum, C. poeyanum, P. lidoense* and *C. decipiens*, *Haynesina depressula, E. advenum* and mostly *Quinqueloculina seminula* among the miliolids. Ostracoda include a variety of *Semicytherura* (*S. acuticostata, S. costata, S. rarecostata*), *Loxoconcha* (*L.* gr. *rhomboidea, L. exagona, L. rubritincta, L. tumida*), *Neocytherideis fasciata* and, locally, valves of *L. elliptica* and *L. stellifera*, likely transported by the river inputs. Peculiar prodelta microfossil assemblages indicative of a fine-grained substrate enriched in organic matter, comparable to the modern shallow North Adriatic mud-belt, were recorded under the modern Po delta plain by Rossi and Vaiani (2008) and Rossi (2009). These assemblages are extremely oligotypic, dominated by *N. turgida* and *Palmoconcha turbida*, opportunistic species typical of shallow marine environments with reduced oxygen concentrations.

3. METHODOLOGICAL APPROACH

Benthic foraminiferal and ostracod data analyzed in my Ph.D. project are represented by modern and late Quaternary meiofaunal (ostracoda and benthic foraminifera) databases. Specifically, the analyzed modern databases are represented by:

- a sub-set of 87 samples from the northern sector of the Adriatic Sea, derived from the pre-existing databases of Breman (1975) for ostracoda and Jorissen (1988) for benthic foraminifera of the Adriatic Sea;
- 64 surface samples collected in the lagoon of Bellocchio ("Sacca di Bellocchio", south of the Po Delta)

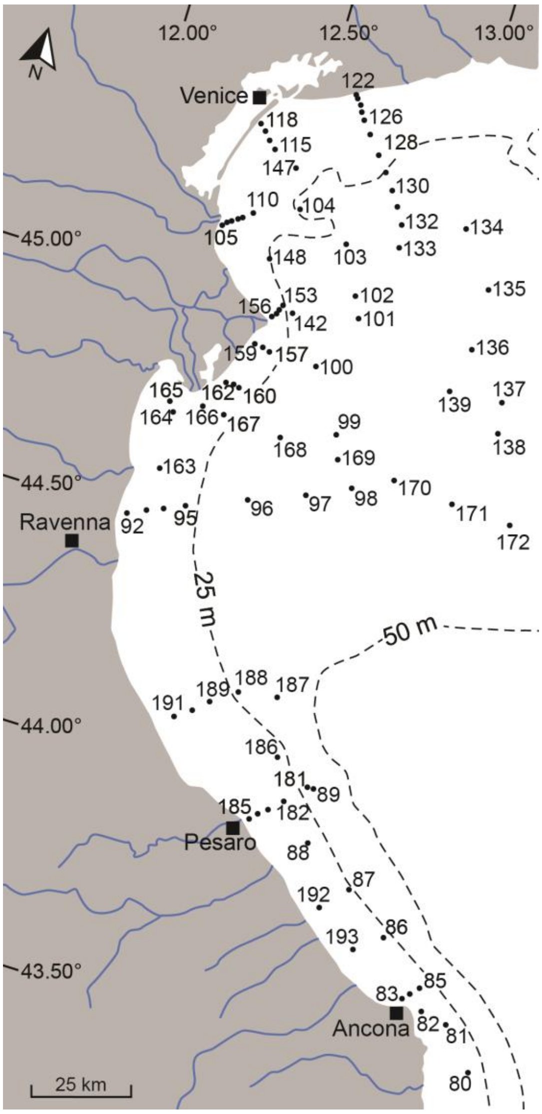

Fig. 3.1 Distribution of samples selected from databases of Breman (1975) and Jorissen (1987), analyzed during my Ph.D. project to determine modern biofacies of ostracoda and benthic foraminifera.

The micropalaeontological samples from the late Quaternary database of the Po coastal plain include a total of 263 samples from three cores (core EM13, 223-S12 and Core 7).

3.1 Modern databases

3.1.1 North Adriatic Sea database

A total of 320 samples for ostracoda and 285 samples for benthic foraminifera compose the Adriatic Sea databases of Breman (1975) and Jorissen (1988), respectively. These databases are formed by the same set of samples (grab samples and piston-core tops), collected during an oceanographic cruise in 1962. The first meiofaunal analyses were performed by Breman (1975) on the ostracod fauna and, in a second instance, by Jorissen (1987, 1988) on benthic foraminifera. Since benthic foraminifera were not stained in the field, both authors analyzed the total assemblages in the sediment fraction >150 µm. Procedures for the treatment and preparation of samples were described at length in the reference works (Breman, 1975; Jorissen, 1988). These samples also include quantitative values of four abiotic factors for each sample: water depth (m), percentage of sand (%), calcium carbonate (%) and organic matter (%).

Therefore, datasets can be considered perfectly comparable in terms of meiofauna and environmental parameters.

Due to their vicinity to the Po coastal plain, the Adriatic meiofaunal databases of Breman (1975) and Jorissen (1988) can be considered the best modern analog for the shallow-marine, late Quaternary meiofaunal assemblages of the Po coastal plain. I performed integrated statistical analyses of the meiofauna on a total of 87 samples from the North Adriatic Sea, between the northern Adriatic coasts and Ancona (Fig. 3.1). Since the meiofauna of the southern sector of the Adriatic show a higher dissimilarity compared to the North Adriatic meiofauna, it was excluded from the analyzed database. This fact could be linked to the different depositional regimes acting on these two sectors of the shallow Adriatic Sea (Frignani et al., 2005).

Within the analyzed databases, the abundance of ostracoda and benthic foraminifera was originally expressed as compositional data in percentage form. Among the additional information included within the databases, the number of total identified valves was reported for ostracoda, whereas the benthic foraminiferal dataset did not include the total number of counted tests. For this reason, the analyzed data could not be transformed into relative abundance (i.e., number of valves/tests) and must be used as percentages. However, the total number of ostracod valves was used to obtain the relative abundance of each taxon, to remove the contribution of obviously transported or reworked freshwater and brackish water taxa (mostly represented by *Candona* spp., *Ilyocypris* spp., *Limnocythere* spp., *Cyprideis torosa*, *Leptocythere lagunae* and *Loxoconcha elliptica*) and finally percentage abundances of the remaining (*in-situ*) taxa were calculated. After these operations, samples including <20 valves were removed from the dataset. This is considered an appropriate threshold value for ostracod studies in marine settings (Cronin, 1999; Bassetti et al., 2010). The final ostracod dataset included 71 samples. In order to reduce the dispersion of the data, selected species were grouped up to genera level according to their taxonomy and ecological characteristics.

Pre-treatment of the data was not required for the benthic foraminiferal dataset, since all the samples originally included >250 tests and the contribution of finely agglutinated taxa (*Eggerella* spp. and *Reophax* spp.) susceptible to fragmentation after burial was already removed by Jorissen (1988). Since nine out of the 87 samples selected for the analyses were not included in the original database due to the scarce fauna (<250 tests), the final benthic foraminiferal dataset included a total of 78 samples. Some species were already partially grouped on the basis of their genera, morphologic groups and/or ecological preferences (Jorissen, 1988), therefore an additional grouping was not performed. Some taxa were gathered together in the original database, since they were considered as *formae* at that time (e.g. *A. parkinsoniana* groups *A. parkinsoniana* and *A. tepida*; *P. granosum* groups *P. granosum* and *P. lidoense*, *C. poeyanum* groups *C. poeyanum* and

C. decipiens; complete list is included in Jorissen, 1988), thus preventing the analysis of the single species distribution.

3.1.2 Sacca di Bellocchio database

The meiofaunal study of the lagoon of Bellocchio is currently in progress. The database will include a series of parameters, specifically:

- Biotic variables: abundances of living (rose Bengal-stained) and dead benthic foraminifera; total abundances of ostracoda;
- Abiotic variables:
    - sediment characteristics: grain size, concentration of $CaCO_3$, C, N, H, S, clay composition;
    - water characteristics: salinity, Ph, temperature, Oxygen Reduction Potential (ORP) and concentration of dissolved oxygen (DO). These parameters were measured by means of a multiparametric probe and are available for a limited number of samples. Specifically, the few cms of water along the tidal creeks in the southern portion of the lagoon prevented the acquisition of the data.

A total of 64 surface samples were collected from the Bellocchio Lagoon (south of the Po Delta) in October 2016 and May-June 2017 (Fig. 3.2). Since the lagoon of Bellocchio is a natural reserve, sampling operations were performed with the permission of the Command for forestry, environmental, food and agricultural protection of the Carabinieri Force (formerly the State Forestry Corps). Samples were collected from relevant areas of the lagoon: permanently submerged areas in the lagoonal basin, channels, creeks and ponds (Fig. 3.2). Sediment samples were collected using a plastic tube of 8 cm of diameter with a sharp ring at one of its extremities, that allowed the collection of undisturbed samples.

Fig. 3.2 Distribution of samples collected from the Sacca di Bellocchio for meiofaunal analyses. Main geomorphological features are indicated. Not-colored areas within the Sacca di Bellocchio are not submerged and characterized by occasional pools and seasonal dry-ponds.

Two aliquots of sediment (ca. 50 ml each one) were collected from the uppermost cm of the undisturbed samples. The first aliquot was stained in the field with buffered rose Bengal dye (2 g of rose Bengal in 1000 ml of 95% ethanol) for at least 14 days to differentiate living and dead benthic foraminifera (Schönfeld, 2012). The second aliquot was collected for grain-size, geochemical (C, N, H, S) and mineralogical ($CaCO_3$, clay composition) analyses. The value of water depth was measured at each site.

Samples were successively oven-dried at 30 °C and weighted. Successively, they were soaked in water for ca. 8 hours and gently washed through a 63 µm sieve with tap water to remove the finer particles and the excess of dye. After washing, samples were dried again at 30°C and weighted in order to quantify the sand fraction.

The quantitative analysis of benthic foraminifera and ostracoda was performed on the sediment fraction >63 µm, due to the extremely low number of living specimens recorded in the fraction >125 µm, which is generally recommended for environmental and biomonitoring studies using benthic foraminifera (Schönfeld, 2012). Only living foraminifera at the time of collection were counted, i.e. the specimens showing a bright stained protoplasm up to the last or penultimate chamber. Living ostracoda are usually recognized on the basis of the presence of soft parts attached to the carapace or valves (e.g. Ruiz et al., 1997). Since the living individuals in our samples were extremely scarce, both living and dead ostracoda were counted, as well as entire carapaces and single valves, on the whole range of the juvenile moults and adults.

3.2 Po coastal plain late Quaternary database

The analyzed late Quaternary micropalaeontological assemblages were collected from three continuously cored boreholes distributed on the modern Po Delta and coastal plain (Fig. 3.3), each one representing specific palaeoenvironmental settings.

- The analyzed shallow marine succession of Core EM13 is chronologically representative of the wave-dominated to river-dominated evolution of the Po Delta.
- The analyzed shallow marine sediment succession of Core 7 is representative of the evolution of the Po Delta under a strong river-dominated regime (i.e. after the Ficarolo avulsion).

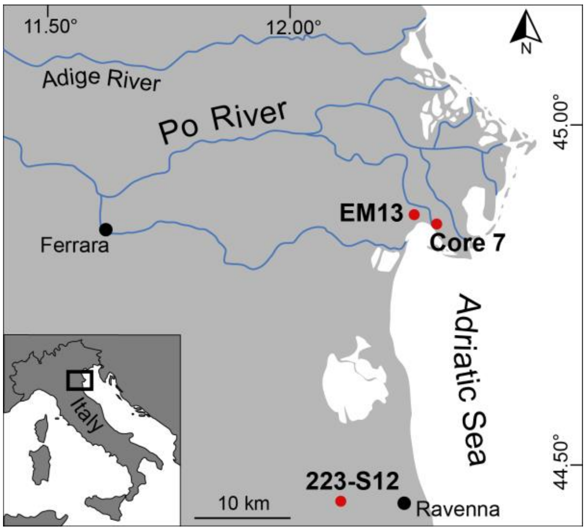

Fig. 3.3 Location of the cores analyzed during the Ph.D. project.

- The Pleistocene back-barrier succession of core 223-S12 represented the peculiar record of a transitional setting developed during the MIS7, one of the rare examples in the Po coastal plain.

3.1.1 Sample collection and treatment

During the research project, 155 samples were directly collected and treated from the 34 m-long core EM13, drilled in collaboration with ExxonMobil. Samples were collected sectioning the core into 2 cm-thick slices, excluding the external surfaces of the sediment core in order to avoid the collection of possibly displaced specimens. Samples were treated following the standard procedures reported, for instance, in Amorosi et al. (2008) and Rossi and Vaiani (2008). Samples were oven-dried at 60 °C for 2-3 days, weighted to obtain the dry weight (ca. 80-100 g per sample) and then soaked in water and hydrogen peroxide (35%) for 8 hours. They were washed through a 63 µm sieve and dried again for 24 hours. Samples from Core 7 and core 223-S12 were already available for the analyses. All the treated samples are stored in the sedimentary laboratory at the BiGeA department of the University of Bologna.

All the studied samples were qualitatively analyzed under a binocular microscope in the fraction >63 µm. Selected samples were dry-sieved and quantitatively analyzed in the fraction >125 µm and relative abundance of benthic foraminifera and ostracoda was obtained. Specifically, a total of 116 samples were quantitatively analyzed from the three previously mentioned cores. All of them were counted for benthic foraminifera, whereas only 42 were quantitatively analyzed for ostracoda, due to: (i) the relatively low abundance of ostracoda within the shallow-marine successions of core EM13 and Core 7 and (ii) the specific aim of the focusing on the benthic foraminiferal record of Core 7. The following table reports the number of samples analyzed during the Ph.D. project and the amount of samples that were quantitatively and statistically analyzed.

ANALYSED SAMPLES FOR THE Ph.D. PROJECT					
Core	Treated	Counted for benthic foraminifera	Counted for ostracoda	Statistically analyzed for benthic foraminifera	Statistically analyzed for ostracoda
EM13	155	49	23	37	17
223-S12	19*	19	19	11	16
Core 7	89*	48	0	37	0

Tab. 1 Samples from the three cores analyzed during the Ph.D. project. The asterisk indicates samples that were already available for the analyses.

3.1.2 Identification and ecological interpretation of benthic foraminifera and ostracoda

Benthic foraminiferal and ostracod taxa were identified following original descriptions and several key papers. Specifically, the identification of benthic foraminifera relies upon the following works: Ellis and Messina (1940), Hansen and Lykke-Andersen (1976), AGIP (1982), Jorissen (1988), Albani and Serandrei Barbero (1990), Cimerman and Langer (1991), Sgarrella and Moncharmont Zei (1993), Hayward et al. (1997), Fiorini and Vaiani (2001), Rasmussen (2005) and Milker and Schmiedl, (2012). Ostracoda were taxonomically identified using the works of Uffenorde (1972), Bonaduce et al. (1975), Breman (1975), Athersuch et al. (1989), Henderson (1990), Mazzini et al. (1999), Faranda and Gliozzi (2008), Frenzel et al. (2010), Cabral and Loureiro (2013) and Salel et al. (2016).

Interpretation of the ecological characteristics of species and the environmental significance of the late Quaternary benthic foraminiferal and ostracod assemblages are inferred from the comparison with modern benthic faunas from shallow-marine (Colalongo, 1969; D'Onofrio, 1969; Uffenorde, 1972; Bonaduce et al., 1975; Breman, 1975; Jorissen, 1987; Murray, 1991; Van der Zwaan and Jorissen, 1991; Barmawidjaja et al.,1992; Donnici and Serandrei Barbero, 2002; Frezza and Carboni 2009; Mojtahid et al. 2009; Goineau et al. 2011, 2012, 2015; Frezza and Di Bella, 2015) and transitional environments (Montenegro and Pugliese, 1996; Debenay et al., 2000; Ruiz et al., 2000; Frenzel and Boomer, 2005; Carboni et al., 2009; Frontalini et al., 2009; Melis and Covelli, 2013; Pint and Frenzel, 2017) of the Mediterranean area. The interpretation of microfossil assemblages also relied upon the comparison with microfaunal associations recovered from late Quaternary coastal successions of Italy (Carboni et al., 2002; Aguzzi et al., 2007; Di Bella et al., 2013, 2014; Amorosi et al., 2014a, 2016), with special attention for works performed on the Po coastal plain (Amorosi et al., 2004, 2008, 2017; Rossi and Vaiani, 2008; Rossi, 2009; Milli et al., 2013; Campo et al., 2017).

3.3 Statistical elaborations

Multivariate statistical techniques were applied to modern and late Quaternary benthic foraminiferal and ostracod faunas for palaeoenvironmental purposes. Prior to the statistical analyses, data matrices were produced grouping taxa with similar ecological preferences up to the genus level and removing rare species (with different threshold values for shallow marine and back-barrier settings) in order to reduce the noise produced by non-significant taxa. Successively, abundance data were transformed using methods adopted in the literature and selected on the basis of the environmental setting (Legendre and Gallagher, 2001; Legendre and Legendre, 2012). In shallow marine settings, data transformation helped to reduce the contribution of minor taxa (e.g. Mojtahid et al., 2009; Rossi and Vaiani, 2009), whereas it was enhanced in back-barrier setting (e.g., Slack et al., 2000). Then, distance matrices were created choosing appropriate similarity (or dissimilarity) measures recommended in the literature (Legendre and Gallagher, 2001; Legendre and Legendre, 2012).

After treatment of the data matrices, two main groups of multivariate statistical methods have been applied:

- *Cluster analyses* (classical Q-mode and Multivariate Regression Trees, MRT), in order to discriminate groups of samples with a similar fauna. This method is often applied in both modern environments and fossil successions, since it allows to place discrete limits between groups. I additionally tested MRT because it has a desirable advantage over classical Q-mode cluster analysis: it partitions groups not only on the basis of biotic variables (i.e., abundances of taxa) but also considering abiotic (i.e., environmental) variables. Therefore, MRT defines quantitative threshold values of environmental variables that create groups with a similar fauna. This is particularly useful in the presence of modern dataset including biotic and abiotic data for each sampling station (e.g., as the case of the North Adriatic database analyzed within this Ph.D. project; see Chapter 5).

- *Ordination analyses* (Metric and non-Metric Multidimensional Scaling, MDS and nMDS), to identify (palaeo-)environmental gradients evidenced by the meiofaunal assemblages. They were applied with the additional aim of checking if the groupings operated by the cluster analyses were reliable and followed natural gradients (e.g. Chapter 8).

A series of additional statistical analyses were performed on the basis of specific questions for each study case.

- *Similarity Percentage (SIMPER) analyses:* how much is the contribution of each taxon to the formation of clusters? (e.g. Chapter 9)

- *Correlation matrices* are usually applied to a single faunal group, in order to understand which taxa can (or cannot) be found together and if they are related to the same set of abiotic parameters. However, I wanted to go further and answer to the following question: which benthic foraminiferal taxa and ostracod taxa could I find in the same meiofaunal assemblage? And, moreover, how both are linked to environmental parameters? (see Chapter 5);

- *Analysis of Similarities (ANOSIM)*: is there a significant difference between groups? ANOSIM is a non-parametric test that works on dissimilarity matrices. It tests if the rank of distances between groups defined *a priori* is greater than the rank of distances within groups. I applied this method to understand if groups of samples showed significant differences in terms of diversity indices (see Chapter 9).

- *Analogue matching (AM*) specifically answers to the following question: which modern samples are most similar to the fossil ones, in terms of faunal composition? This technique operates on two databases, one composed a set of fossil assemblages and the second one composed by modern assemblages. It calculates the dissimilarity (or similarity) between every fossil and modern samples and it finds modern samples that are most similar (i.e., that show the minimum dissimilarity) to the fossil ones. I used AM to find the closest modern analogue to each fossil sample of core EM13, in terms of both benthic foraminiferal and ostracod assemblages (see Chapter 6). It should be mentioned that modern databases for the Adriatic Sea (Breman, 1975; Jorissen, 1988) report meiofaunal data analyzed in the fraction >150 µm. On the other hand, fossil assemblages from sediment cores were analyzed in the fraction >125 µm as suggested by reference works (Boomer, 2003; Schönfeld et al., 2012; Weinkauf and Milker, 2018). Nevertheless, this discrepancy is not significant, since benthic foraminiferal data from these two size fractions are considered fully comparable and do not imply significant problems for palaeoenvironmental reconstructions (Weinkauf and Milker, 2018).
- *Calculation of faunal parameters:* what is the structure of benthic foraminiferal and ostracod assemblages? Indices of species diversity, dominance, distribution of individuals among taxa and faunal density were computed to detect changes in the structure of benthic communities connected to shifts of palaeoecological conditions. This procedure was exclusively applied when it was considered essential for the purpose of the work, as in the case of Chapter 9. Conversely, it was not applied to Chapter 5 and 6, where taxonomic categories are derived from literature data that often gather several species into groups of higher taxonomic rank. The Foraminiferal Abnormality Index (FAI; Frontalini and Coccioni, 2008) was expressed in presence of significant values of aberrant benthic foraminifera indicative of stressed conditions (FAI>1%), as in Chapter 9. Except for core 223-S12, abnormal tests of benthic foraminifera within the Po Plain sediment successions are always very rare (FAI<1%). Literature data presented in Chapter 5 do not include quantitative information about deformed tests of benthic foraminifera. The FAI and the structure of the meiobenthic community of the Bellocchio Lagoon (Chapter 10) will be analyzed when the full database will be compiled.

4. RESEARCH SUMMARY

The purpose of this Ph.D. project is to detect coastal and delta dynamics within the late Quaternary sediment succession of the eastern Po Plain through the analysis of benthic foraminifera and ostracoda. In order to track even small palaeoenvironmental changes, is essential to understand the mechanisms that drive the faunal turnover in each group. The cornerstone of the project is the integration of benthic foraminifera and ostracoda, combined with the comparison of the distinct palaeoecological information provided by each group.

To achieve these goals, shallow marine and back-barrier settings were investigated, since they represent extremely fragile and unstable environments that change in response to allogenic (e.g., sea-level oscillations) as well as autogenic (e.g., channel avulsions, delta lobe switching, closure of tidal inlets) processes. Both modern and fossil faunas were investigated within each setting: a comprehensive knowledge of present-day fauna would allow to interpret in detail the fossil record. This operation should be performed in the same geographical area, in order to retain comparable benthic assemblages.

This resulted in the analysis of six study cases during my Ph.D. project (Fig. 4.1):

Modern settings	Late Quaternary Po Plain sediment succession
North Adriatic shelf	EM13 Holocene shallow marine succession
	Po coastal plain HST
	Core 7 late Holocene shallow marine succession
Lagoon of Bellocchio	Core 223-S12 Pleistocene back-barrier succession

Most of the obtained results were reported in four research papers, which were already published (chapters 8 and 9) or either submitted (chapters 5 and 7). Preliminary results about the fossil meiofauna of core EM13 and the modern meiofauna of the Lagoon of Bellocchio are presented in chapter 6 and chapter 10, respectively.

- **First study case:** *Modern meiofauna of the North Adriatic Sea (Chapter 5)*. The North Adriatic shelf faces the Po coastal plain and its sedimentary dynamics are strongly influenced by the Po River, particularly in the shallowest (<40 m water depth) sector, therefore it represents the best modern analog for late Quaternary shallow marine successions of the Po Plain. This chapter presents the multivariate analysis of modern benthic foraminifera and ostracoda from this sector of the basin. Even though data were derived from literature sources (Breman, 1975; Jorissen, 1988), we obtained new insights about the environmental drivers influencing the distribution of the meiofauna: benthic foraminifera are mostly related to organic matter, whereas bathymetry and grain-size (i.e. sand concentration) drive ostracod assemblages.

Moreover, we show that the combination of the two meiofaunal groups allow to obtain a refined characterization in terms of depositional environments on river-influenced shelves.

Authors contribution to the paper: all the authors defined the design of the work. I performed the statistical analyses, prepared all the figures and the majority of the supplementary and in-text tables, with the exception of table 5 which was prepared by VR. I, VR and SV interpreted the data. All the authors contributed to the writing of the paper.

- **Second study case:** *The palaeoecological record of delta dynamics (Chapter 6)*. In chapter 6, modern meiofaunal assemblages were quantitatively compared to the fossil fauna of the Holocene shallow marine succession of core EM13, which chronologically encompasses the wave-to-river dominated Holocene evolution of the Po Delta. Here, I show that each group shows a different palaeoecological record: in accordance with modern data, benthic foraminifera are related to organic matter fluxes, whereas ostracoda seem to be indicative of the amount of sediment input. Included in the well-known evolutionary frame of the Po Delta, I show that the integration of benthic foraminifera and ostracoda represents a powerful tool to obtain an high-resolution characterization of shallow marine, river-influenced sediment successions.

Fig. 4.1 Location of the study cases presented in the Ph.D. thesis. Modern databases from literature sources in green, based on new data in red, sediment successions in yellow.

- **Third study case:** *Three-fold nature of the Po Plain highstand succession (Chapter 7)*.The further step was to test benthic foraminifera and ostracoda as palaeoecological indicators at a wider scale: in chapter 7 they were applied for the characterization of the depositional systems of the high-stand succession of the Po coastal plain. They provide information about palaeoenvironmental conditions along the whole stratigraphic interval, from proximal to distal locations, in both sand and fine-grained deposits, over three phases of coastal evolution: i) uppermost TST: bay-head delta progradation in an estuarine environment, ii) lower HST: predominant aggradation of wave-dominated deltas, and iii) upper HST: rapid progradation of the river-dominated Po Delta.

  Authors contribution to the paper: the paper was mostly ideated by AA, in collaboration with LB and BC. Sedimentological and stratigraphic analyses were performed by AA, LB and BC. Geochemical data were analyzed and interpreted by AA and IS. Most of the radiocarbon dates were determined by WH. Mollusks data were collected, treated and interpreted by DS.

Micropalaeontological data were collected, treated and interpreted by SV, VR and GB. Specifically, I treated, analyzed and interpreted benthic foraminifera and ostracoda from Core 7 and core EM13, therefore my contribution was mostly focused on the wave-dominated and river-dominated facies in the seaward portion of the succession (phases 2 and 3 of the model). I produced Figure 4, I contributed to the writing of the micropalaeontological contents of the paper and to the preparation of Table 1. The majority of the figures were prepared by LB and BC. Writing of the paper was mostly performed by AA with the subordinate collaboration of all the authors.

- **Fourth study case:** *Benthic foraminifera: a key tool in river-dominated successions (Chapter 8)*.The shallow marine succession of Core 7 was studied to specifically focus on the prograding portion of the upper HST, in order to investigate the ability of benthic foraminifera to detect subtle, short-time palaeoenvironmental changes within a river-dominated succession of the Po Plain. In chapter 8 we show that these microfossils track changes of river influence, related to short time-scale autogenic deltaic processes that governed deltaic evolution in the last millennia.

  Authors contribution to the paper: all the authors contributed to the ideation and writing of the paper. Analysis of benthic foraminifera were performed by me and SV. I performed the statistical analyses and contributed for the 80% to the preparation of the figures. Interpretation of microfossil fauna was done by me and SV, whereas geochemical data were interpreted by AA.

- **Fifth study case:** *Accuracy of benthic foraminifera and ostracoda in back-barrier successions (Chapter 9)*. Within the Pleistocene back-barrier succession of core 223-S12, benthic foraminifera and ostracoda were compared to test which group shows the highest palaeoenvironmental resolution potential in such settings. The amount of aberrant specimens within the two benthic foraminiferal assemblages suggests the development of stressed/unstressed conditions, whereas three ostracod assemblages were determined by salinity and thus can be correlated to different degrees of isolation from the sea. In this case, ostracoda gave more straightforward indications about palaeoenvironmental conditions, even though benthic foraminifera provided relevant additional information and integrated the palaeoecological record in presence of monospecific ostracod assemblages. Additionally, a detailed taxonomic analysis of Elphidiidae, Rotaliidae, and Nonionidae was performed to increase our knowledge on peculiar taxa recovered in the analyzed deposit.

  Authors contribution to the paper: I and SV defined the design of the work and carried out benthic foraminiferal analyses, whereas I performed the ostracod analyses and statistical elaborations. Interpretation of fossil data and preparation of the paper was contributed to by both authors.

- **Sixth study case:** *Modern meiofauna of the Lagoon of Bellocchio (Chapter 10)*. Despite the exceptional level of detail obtained in the Pleistocene back-barrier succession of core 223-S12, some features of the fossil assemblages were not fully understood (e.g. environmental factors that determined the development of stressed conditions, connection between ostracod assemblages and effective distance from inlets, etc.). Therefore, the study of the modern meiofauna of the Bellocchio Lagoon started with the aim of understanding the dynamics that govern the meiofaunal turnover within these settings. This chapter presents preliminary results about living benthic foraminifera, live and dead ostracoda and the future perspectives of this project, such as the identification of benthic foraminiferal biotopes (using living individuals) and meiofaunal thanatofacies (dead benthic foraminifera and ostracoda) to develop a proxy for palaeoenvironmental reconstructions within back-barrier successions.

5. MODERN MEIOFAUNA OF THE NORTH ADRIATIC SEA

5.1 Manuscript I

Benthic ostracoda and foraminifera from the North Adriatic Sea (Italy, Mediterranean Sea): a proxy for the depositional characterization of river-influenced shelves*

Giulia Barbieri, Veronica Rossi, Stefano Claudio Vaiani and Benjamin Peter Horton

*****Submitted to **Marine Micropaleontology**

Benthic ostracoda and foraminifera from the North Adriatic Sea (Italy, Mediterranean Sea): a proxy for the depositional characterization of river-influenced shelves

Giulia Barbieri[a*], Veronica Rossi[a], Stefano Claudio Vaiani[a] and Benjamin Peter Horton[b, c]

[a] Dipartimento di Scienze Biologiche, Geologiche e Ambientali, University of Bologna, via Zamboni 67 Bologna, 40127, Italy

[b] Asian School of the Environment, Nanyang Technological University, Singapore 639798

[c] Earth Observatory of Singapore, Nanyang Technological University, Singapore 639798

* Corresponding author: Giulia Barbieri. E-mail: giulia.barbieri21@unibo.it Telephone: +39 051 2094588

E-mail addresses: veronica.rossi4@unibo.it (V. Rossi), stefano.vaiani@unibo.it (S.C. Vaiani), bphorton@ntu.edu.sg (B.P. Horton)

Abstract

In this study we investigate the distribution of ostracoda and benthic foraminifera from the shallow (<40 m water depth) North Adriatic shelf fed by the Po River and, to a lesser extent, Apennines and Alpine rivers. We recognize the main environmental drivers on each benthic group and identify depositional settings under different degrees of river influence, integrating faunistic and environmental data from a sub-set of samples of previously published databases (Breman, 1975; Jorissen, 1988). Multivariate statistical analyses, including Analogue Matching technique and Multidimensional Scaling, indicate that distinct environmental parameters drive the meiofaunal turnover across the North Adriatic inner shelf: grain-size (sand %) and bathymetry for ostracoda; organic matter concentration for benthic foraminifera. The integration between ostracoda and benthic foraminifera, which show seven and five biofacies respectively, gives us the opportunity to distinguish three main areas with respect to the relative position to the main source of riverine material (i.e., the Po River) and the accumulation of river inputs. In proximity of the Po Delta, where high fluxes of sediment occur, taxa tolerant to organic-rich (2.7% on average) muddy (0.5-15.6% of sand) substrates and periodical oxygen deficiency are abundant (*Palmoconcha turbida, Leptocythere ramosa, Ammonia parkinsoniana-Ammonia tepida, Nonionella turgida*). Downdrift of the main feeding mouths, under the combined influence of the Po and Apennine rivers, ostracoda discriminate between shallow (8-13 m water depth), sandy (15.9-73.3%) substrates (*Semicytherura incongruens, Xestoleberis* spp.) subject to the action of longshore currents and deeper (13-20 m water depth) more clayey (1.1-11.2% of sand) bottoms (*S. incongruens, Palmoconcha turbida*). Conversely, benthic foraminifera are monotonous from coast to offshore, being represented by taxa tolerant to moderate concentrations of organic matter (0.1-1.3%) as *A. parkinsoniana-A. tepida* and *Aubignyna perlucida*. The mud-lover species *Cytheridea neapolitana* and *Bulimina marginata,* tolerating high organic matter concentrations (1.35% on average), are abundant in the Adriatic mud-belt subject to major accumulation of riverine material at 20-40 m water depth. Updrift of the Po Delta, on sandy substrates with low organic matter (0.65% on average) the meiofauna mostly include *S. incongruens, Pontocythere turbida* and Milioloidea. Out of the fluvial influence at ca. >20 m water depth, diversified meiofaunal assemblages characterize the North Adriatic inner shelf, where ostracoda discriminate sediment-starved areas enriched in sand (19.4-97.4%). Our results show that the combined application of ostracoda and benthic foraminifera would represent a valuable tool to obtain refined depositional characterization of river-influenced shelves, and to achieve detailed palaeogeographical reconstructions of late Quaternary shallow marine successions.

Keywords: Ostracoda; Benthic foraminifera; Adriatic Sea; depositional environment; prodelta; multivariate analysis

1. INTRODUCTION

Benthic ostracoda and foraminifera represent useful ecological indicators of the depositional dynamics of continental shelves, due to their abundance and adaptability to different environmental conditions (Athersuch et al., 1989; Murray, 2006). However, multiple factors are potentially responsible for the meiofaunal community turnover in shelf settings which are complex ecosystems subject to the interaction of several sedimentary, hydrodynamic and biological processes and their variation in time and space (e.g. Jorissen, 1987; Murray, 2006; Rodriguez-Lazaro and Ruiz-Muñoz, 2012). This is further emphasized on river-influenced shelves, as changes in spatial distribution patterns of the riverine inputs are known to strongly affect meiofaunal assemblages (e.g., Van der Zwaan and Jorissen, 1991; Mojtahid et al., 2009; Goineau et al., 2015).

The interpretation of ostracod and benthic foraminiferal assemblages exclusively based on environmental affinities to extant taxa produces palaeoecological reconstructions that implicitly include several palaeoenvironmental parameters commonly estimated on a qualitative way. This is partially in contrast with the requirements of modern palaeoecology that aspires to quantify palaeoenvironmental changes through time, connecting biotic assemblages with a reduced set of significant abiotic (i.e., environmental) factors (Holland, 2005; Patzkowsky and Holland, 2012). When multiple fossil groups are applied as proxies, the necessity of finding independent connections between single faunal groups and controlling factors is even more important to obtain detailed palaeoenvironmental reconstructions (Amorosi et al., 2014; Barbieri and Vaiani, 2018). Several stratigraphic studies have taken the advantage of the combined application of ostracoda and foraminifera as palaeoenvironmental proxies (Alberti et al., 2013; Fanget et al., 2016; Amorosi et al., 2017; Rossi et al., 2017; Moissette et al., 2018), but only few of them clearly linked the stratigraphic distribution of fossils to specific controlling factors (Morigi et al., 2005; Yasuhara et al., 2012; Amorosi et al., 2014; Azzarone et al., 2018; Rossi et al., 2018). Moreover, the integration of ostracoda and benthic foraminifera was never adopted on river-influenced shelves, even though these settings represent a common situation all over the world (Walsh and Nittrouer, 2009). If the contribution of single environmental parameters on their distribution is disentangled, it will be feasible to obtain more accurate interpretations of the fossil record.

In order to understand the ecological response of both ostracoda and benthic foraminifera, modern databases should be comparable in terms of study area, measured variables and sampling techniques. In the Mediterranean basin, several databases were created to examine the relationships among the distribution patterns of ostracoda or benthic foraminifera and a set of environmental parameters in marine areas (e.g., Donnici and Serandrei Barbero, 2002; Goineau et al., 2011, 2015; Frezza and Di Bella, 2015). However, the integrated meiofauna analysis for the ecological characterisation of modern marine environments is scarcely adopted (Pascual et al., 2008; Angue Minto'o et al., 2013), and the most part of these studies focus on the effects of anthropogenic activities on specific coastal areas (Frontalini et al., 2011; Salvi et al., 2015; Balassone et al., 2016).

The Adriatic Sea databases produced by Breman (1975) for ostracoda and Jorissen (1988) for benthic foraminifera share the same abiotic variables with a significant relevance for the analysed environmental setting (i.e., water depth, percentage of organic matter, sand and calcium carbonate), furnishing the opportunity to compare meiofauna dynamics. We use in our work part of these databases focusing on the North Adriatic inner shelf (i.e., <40 m water depth), which is subject to the major influence of the Po River and several subordinate Alpine and Apennine rivers distributed along the eastern Italian coast (Frignani et al., 2005; Fig. 1).

Here, we describe the quantitative distribution, composition and species-environmental relations of modern ostracoda and benthic foraminifera on the North Adriatic river-influenced shelf, subject to the interaction among river sediment inputs, oceanographic processes, physiographic setting and their variation in time and space. Specifically, we define the main biofacies and discern the contribution of single environmental parameters on the distribution of ostracoda and benthic foraminifera groups, applying a set of multivariate statistical analyses that jointly consider faunal and abiotic variables. Moreover, we illustrate that ostracoda and benthic foraminifera are complementary (palaeo)biological indicators able to identify depositional environments under different degrees of river inputs, providing an improved characterization of continental shelves, also in a stratigraphic perspective.

2. STUDY AREA

The Adriatic Sea is a narrow (ca. 200 x 800 km) epicontinental basin elongated in a northwest-southeast direction in the Mediterranean Sea (Fig. 1). It represents the foreland basin of the Apennine and Dinaric thrust belts, resulted from the subduction of the Adriatic plate and the accretion of the Apennine chains in the Meso-Cenozoic (Doglioni, 1993). The western side of the

Adriatic Sea is a Plio-Quaternary foredeep divided in two sectors by a structural high in proximity of Ancona (Ori et al., 1986; Ricci Lucchi, 1986).

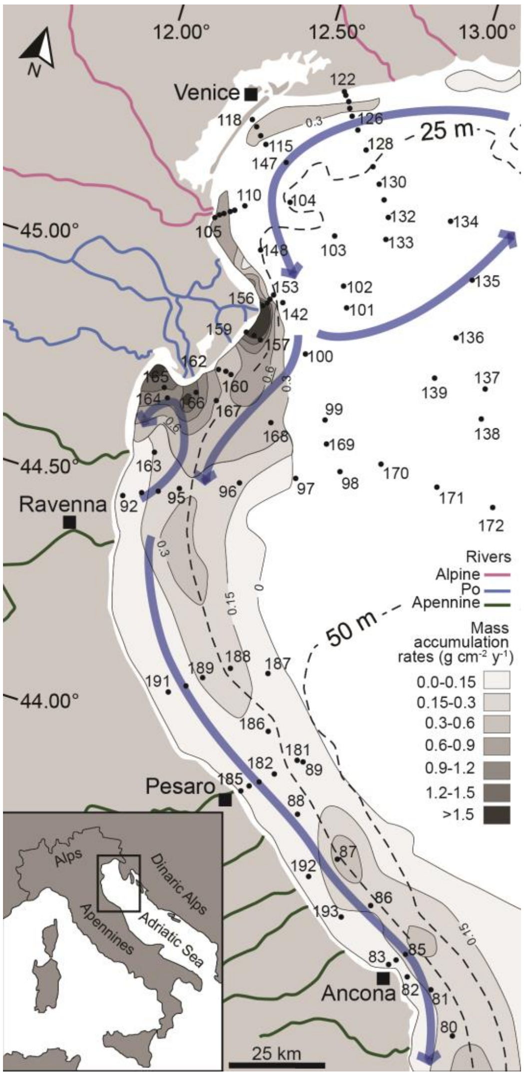

Figure 1 Map of the northern Adriatic Sea and distribution of samples analysed within this work for ostracoda (Breman, 1975) and benthic foraminifera (Jorissen, 1988). Rivers are coloured according to their geographical grouping (after Cattaneo et al., 2003). Mass accumulation rates are derived from Frignani et al. (2005). Blue arrows indicate the simplified pattern of sediment flux, influenced by surface circulation pattern of the Adriatic Sea (after Harris et al., 2008.

The Adriatic Sea can be divided into three morphological domains: i) the northern Adriatic, characterized by a 300 km-long platform dipping towards SE of about 0.02°, bordered by the shelf break at ca. 120 m water depth; ii) the central Adriatic, that reaches a depth of 260 m in the Meso-Adriatic Depression and is bordered by a narrower (ca. 50 km) and steeper (ca. 0.5°) shelf; iii) the southern Adriatic, the deepest portion with a maximum depth of 1200 m (Cattaneo et al., 2003; Storms et al., 2008).

The microtidal Adriatic Sea is strongly influenced by a cyclonic thermohaline circulation prone to seasonal variability, and driven by wind forcing and freshwater input from rivers. Three main water masses are present: i) a surficial temperature-mixed layer (0-30 m) characterized by less saline and cooler waters mainly derived by Po river runoff (Western Adriatic Coastal Current, WACC); ii) a Levantine Intermediate Water layer (30-130 m) and iii) a deep (>130 m), very dense water (Cattaneo et al., 2003).

Sediment inputs are mostly provided by the rivers located along the northern and western sides of the Adriatic Sea (Fig. 1). The main sources are the Eastern Alpine rivers (providing 3.2 Tg·yr^{-1} of sediments, mainly by the Adige River), the Po River (12.22 Tg·yr^{-1}, representing the major source of sediments of the whole Adriatic Sea) and Apennine rivers down to Ancona (16.9 Tg·yr^{-1}). In this sector of the basin, the river input is higher than sediment accumulation, i.e. the amount of sediment provided by rivers is higher than the amount of sediment deposited on the seafloor (Frignani et al., 2005). The surficial counter-clockwise WACC transports and deposits the excess of sediment in the central and southern Adriatic, where the sediment accumulation on the sea bottom overcomes the low fluvial supply (Frignani et al., 2005). The interaction between sea currents and riverine inputs also determines the distribution of sediments on belts parallel to the Adriatic coastline according to the grain size, with sands along the coast followed basinward by mud and offshore relict sands (Brambati et al., 1983).

Based on mass accumulation rates and sediment characteristics, three main areas can be distinguished on the North Adriatic inner shelf (Frignani et al., 2005; Fig. 1): i) North of the Adige River, where the low sediment accumulation promotes the formation of scattered mud patches exclusively in front of the river outlets; ii) from the Po outlets to Ravenna, where the maximum values of mass accumulation rates are recorded; iii) from Ravenna to Ancona, where values of sedimentation rates are moderate. South of the Po Delta, high amounts of sediments are accumulated at 20-40 m water depth along the “Adriatic mud-belt” (Van der Zwaan and Jorissen, 1991). Here and in areas of maximum sediment deposition immediately south of the Po Delta, periodical/seasonal oxygen deficiency occur at the sediment-water interface due to the intense accumulation and degradation of organic matter (Van der Zwaan and Jorissen, 1991; Alvisi et al., 2013). The organic material included in prodelta sediments is mainly represented by refractory organic matter of terrestrial origin, with a great contribution of soil-derived OM (Tesi et al., 2007). Labile organic matter derived from phytoplankton represents a minor portion of the organic material deposited on the shelf and it is rapidly degraded (Miserocchi et al., 2007; Tesi et al., 2013).

The highest values of mass accumulation rate (3.3 g·cm^{-2}·y^{-1}) are recorded in front of the Po River outlets, where both continuous and episodic sedimentation phases occur (Frignani et al., 2005; Palinkas and Nittrouer, 2007; Fig. 1). The latter are related to major flood events with a sub-decadal return time (Cattaneo et al., 2003), leading to the deposition of thick fine-grained layers becoming progressively thinner in a southward direction (Wheatcroft et al., 2006). Two main peaks in water and sediment discharge occur yearly, one during the late autumn related to the precipitation maxima and the other in the late spring triggered by snow melting (Cattaneo et al., 2003).

In the sectors of the North Adriatic shelf not affected by riverine sedimentation, sediment-starved conditions occur and the modern seafloor is represented by remains of alluvial plain deposits developed during the last glacial period and, to a lesser extent, by patches of transgressive back barrier-coastal deposits that represent the result of the backstepping migration of a wide barrier-lagoon-estuary system in response to the Holocene transgression (Trincardi et al., 1994; Storms et al., 2008; Ronchi et al., 2018).

3. METHODOLOGICAL APPROACH

3.1 The Adriatic Sea database

The analysed data were derived from the modern ostracod and benthic foraminiferal databases of the Adriatic Sea, published by Breman (1975) and Jorissen (1988). A total of 357 grab samples and piston-core tops were collected during the oceanographic cruise in 1962 from 7.5 to 1205 m of water depth in the whole Adriatic Sea to perform analyses on ostracoda and benthic foraminifera. Treatment and preparation of samples for meiofaunal analyses followed standard procedures described in detail in Breman (1975) and Jorissen (1988). Analyses were performed on the sediment fraction between 150-450 µm for ostracoda and 150-595 µm for benthic foraminifera. The fraction >150 µm was selected by the authors in order to retain most of the adult individuals and keep the data comparable to other (palaeo-)ecological studies (Breman, 1975; Jorissen, 1987, 1988). Each sampling station was also characterised in terms of water depth (m), content of sand (%), calcium carbonate (%) and organic matter (%) by Van Straaten (1970).

Basic statistical analyses were previously performed on original works (Breman, 1975; Jorissen, 1987, 1988). Specifically, Breman (1975) run a Q-mode PCA on a reduced set (120) of ostracod samples from the whole Adriatic Sea, selected due to the limited storage space of the employed statistical program. Concerning benthic foraminifera, statistical analyses were performed on: i) the entire dataset (285 samples), analysed with a Q-mode PCA and an R-mode cluster analysis on the 50 most abundant taxa (Jorissen, 1987); ii) a subset of 124 samples from biofacial units II and IV, analysed with an R-mode cluster analysis on the 40 most abundant taxa (Jorissen, 1988). Here, we apply a suite of most recent statistical methods to ostracoda and benthic foraminifera from a North Adriatic subset of stations (n = 87) at maximum 40 m water depth, distributed from the northern coasts down to the Conero promontory near Ancona (Fig. 1), in order to characterize in detail the portion of the shelf directly influenced by river inputs.

Ostracod taxa were reported by the author at species level as standardized relative frequencies on the total assemblage and the total number of identified valves was included (Breman, 1975). We removed transported or reworked freshwater and brackish water taxa (such as *Candona* spp., *Ilyocypris* spp., *Limnocythere* spp., *Cyprideis torosa*, *Leptocythere lagunae* and *Loxoconcha elliptica*; complete list included in Supplementary Material Tab. 1) from the original data and recalculated relative frequencies. Afterwards, only seventy-one samples including at least 20 valves were retained for the construction of the ostracod matrix; this number is considered a suitable threshold value to discern small samples (valves <20) not suitable for quantitative studies in marine settings (Cronin, 1999; Bassetti et al., 2010). Finally, we grouped selected species up to genera level according to their taxonomy and ecological characteristics to reduce the dispersion of the data (list of taxa in Supplementary Material Tabs. 1, 2).

The benthic foraminiferal matrix is composed of 78 samples including more than 250 counted tests of unstained individuals (i.e. total assemblages), excluded the contribution of finely agglutinated taxa such as *Eggerella scabra* and *Reophax* spp. due to their susceptibility to fragmentation after burial (Jorissen, 1988). Relative abundances of taxa were expressed in the original dataset as compositional data in percentage form.

3.2 Multivariate statistical analyses

The most common ostracod and benthic foraminiferal taxa with a relative abundance >5% in at least one sample were included in the matrices for multivariate statistical analyses, following reference works on Mediterranean river-influenced shelves (Frezza and Di Bella, 2015; Goineau et al., 2015). We calculated the square root of the relative proportions of the data (Hellinger transformation) and then applied the Euclidean distance to compute the Hellinger distance, a measure recommended for clustering and ordination of quantitative species data, which gives less statistical weight to rare taxa (Legendre and Gallagher, 2001). We standardized to zero mean and unit variance (z-standardization) the abiotic variables in order to compare environmental parameters with different orders of magnitude (e.g. absolute values of water depth and concentration-like data of sediment composition).

Finally, we separately performed the following statistical analyses on both ostracod (71 samples and 27 taxa) and benthic foraminiferal (78 samples and 22 taxa) matrices:

1. Multivariate Regression Trees (MRT) were performed to determine biofacies focusing on the relationship between sites with similar meiofaunal content and environmental conditions (De’ath, 2002). MRT is a constrained clustering technique that defines quantitative values of environmental variables to discriminate groups with a similar faunal composition (De’ath, 2002). This operation is performed on the whole dataset (including biotic and abiotic variables) to obtain the first partition and then it is successively repeated for every defined group until each sample forms a single group. The resulting tree must be “pruned”, i.e. its dimension must be reduced until it retains the most informative partitions, expressed as the

best predictive performance of the tree. Usually, it is the smallest solution within one standard error of the lowest value of cross-validated relative error (CVRE). The final tree is formed by a series of splits (nodes) with a related value of one explanatory variable, and terminal nodes (leaves) represent groups of sites (clusters) resulting from the chosen partition. In order to assess if MRT groups significantly differ in terms of environmental variables, a Kruskal-Wallis test was applied (Supplementary Material Tab. 3). If the p-value was significant (<0.05), a post-hoc test was performed to identify significantly different groups by means of a pairwise Wilcoxon test for multiple sample, with a Bonferroni correction to reduce the probability of making Type-I errors (Supplementary Material Tabs. 4, 5).

2. A Similarity Percentage analysis (SIMPER) based on the Euclidean distance was applied to groups derived from MRT to quantify biotic and abiotic variables responsible for the grouping of samples, and to assess which species mostly contribute to the similarity between samples of the same group (Tables 1-4; Clarke, 1993).

3. A Metric Multidimensional Scaling (MDS; Gower, 1966) was performed on each matrix to further test the relationships between assemblages and environmental parameters and to determine the main factor(s) driving meiofauna turnover across the study area. MDS was computed exclusively using faunistic data, in order to assess if MRT clusters could still be discriminated from the faunal composition of samples. This ordination technique allows to obtain a Euclidean representation of points projected onto a space of reduced dimensionality, preserving their distance relationships. Since both MRT and MDS use the same metric distance, this type of ordination is recommended to order groups of points defined by the MRT in a low-dimensional space (De'ath, 2002). The connection between samples and environmental variables was visualized fitting the latter as vectors and contour plots on the MDS graphs.

4. Ostracod and benthic foraminiferal databases were correlated by means of a Spearman's correlation matrix, in order to assess the relationship among ostracod, benthic foraminiferal taxa and environmental variables (p-values and R-values provided in Supplementary Material Tab. 6). Only the stations shared by both databases were included (69 samples).

All the analyses were carried out with the R software (R Core Team, 2018), except for the calculation of SIMPER, performed using the software PAST (PAlaeontological STatistic – version 3.10 by Hammer et al., 2001). The following R packages were used: base (base statistics, Kruskal-Wallis and Wilcoxon tests, MDS), mvpart and MVPARTwrap (MRT), vegan (fitting environmental vectors and contours on MDS), ade4 (for the function is.euclid), ggplot2 and ggthemes (MDS plots), Hmisc and corrplot (computation and graphical representation of correlation matrices).

Moreover, we produced spatial distribution maps of the environmental variables included in the Adriatic Sea database using the software Surfer (Golden Software, version 11.0) and the kriging interpolation as gridding method, since it provides the best resolution for irregularly spaced data. Some stations not included in the analysed sub-set of samples were added to obtain a complete map of the area. The blank boundary in correspondence to the Adriatic coasts was defined digitizing the coastline and adding it as a breakline for the grids.

4. RESULTS: NORTH ADRIATIC MEIOFAUNAL BIOFACIES

The combination of MRT, SIMPER and Kruskal-Wallis test reveals a distinctive set of meiofaunal biofacies (*sensu* Jackson, 1997) distributed across the inner portion (<40 m water depth) of the North Adriatic shelf. In total, we identify seven ostracod biofacies and five benthic foraminiferal biofacies.

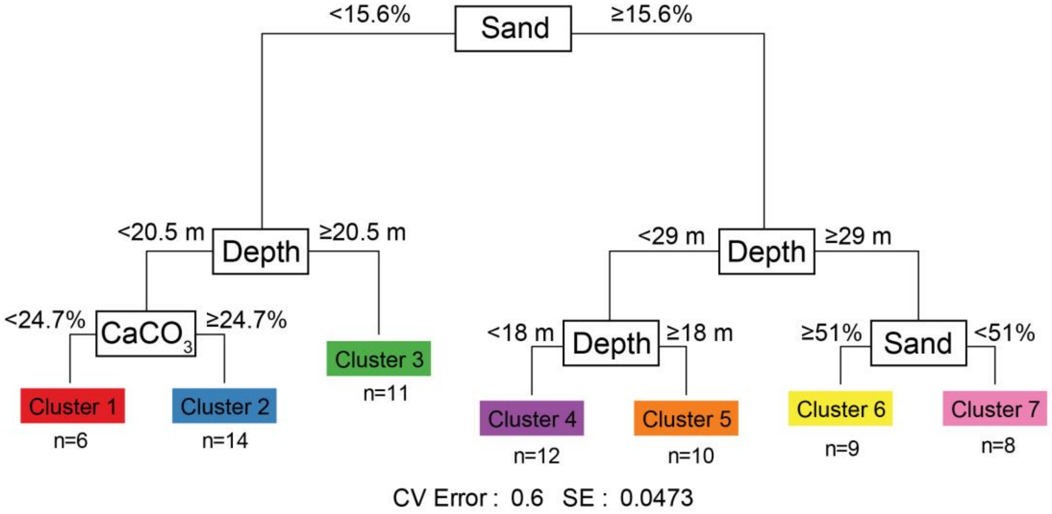

Figure 2 Multivariate Regression Tree (MRT) obtained from the ostracod matrix and four explanatory variables (concentrations of sand, organic matter, $CaCO_3$ and water depth in m). Discriminant variables and threshold values are reported at each node of the tree. Cross validation error and Standard error are also indicated.

4.1 Ostracod biofacies

The MRT performed on the ostracod matrix gathered the analysed samples into 7 groups/clusters (Fig. 2), which correspond to specific environmental conditions (Figs. 3, 4a-c) characterized by a distinctive faunal assemblage (Tables 1, 2).

The first node separates samples on the basis of the sand content in the sediment, with a threshold value of 15.6%. Depth determines the second subdivisions at each side of the tree: for samples on the left side, the boundary is placed at 20.5 m, whereas it corresponds to 29 m for the samples on the right side. The lowermost nodes are related to different abiotic variables. On the left portion of the tree, samples with <15.6% of sand and at depth <20.5 m are further separated by the $CaCO_3$ limit placed at 24.7%, that defines the first two leaves of the tree (cluster 1 and cluster 2). On the right part of the diagram, samples with ≥15.6% of sand content placed at <29 m water depth are divided between samples at <18 m water depth (cluster 4) and samples comprised between 18 and 29 m water depth (cluster 5). On the other hand, samples located at ≥29 m water depth are split into cluster 6 and cluster 7, based on the concentration of sand (≥51% and <51%, respectively).

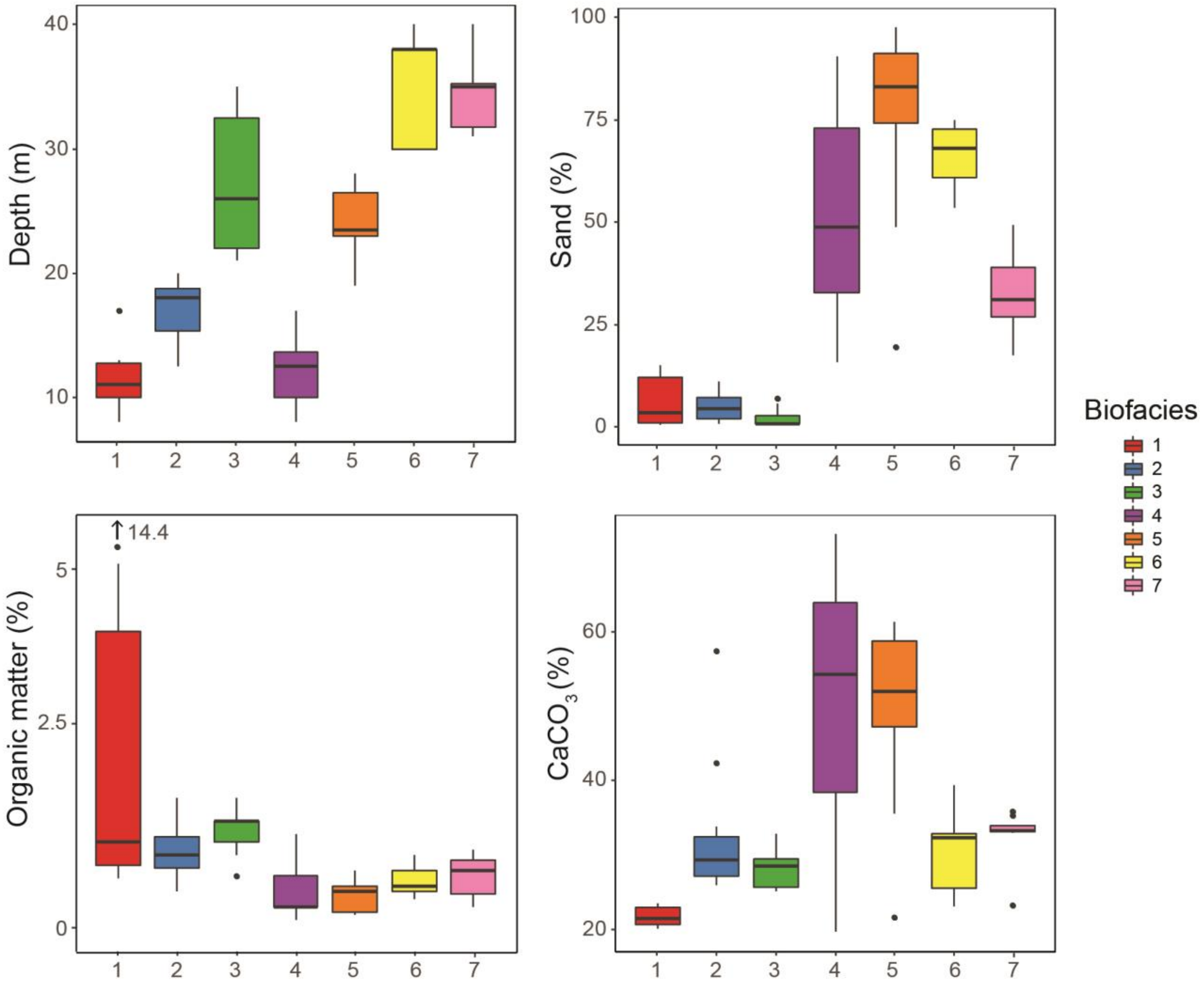

Figure 3 Box plot summarizing the values of the four environmental variables for each ostracod biofacies. The thick line within the box represents the median, and limits of the box represent the upper and lower quartiles.

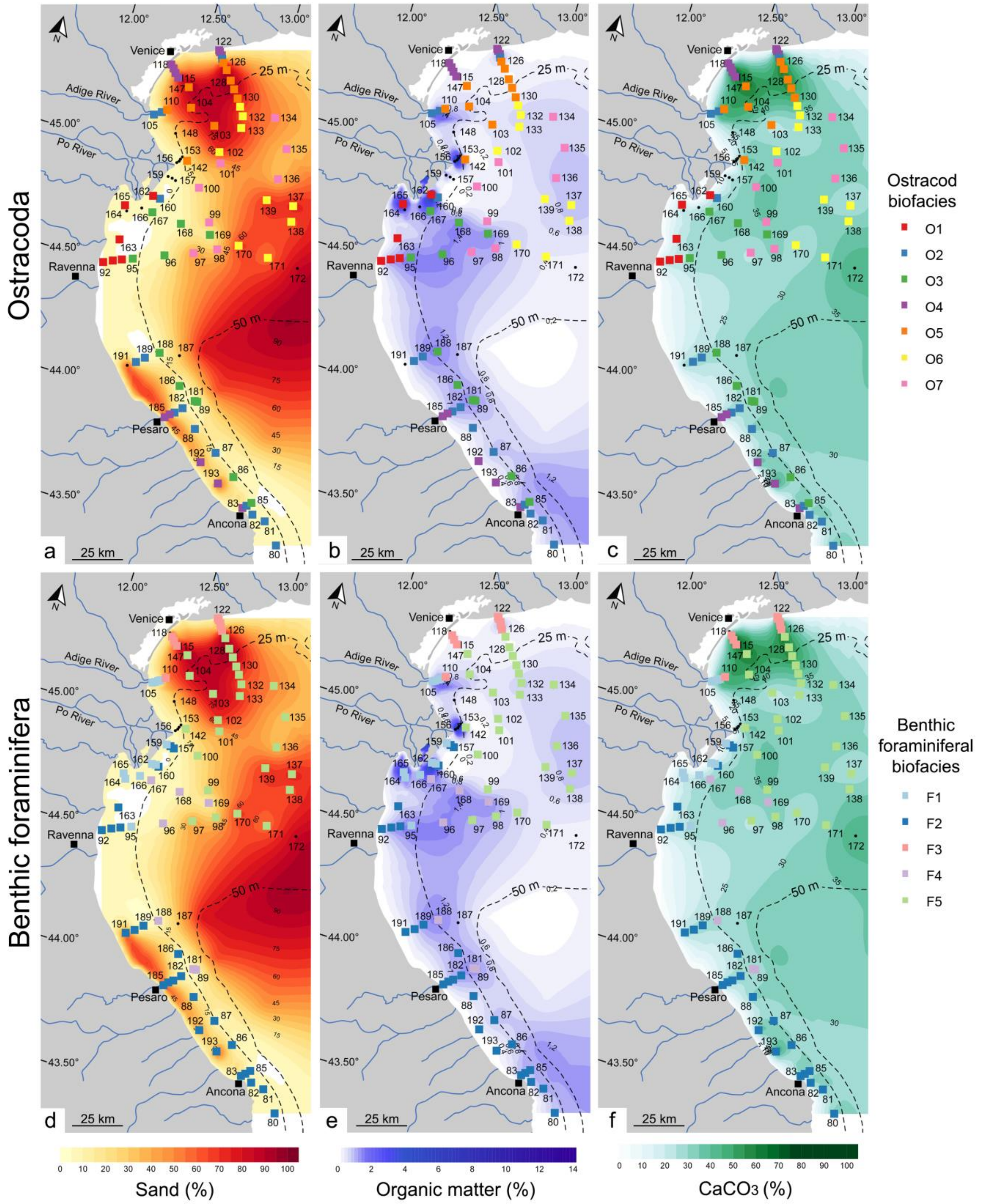

Figure 4 Distribution of samples for ostracoda (a-c) and benthic foraminifera (d-f) coloured according to biofacies defined by the MRT, superimposed to the distribution of sand (a, d), organic matter (b, e) and calcium carbonate (c, f) concentrations.

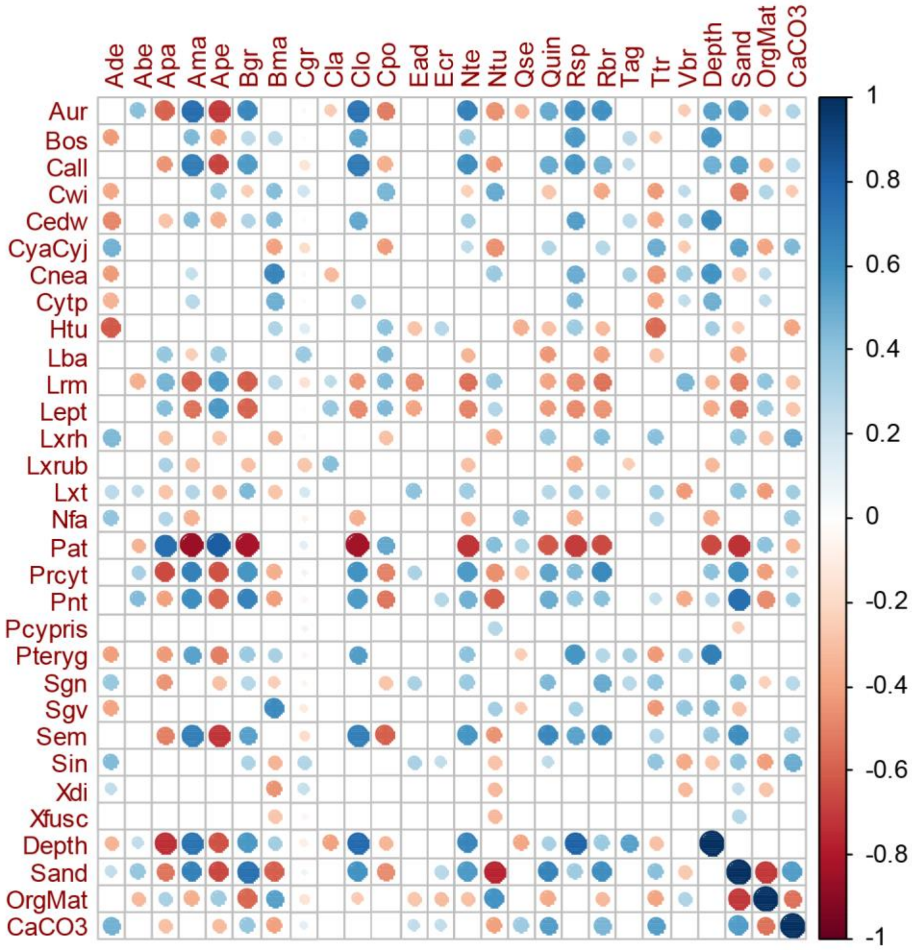

Figure 5 Correlation matrix between abundances of ostracod and benthic foraminifera and environmental variables. R-values (positive in blue and negative in red) are exclusively reported for significant correlations (p-values<0.05, Supplementary Material Tab. 6).

Biofacies O1 (cluster 1)

Biofacies O1 comprises stations located south of the Po Delta down to Ravenna (Fig. 4a-c). These samples are placed at shallow water depths (8–17 m), show a low concentration of sand (0.5–15.2%) and calcium carbonate (20.1–23.5%), and the highest values of organic matter concentration (3.9%; Figs. 3, 4a-c). The most abundant species of this biofacies are *Palmoconcha turbida*, *Leptocythere ramosa* and other *Leptocythere* species that includes *L. laevis*, *L. tenera*, *L. rara* and *Leptocythere* sp. A (average abundances of 28.8%, 8.6% and 23.7%, respectively). All these taxa show a significant (p-value<0.05, Supplementary Material Tab. 6) negative correlation with sand and depth and have the highest positive correlation with organic matter of the entire dataset (Fig. 5).

Biofacies O2 (cluster 2)

This biofacies groups samples mainly positioned in front of the Adige River mouth and along the Adriatic coast south of Ravenna between ca. 13 and 20 m water depth (Figs. 3, 4a-c). Two scattered samples are also present near the Po Delta and along the northern Adriatic coast (Fig. 4). Stations of biofacies O2 have a low sand content (0.7–11.2%) and moderate $CaCO_3$ values (25.9–57.4%; Fig. 3). This biofacies includes relatively high frequencies of *Semicytherura incongruens* and *Palmoconcha turbida* (average values of 26.6% and 23%, respectively). *Loxoconcha tumida* and *Loxoconcha* ex gr. *rhomboidea* reach their maximum average abundance, even though with relatively low frequencies (6.2% and 2.2%, respectively), within this biofacies. These taxa, as well as *S. incongruens*, show a positive correlation with sand and $CaCO_3$ percentages and are negatively correlated to organic matter (Fig. 5).

Biofacies O3 (cluster 3)

Biofacies O3 includes samples distributed along the Adriatic coast south of the Po Delta between 21 and 35 m of water depth (Figs. 3, 4a-c). A very low sand content (0.5-7%) and relatively high organic matter concentration (0.7-1.8%, average value of 1.35%) characterise this biofacies (Fig. 3). *Cytheridea neapolitana* is the most abundant species, with an average abundance of 24.7%. It shows a positive correlation with depth and organic matter, and a negative correlation with sand (Fig. 5). Relatively high frequencies of *Palmoconcha turbida* and *S. incongruens* (average abundances of 13.8% and 12.5%, respectively) are recorded, together with *Carinocythereis whitei*, *L. ramosa* and *Sagmatocythere versicolor* (average values of 8.9%, 7.5% and 4.2%, respectively). These species are negatively correlated to sand, and *C. whitei* and *L. ramosa* show a significant positive correlation to organic matter (Fig. 5).

Biofacies O4 (cluster 4)

This biofacies includes samples characterised by sandy sediments (15.9-90.4% of sand content) and distributed along the Adriatic coasts at shallow depths (8-17 m water depth), specifically in the northern sector and from Pesaro to Ancona (Figs. 3, 4a-c). The most common species is *S. incongruens* (average value of 36.7%), followed by *Pontocythere turbida* (17.9%). Both are positively correlated to sand and negatively correlated to organic matter (Fig. 5). Even though with relatively low values, *Xestoleberis dispar* and *Xestoleberis fuscomaculata* show their highest average concentrations within this biofacies (1.75% and 1.63%, respectively).

Biofacies O5 (cluster 5)

Biofacies O5 includes samples restricted to the shelf north of the Po Delta, with high sand content (19.4-97.4%) at 18-29 m water depth (Figs. 3, 4a-c). *Semicytherura incongruens* and *Pontocythere turbida* are the most abundant species (average values of 31.8% and 19.5%, respectively). The ostracod fauna also includes taxa positively correlated to sand (Fig. 5), such as *Aurila* spp. (mainly *A. speyeri* and *A. convexa*), *Cytheretta* spp. (*C. adriatica* and *C. judaea*), *Loxoconcha tumida, Paracytheridea* spp., *Sagmatocythere napoliana* and *Semicytherura* spp.

Biofacies O6 (cluster 6)

Samples of biofacies O6 are located at 30-40 m water depth on the North Adriatic shelf (Fig. 4a-c), in correspondence of bottoms enriched in sand (53.5-74.8% of sand). *Pontocythere turbida* is the species recorded with the highest frequencies (average value of 34.6%), followed by *S. incongruens* (18.7%). Both species show a positive correlation to sand and a negative correlation to organic matter (Fig. 5). Subordinate taxa are *Aurila* spp. and *Semicytherura* spp.

Biofacies O7 (cluster 7)

This biofacies is located in front of the Po Delta, at water depths between 30 and 40 m (Figs. 4a-c) on moderately sandy substrates (17.6-49.2%; Fig. 3). Biofacies O7 shows relatively high frequencies of a variety of taxa. *Cytheridea neapolitana* is the most abundant species (average frequency: 22.7%), associated to lower percentages of other taxa with a significant positive correlation to water depth (Fig. 5), such as *Callistocythere* spp. (mostly *C. adriatica* and *C. intricadoides*), *C. whitei, H. turbida*, *Pterygocythereis* spp. (mostly *P. jonesii*) and *Semicytherura* spp. (mostly *S. ruggierii* associated to other species with low frequencies). *Bosquetina carinella*, *Costa edwarsii* and *Cytheropteron* spp. (mostly represented by *C. rotundatum*) reach their highest frequencies within biofacies O7, while they are almost absent in the other biofacies.

Taxon	Av. dissim.	Contrib. %	Cumulative %	Assemblage O1	Assemblage O2	Assemblage O3	Assemblage O4	Assemblage O5	Assemblage O6	Assemblage O7
Semicytherura incongruens	562.3	26.1	26.1	2.8	26.6	12.5	36.7	31.8	18.7	10.3
Pontocythere turbida	403.7	18.7	44.8	1.3	6.8	0.5	17.9	19.5	34.6	12.4
Palmoconcha turbida	354.6	16.4	61.2	28.8	23.0	13.8	11.0	0.8	0.0	1.0
Cytheridea neapolitana	287.3	13.3	74.5	0.3	2.1	24.7	0.5	0.8	5.3	22.3
Leptocythere spp.	159.8	7.4	81.9	23.8	4.8	4.9	2.2	0.3	0.4	0.6
Loxoconcha tumida	56.7	2.6	84.6	0.0	6.2	2.7	4.6	11.7	4.7	4.9
Leptocythere ramosa	46.6	2.2	86.7	8.6	2.3	7.5	3.2	0.0	0.1	0.4
Carinocythereis whitei	45.8	2.1	88.8	8.0	6.1	8.9	3.6	0.7	4.1	9.4
Hiltermannicythere turbida	38.0	1.8	90.6	6.0	5.3	8.7	3.4	2.2	7.9	9.5
Cytheretta spp.	37.6	1.7	92.3	1.5	3.2	0.2	4.0	7.7	1.4	0.7
Aurila spp.	28.5	1.3	93.7	0.0	0.4	0.1	0.1	6.1	3.9	2.3
Semicytherura spp.	28.1	1.3	95.0	4.1	0.7	0.7	2.2	6.1	5.9	5.1
Xestoleberis dispar	18.1	0.8	95.8	4.3	1.3	0.0	1.8	0.6	0.7	0.4
Loxoconcha ex gr. *rhomboidea*	16.1	0.7	96.5	0.0	2.2	0.0	1.4	1.1	0.5	0.2
Callistocythere spp.	12.7	0.6	97.1	1.8	0.5	1.1	1.2	2.2	3.1	5.9
Sagmatocythere versicolor	10.8	0.5	97.6	0.5	1.1	4.2	0.0	0.5	0.9	1.3
Leptocythere bacescoi	9.3	0.4	98.1	3.1	3.5	1.6	1.2	0.5	1.1	2.7
Pterigocythereis spp.	8.8	0.4	98.5	0.0	0.1	2.4	0.0	0.2	2.2	4.1
Loxoconcha rubritincta	6.0	0.3	98.8	2.2	0.2	0.0	0.9	0.0	0.0	0.0
Xestoleberis fuscomaculata	5.3	0.2	99.0	0.0	0.6	0.3	1.6	0.5	0.4	0.5
Costa edwarsii	5.2	0.2	99.2	0.0	0.0	1.6	0.0	0.1	0.3	3.2
Cytheropteron spp.	3.9	0.2	99.4	0.2	0.1	1.7	0.0	0.1	0.5	2.4
Bosquetina spp.	3.2	0.1	99.6	0.0	0.0	0.5	0.0	0.0	0.5	2.5
Pontocypris spp.	2.7	0.1	99.7	0.2	1.4	0.5	0.1	0.2	0.1	0.3
Paracytheridea spp.	2.7	0.1	99.8	0.0	0.0	0.0	0.1	2.2	1.4	0.1
Loxoconcha napoliana	2.7	0.1	99.9	0.0	0.1	0.0	0.1	2.2	0.0	0.3
Neocytherideis fasciata	1.3	0.1	100.0	0.0	0.5	0.1	1.0	0.0	0.0	0.0

Table 1 Similarity percentage (SIMPER) analysis performed on faunal composition of ostracod assemblages defined by the MRT (Fig. 2).

Variable	Av. dissim.	Contrib. %	Cumulative %	Assemblage O1	Assemblage O2	Assemblage O3	Assemblage O4	Assemblage O5	Assemblage O6	Assemblage O7
Sand (%)	2356.0	79.7	79.7	6.3	4.9	2.2	51.9	75.8	66.4	32.7
$CaCO_3$ (%)	394.2	13.3	93.0	21.8	32.1	28.1	50.4	49.6	30.6	32.5
Depth (m)	200.4	6.8	99.8	11.7	17.0	27.5	12.3	24.2	35.0	34.4
Organic matter (%)	6653.0	0.2	100.0	3.9	1.1	1.4	0.5	0.5	0.7	0.7

Table 2 Similarity percentage (SIMPER) analysis performed on abiotic parameters related to ostracod assemblages defined by the MRT (Fig. 2).

4.2 Benthic foraminiferal biofacies

The MRT performed on the benthic foraminiferal matrix grouped the analysed samples into 5 clusters (Fig. 6), which correspond to peculiar environmental conditions (Figs. 4d-f, 7) where distinctive associations of taxa occur (Tables 3, 4). With respect to the biofacial units previously identified in the Adriatic Sea by Jorissen (1987), clusters 1-3 are gathered within biofacial unit II, while cluster 4 roughly coincides with biofacial unit IV and cluster 5 corresponds to biofacial unit III.

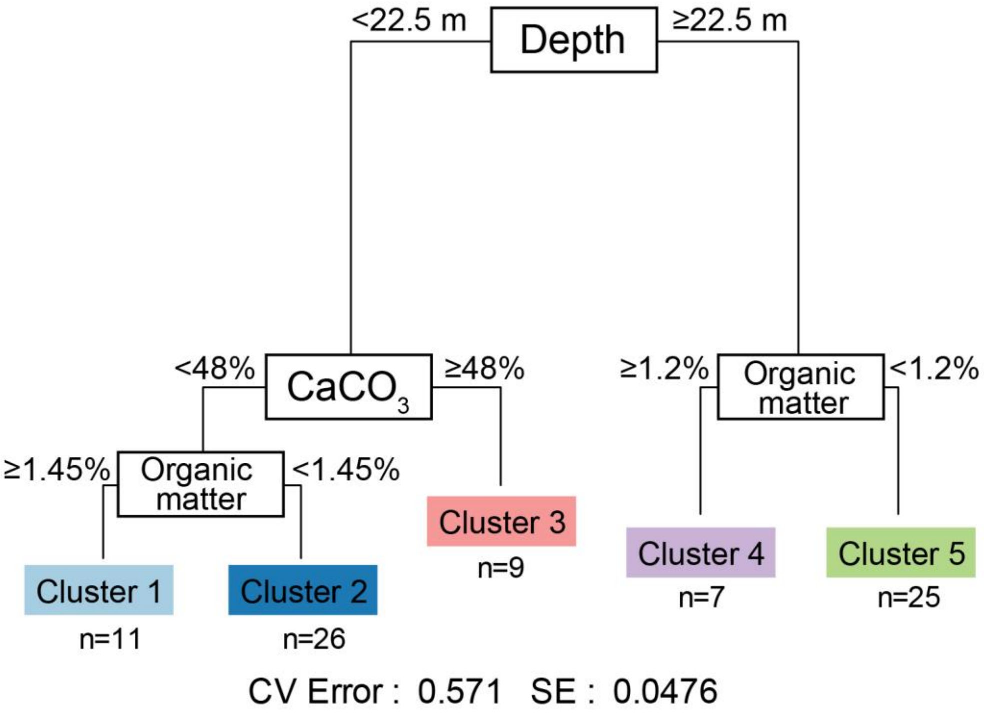

Figure 6 Multivariate Regression Tree (MRT) obtained from the benthic foraminiferal matrix and four explanatory variables (concentrations of sand, organic matter, $CaCO_3$ and water depth in m). Discriminant variables and threshold values are reported at each node of the tree. Cross validation error and Standard error are also indicated.

In the MRT tree (Fig. 6), the discriminant environmental parameter for the first node is water depth, with the limit placed at 22.5 m. The shallower samples on the left portion of the tree are subdivided by the $CaCO_3$ content: samples with <48% of $CaCO_3$ are further split on the basis of the percentage of organic matter (cluster 1 with ≥1.45%, cluster 2 with <1.45%), whereas samples including ≥48% of $CaCO_3$ are gathered into cluster 3. On the right portion of the tree (samples at water depths ≥22.5 m), the last two leaves are discriminated by the organic matter concentration (≥1.2% in cluster 4 and <1.2% in cluster 5).

Biofacies F1 (cluster 1)

This biofacies is characterised by a shallow water depth (9-22 m), low sand (0.7-14.4%) and $CaCO_3$ content (20.1-42.3%) and high organic matter concentration (1.6-14.4%; Fig. 7). Samples of biofacies F1 are situated in proximity of the Adige and Po outlets and south of the Po Delta near

Ravenna (Fig. 4d-f). The dominant taxa is *Ammonia parkinsoniana-Ammonia tepida* with subordinate *Nonionella turgida* (average frequencies of 57.2% and 8.3%, respectively). These taxa show a significant positive correlation to organic matter and a negative correlation to sand and $CaCO_3$ (Fig. 5).

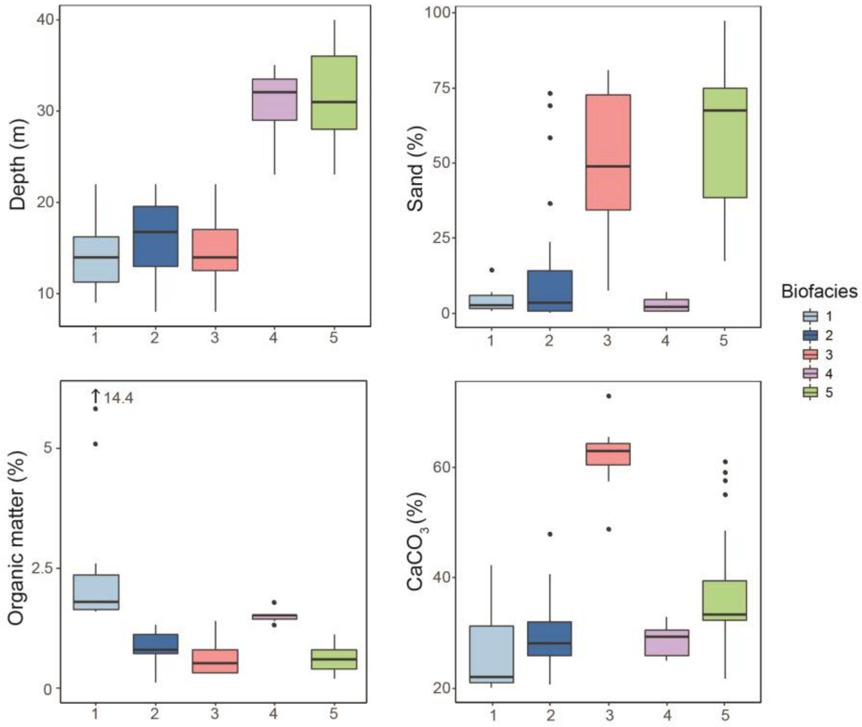

Figure 7 Box plot summarizing the values of the four environmental variables for each benthic foraminiferal biofacies. The thick line within the box represents the median, and limits of the box represent the upper and lower quartiles.

Biofacies F2 (cluster 2)

Biofacies F2 is distributed from the Po Delta to Ancona along the Adriatic coast between 8 and 22 m water depth (Figs. 4d-f, 7). Samples of this clusters have a moderate organic matter concentration (0.1-1.3%), relatively low $CaCO_3$ (20.7-48%) and variable sand content (0.2-73.3%). *Ammonia parkinsoniana-A. tepida* is the most common taxa (average frequency of 36.8%). This biofacies is characterised by the maximum average frequency of *Aubignyna perlucida* (9.19%), which shows a negative correlation to depth and sand (Fig. 5). Additional secondary taxa are *Porosononion* ex gr. *granosum* and *Cribroelphidium* ex gr. *poeyanum* (on average 9.7% and 9.3%, respectively). The former does not show any significant correlation with environmental parameters, whereas the latter is negatively correlated to organic matter and water depth.

Biofacies F3 (cluster 3)

This biofacies is located north of the Po Delta at shallow water depth (8-22 m, Fig. 4d-f). Biofacies F3 shows the highest values of $CaCO_3$ of the entire database (48.9-73%), along with high sand (7.6-80.8%) and moderate organic matter concentrations (0.3-1.4%; Fig. 7). The highest frequency of Milioloidea (including *Adelosina* spp., *Quinqueloculina seminula*, *Quinqueloculina* spp. and *Triloculina trigonula*) is recorded within this biofacies (average value of 23.8%). All the mentioned taxa show a significant positive correlation with $CaCO_3$ (Fig. 5). Moderate concentrations of *A. tepida* and *A. parkinsoniana* (14.7% on average), *Porosononion* ex gr. *granosum* (11%) and *Cribroelphidium* ex gr. *poeyanum* (9.5%) are also recorded.

Biofacies F4 (cluster 4)

Biofacies F4 gathers stations distributed south of the Po Delta down to Pesaro at 23-35 m water depth (Fig. 4d-f) and is characterized by high organic matter (1.3-1.8%) and low sand concentrations (0.5-7%; Fig. 7). *Bulimina marginata*, with an average frequency of 21.1%, is the most abundant species of this biofacies, positively correlated to organic matter and depth, negatively correlated to sand and $CaCO_3$ (Fig. 5). Accompanying taxa are *Textularia agglutinans* (average frequency of 12.7%), *A. parkinsoniana- A. tepida* (12.6%), *Cribroelphidium* ex gr. *poeyanum* (7.8%), *Porosononion* ex gr. *granosum* (6.4%) and *N. turgida* (5.9%). Even though with low frequencies, *Valvulineria bradyana* shows its maximum concentration within this biofacies (average value of 2.1%).

Biofacies F5 (cluster 5)

This biofacies occurs between 23-40 m water depth, relatively far from the North Adriatic coast (>23 m water depth; Figs. 4d-f, 7). Stations of biofacies F5 show high percentages of sand (21.7-61%), moderate $CaCO_3$ (21.7-61%) and low organic matter content (0.2-1.1%; Fig. 7). The benthic foraminiferal fauna is highly diversified, mainly composed of taxa positively correlated to depth and sand and negatively correlated to organic matter (Fig. 5), such as *Buccella granulata* (average frequency of 11%), *Ammonia beccarii* (8.4%), *Asterigerinata mamilla* (7.2%), *Lobatula lobatula* (5.8%)*, Neoconorbina terquemi* (3.4%) and *R. bradyi* (1.9%). Moderate concentrations of *T. agglutinans*, *Porosononion* ex gr. *granosum* and *A. parkinsoniana-A. tepida* are also recorded within this biofacies.

Taxon	Av. dissim.	Contrib. %	Cumulative %	Assemblage F1	Assemblage F2	Assemblage F3	Assemblage F4	Assemblage F5
Ammonia parkinsoniana - A. tepida	1220.0	61.2	61.2	57.2	36.8	14.7	12.6	7.4
Bulimina marginata	114.4	5738.0	67.0	2.3	1.3	0.1	21.1	1.6
Nonionella turgida	103.3	5183.0	72.1	8.3	4.6	0.4	5.9	0.6
Textularia agglutinans	88.5	4441.0	76.6	5.4	6.1	6.4	12.7	9.0
Buccella granulata	70.5	3535.0	80.1	0.1	1.6	4.8	1.9	11.0
Aubignyna perlucida	58.5	2933.0	83.1	2.4	9.2	3.9	5.0	0.2
Cribroelphidium granosum gr.	54.0	2709.0	85.8	0.9	9.7	11.0	6.4	9.0
Cribroelphidium poeyanum gr.	43.9	2202.0	88.0	2.8	9.2	9.5	7.8	4.4
Asterigerinata mamilla	36.1	1.8	89.8	0.0	0.0	0.6	0.6	7.2
Ammonia beccarii	33.4	1.7	91.4	3.4	4.7	4.4	3.0	8.4
Reussella spinulosa	30.4	1.5	93.0	0.1	0.3	0.8	2.2	5.9
Quinqueloculina seminula	23.8	1.2	94.2	3.5	2.3	7.7	4.1	1.3
Cibicides lobatulus	22.8	1.1	95.3	0.2	0.1	0.1	1.1	5.8
Quinqueloculina spp.	16.7	0.8	96.1	0.1	0.2	3.2	1.0	3.4
Adelosina spp.	16.0	0.8	97.0	1.8	1.3	6.9	0.5	1.4
Neoconorbina terquemi	13.9	0.7	97.7	0.0	0.0	0.5	0.5	3.4
Triloculina trigonula	13.1	0.7	98.3	2.2	1.6	5.9	0.5	1.8
Elphidium advenum	13.0	0.7	99.0	2.5	2.7	2.7	2.0	3.1
Elphidium crispum gr.	11.7	0.6	99.5	0.3	3.7	3.3	3.2	3.8
Rosalina bradyi	5267.0	0.3	99.8	0.1	0.0	1.7	0.7	1.9
Valvulineria bradyana	2427.0	0.1	99.9	0.0	0.0	0.0	2.1	0.0
Cassidulina laevigata gr.	1445.0	0.1	100.0	1.0	0.1	0.0	0.0	0.0

Table 3 Similarity percentage (SIMPER) analysis performed on faunal composition of benthic foraminiferal assemblages defined by the MRT (Fig. 2).

Variable	Av. dissim.	Contrib. %	Cumulative %	Assemblage F1	Assemblage F2	Assemblage F3	Assemblage F4	Assemblage F5
Sand (%)	2317.0	78.5	78.5	4.2	13.5	49.7	2.9	59.7
$CaCO_3$ (%)	416.0	14.1	92.6	26.5	29.5	62.0	28.6	36.8
Depth (m)	210.3	7.1	99.8	14.3	16.0	14.5	30.7	31.6
Organic matter (%)	6.7	0.2	100.0	3.3	0.8	0.6	1.5	0.6

Table 4 Similarity percentage (SIMPER) analysis performed on abiotic parameters related to benthic foraminiferal assemblages defined by the MRT (Fig. 2).

4.3 MDS analysis of the North Adriatic meiofauna

The application of the MDS to the ostracod and benthic foraminiferal data (Fig. 8) refines the results obtained by the MRT, furnishing new insights on the species-environmental variables relationship (Figs. 2, 5, 6). Indeed, except for scattered samples, the distribution in the MDS graphs is consistent with the biofacies occurrence across the North Adriatic inner shelf (Figs. 4 and 8).

About ostracoda, the strong environmental gradient underlying the major axis of variation (axis 1 - MDS1 in Fig. 8) corresponds to the substrate grain-size (specifically, the sand concentration). Fitted vectors and contour plots clearly display that the arrangement of the samples from positive to negative eigenvalues of axis 1 (explaining 33.5% of variance) can be connected to an increase of sand content in the substrate. Biofacies characterized by a low sand content (O1-O3; Figs. 3, 4a-c) plot on the right side of the graph (<20% of sand), whereas samples with intermediate (20-60%; biofacies O4-O7) and high (>60%; biofacies O5-O6) percentages of sand are plotted towards the left side. As indicated by the direction of environmental vectors, axis 2 (MDS2, explaining 20.7% of variance) has a strong positive correlation with bathymetry. Samples belonging to biofacies O1, O2 and O4 plot in correspondence of low MDS2 values underlying water depths <20 m; in contrast, biofacies O3, O5-O7 samples attain higher MDS2 values and water depths ranging between ca. 20-40 m.

Concerning benthic foraminifera, a high percentage of the total variance (42.5%) is explained by MDS axis 1, which is negatively correlated to the organic matter concentration in the substrate (Fig. 8). This is indicated by the low angle between this axis and the vector underlying the organic matter parameter, even if the strength of the gradient (i.e., the length of the arrow) is relatively low. According to this interpretation, the position of biofacies (F1-F5) follows a negative organic matter gradient from negative to positive scores of MDS1 (Fig. 8). Biofacies F1, F2 and F4, with organic matter concentration (>0.8%), plot on the left side of the graph, while biofacies F3 and F5 occur on the right in correspondence of lower organic matter concentrations (Figs. 7 and 8). Conversely, a clear correlation between MDS axis 2 (explaining the 13.2% of the total variance) and any available environmental parameters is difficult to assess. None of the plotted environmental vectors can be easily related (i.e., is more or less parallel to) to axis 2, therefore this axis could be directly correlated to a different environmental variable (or a combination of two or more variables) not included into the analysed database. Nevertheless, taking into account the direction of the vector corresponding to the water depth, which was recognized by the MRT as the first parameter influencing benthic foraminifers biofacies (Fig. 6), a distribution of biofacies along a bathymetric gradient from the upper-left (lower depths) to the lower-right (higher depths) corner of the graph (Fig. 8) is recognized.

5. DISCUSSION

5.1 Drivers of changes in meiofauna composition across a river-influenced shelf

The employment of multiple statistical analyses on the modern ostracod fauna of the North Adriatic shelf suggests that the primary factor influencing biofacies composition and distribution is the substrate grain-size (i.e., sand content), while water depth represents the second most important environmental driver (Figs. 2, 8). Bathymetry seems to play a significant but not primary role also for the distribution of benthic foraminifera, that are mainly controlled by the organic matter content (Figs. 6, 8). Bathymetry is considered a complex gradient that commonly drives faunal distribution in modern and fossil marine settings (Scarponi and Kowalewski, 2004; Tyler and Kowalewski, 2014; Benito et al., 2016; Danise and Holland, 2017; Rossi et al., 2018). Although the water-depth distribution of ostracod and benthic foraminiferal species can vary from basin to basin, bathymetry was commonly identified as the main driver for the meiofaunal turnover from the coast to the lower continental slope (ca. 5-900 m water depth; Jorissen, 1987; Mendes et al., 2004; Avnaim-Katav et al., 2015; Bernasconi et al., 2018; Angue Minto'o et al., 2013), as well as from the

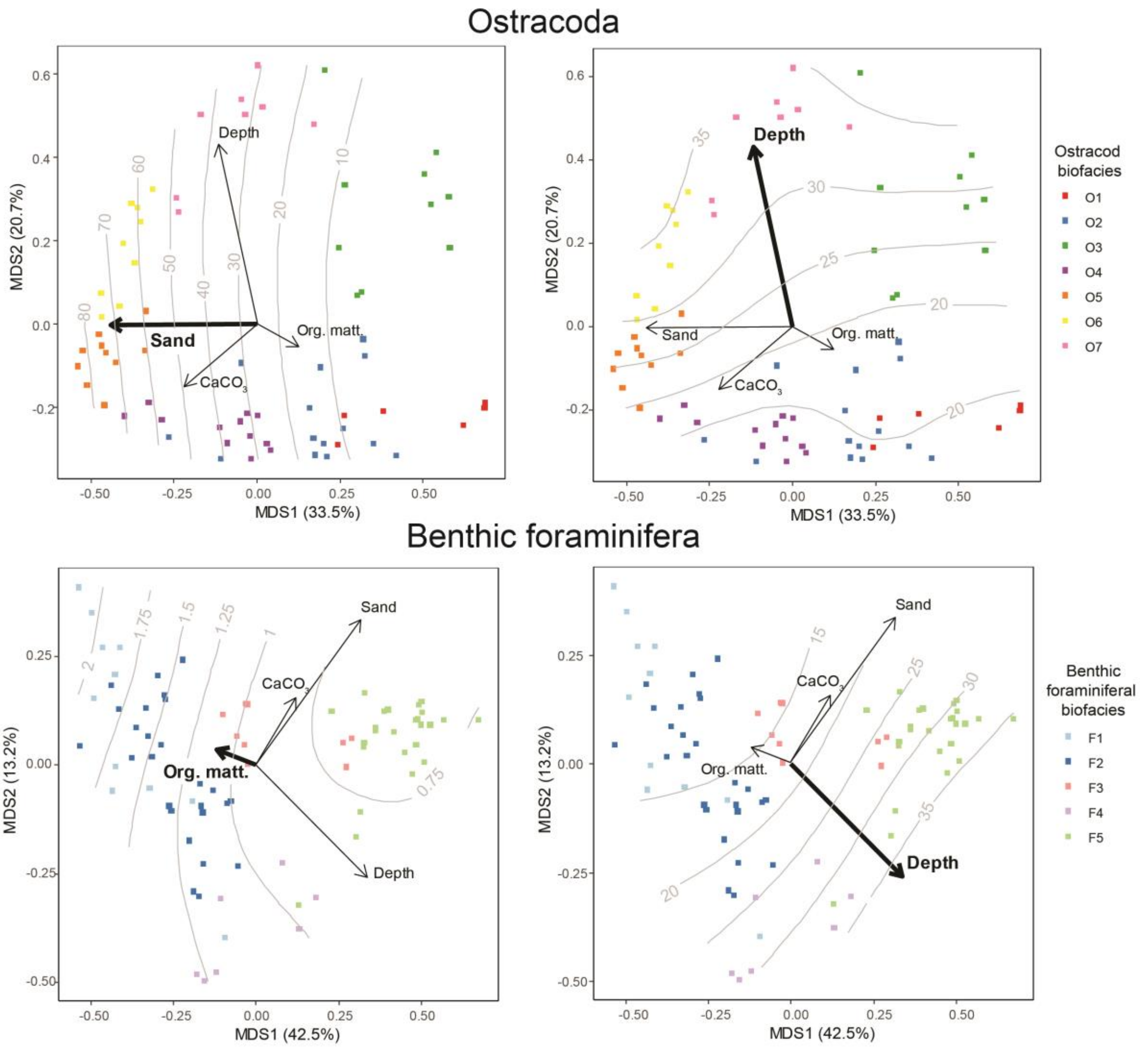

Figure 8 Metric multidimensional scaling (MDS) for ostracod and benthic foraminiferal species composition of stations based on the Euclidean distance. Colours of groups are in accordance to biofacies defined by the MRT. Contours display the distribution of the main environmental drivers on assemblages: depth and sand for ostracoda, organic matter and depth for benthic foraminifera.

inner to the middle-outer shelf depths (Hayward et al., 1999; Pascual et al., 2008; Azzarone et al., 2018; Rossi et al., 2018). Also considering a narrower water-depth range on continental shelves facing delta systems, the zonation of meiofaunal assemblages seems to be related to bathymetry (e.g., Horton et al., 2003; Rossi and Horton, 2009; Frezza and Di Bella, 2015; Benito et al., 2016), but it should be reminded that water depth is a complex factor strictly related to many biotic (e.g., life strategy) and abiotic parameters (e.g., grain-size and vegetation cover of substrate, organic matter concentration, oxygen content). In turn, the distribution of these parameters is influenced by the geomorphological features and sedimentary dynamics of the basin, including the position of river mouths with respect to longshore currents and the amounts of riverine input in terms of sediment and organic matter (Puig et al., 2007; Hanebut et al., 2015; Liu et al., 2018). Therefore, in shallow marine, fluvial-influenced environments, bathymetry can be considered an indirect influencing factor on the distribution of marine meiofauna that exclusively defines a specific location in the three dimensional space (Rossi and Horton, 2009).

In the Mediterranean basin, among the several parameters underlying water depth, a strong influence on the distribution of present-day ostracoda seems to be played by the grain-size of the substrate (Bonaduce et al., 1975; Ruiz et al., 1997; Arbulla et al., 2004; Frezza and Di Bella, 2015; Sciuto et al., 2015). However, to our knowledge, its effect was statistically validated in just one case (Pascual et al., 2008).

Sand concentration, which is the first influencing factor on ostracod assemblages of the North Adriatic Sea, defines two major groups of ostracod biofacies: the first is related to muddy substrates (biofacies O1-O3) and the second to more sandy sediments (biofacies O4-O7). Within these two major groups of biofacies, further subdivisions reflect minor changes in organic matter/$CaCO_3$ conditions along the bathymetric gradient (Figs. 2, 4, 8). Muddy substrates are formed by the deposition of fine-grained particles of river plumes rich in soil-derived organic matter (Tesi et al., 2007), mostly provided by the Po River (Cattaneo et al., 2003; Frigani et al., 2005), which are distributed on specific areas (and at well-defined bathymetric ranges) of the shelf by surficial currents (Harris et al., 2008; Fig. 1). Within these areas oxygen deficiency as well as dissolution phenomena, which determines low $CaCO_3$ values, can be developed in response to the high organic matter concentration (Van der Zwaan and Jorissen, 1991).

The organic matter is, indeed, an important controlling factor that exerts a primary influence on the distribution of benthic foraminifera in the North Adriatic Sea (Fig. 8), as previously assessed by Jorissen (1988). High concentrations of organic matter occur in areas subject to high accumulation of riverine sediments (Figs. 1, 4d-f), where a series of opportunistic taxa (*sensu* Jorissen et al., 2018) characterize the benthic foraminiferal biofacies (i.e., F1, F2, F4). Conversely, where the input of riverine material is substantially negligible and the concentration of organic matter is lower (Figs. 1, 4d-f), benthic foraminiferal assemblages are more diversified and opportunistic taxa are scarce (biofacies F3, F5). This is consistent with several studies undertaken on other river-influenced shelves of the Mediterranean Sea (e.g., Rhone Delta and Ombrone Delta; Frezza and Carboni, 2009; Mojtahid et al., 2009; Goineau et al., 2011).

The contribution of other abiotic parameters, such as sand and $CaCO_3$, is less significant (Figs. 6, 8); however, a clear distinction between shallow-water (biofacies F1-F3) and relatively deep-water (biofacies F4, F5) assemblages is recognizable in the North Adriatic Sea (Figs. 4d-f, 8). Among additional abiotic parameters, salinity is often regarded as one of the most influencing factors on benthic assemblages from marginal marine settings (e.g. Murray, 2006; Frenzel and Boomer, 2005). Even though salinity values are not provided in the analysed database, its influence on meiofaunal benthic assemblages can be excluded. In the Adriatic Sea, the lowest salinity values are recorded during major flood events, when high amounts of riverine water is delivered to the prodelta and water stratification is produced, especially if geostrophic currents are weak (Frascari et al., 2006). Under these conditions, cold, less saline waters are restricted in the upper layer of the water column, especially in proximity to the Po River mouths; nevertheless, at these locations salinity rapidly increases to values of 36 psu at ca. 8-9 m water depth (Fox et al., 2004; Frascari et al., 2006). Since the shallowest samples analysed in this work were collected at 8 m water depth, benthic foraminifera and ostracoda should not be affected by salinity variations related to intense fluvial discharge.

5.2 Integrating ostracoda and benthic foraminifera: a multi-proxy tool for river-influenced depositional environments

On marine settings, riverine influence is considered a qualitative parameter primarily dependent on the amount of river supply (in terms of organic matter and sediment) and it defines a position in the basin with respect to the main source of fluvial material (Goineau et al., 2011). The linkage between meiofaunal assemblages and riverine influence was previously recognized even in the Rhône (Mojtahid et al., 2009; Goineau et al., 2011, 2012) and Ombrone prodelta (Frezza and Carboni, 2009; Frezza and Di Bella, 2015), but not fully explored combining the two groups in a quantitative framework. Our approach demonstrates that ostracoda and benthic foraminifera of the North Adriatic shelf are primarily related to different environmental parameters (i.e., grain-size and organic matter, apart from the water depth). Therefore, only their combination allows to recognize different (palaeo)depositional environments within the water-depth range 8-40 m, as defined by a set of abiotic parameters (Fig. 9, Tab. 5) which depends on the sediment supply and relative position to the Po River mouths (i.e., riverine influence). In a stratigraphic perspective, changes in meiofauna structure and abundance of key species can track variations in riverine inputs within past sedimentary successions, highlighting the lateral shifts and/or the approaching of river mouths during highstand periods.

Prodelta in proximity of the main feeding mouths

Near the Po Delta at <20 m water depth (Fig. 9), where the substrate is enriched in mud and organic matter, the maximum values of sediment accumulation are recorded (Frignani et al., 2005) and frequent hypoxic events occur due to the deposition of abundant organic matter of riverine origin coupled with scarce water circulation (Palinkas and Nittrouer, 2007; Alvisi et al., 2013). All these environmental conditions are marked by a peculiar meiofauna (biofacies O1+F1), mainly composed of *Palmoconcha turbida*, *L. ramosa* and *A. parkinsoniana-A. tepida. Ammonia tepida* shows high concentrations in proximity to fluvial outlets under unstable environmental conditions (Mojtahid et al., 2009; Goineau et al., 2011, 2012). *Palmoconcha turbida* and *L. ramosa* prefer fine-grained substrates at shallow depths (Colalongo, 1969; Frezza and Di Bella, 2015) and the former is considered tolerant to low oxygen conditions (Bodergat et al., 1998). *Nonionella turgida* is common at the transition with the mud belt and, locally, south of the Po Delta where organic matter accumulates and periodical oxygen deficiency occur (Van der Zwaan and Jorissen, 1991; Alvisi et al., 2013). This species thrives under strong inputs of fresh organic matter derived from riverine phytoplankton (Goineau et al., 2012), but it even survives in sediments enriched by high low-quality organic matter inputs near river mouths (Mojtahid et al., 2009; Goineau et al., 2011) under hypoxic conditions (Barmawidjaja et al., 1992).

In front of the main Po River outlets, the deposition of seasonal floods determines a non-steady state accumulation of sediment (Palinkas and Nittrouer, 2007). Here, ostracod assemblages are extremely poor (<20 valves, not included in the statistical analyses) and usually include high percentages of transported brackish and freshwater taxa. In contrast, benthic foraminifera are characterized by more abundant assemblages, and mostly by the biofacies F1. This implies that unstable conditions in proximity of river outlets hamper the development of an autochthonous ostracod fauna, whereas benthic foraminifera are more abundant and dominated by the opportunistic *A. parkinsoniana-A. tepida* (Jorissen et al., 2018). However, it should be specified that at depth shallower than our minimum values (<8 m), in correspondence of the Po delta front, both ostracod and benthic foraminiferal assemblages are very scarce (Colalongo, 1969; D’Onofrio, 1969).

Prodelta downdrift of the main feeding mouths

This prodelta area, located at <20 m water depth from Ravenna to Ancona, is affected by the accumulation of sediments transported by Apennine rivers and, subordinately, by the Po River (Fig. 9). The substrate has a variable grain-size (1.1-73.3% of sand), it is characterized by relatively high organic matter content (0.9% on average) and sediment accumulation rates are moderate (Frignani et al., 2005; Fig. 1). This area shows abundant concentrations of the ostracod *S. incongruens* (biofacies O2 and O4), a species distributed on all kind of sediments in the Adriatic Sea, even though it shows a slight preference for sediments enriched in sands. The characteristic benthic foraminiferal taxa are *A. parkinsoniana-A. tepida* and *A. perlucida* (biofacies F2), that tolerate relatively high organic matter concentrations and prefer muddy substrates (Fig. 5). *Aubignyna perlucida* is known to have a limited tolerance for oxygen deficiency (Barmawidjaja et al., 1992; Donnici and Serandrei Barbero, 2002). The associated *Porosononion* ex gr. *granosum* and *Cribroelphidium* ex gr. *poeyanum* seem to be relatively indifferent to organic matter, in accordance with Jorissen (1988, 2018). Within this area, ostracoda discriminate significantly different substrate conditions. Biofacies O4 occurs in the shallowest portion (ca. 8-13 m water depth), on sandy sediments (15.9-73.3%) with low organic matter content (0.6% on average) and includes, apart from *S. incongruens*, other species as *Pontocythere turbida* and *Palmoconcha turbida*, both widespread in the Adriatic Sea between 5-40 m water depth. Even though they are

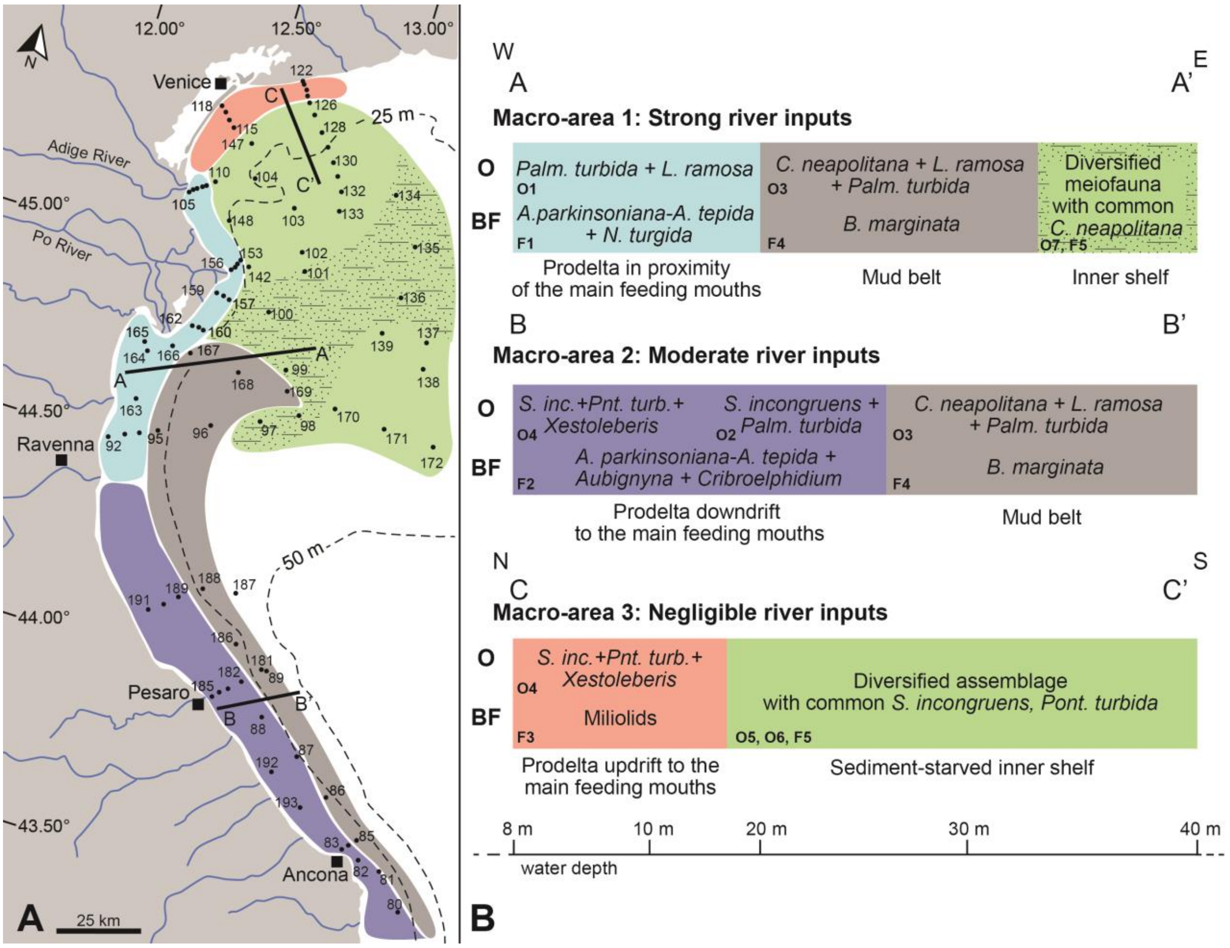

Figure 9 A) Distribution of the five depositional environments defined by the combined application of ostracoda and benthic foraminifera on the shallow (<40 m) North Adriatic Shelf. B) Variation of the meiofaunal biofacies along a bathymetric gradient for three macro-areas subject to different degrees of river inputs of the North Adriatic Sea.

Depositional settings	Environmental conditions	Meiofaunal assemblage	Key species (D: dominant; S: secondary)
prodelta in proximity of the main feeding mouths	high fluxes of OM and periodic oxygen deficiency low sand content very high accumulation rates	Ostracoda and foraminifera: mud-lover taxa tolerant to high OM and low oxygen conditions at shallow depths	Palmoconcha turbida (D); Leptocythere ramosa (D); Ammonia tepida-parkinsoniana (D); Nonionella turgida (S)
prodelta downdrift of the main feeding mouths	moderate fluxes of OM variable sand content moderate accumulation rates	Ostracoda: indifferent to grain-size. Foraminifera: tolerant to high OM; mainly on clay sediments.	Semicytherura incongruens (D); Pontocythere turbida (S); Palmoconcha turbida (S); Ammonia tepida-parkinsoniana (D); Aubignyna perlucida (S); Cribroelphidium ex gr. granosum and C. ex gr. poeyanum (S)
prodelta updrift of the main feeding mouths	low fluxes of OM moderate sand content moderate to low accumulation rates	Ostracoda: indifferent to grain-size. Foraminifera: preferring low OM.	Semicytherura incongruens (D); Pontocythere turbida (S); Miliolids (D); Cribroelphidium granosum gr. and C. poeyanum gr. (S)
mud belt	high fluxes of OM low sand content high accumulation rates	Ostracoda and foraminifera: tolerant to high OM and low oxygen conditions at high depths	Cytheridea neapolitana (D); Leptocythere ramosa (S), Palmoconcha turbida (S); Bulimina marginata (D), Nonionella turgida (S)
inner shelf	low fluxes of OM moderate to high sand content low accumulation rates	Ostracoda and foraminifera: mainly indicative of low OM and indifferent to grain-size	Diversified assemblages with benthic foraminifera sensitive to organi matter

Table 5 Depositional environments recognized on the basis of ostracod, benthic foraminiferal biofacies and environmental parameters on the shallow (<40 m) North Adriatic shelf. A summary of the most significant environmental features, main characteristics of the meiofaunal assemblage and key ostracod and benthic foraminiferal taxa are reported for each depositional setting.

abundant under different conditions (the former on sandy sediments and the latter on muddy substrates), they seem to be able to live on different substrate grain-size, as similarly observed in other Mediterranean shallow marine settings (Arbulla et al., 2004; Angue Minto'o et al., 2013; Frezza and Di Bella, 2015). The occurrence of the highest frequencies of two phytal species of the genus *Xestoleberis* (*X. dispar* and *X. fuscomaculata;* Lachenal and Boodergat, 1988; Triantaphyllou et al., 2005) indicates a vegetated prodelta setting.

Conversely, the deepest sector (ca. 13-20 m water depth) with more fine-grained bottoms (1.1-11.2% of sand) and higher organic matter concentration (0.9% on average; Fig. 4) is colonized by Palmoconcha turbida in association with S. incongruens (biofacies O2) and the above-mentioned benthic foraminifera (biofacies F2), pointing to a muddy prodelta not affected by hypoxic conditions.

Prodelta updrift of the main feeding mouths

At shallow depths (<20 m) in the northern Adriatic Sea (Fig. 9), the sediment accumulation is extremely low due to the negligible inputs provided by the Alpine rivers, with the exception of the Adige River (Cattaneo et al., 2003; Frignani et al., 2005). Moreover, the efficient distribution of the riverine inputs by strong longshore currents prevents the sediment accumulation in proximity to river mouths (Harris et al., 2008). A peculiar benthic foraminiferal assemblage dominated by Milioloidea – biofacies F3 (i.e., *Adelosina* spp., *Q. seminula*, *Quinqueloculina* spp. and *T. trigonula*) occurs in this depositional setting, characterized by high concentration of sand and $CaCO_3$ (respectively 49.7% and 62.0% on average). The ostracod fauna (biofacies O4) is consistent with a shallow marine area with vegetated bottoms.

Mud belt

South of the Po Delta at ca. 20-35 m water depth, the peculiar setting of the Adriatic mud-belt (Fig. 9) occurs and high abundances of *C. neapolitana* (biofacies O3) and *B. marginata* (biofacies F4) are recorded, along with subordinate *L. ramosa, Palmoconcha turbida* and *N. turgida*. These species thrive under eutrophic and hypoxic conditions typical of the clay belts (Donnici and Serandrei Barbero, 2002; Mendes et al., 2004; Di Bella et al., 2013; Frezza and Di Bella, 2015). *Sagmatocythere versicolor* and *V. bradyana* are additional characteristic taxa with environmental affinities similar to those of the most abundant species, such as a slight preference for muddy bottoms at relatively high depths (Bonaduce et al., 1975; Frezza et al., 2005; Frezza and Carboni, 2009; Mojtahid et al., 2009; Frezza and Di Bella, 2015).

Inner shelf

Far from the river mouths at water depths >20 m (Fig. 9), the organic matter content is low (0.6% on average) as well as the riverine influence in terms of sediment supply (Cattaneo et al., 2003;

Frignani et al., 2005). Overall, ostracoda (biofacies O5-O7) and benthic foraminifera (biofacies F5) are highly diversified in terms of number and relative abundance of taxa. Widespread ostracod taxa indifferent to bottom grain-size such as *S. incongruens* and *Pontocythere turbida* are abundant and are associated to epiphytic benthic foraminifera such as *A. mamilla, B. granulata, L. lobatula, N. terquemi, R. bradyi* (Sgarrella and Moncharmont Zei, 1993; Frezza and Carboni, 2009), sensitive to organic enrichment (Jorissen et al., 2018).

However, ostracod biofacies identify different areas in terms of sediment grain-size. Specifically, biofacies O7 shows a significantly lower sand concentration than biofacies O5-O6 (Fig. 3) which mark the sediment-starved portions of the inner shelf (Fig. 9). In front of the Po Delta, a minor portion of fine-grained riverine sediments is episodically transported by water currents (Harris e al., 2008). Here, the most common species is *C. neapolitana*, which is also abundant in the Adriatic mud-belt: this taxa does not seem to be disturbed by organic matter enrichment and oxygen depletion, rather its distribution seems to be related to the presence of fine-grained sediments at water depths >20 m. Within this depositional setting, it is associated to several depth-related taxa, such as *Bosquetina carinella*, *Callistocythere* spp., *C. whitei, Costa edwarsii, Cytheropteron* spp., *H. turbida*, *Pterygocythereis* spp. and *Semicytherura* spp. (biofacies O7), indicative of an open marine environment (Bonaduce et al., 1975; Faranda et al., 2007).

5.3 Patterns in the spatial turnover of meiofauna

The general distribution patterns of the meiofaunal biofacies reflects the presence of three macro-areas (Fig. 9) with peculiar environmental characteristics related to different degrees of river inputs from the coast to the basin, according to Frignani et al. (2005):

1. *Macro-area subject to strong river inputs: in front of the Po Delta, from the Adige outlet down to Ravenna.* Maximum values of sedimentation rates occur near the major source of river inputs (Fig. 1), where the meiofauna is characterized by mud-lover taxa tolerant to high organic matter and lowered oxygen content, such as *L. ramosa*, *Palmoconcha turbida, A. parkinsoniana-A. tepida* and *N. turgida.* At water depths >15 m, fine-grained substrates enriched in organic matter (the Adriatic mud-belt *sensu* Van der Zwaan and Jorissen, 1991) are characterized by high frequencies of opportunistic taxa such as *C. neapolitana* and *B. marginata*, whereas deepward (>25 m water depth) the meiofauna is diversified and typical of an inner shelf setting. A similar pattern in terms of species and distribution of benthic foraminifera was identified across the Rhône prodelta under the influence of the river plumes, from the main river mouths to the offshore (Goineau et al., 2011, 2015). As far as we know, no comparable ostracod patterns have been recorded in the Mediterranean area.

2. *Macro-area subject to moderate river inputs: from Ravenna to Ancona*. This area is subject to the riverine inputs provided by the Apennine rivers as well as to the deposition of slow-

settling mud and organic matter particles provided by the Po River (Fig. 1; Frignani et al., 2005; Harris et al., 2008). The strong, persistent southward along-shelf WACC distributes at shallow depths (<13 m) the coarse-grained sediments supplied by rivers (Puig et al., 2007; Fain et al., 2007). In these proximal areas, the sandy substrate (Fig. 4; Brambati et al., 1983) is mainly colonized by *Semicytherura incongruens,* associated to the phytal taxa *Xestoleberis* spp. A small portion of sediment flux from the Apennine rivers is deposited at 13-25 m water depth, where fine-grained bottoms are characterized by higher frequencies of the mud-lover species *Palmoconcha turbida*. Benthic foraminifera are indifferent to change in grain-size substrate and the assemblages are characteristic of shallow depths with dominance of taxa tolerant to organic matter (e.g., *A. parkinsoniana-A. tepida, A. perlucida* and *Porosononion* ex gr. *granosum*). The Adriatic mud-belt is still present at 25-40 m water depth. A similar distribution of meiofauna was reported from the Tyrrhenian shelf in front of the Ombrone River (Frezza and Carboni, 2009; Frezza and Di Bella, 2015).

3. *Macro-area subject to low river inputs: the northern shelf of the Adriatic Sea, north of the Adige Delta.* Sandy substrates at 8-20 m water depth result from the low sediment inputs provided by Eastern Alpine rivers (Adige River excluded) coupled with the longshore currents (Fig. 1; Frignani et al., 2005). Here, the local riverine sediment supply is not overcome by the higher contribution of upstream rivers (Harris et al., 2008), determining a lower concentration of mud and organic matter, and a consequent enrichment in $CaCO_3$ reflected by the abundance of Milioloidea. Ostracod fauna is typical of sandy substrates and is similar to that recovered within the proximal prodelta of macro-area 2. The general geographical context also prevents the basinward development of a continuous mud belt, and only scattered mud patches occur in front of the river mouths out of the investigated area (Fig. 1; Brambati et al., 1983; Frignani et al., 2005). Therefore, at ca. 20 m water depth, the meiofauna directly turns into an inner shelf assemblage typical of the sandy, sediment-starved North Adriatic shelf.

6. CONCLUSIONS

The availability of ostracod and benthic foraminiferal data from the same set of samples gave us the opportunity to compare the zonation of both groups in the northern sector of the Adriatic Sea, and to explore the environmental factors that control their spatial distribution over a river-influenced shelf in a deltaic progradational context.

- The integrated multivariate analysis of the North Adriatic modern meiofaunal databases revealed that communities are primarily controlled by different environmental drivers: ostracoda by grain-size and bathymetry, benthic foraminifera by organic matter.

- The combined application of the seven ostracod biofacies and the five benthic foraminiferal biofacies allowed the identification of five depositional environments determined by the position respect to the Po River: 1) In proximity of its mouths, the meiofauna is dominated by species tolerant to high mud, organic matter inputs, and oxygen deficiency such as *Palmoconcha turbida, L. ramosa, A. parkinsoniana-A. tepida* and *N. turgida*. 2) Downdrift of the main fluvial mouths, generalist ostracoda in terms of grain-size (*S. incongruens*) are associated with benthic foraminifera tolerant to moderate levels of organic matter (*A. parkinsoniana-A. tepida, A. perlucida, Porosononion* ex gr. *granosum*, *Cribroelphidium* ex gr. *poeyanum*). Here, ostracoda discriminate between shallower sandy sediments (*Pontocythere turbida, Xestoleberis* spp.) and deeper fine-grained bottoms (abundant *Palmoconcha turbida*). 3) Updrift of the fluxes of riverine material, shallow-marine ostracoda typical of sandy substrates and Milioloidea occur. 4) In the shallow Adriatic mud belt, species tolerant to high organic matter concentrations and oxygen deficiency (*C. neapolitana, L. ramosa, B. marginata* and *N. turgida*) dominate. 5) On the inner shelf, meiofaunal assemblages are well-diversified and ostracoda mark changes of substrate grain-size in relationship with sediment inputs (sediment-starved areas enriched in sand vs. fine-grained bottoms subject to episodic riverine inputs).

- Distinct sequences of depositional environments are recognized from coastal to offshore locations on three macro-areas of the North Adriatic shelf subject to different degrees of riverine inputs.

- Ostracoda and benthic foraminifera have proven to be complementary indicators on river-influenced shelves, allowing a refined characterization of depositional environments in relationship with the main riverine inputs. Therefore, they represent a useful tool to investigate the evolution of fine-grained sediment successions in deltaic progradational contexts.

7. ACKNOWLEDGMENTS

GB acknowledges the funding from Marco Polo Programme for research mobility and fruitful collaborative research work. BPH acknowledges the funding from Singapore Ministry of Education Academic ResearchFund Tier 2 MOE218-T2-1-030, the National Research Foundation Singapore, and the Singapore Ministry of Education, under the Research Centres of Excellence initiative. This article is a contribution to PALSEA2 (Palaeo-Constraints on Sea-Level Rise), InternationalGeoscience Program (IGCP) Project 639, “Sea Level Change from Minutes to Millennia,” and INQUA Project 1601P “Geographic variability of HOLocene relative SEA level (HOLSEA).” This work is Earth Observatory of Singapore contribution no. XXX.

Supplementary Tables*

*Supplementary tables will be available upon request

Suppl. Tab. 1 – Abbreviations used for ostracod taxa and list of freshwater and brackish water taxa removed from the original ostracod matrix.

Suppl. Tab. 2 – Abbreviations used for benthic foraminiferal taxa.

Suppl. Tab. 3 – Results of the Kruskal-Wallis test to ascertain differences in environmental variables among biofacies, performed on ostracoda and benthic foraminifera. Significance: *<0.05 **<0.01 ***<0.001

Suppl. Tab. 4 – Results of the pairwise Wilcoxon test to identify ostracod biofacies that significantly differ in terms of environmental parameters. Significant values (<0.05) are shaded in grey.

Suppl. Tab. 5 – Results of the pairwise Wilcoxon test to identify benthic foraminiferal biofacies that significantly differ in terms of environmental parameters. Significant values (<0.05) are shaded in grey.

Suppl. Tab. 6 – Quantitative p-values and R-values of the Spearman’s correlation between ostracoda, benthic foraminifera and environmental variables. Significant (<0.05) p-values are reported. R-values are shown as follows: significant positive (>0.25) in green and significant negative (<-0.25) in red.

Suppl. Tab. 7 – Data matrix for analysis of ostracoda and environmental parameters, from Breman (1975). Abbreviations of taxa as reported in *Suppl. Tab. 1*. Cluster number of each sample resulting from the MRT is included.

Suppl. Tab. 8 – Data matrix for analysis of benthic foraminifera and environmental parameters, from Jorissen (1988). Abbreviations of taxa as reported in *Suppl. Tab. 2*. Cluster number of each sample resulting from the MRT is included.

8. REFERENCES

Alberti, M., Hethke, M., Fürsich, F.T. and Liu, C., 2013. Macro- versus microfauna: resolution potential of bivalves, gastropods, foraminifera and ostracods in reconstructing the Holocene palaeoenvironmental evolution of the Pearl River delta, China. Palaeobio. Palaeoenv. 93, 327–353.

Alvisi, F., Giani, M., Ravaioli, M. and Giordano, P., 2013. Role of sedimentary environment in the development of hypoxia and anoxia in the NW Adriatic shelf (Italy). Estuar. Coast. Shelf Sci. 128, 9–21.

Amorosi, A., Rossi, V., Scarponi, D., Vaiani, S.C., Ghosh, A., 2014. Biosedimentary record of postglacial coastal dynamics: high-resolution sequence stratigraphy from the northern Tuscan coast (Italy). Boreas 43, 939–954.

Amorosi, A., Bruno, L., Campo, B., Morelli, A., Rossi, V., Scarponi D., Hong, W., Bohacs, K.M. and Drexler, T., 2017. Global sea-level control on local parasequence architecture from the Holocene record of the Po Plain, Italy. Mar. Petrol. Geol. 87, 99–111.

Angue Minto'o, C.M., Bassetti, M.-A., Jouet, G. and Toucanne, S., 2013. Distribution of modern ostracoda and benthic foraminifera from the Golo margin (East-Corsica). Revue de Paléobiologie 32 (2), 607–628.

Arbulla, D., Pugliese, N., and Russo, A., 2004. Ostracods from the National Park of La Maddalena Archipelago (Sardinia, Italy). B. Soc. Paleontol. Ital. 43, 91–99.

Athersuch, J., Horne, D. J. and Whittaker, J. E., 1989. Marine and brackish water ostracods. In: Kermack, D. M. and Barnes, R. S. K., (Eds.), Synopses of the British Fauna (New Series), Vol. 43. Brill E.J., Leiden, 345 pp.

Avnaim-Katav, S., Hyams-Kaphzan, O., Milker, Y. and Almogi-Labin, A., 2015. Bathymetric zonation of modern shelf benthic foraminifera in the Levantine Basin, eastern Mediterranean Sea. J. Sea Res. 99, 97-106.

Azzarone, M., Rossi, V., Capraro, L., Faranda, C., Ferretti, P., Macrì, P., Scarponi, D., 2018. Early-Middle Pleistocene Benthic turnover and oxygen isotope stratigraphy from the Central Mediterranean (Valle di Manche, Crotone Basin, Italy): data and trends. Data in Brief 17, 1099–1107.

Balassone, G., Aiello, G., Barra, D., Cappelletti, P., De Bonis, A., Donadio, C., Guida, M., Melluso, L., Morra, V., Parisi, R., Pennetta, M. and Siciliano, A., 2016. Effects of anthropogenic activities in a Mediterranean coastland: the case study of the Falerno-Domitio littoral in Campania, Tyrrhenian Sea (southern Italy). Mar. Pollut. Bull. 112, 271–290.

Barbieri, G. and Vaiani, S.C., 2018. Benthic foraminifera or Ostracoda? Comparing the accuracy of palaeoenvironmental indicators from a Pleistocene lagoon of the Romagna coastal plain (Italy). J. Micropalaeontol. 37, 203–230.

Barmawidjaja, D.M., Jorissen, F.J., Puskaric, S. and Van der Zwaan, G.J., 1992. Microhabitat selection by benthic foraminifera in the Northern Adriatic sea. J. Foramin. Res. 22, 297–317.

Bassetti, M.A., Carbonel, P., Sierro, F.J., Perez-Folgado, M., Jouët, G., Berné, S., 2010. Response of ostracods to abrupt climate changes in the Western Mediterranean (Gulf of Lions) during the last 30 kyr. Mar. Micropaleontol. 77, 1–14.

Benito, X., Trobajo, R., Cearreta, A. and Ibáñez, C., 2016. Benthic foraminifera as indicators of habitat in a Mediterranean delta: implications for ecological and palaeoenvironmental studies. Estuar. Coast. Shelf Sci. 180, 97–113.

Bernasconi, E., Mansilla, M. and Cusminsky, G., 2018. Recent benthic foraminifers from the South Atlantic shelf of Argentina. J. Foramin. Res. 48, 210-222.

Bodergat, A.M., Ikeya, N. and Irzi, Z., 1998. Domestic and industrial pollution: use of ostracods (Crustacea) as sentinels in the marine coastal environment. Journal de Recherche Océanographique 23, 139–144.

Bonaduce, G., Ciampo, G. and Masoli, M., 1975. Distribution of Ostracoda in the Adriatic Sea. LS Olschki; Taylor and Francis.

Brambati, A., Ciabatti, M., Fanzutti, G.P., Marabini, F. and Marocco, R., 1983. A new sedimentological textural map of the northern and central Adriatic Sea. Boll. Oceanog. Teor. Appl. I, 267– 271.

Breman, E., 1975. The distribution of Ostracodes in the bottom sediments of the Adriatic Sea. PhD thesis, Free University of Amsterdam, the Netherlands.

Cattaneo, A., Correggiari, A., Langone, L. and Trincardi, F., 2003. The late-Holocene Gargano subaqueous delta, Adriatic shelf: sediment pathways and supply fluctuations. Mar. Geol. 193, 61–91.

Clarke, K. R., 1993. Non-parametric multivariate analyses of changes in community structure. Aust. J. Ecol., 18, 117–143.

Colalongo M.L., 1969. Ricerche sugli Ostracodi nei fondali antistanti il delta del Po. Giornale di Geologia 36, 335–362.

Cronin, T.M., De Martino, D.M., Dwyer, G.S., Rodriguez-Lazaro, J., 1999. Deep-sea ostracode species diversity: response to late Quaternary climate change. Mar. Micropaleontol. 37, 231–249.

Danise, S. and Holland, S., 2017. Faunal response to sea-level and climate change in a short-lived seaway: Jurassic of the Western Interior, Usa. Palaeontology 60, 213-232.

De'ath, G., 2002. Multivariate Regression Trees: a new technique for modeling species–environment relationships. Ecology, 83(4), 1105–1117.

Dessandier, P.-A., Bonnin, J., Kim, J.-H., Bichon, S., Deflandre, B., Grémare, A. and Sinninghe Damsté, J.S., 2016. Impact of organic matter source and quality on living benthic foraminiferal distribution on a river-dominated continental margin: A study of the Portuguese margin. J. Geophys. Res.-Biogeo. 121, 1689–1714.

Di Bella, L., Bellotti, P. and Milli, S., 2013. The role of foraminifera as indicators of the Late Pleistocene-Holocene palaeoclimatic fluctuations on the deltaic environment: The example of Tiber delta succession (Tyrrhenian margin, Italy). Quatern. Int. 303, 191-209.

D'Onofrio, S., 1969. Ricerche sui Foraminiferi nei fondali antistanti il Delta del Po. Giornale di Geologia 36, 283–334.

Doglioni, C., 1993. Some remarks on the origin of foredeeps. Tectonophysics 228, 1–20.

Donnici, S. and Serandrei Barbero, R., 2002. The benthic foraminiferal communities of the northern Adriatic continental shelf. Mar. Micropaleontol. 44, 93–123.

Fain, A.M.V., Ogston, A.S. and Sternberg, R.W., 2007. Sediment transport event analysis on the western Adriatic continental shelf. Cont. Shelf Res. 27, 431–451.

Fanget, A.S., Bassetti, M.A., Fontanier, C., Tudryn, A., Berné, S., 2016. Sedimentary archives of climate and sea-level changes during the Holocene in the Rhône prodelta (NW Mediterranean Sea). Clim. Past 12, 2161–2179.

Faranda, C., Gliozzi, E. and Mazzini, I., 2007. Palaeoenvironmental evolution of the Plio-Pleistocene Monte Mario succession (Rome, Italy) inferred from ostracod assemblages. Riv. Ital. Paleontol. S. 113, 473-485.

Fox, J.M., Hill, P.S., Milligan, T.G. and Boldrin, A., 2004. Flocculation and sedimentation on the Po River Delta. Mar. Geol. 203, 95-107.

Frascari, F., Spagnoli, F., Marcaccio, M. and Giordano, P., 2006. Anomalous Po River flood event effects on sediments and the water column of the northwestern Adriatic Sea. Clim. Res. 31, 151-165.

Frenzel, P. and Boomer, I., 2005. The use of ostracods from marginal marine, brackish waters as bioindicators of modern and Quaternary environmental change. Palaeogeogr. Palaeocl. Palaeoecol., 225, 68–92.

Frezza, V., Bergamin, L. and Di Bella, L., 2005. Opportunistic benthic foraminifera as indicators of eutrophicated environments. Actualistic study and comparison with the Santernian middle Tiber Valley (Central Italy). B. Soc. Paleontol. Ital. 44, 193–201.

Frezza, V. and Carboni, M.G., 2009. Distribution of recent foraminiferal assemblages near the Ombrone River mouth (Northern Tyrrhenian Sea, Italy). Rev. Micropaléontol. 52, 43–66.

Frezza, V., and Di Bella, L., 2015. Distribution of recent ostracods near the Ombrone River mouth (Northern Tyrrhenian Sea, Italy). Micropaleontology 61, 101–114.

Frignani, M., Langone, L., Ravaioli, M., Sorgente, D., Alvisi, F. and Albertazzi, S., 2005. Fine-sediment mass balance in the western Adriatic continental shelf over a century time scale. Mar. Geol. 222–223, 113– 133.

Frontalini, F., Semprucci, F., Coccioni, R., Balsamo, M., Bittoni, P. and Covazzi-Harriague, A., 2011. On the quantitative distribution and community structure of the meio and macrofaunal communities in the coastal area of the Central Adriatic Sea (Italy). Environ. Monit. Assess., 180, 325–344.

Goineau, A., Fontanier, C., Jorissen, F. J., Lansard, B., Buscail, R., Mouret, A., Kerhervé, P., Zaragosi, S., Ernoult, E., Artéro, C., Anschutz, P., Metzger, E. and Rabouille, C., 2011. Live (stained) benthic foraminifera from the Rhône prodelta (Gulf of Lion, NW Mediterranean): Environmental controls on a river-dominated shelf. J. Sea Res. 65, 58–75.

Goineau, A., Fontanier, C., Jorissen, F. J., Buscail, R., Kerhervé, P., Cathalot, C., Pruski, A. M., Lantoine, F., Bourgeois, S., Metzger, E. , Legrand, E. and Rabouille, C., 2012. Temporal variability of live (stained) benthic foraminiferal faunas in a river-dominated shelf: faunal response to rapid changes of the river influence (Rhône prodelta, NW Mediterranean). Biogeosciences 9, 1367–1388.

Goineau, A., Fontanier, C., Mojtahid, M., Fanget, A.-S., Bassetti, M.-A., Berné, S. And Jorissen F., 2015. Live–dead comparison of benthic foraminiferal faunas from the Rhône prodelta (Gulf of Lions, NW Mediterranean): Development of a proxy for palaeoenvironmental reconstructions. Mar. Micropaleontol. 119, 17–33.

Gower, J. C. 1966. Some distance properties of latent root and vector methods used in multivariate analysis. Biometrika, 53, 325–338.

Hammer, Ø., Harper, D. A. T., and Ryan, P. D., 2001. PAST: Paleontological Statistics Software Package for Education and Data Analysis, Palaeontol. Electron., 4, 1–9.

Hanebuth, T.J.J., Lantzsch, H. and Nizou, J., 2015. Mud depocenters on continental shelves—appearance, initiation times, and growth dynamics. Geo-Mar. Lett 35, 487-503.Harris, C.K., Sherwood, C.R., Signell, R.P., Bever, A.J. and Warner, J.C., 2008. Sediment dispersal in the northwestern Adriatic Sea. J. Geophys. Res. 113, C11S03.

Harris, C. K., Sherwood, C. R., Signell, R. P., Bever, A. J. and Warner, J. C., 2008. Sediment dispersal in the northwestern Adriatic Sea. J. Geophys. Res. 113, C11S03, doi:10.1029/2006JC003868.

Hayward, B.W., Grenfell, H.R., Reid, C.M. and Hayward, K.A., 1999. Recent New Zealand shallow-water benthic foraminifera: taxonomy, ecologic distribution, biogeography, and use in paleoenvironmental assessment. Inst. Geol. Nucl. Sci. Monogr. 21, 264 pp.

Holland, S.M., 2005. The signatures of patches and gradients in ecological ordinations. Palaios 20, 573-580.

Horton, B.P., Larcombe, P., Woodro¡e, S.A., Whittaker, J.E., Wright, M.R. and Wynn, C., 2003. Contemporary foraminiferal distributions of a mangrove environment, Great Barrier Reef coastline, Australia: implications for sea-level reconstructions. Mar. Geol. 198, 225-243.

Jackson J.A. (Ed.), 1997. Glossary of Geology, fourth edition. Am. Geol. Inst., 769 pp.

Jorissen, F.J., 1987. The distribution of benthic foraminifera in the Adriatic Sea. Mar. Micropaleontol. 12, 21–48.

Jorissen, F. J., 1988. Benthic Foraminifera from the Adriatic Sea; principles of phenotypic variation, Utrecht Micropaleontological Bulletins, 37, 176 pp.

Jorissen, F.J., Nardelli, M.P. , Almogi-Labin, A., Barras, C., Bergamin, L., Bicchi, E., El Kateb, A., Ferraro, L., McGann, M., Morigi, C., Romano, E., Sabbatini, A., Schweizer, M. and Spezzaferri, S., 2018. Developing Foram-AMBI for biomonitoring in the Mediterranean: species assignments to ecological categories. Mar. Micropaleontol., 33-45. 10.1016/j.marmicro.2017.12.006

Lachenal, A. M. and Bodergat, A. M., 1988. Les ostracodes et l'évolution paléogéographique au Quaternaire récent du site d'Ashtart (Golfe de Gabès, Tunisie Orientale). Geobios, 21, 73–80.

Legendre, P. and Gallagher, E.D., 2001. Ecologically meaningful transformations for ordination of species data. Oecologia, 129, 271–280.

Liu, J.T., Hsu, R.T., Yang, R.J., Ping Wang, Y., Wu, H., Du, X., Li, A., Chien, S.C., Lee, J., Yang, S., Zhu, J., Su, C., Chang, Y. and Huh, C., 2018. A comprehensive sediment dynamics study of a major mud belt system on the inner shelf along an energetic coast. Sci. Rep. 8:4229. DOI:10.1038/s41598-018-22696-w.

Mendes, I., Gonzalez, R., Dias, J. M. A., Lobo, P., and Martins, V., 2004. Factors influencing recent benthic foraminifera distribution on the Guadiana shelf (southwestern Iberia). Mar. Micropaleontol. 51, 171–192.

Miserocchi, S., Langone, L. and Tesi, T., 2007. Content and isotopic composition of organic carbon within a flood layer in the Po River prodelta (Adriatic Sea). Continental Shelf Research 27, 338–358.

Mojtahid, M., Jorissen, F., Lansard, B., Fontanier, C., Bombled, B. and Rabouille, C., 2009. Spatial distribution of live benthic foraminifera in the Rhône prodelta: Faunal response to a continental–marine organic matter gradient. Mar. Micropaleontol. 70, 177–200.

Moissette, P., Cornéec, J.-J., Antonarakou, A., Kontakiotis, G., Drinia, H., Koskeridou, E., Tsourou, T., Agiadi, K. and Karakitsios, V., 2018. Palaeoenvironmental changes at the Tortonian/Messinian boundary: A deep-sea sedimentary record of the eastern Mediterranean Sea. Palaeogeogr. Palaeocl. 505, 217–233.

Morigi, C., Jorissen, F.J., Fraticelli, S., Horton, B.P., Principi, M., Sabbatini, A., Capotondi, L., Curzi, P.V. and Negri, A., 2005. Benthic foraminiferal evidence for the formation of the Holocene mud-belt and bathymetrical evolution in the central Adriatic Sea. Mar. Micropaleontol. 57, 25– 49.

Murray, J. W., 2006. Ecology and applications of benthic foraminifera. Cambridge University Press, Cambridge, 426 pp.

Ori, G.G., Roveri, M. and Vannoni, F., 1986. Plio-Pleistocene sedimentation in the Apenninic-Adriatic foredeep (Central Adriatic sea, Italy). In: Allen, P.A., Homewood, P. (Eds.), Foreland Basins. IAS Spec. Publ. 8, pp. 183-198.

Palinkas, C.M. and Nittrouer, C.A., 2007. Modern sediment accumulation on the Po shelf, Adriatic Sea. Cont. Shelf. Res. 27, 489–505.

Pascual, A., Rodriguez-Lazaro, J., Martín-Rubio, M., Jouanneau, J.-M. and Weber, O., 2008. A survey of the benthic microfauna (foraminifera, Ostracoda) on the Basque shelf, southern Bay of Biscay. J. Marine Syst. 72, 35–63.

Patzkowsky, M.E. and Holland, S.M., 2012. Stratigraphic Paleobiology: Understanding the Distribution of Fossil Taxa in Time and Space. University of Chicago Press, 256 pp.

Puig, P., Ogston, A.S., Guillén, J., Fain, A.M.V. and Palanques, A., 2007. Sediment transport processes from the topset to the foreset of a crenulated clinoform (Adriatic Sea). Cont. Shelf Res. 27, 452–474.

R Core Team, 2018. R: A language and environment for statistical computing. R Foundation for Statistical Computing, Vienna, Austria.

Ricci Lucchi, F., 1986. The Oligocene to recent foreland basins of the Northern Apennines. In: Allen, P.A., Homewood, P. (Eds.), Foreland Basins. IAS Spec. Publ. 8, 105-139.

Rodriguez-Lazaro, J. and Ruiz-Muñoz, F., 2012. A General Introduction to ostracods: morphology, distribution, fossil record and applications. In: Horne, D. J., Holmes, J. A., Rodriguez-Lazaro, J., and Viehberg, F. (Eds.), Ostracoda as proxies for Quaternary climate change. Developments in Quaternary Science 17, Elsevier, 1–14.

Ronchi, L., Fontana, A., Correggiari, A. and Asioli, A., 2018. Late Quaternary incised and infilled landforms in the shelf of the northern Adriatic Sea (Italy). Mar. Geol. 405, 47-67.

Rossi, V. and Horton, B.P., 2009. The application of a subtidal foraminifera-based transfer function to reconstruct Holocne paleobathymetry of the Po Delta, Northern Adriatic Sea. J. Foramin. Res. 39, 180-190.

Rossi, V., Amorosi, A., Sarti, G. and Mariotti, S., 2017. Late Quaternary multiple incised valley systems: An unusually well-preserved stratigraphic record of two interglacial valley-fill successions from the Arno Plain (northern Tuscany, Italy). Sedimentology 64, 1901-1928.

Rossi, V., Azzarone, M., Capraro, L., Faranda, C., Ferretti, P., Macrì, P. and Scarponi, D., 2018. Dynamics of benthic marine communities across the Early-Middle Pleistocene boundary in the Mediterranean region (Valle di Manche, Southern Italy): Biotic and stratigraphic implications. Palaeogeogr. Palaeocl. 495, 127–138.

Ruiz, F., González-Regalado, M.L. and Muñoz, J.M., 1997. Multivariate analysis applied to total and living fauna: seasonal ecology of recent benthic Ostracoda off the North Cádiz Gulf coast (southwestern Spain). Mar. Micropaleontol. 31, 183-203.

Salvi, G., Buosi, C., Arbulla, D., Cherchi, A., De Giudici, G., Ibba, A. and De Muro, S., 2015. Ostracoda and foraminifera response to a contaminated environment: the case of the Ex-Military Arsenal of the La Maddalena Harbour (Sardinia, Italy). Micropaleontology 61, 115–133.

Scarponi, D. and Kowalewski, M., 2004. Stratigraphic paleoecology: Bathymetric signatures and sequence overprint of mollusk associations from upper Quaternary sequences of the Po Plain, Italy. Geology 32, 989-992.

Sciuto F., Rosso, A., Sanfilippo R. and Di Martino, E., 2015. Ostracods from mid-outer shelf bottoms of the Ciclopi Islands Marine Protected Area (Ionian Sea, Eastern Sicily). B. Soc. Paleontol. Ital. 54, 1-15.

Sgarrella, F. and Moncharmont Zei, M., 1993. Benthic Foraminifera of the Gulf of Naples (Italy): systematics and autoecology. B. Soc. Paleontol. Ital. 32, 145–264.

Storms, J.E.A., Jan Weltje, G., Terra, G.J., Cattaneo, A. and Trincardi, F., 2008. Coastal dynamics under conditions of rapid sea-level rise: Late Pleistocene to Early Holocene evolution of barrier–lagoon systems on the northern Adriatic shelf (Italy). Quaternary Sci. Rev. 27, 1107– 1123.

Tesi, T., Miserocchi, S., Goni, M.A., Langone, L., Boldrin, A. and Turchetto, M., 2007. Organic matter origin and distribution in suspended particulate materials and surficial sediments from the western Adriatic Sea (Italy). Estuarine, Coastal and Shelf Science 73 (3–4), 431–446.

Tesi, T., Langone, L., Giani, M., Ravaioli, M. and Miserocchi, S., 2013. Source, diagenesis, and fluxes of particulate organic carbon along the western Adriatic Sea (Mediterranean Sea). Mar. Geol. 337, 156-170.

Trincardi, F., Correggiari, A. and Roveri, M., 1994. Late Quaternary transgressive erosion and deposition in a modern epicontinental shelf: the Adriatic Semienclosed Basin. Geo-Mar. Lett. 14, 41–51.

Triantaphyllou, M.V., Tsourou, T., Koukousioura, O. and Dermitzakis, M.D., 2005. Foraminiferal and ostracod ecological patterns in coastal environments of SE Andros Island (Middle Aegean Sea, Greece). Revue de micropaléontologie 48, 279-302.

Tyler, C.L. and Kowalewsky, M., 2014. Utility of Marine Benthic Associations as a Multivariate Proxy of Paleobathymetry: A Direct Test from Recent Coastal Ecosystems of North Carolina. PLoS ONE 9(4): e95711. doi:10.1371/journal.pone.0095711.

Van der Zwaan, G. J. and Jorissen, F. J., 1991. Biofacial patterns in river-induced shelf anoxia. In: Tyson, R. V., Pearson, T.H., (Eds.), Modern and Ancient Continental Shelf Anoxia. Geological Society Special Publication, vol. 58, pp. 65–82, London.

Van Straaten, L.M.J.U., 1970. Holocene and Late Pleistocene sedimentation in the Adriatic Sea. Geologische Rundschau 60, 106-131.

Walsh, J.P. and Nittrouer, C.A., 2009. Understanding fine-grained river-sediment dispersal on continental margins. Mar. Geol. 263, 34-45.

Wheatcroft, R. A., Hunt, L., Stevens, A. and Lewis, R., 2006. The large-scale distribution and internal geometry of the fall 2000 Po River flood deposit: evidence from digital X-radiography. Cont. Shelf Res. 26, 499–516.

Yasuhara, M., Hunt, G., Cronin, T.M., Hokanishi, N., Kawahata, H., Tsujimoto, A., Ishitake, M., 2012. Climatic forcing of Quaternary deep-sea benthic communities in the North Pacific Ocean. Paleobiology 38, 162–179.

6. THE PALAEOECOLOGICAL RECORD OF DELTA DYNAMICS

6.1 Introduction

Holocene sediment succession buried beneath the modern Po coastal plain has been proven to be an excellent archive for palaeoenvironmental studies, since it was formed under a strong subsidence rate that allowed the formation of a suite of palaeoenvironments in a retrogradational to progradational trend (Amorosi et al., 2005, 2017). In this context, benthic foraminifera and ostracoda were jointly applied as palaeoenvironmental indicators, mostly in a qualitative or semi-quantitative fashion (Amorosi et al., 2004, 2008). Numerical palaeoecology (which naturally derives from numerical ecology), represents a powerful instrument to obtain refined palaeoenvironmental trends, giving insights about palaeocommunities' structure, faunal turnover as well as connection between biotic (i.e., faunistic) and abiotic (i.e., palaeoenvironmental) variables (Legendre & Legendre, 2012). Statistical approaches were adopted in very few cases for the analysis of Holocene meiofauna of the Po Plain, but benthic foraminifera and ostracoda were treated separately (Rossi and Vaiani, 2008; Rossi, 2009).

Here, I report the record of benthic foraminifera and ostracoda from the Holocene shallow marine succession of core EM13. The two benthic groups were analyzed in parallel using the same statistical analyses, with the aim of: i) understand the independent palaeoecological response of each group to the overall Holocene coastal progradation; ii) assess which group provides the best palaeoenvironmental resolution within a shallow marine, river-influenced succession.

6.2 Materials and methods

The continuous core EM13 was drilled in the southern Po Delta plain, about 3.5 km from the modern coastline (Fig. 6.1) as part of the research project in collaboration with ExxonMobil Upstream Research Company. It is 35 m in length and core recovery was >95%. Qualitative micropalaeontological analyses were performed on 155 samples from the whole length of the core. Here, we focus on the thick shallow marine succession between 26 and 5 m core depth. A total of 115 samples of ca. 80 g of dry weight were collected every 20 cm from this stratigraphic interval.

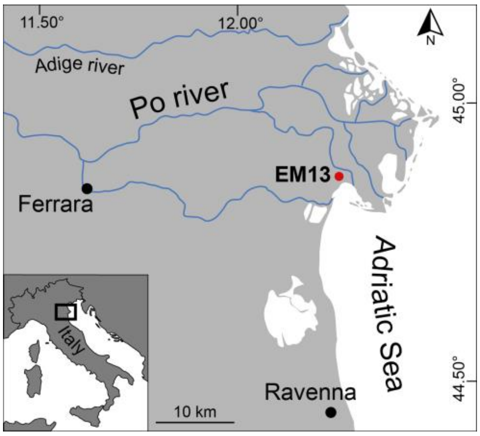

Fig. 6.1 Location of core EM13

All samples were treated as follow: i) oven-dried at 60°C for at least 8 hours; ii) soaked in water and H_2O_2 (35% vol.); iii) wet-sieved at 63 µm using tap water; iii) oven-dried again at 60°C for 8 hours. Forty-nine samples containing abundant and well preserved meiofauna were dry-sieved to retain the fraction >125 µm and split in order to obtain sub-samples including at least 300 individuals of benthic foraminifera and 20 valves of ostracoda. All 49 samples were counted to obtain the number of benthic foraminiferal tests, whereas 23 samples were quantitatively analyzed for ostracoda (exclusively adult or eventually A1 valves were counted). Taxa were identified on the basis of original descriptions (Ellis and Messina,1940) and literature sources concerning modern as well as fossil material (Uffenorde, 1972; Bonaduce, 1975; Breman, 1975; Jorissen, 1988; Athersuch et al., 1989; Sgarrella and Moncharmont Zei, 1993; Fiorini and Vaiani, 2001; Faranda and Gliozzi, 2008).

To obtain a robust chronological framework of the cored succession, a total of eight radiocarbon dates were performed on selected samples of mollusk shells, peat and wood material using accelerator mass spectrometry (AMS) at KIGAM laboratory (Daejeon City, Korea) (Table 6.1).

Sample depth (m)	Radiocarbon-dated material	Radiocarbon age	Calibrated age (yr BP)
10.90	Shell	840±40	580±40
17.50	Wood	1060±30	985±35
22.65	Shell	1900±400	1570±50
25.60	Shell	5290±40	5515±55
25.78	Shell	2220±30	1655±60
26.75	Wood	8040±50	8900±100
29.00	Peat	8500±50	9500±30
32.00	Wood	9080±50	10250±50

Tab. 6. 1 List of radiocarbon dates performed on samples from core EM13.

6.2.1 Statistical analysis

Analogue matching (AM) technique finds modern sites that are faunistically similar to each fossil sample based on any dissimilarity (or similarity) measure. Benthic foraminiferal and ostracod matrices for the AM technique were produced grouping selected species with similar ecological characteristics up to genera level in accordance with the modern databases of Jorissen (1988) and Breman (1975) presented in chapter 5. Accordingly, the contribution of finely agglutinated benthic foraminifera (such as *Eggerella* spp.) and freshwater/brackish water ostracoda was removed. After these operations, 27 samples with >300 tests of benthic foraminifera and 17 samples with >20 ostracod valves were retained for statistical analyses. The most abundant 24 benthic foraminiferal and ostracod taxa present with a frequency >5% in at least one sample were included in the final matrices for the AM. Since in modern databases data are expressed as percentage abundances, the fossil data were accordingly transformed in percentage form. Then, the square-root of the percentage abundances for both modern and fossil meiofaunal matrices was calculated, and the Euclidean distance applied to obtain the Hellinger distance (Legendre and Gallagher, 2001) as a measure of dissimilarity between modern and fossil samples. It emphasizes the contribution of mid-range species and downweight species with low abundances (Legendre and Gallagher, 2001;

Legendre and Legendre, 2012). The first four analogues with the lower values of dissimilarity were considered.

6.3 Results

A total of 118 benthic foraminiferal and 67 ostracod taxa were identified in the sediment succession between 25.88 and 8.80 m core depth. AM technique allowed to identify the most similar modern samples to each fossil assemblage in terms of faunal composition. Modern assemblages of benthic foraminifera and ostracoda are grouped in accordance with the biofacies recognized in the modern North Adriatic Sea, described at length in chapter 5 and indicated here with the reference colours.

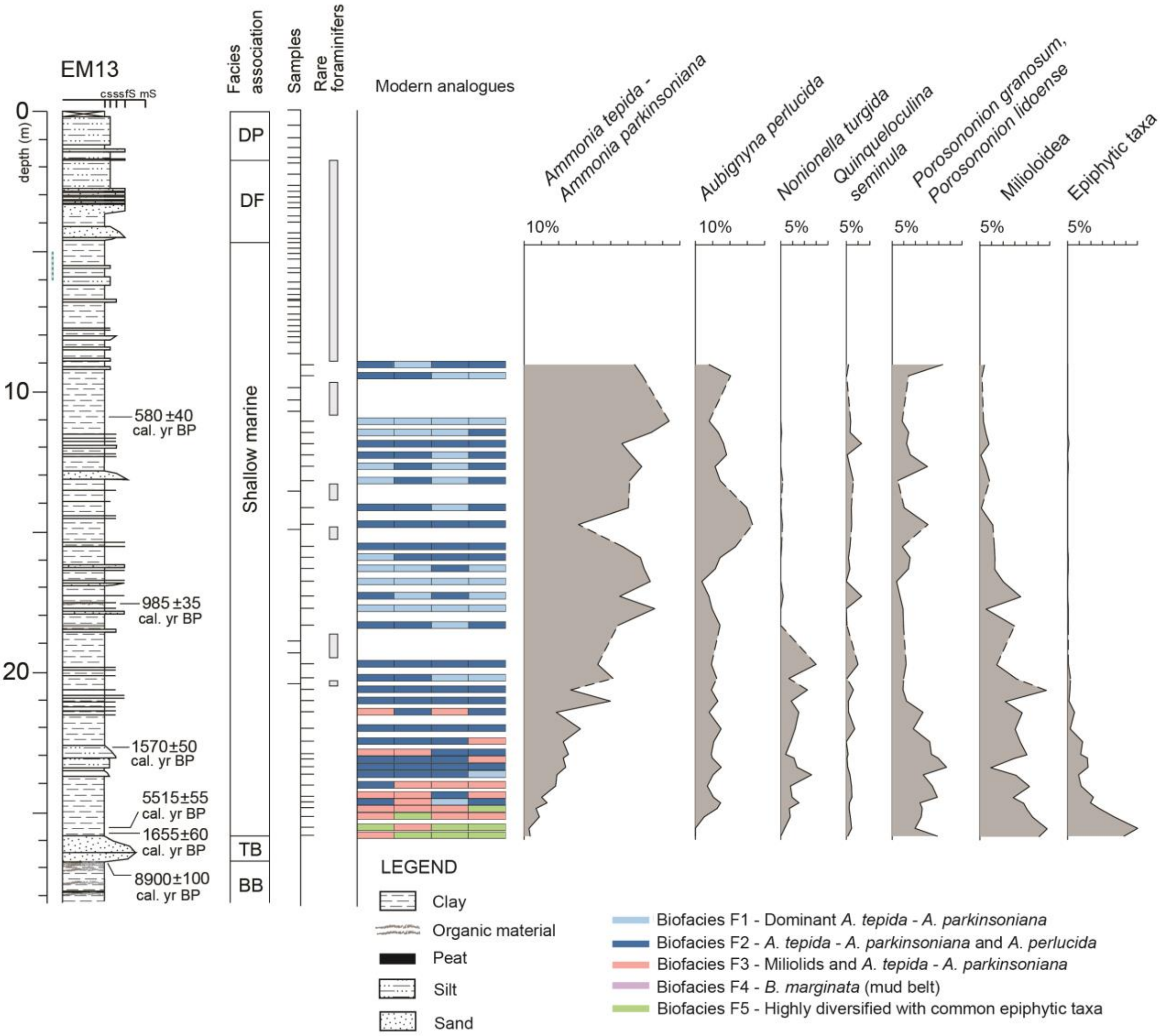

Fig. 6.2 Stratigraphy and vertical distribution of the most common taxa of benthic foraminifera or ecological groups and facies association (BB: Back-barrier; TB: transgressive barrier; DF: delta front; DP: delta plain). Quantitatively analyzed samples are reported on the right side of the sample column, samples qualitatively analyzed on the left. Colors of modern analog samples are referred to benthic foraminiferal biofacies described at length in chapter 5.

6.3.1 Benthic foraminifera

Above the transgressive barrier sands that mark the passage to marine deposits, benthic foraminifera between 25.88-25.40 m core depth are characterized by relatively high frequencies of Milioloidea (25.5-28.9%; Fig. 6.2). Among them, the most abundant genera are represented by *Triloculina* (with the most abundant species *Triloculina trigonula,* 5.4-9.5%) and *Adelosina* (5.7-6.7%). This stratigraphic portion also includes high proportions of epiphytic taxa (24.8-29.2%), mostly represented by *Asterigerinata mamilla, Buccella granulata, Neoconorbina terquemi, Rosalina bradyi* and *Siphonaperta aspera*. *Porosononion lidoense* (2.9-10.2%) and *P. granosum* (7.0-9.2%), gathered into *Porosononion* ex. gr. *granosum* are common. These benthic foraminiferal assemblages are similar to those nowadays recorded on the northern Adriatic shelf at 17-24 m water depth, with a diversified fauna characteristic of the inner shelf out of the fluvial influence of the Po River (Suppl. Tab. 6.2).

Between 25.40-23.89 m core depth, Milioloidea are still abundant (14.3-22.7%), but the concentration of epiphytic taxa progressively decreases (5.0-16.8%), replaced by increasing *Ammonia parkinsoniana-Ammonia tepida* (8.8-18.2%). Moderate frequencies of *P. granosum* (9.7-17.6%) and *Aubignyna perlucida* (5.1-14.6%) are recorded. Similar modern benthic foraminiferal assemblages are mostly located at shallow depths (8-22 m water depth) north of the Po Delta, updrift of the main feeding mouths, where sediment inputs and organic matter concentration are low.

Even though Milioloidea are abundant even between 23.89-18.00 m core depth (4.7-28.6%), *T. trigonula* becomes very scarce (0.3-3.3%) and it is replaced by higher frequencies of *Quinqueloculina* (with the exclusion of *Q. seminula*; 1.9-19.9%). The most abundant taxa becomes *A. parkinsoniana-A. tepida* (18.5-54.1%), whereas the concentration of *P. granosum* progressively decreases (20.6-4.6%) and moderate frequencies of *Nonionella turgida* are recorded (up to 15%). Similar modern assemblages are located downdrift of the Po River at 12-18 m water depth, on fine-grained substrates (0.5-36.6% sand) with moderate concentration of organic matter (1% on average).

Upwards, from 18.00 to 8.80 m core depth, benthic foraminiferal assemblages are dominated by *A. parkinsoniana-A. tepida* (31.4-83.7%, 64.1% on average). *Aubignyna perlucida* is relatively abundant, but at 15.75-13.66 m core depth this species reaches its maximum concentration (23.2-33%), at the expense of *A. parkinsoniana-A. tepida* which significantly decrease within this interval (57.1-31.4%). Epiphytic taxa almost disappear, as well as *N. turgida*, a dominant species in the shallow Adriatic mud belt but rare in proximity to fluvial outlets. Samples between 18.00-15.75 m and 13.66-8.80 m core depth are mostly similar to those nowadays located in proximity of the Po and Adige river mouths, where high amounts of riverine material (sediment and organic matter) are deposited. Benthic foraminiferal assemblages between 15.75 and 13.66 m core depth are similar to the modern ones located downdrift of the Po Delta at shallow depth (8-13 m water depth) with moderate concentration of organic matter (0.68% on average). Benthic foraminifera are rare in the uppermost portion of the succession and dominated by *A. parkinsoniana-A. tepida.*

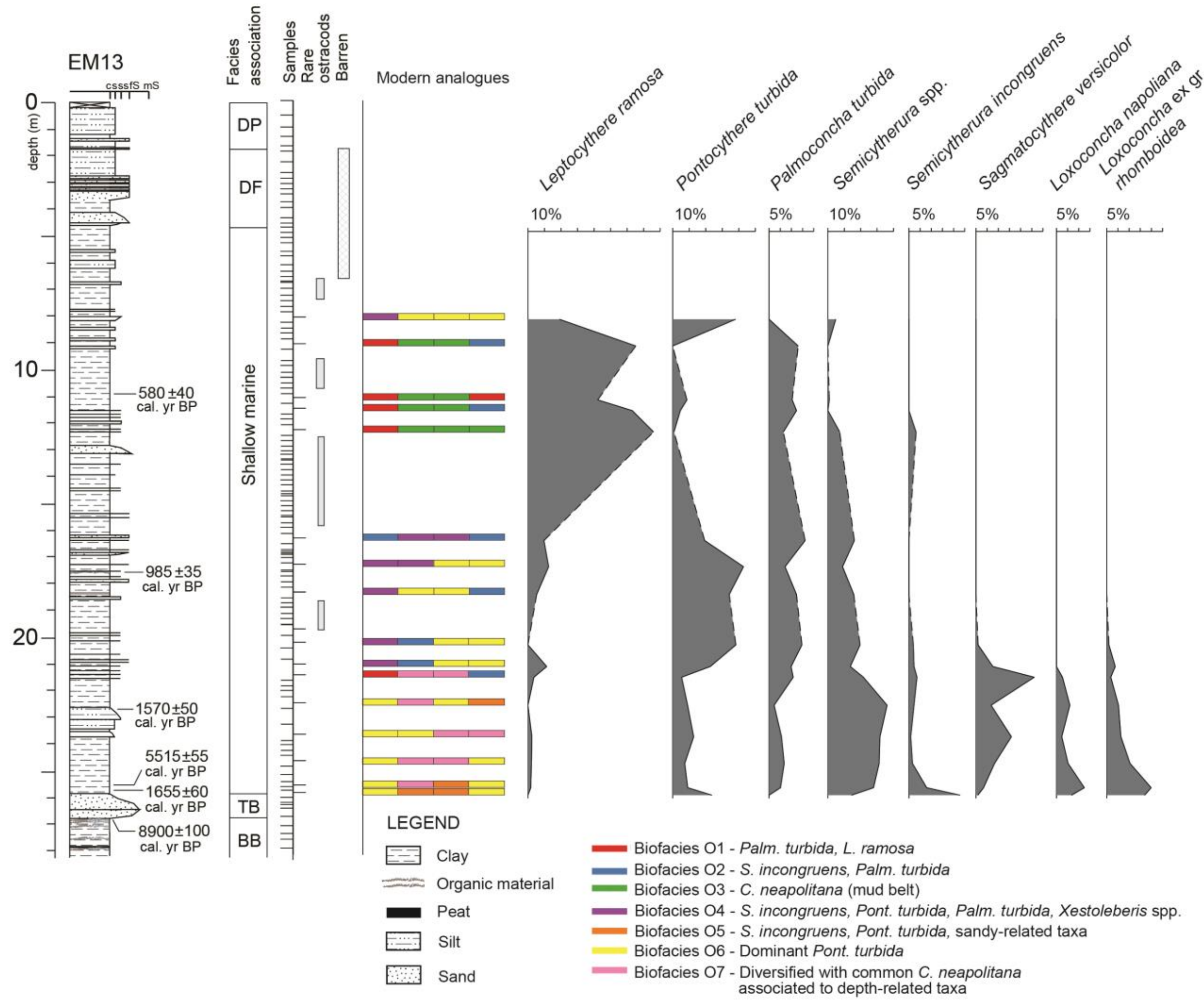

Fig. 6.3 Stratigraphy and vertical distribution of the most common taxa of ostracoda and facies association (BB: Back-barrier; TB: transgressive barrier; DF: delta front; DP: delta plain). Quantitatively analyzed samples are reported on the right side of the sample column, samples qualitatively analyzed on the left. Colors of modern analog samples are referred to ostracod biofacies described at length in chapter 5.

6.3.2 Ostracoda

From 25.88 to 21.26 m core depth, ostracod assemblages include high frequencies of *Semicytherura incongruens* (0.8-23.3%; Fig. 6.3) and a variety of other *Semicytherura* species (mostly *Semicytherura* cf. *sella, S. rarecostata, S. ruggierii, S. acuta*; 14.4-36.1%). *Loxoconcha* ex gr. *rhomboidea* (5.3-19.7%), *Pontocythere turbida* (9.0-24.1%) and *Sagmatocythere versicolor* (0.9-26.1%) are common, associated to lower frequencies of and *Sagmatocythere napoliana* (2.4-12.4%), *Palmoconcha turbida* (up to 10.8%) and *Xestoleberis* spp. (up to 6.8%). The ostracod assemblage recorded at 25.88 m core depth is similar to faunas nowadays developed on the sediment-starved Adriatic shelf at 25-30 m water depth, out of the influence of the riverine inputs. Upper samples are both similar to faunas of the sediment-starved portion of the shelf, as well as those of the inner shelf sligthly influenced by the Po River runoff (please refer to chapter 5), placed at 25-40 m water depth. However, it should be noticed that the similarity to these samples is driven by the moderate frequencies of *Pontocythere turbida* and *Semicytherura* spp., whereas *Cytheridea neapolitana* typical of the slightly river-influenced inner shelf, is totally absent in core assemblages. The increase in *Palmoconcha turbida* and the decrease of *Semicytherura* spp. at 21.46 m core depth create a mixed signal, since this sample is related to three different modern biofacies.

Ostracod assemblages between 21.26-14.30 m core depth are dominated by *Pontocythere turbida* (5.4-42.9%). Compared to the lower stratigraphic interval, frequencies of *Palmoconcha turbida* increases (7.1-16.1%), whereas *Semicytherura* spp. (8.9-21.6%) slightly decrease. Scarce frequencies of *Leptocythere ramosa* (up to 12.5%) and *Xestoleberis* spp. (up to 9.7%) are recorded. *Loxoconcha* ex gr. *rhomboidea, S. versicolor* and *S. incongruens* are rare at the base of this stratigraphic interval and gradually disappear. These assemblages are similar to modern faunas located far from the main sources of riverine materials, on substrates enriched in sand. They are mostly similar to faunas recovered at relatively shallow water depth (12.5-20 m), however they also show a certain degree of similarity to deeper faunas of the sediment-starved shelf (31-40 m water depth).

Between 14.30-8.80 m core depth *L. ramosa* strongly dominates the ostracod assemblages (42.2-76.0%), associated to relatively scarce frequencies of *Palmoconcha turbida* (6.4-13.0%) and *Pontocythere turbida* (up to 8.6%). Ostracod assemblages within this interval are mostly similar to those found in proximity of the modern Po Delta, subject to strong and unstable inputs of sediment and organic matter. The similarity to modern mud belt faunas is produced by the high frequencies of *L. ramosa* recorded in fossil assemblages, even though they do not include *Cytheridea neapolitana*. From 8.80 to 6.50 m core depth, the shallow marine succession includes rare ostracod valves mostly represented by *L. ramosa*, whereas the uppermost portion is barren in ostracoda.

6.4 Discussion

6.4.1 Benthic foraminifera as tracers of organic matter fluxes

As it is shown in chapter 5, the distribution of modern benthic foraminiferal assemblages of the Adriatic Sea is strongly influenced by organic matter concentration and, subordinately by water depth (even though the contribution of additional factors could not be excluded). The thigh correlation between benthic foraminifera and organic matter fluxes was demonstrated in other Mediterranean river-influenced shelves as well (Goineau et al., 2011; Frezza and Carboni, 2009; Jorissen et al., 2018 an references therein).

The comparison between fossil and modern assemblages by means of AM indicates that benthic foraminifera record low levels of organic matter from 25.88 to 23.89 m core depth (Fig. 6.4). Specifically, they are analogous to deeper faunas of the inner shelf far from river mouths from 25.88 to 25.40 m core depth. Conversely, they are indicative of lower depths in the upper portion of the stratigraphic interval, suggesting the passage to a shallow prodelta affected by very low organic matter inputs, as nowadays occur along the northern Adriatic coasts updrift of the main sources of riverine inputs (chapter 5). From 23.89 to 18.00 m core depth, the similarity to modern assemblages located downdrift of the Po Delta suggests an increase in the concentration of organic matter provided by rivers. Foraminiferal assemblages recovered between 18.00-15.75 m and 13.66-8.80 are related to high levels of organic matter deposited in proximity of a river mouth, as suggested by the similarity with present-day fauna found in proximity of the Po and Adige river mouths. However, assemblages indicate a decrease of organic matter inputs from 15.75 to 13.66 m core depth, likely caused by a phase of diminished river discharge or by a shift of the river mouth in a relatively more distal position.

6.4.2 Ostracoda as tracers of sediment supply

Modern ostracoda of the shallow North Adriatic Sea show a distribution pattern mostly determined by water depth and grain-size of the substrate (chapter 5). Bathymetry is known to be a complex factor that implicitly includes several environmental parameters, therefore it simply indicates a position in the geographical space (Rossi and Horton, 2009). In the case of the North Adriatic shelf, the influence of the Po River in terms of sediment supply exerts a primary role on the spatial distribution of bottom grain-size and hence on ostracod assemblages. In fact, fine-grained sediments provided by the Po and, subordinately, Apennine rivers determine the zonation of the bottom sediments on parallel belts according to grain-size. These sediments are transported by the surface WACC tens of km south (Cattaneo et al., 2003; Harris et al., 2008), creating a fine-grained silty/clayey belt at ca. 15-40 m water depth parallel to the coastline and up to 8 m water depth in proximity of the Po Delta (Brambati et al., 1983). On such substrates, specific biofacies are developed in response to very high (e.g., biofacies O1) or relatively lower (e.g., biofacies O2, O3) rates of sediment supply. This process also affect the distribution of ostracoda at higher depths, far from the river mouths, where sediment-starved areas are marked by peculiar assemblages (e.g., biofacies O5, O6). However, on areas subject to similar mass accumulation rates, the occurrence of different ostracod assemblages at specific bathymetric intervals (e.g., biofacies O4, O2 downdrift of the Po Delta) are due to differences in the sediment dynamics, as explained in chapter 5. In this context, ostracoda can represent proxies for conditions of sedimentation, in terms of sediment supply derived from riverine inputs, but they also furnish insights on the processes that governed sediment dynamics.

Ostracod assemblages between 25.88-21.26 m core depth indicate an extremely low riverine sediment supply (Fig. 6.4). In fact, all the assemblages indicate a shallow marine environment subject to low sedimentation rates. The absence of *C. neapolitana* in core assemblages confirms this interpretation, since this species exclusively occur on fine-grained substrates affected by riverine inputs at high depths (chapter 5). Upward, from 21.26 to 14.30 m core depth, the similarity to modern sites at shallow depths subject to the inputs of Apennine rivers suggest a slight increase in sediment supply. However, at these sites the action of longshore currents is still prevalent over the fine-grained sediment input provided by rivers. Analogs of the upper sample at 16.34 m core depth indicate a progressive increase in sediment supply. The upper portion of the sediment succession suggests high riverine sediment supply and possible oxygen deficiency at the bottom.

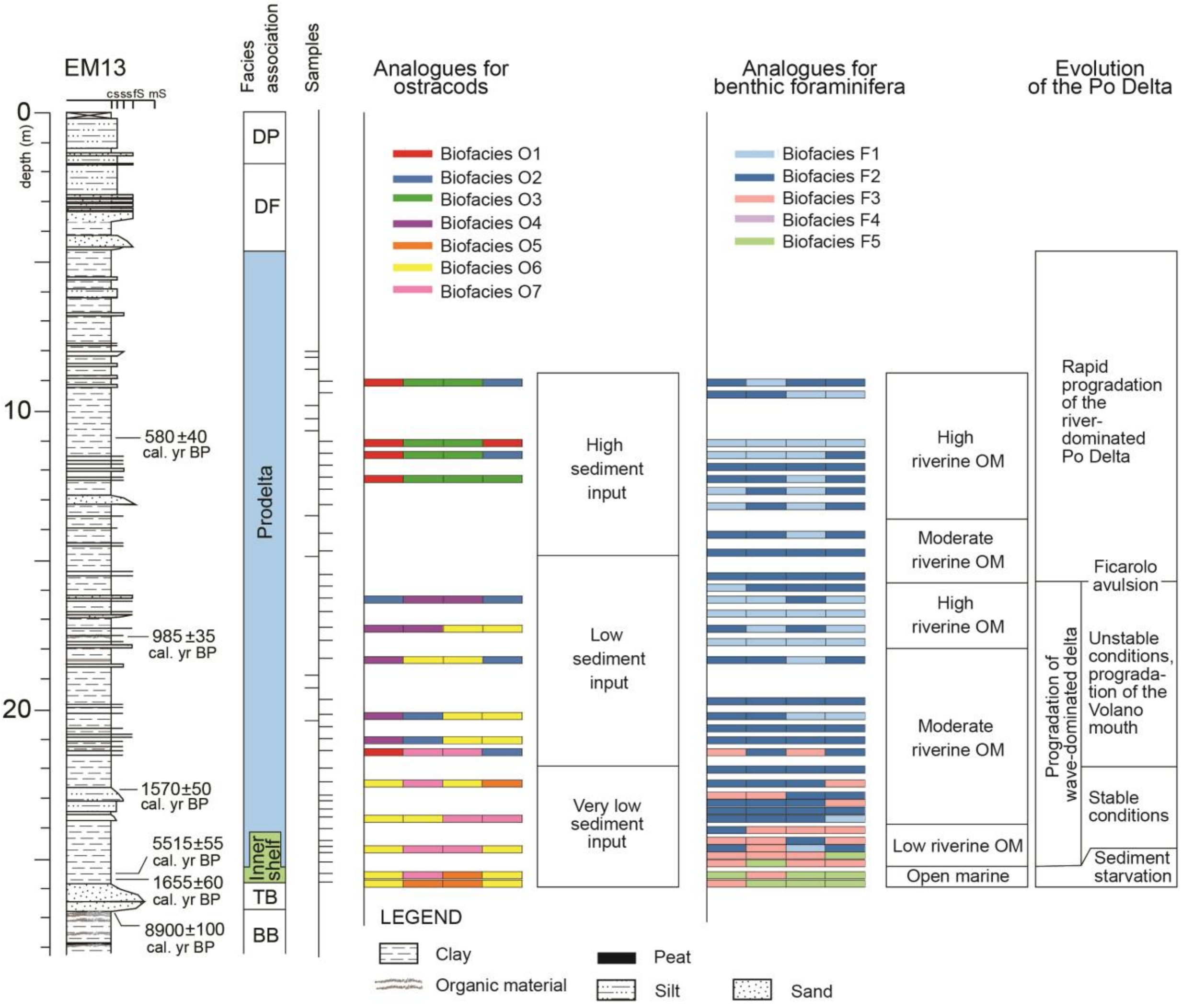

Fig. 6.4 Stratigraphy and vertical distribution of modern analogues for ostracoda and benthic foraminifera, interpretation and phases of evolution of the Po Delta. Colors of modern analog samples are referred to ostracod and benthic foraminiferal biofacies reported in chapter 5.

6.4.3 The record of delta dynamics: integrating benthic foraminifera and ostracoda

The combination of benthic foraminifera and ostracoda with radiocarbon dates from the shallow marine succession of core EM13 allows to understand the palaeoecological response of those benthic groups to delta dynamics.

The inverse trend shown by radiocarbon dates at the base of the succession indicates the presence of a condensed section, with ca. 4 cal. kyr of stratigraphic condensation. At distal locations from the shoreline position at the peak of marine transgression (ca. 7.7 cal kyr BP; Bruno et al., 2017), as the case of core EM13, the estimated accumulation rates are <<1 mm/yr (Campo et al., 2017). The low sediment supply were caused by the sediment trapping in estuaries, where river mouths formed prograding bay-head delta ca. 30 km inland from the modern shoreline (Amorosi et al., 2017; Bruno et al., 2017). After the infilling of the estuaries, the counter-clockwise circulation pattern of the Adriatic Sea favored the sediment transport at shallow depth along the coast, feeding coastal sand bars at proximal locations (Amorosi et al., 2016a; Bruno et al., 2017). The meiofauna included within the lowermost portion of the sediment succession, at 25.88-25.40 m core depth, is in accordance with these conditions, since ostracoda clearly indicate an inner shelf environment not subject to riverine inputs, i.e. under sediment-starved conditions. Benthic foraminifera similar to modern inner shelf assemblages indicate a generic shallow, relatively open-marine palaeoenvironment.

The stratigraphic interval at 25.40-22.00 m core depth is chronologically in accordance with a phase of warm climate and the development of the Roman Empire, that favored riverine stability and the progradation of a delta lobe south of the study area (Stefani and Vincenzi, 2005). At these times, the Po coastal plain was characterized by a series of wave-dominated, arcuate deltas that laterally shifted to rectilinear strandplains (Stefani and Vincenzi, 2005). Benthic foraminifera consistently mark the first signal of an approach to the coastline (i.e., coastal progradation) with the abrupt shift to shallower conditions at 25.40 m core depth and then a progressive increase in organic matter inputs resulting from the progradation of the wave-dominated delta. Within this interval ostracoda still suggest low sediment input, in accordance with the dominant longshore transport at shallow depths operated by longshore currents.

After the demise of the Roman Empire (ca. 1500 yr BP), more humid and cold climate conditions led to instability of the drainage network and repeated flood events (Stefani and Vincenzi, 2005) are recorded by ostracoda in terms of a relative (even though slight) increase in sediment supply in the study area from 22.00 m core depth. Moreover, ostracoda are suggestive of the predominant action of longshore currents, in accordance with the wave-dominated phase of the Po Delta during these times. The progressive approach of the Volano mouth (Correggiari et al., 2005; Fig. 2.16) is recorded by benthic foraminifera, that indicate a progressive increase of organic matter and vicinity to a river mouth at 18.00-15.75 m core depth.

The Ficarolo avulsion, a major avulsion event that shifted the entire Po drainage system to the northern sector of the Po Plain, occurred in 1152 AD (ca. 800 yr BP; Ciabatti, 1967). This event is likely recorded by benthic foraminifera, that indicate a decrease of organic matter inputs at 15.75-13.66 m core depth. Up to 8.80 m core depth the signal of benthic foraminifera and ostracoda is uniform: the former suggest high organic matter inputs, the latter high sediment supply, in proximity to the rapidly prograding Po River mouths. The uppermost portion of the succession, with rare benthic foraminifera and ostracoda is in accordance with deposition at the immediate vicinity of a fluvial mouth interested by flood sedimentation.

6.5 Conclusion and future perspectives

In this chapter I presented the record of benthic foraminifera and ostracoda within the shallow marine succession of core EM13, compared with the modern meiofaunal assemblages described in chapter 5. Benthic foraminifera and ostracoda provided different palaeoecological signal: the former gave insights about organic matter inputs ad relative distance from river mouths, the latter furnished indications about sediment input and dynamics. The stratigraphic distribution of meiofauna is in accordance with specific phases of the Po Delta evolution. Exclusively the combination of both meiofaunal represents a comprehensive tool to reconstruct in detail delta dynamics, at least within this fine-grained succession.

This is the first attempt of a quantitative assessment of the similarity between fossil and modern samples. In the next future, data about sediment geochemistry will be included to obtain indications about the sediment provenance and age-depth model will be constructed. I intend to apply the same techniques to shallow marine benthic foraminifera and ostracoda of a nearby Holocene sediment succession of the Po Delta, in order to test the reliability of meiofauna in a sector of the coastal plain that was subject to different coastal dynamics..

6.6 Supplementary material

	A. parkinsoniana-A. tepida	*A. perlucida*	*A. beccarii*	*N. turgida*	*Q. seminula*	*Cribroelphidium* ex gr. *granosum*	*Cribroelphidium* ex gr. *poeyanum*	*Adelosina* spp.	*A. mamilla*	*B. marginata*	*B. granulata*	*C. laevigata*	*Cribroelphidium* spp.	*Cycloforina* spp.	*E. advenum*	*E. crispum*	*L. lobatula*	*N. terquemi*	*Quinqueloculina* spp.	*R. bradyi*	*R. spinulosa*	*T. agglutinans*	*T. trigonula*	*S. aspera*
25.88	3.5	0.0	1.9	0.0	0.6	19.4	1.0	6.7	2.9	0.0	6.4	0.0	0.0	7.3	1.6	1.3	0.0	3.8	2.5	5.1	0.3	3.5	5.4	6.7
25.6	2.9	0.0	2.2	1.6	2.2	9.8	0.0	5.7	5.4	0.0	2.5	0.0	1.6	5.1	4.8	1.0	0.0	7.9	3.2	6.3	0.3	3.2	9.5	7.0
25.19	8.8	5.1	0.0	4.0	1.7	12.5	0.3	6.0	4.3	0.3	1.7	0.0	2.0	2.0	3.7	0.3	0.0	3.4	5.1	7.4	0.9	1.4	4.0	3.4
24.89	6.9	12.6	0.6	3.6	1.2	12.9	0.9	5.7	4.5	0.0	0.3	0.0	3.9	1.5	1.8	0.3	0.3	3.0	8.4	2.4	1.8	6.9	1.8	3.9
24.69	13.3	14.6	1.1	7.7	1.3	11.9	0.3	4.5	3.2	0.0	0.5	0.0	2.7	1.9	1.9	0.0	0.3	3.4	5.6	1.9	0.3	2.1	2.1	1.1
24.49	10.1	10.4	0.9	4.8	2.4	19.4	0.9	6.0	3.9	0.0	0.6	0.0	4.2	0.9	1.8	0.0	0.3	2.4	2.4	2.1	1.5	3.3	1.8	2.1
24.09	18.2	6.9	1.6	4.1	2.2	17.2	0.0	2.5	1.6	0.0	0.3	0.0	4.7	0.6	0.6	0.6	0.0	0.9	7.8	1.6	0.6	6.3	6.0	1.6
23.69	18.9	10.2	0.6	13.0	1.6	13.4	0.3	3.7	0.6	0.0	0.3	0.0	7.5	0.6	0.9	0.0	0.0	0.0	6.5	0.9	0.6	1.9	3.1	1.2
23.42	24.0	15.0	0.0	6.9	0.6	23.4	0.6	0.9	3.7	0.0	0.3	0.0	1.2	0.0	1.6	0.0	0.0	1.2	1.9	2.8	0.9	1.9	1.6	0.3
23.09	22.6	9.8	0.7	5.6	0.3	19.7	0.7	1.3	4.3	0.0	0.7	0.0	1.6	0.7	2.0	0.3	0.0	1.0	11.1	1.0	1.0	1.3	1.0	1.0
22.96	25.6	9.2	0.0	2.0	0.8	16.9	1.8	3.3	2.3	0.0	0.5	0.0	4.6	0.8	2.3	0.3	0.0	1.3	9.0	1.3	0.5	1.3	3.3	1.5
22.51	22.6	10.6	1.0	4.2	0.0	16.1	1.6	3.9	4.5	0.0	0.3	0.0	2.9	0.6	1.9	0.0	0.0	0.0	9.4	1.0	0.3	3.2	1.9	0.6
22.05	32.5	14.9	0.0	6.1	3.6	9.1	5.5	5.5	0.6	0.0	0.6	0.0	2.8	0.0	1.4	0.3	0.0	0.0	5.2	0.0	0.3	1.4	1.4	0.0
21.46	18.5	7.9	1.3	7.6	1.0	13.2	4.3	4.6	0.0	0.0	2.0	0.0	2.0	0.0	2.0	3.3	0.0	0.3	6.6	1.0	1.0	3.0	2.0	0.0
21.06	49.9	13.0	0.9	4.4	0.9	6.2	6.5	3.5	0.3	0.0	0.0	0.0	0.3	0.0	0.9	0.0	0.0	0.0	5.6	0.0	0.0	0.6	1.5	0.3
20.66	26.9	9.3	0.0	11.3	3.0	4.7	4.0	6.0	0.3	0.0	0.0	0.3	1.0	0.0	1.7	0.0	0.0	0.0	19.9	0.7	0.0	0.0	1.0	0.0
20.25	51.4	12.4	0.6	3.4	0.3	4.9	0.3	4.3	0.3	0.0	0.3	0.0	0.9	0.0	0.3	0.0	0.0	0.0	9.0	0.0	0.0	0.0	0.6	0.6
19.75	42.5	9.3	0.7	15.0	5.0	6.0	8.0	0.7	0.3	0.0	0.0	0.0	0.3	0.0	0.0	0.0	0.0	0.0	5.3	0.0	0.0	0.0	0.3	0.0
18.36	54.1	14.3	0.0	0.0	0.3	4.9	1.8	1.2	0.0	0.0	0.3	0.0	0.6	0.3	0.0	0.0	0.0	0.0	11.2	0.0	0.0	0.0	0.3	0.0
17.76	75.4	9.6	0.0	0.0	0.0	4.7	0.7	0.3	0.0	0.0	0.0	0.0	0.0	0.0	0.0	0.0	0.0	0.0	0.7	0.0	0.0	0.0	0.0	0.3
17.32	55.2	7.8	0.0	1.0	6.5	3.4	0.7	5.6	0.0	0.0	0.0	0.0	0.0	0.3	0.0	0.0	0.0	0.0	8.8	0.0	0.0	0.0	0.7	0.0
16.79	72.9	3.8	0.0	0.0	0.0	1.9	0.3	0.6	0.0	0.0	0.0	0.0	0.6	0.0	0.0	0.0	0.0	0.0	8.5	0.0	0.0	0.0	0.3	0.0
16.34	69.3	11.6	0.3	0.0	1.5	7.0	1.2	1.8	0.0	0.0	0.0	0.0	0.0	0.0	0.0	0.0	0.0	0.0	2.7	0.0	0.0	0.0	0.3	0.3
15.94	67.2	14.2	0.0	0.0	0.9	7.7	2.2	2.5	0.3	0.0	0.0	0.0	0.0	0.0	0.0	0.0	0.0	0.0	4.0	0.0	0.0	0.0	0.0	0.0
15.55	57.1	23.2	0.0	0.3	1.6	4.4	4.4	2.5	0.0	0.0	0.0	0.0	1.6	0.0	0.0	0.0	0.0	0.0	2.5	0.0	0.0	0.0	0.0	0.0
14.76	31.4	33.0	0.0	0.7	2.3	15.4	9.2	3.3	0.0	0.0	0.0	0.0	0.0	0.0	0.3	0.0	0.0	0.0	2.0	0.0	0.0	0.0	0.0	0.0
14.16	60.2	29.8	0.0	0.0	2.1	5.2	0.6	0.6	0.0	0.0	0.0	0.0	0.0	0.0	0.0	0.0	0.0	0.0	0.0	0.0	0.0	0.0	0.0	0.0
13.19	61.0	14.3	9.1	0.7	3.0	2.5	3.0	1.7	0.0	0.0	0.0	0.0	0.0	0.0	0.2	0.0	0.0	0.0	1.7	0.0	0.0	0.0	0.0	0.0
12.69	67.9	11.4	0.3	0.0	1.5	15.1	0.3	1.9	0.0	0.0	0.3	0.0	0.0	0.0	0.0	0.0	0.0	0.0	0.6	0.0	0.0	0.0	0.0	0.0
12.27	61.8	18.1	0.0	0.0	0.4	7.8	10.2	0.2	0.0	0.0	0.0	0.2	0.0	0.0	0.0	0.0	0.0	0.0	0.2	0.0	0.0	0.0	0.0	0.0
11.87	56.5	16.3	0.3	0.0	6.5	6.2	5.1	2.2	0.0	0.0	0.6	0.3	0.0	0.0	0.3	0.0	0.0	0.0	1.7	0.0	0.0	0.0	0.0	0.0
11.47	73.5	13.2	0.0	0.3	1.6	7.1	1.3	0.6	0.0	0.0	0.0	0.0	0.0	0.0	0.0	0.0	0.0	0.0	1.9	0.0	0.0	0.0	0.0	0.0
11.07	83.7	8.0	0.0	0.0	1.8	4.3	0.0	0.3	0.0	0.0	0.0	0.0	0.0	0.0	0.0	0.0	0.0	0.0	1.2	0.0	0.0	0.0	0.0	0.0
9.45	68.3	20.4	0.0	0.0	0.2	7.0	1.3	0.0	0.0	1.4	0.0	0.0	0.0	0.0	0.0	0.0	0.0	0.0	0.0	0.0	0.0	0.0	0.2	0.0
9.05	63.8	7.9	0.3	0.0	1.0	21.7	2.3	0.7	0.0	0.0	0.0	0.0	0.0	0.0	0.0	0.0	0.0	0.0	1.0	0.0	0.0	0.0	0.3	0.0

Tab. 6.2 Percentage values of the most common (>5%) taxa of benthic foraminifera recorded within analyzed samples of core EM13 including >300 tests.

	Aurila spp.	*Callistocythere* spp.	*C. whitei*	*Cytheretta* spp.	*Cytheropteron* spp.	*F. sphaerulolineata*	*Hemicytherura* spp.	*H. turbida*	*L. bacescoi*	*L. ramosa*	*Leptocythere* spp.	*Loxoconcha* ex gr. *rhomboidea*	*S. napoliana*	*Loxoconcha* aff. *bonaducei*	*N. fasciata*	*Palmoconcha turbida*	*P. jonesii*	*Paracytheridea* spp.	*Pontocypris* spp.	*Pontocythere turbida*	*Semicytherura* spp.	*S. incongruens*	*S. versicolor*	*X. dispar*
25.88	0.0	0.8	0.0	0.0	0.0	0.8	0.0	1.7	0.0	0.0	2.5	16.9	6.8	1.7	0.8	0.0	0.8	0.0	0.0	23.7	14.4	22.9	0.8	0.0
25.60	0.6	0.0	0.6	0.0	0.0	1.1	0.0	2.3	0.0	1.7	0.6	19.9	12.5	4.0	0.6	5.1	0.0	0.0	0.6	9.1	27.8	8.0	3.4	0.0
24.69	0.0	1.6	0.0	3.1	0.0	3.1	0.0	1.0	0.0	2.1	0.0	10.4	5.2	8.3	1.0	6.8	0.0	1.0	0.0	7.3	31.3	1.6	8.3	3.6
23.69	0.0	0.0	0.0	0.0	0.0	2.4	0.0	0.8	0.0	2.4	2.4	6.3	2.4	0.8	1.6	5.6	0.0	0.8	1.6	12.7	31.7	0.8	15.9	0.0
22.51	0.0	0.8	0.0	0.8	0.0	2.3	0.8	0.0	5.3	0.0	1.5	5.3	6.0	6.0	2.3	2.3	0.0	0.8	0.0	9.0	36.1	2.3	6.8	5.3
21.46	0.0	0.0	0.0	0.0	0.0	4.5	0.0	0.0	5.4	3.6	2.7	1.8	2.7	0.0	0.9	10.8	0.0	0.0	0.9	5.4	21.6	3.6	26.1	1.8
21.06	0.0	0.8	2.3	0.0	0.0	1.5	0.0	0.0	0.8	11.4	6.1	3.8	0.0	0.8	5.3	9.8	0.0	0.0	0.0	22.7	13.6	2.3	7.6	6.1
20.25	0.0	0.0	0.0	1.0	1.0	2.9	1.0	1.0	5.9	0.0	2.0	1.0	0.0	0.0	3.9	14.7	0.0	0.0	0.0	38.2	19.6	2.0	1.0	2.0
18.36	0.0	0.0	0.0	0.0	0.0	7.9	5.3	0.0	0.9	5.3	13.2	0.0	0.0	0.0	1.8	12.3	0.0	0.0	0.0	34.2	15.8	0.0	0.0	1.8
17.32	0.0	0.0	1.8	1.8	0.0	1.8	0.0	0.0	1.8	12.5	16.1	0.0	0.0	0.0	1.8	7.1	0.0	0.0	0.0	42.9	8.9	0.0	0.0	0.0
16.34	0.0	0.0	3.2	0.0	0.0	0.0	0.0	0.0	0.0	9.7	12.9	0.0	0.0	0.0	3.2	16.1	0.0	0.0	6.5	19.4	16.1	0.0	0.0	9.7
12.27	0.0	0.0	0.8	0.0	0.0	0.0	0.0	0.0	0.0	76.0	5.6	0.0	0.0	0.0	0.0	6.4	0.0	0.0	0.0	0.8	7.2	3.2	0.0	0.0
11.47	0.0	0.0	0.0	0.0	0.0	3.1	0.0	1.5	0.0	63.1	12.3	0.0	0.0	0.0	0.0	12.3	0.0	0.0	0.0	4.6	0.0	0.0	0.0	0.0
11.07	0.0	0.0	0.9	0.0	0.0	0.0	0.0	25.9	0.0	42.2	8.6	0.0	0.0	0.0	0.0	10.3	0.0	0.0	0.0	8.6	0.9	0.0	0.0	1.7
9.05	0.0	0.0	0.0	0.0	0.0	0.0	0.0	0.0	0.0	65.2	13.0	0.0	0.0	0.0	4.3	13.0	0.0	0.0	0.0	0.0	0.0	0.0	0.0	4.3
8.05	2.4	7.1	0.0	0.0	0.0	2.4	0.0	0.0	0.0	19.0	7.1	0.0	0.0	0.0	2.4	0.0	0.0	0.0	2.4	38.1	4.8	0.0	0.0	2.4

Tab. 6. 3 Percentage values of the most common (>5%) taxa of ostracoda recorded within analyzed samples of core EM13 including >20 valves.

k-closest analogues

k	25.88	25.6	25.19	24.89	24.69	24.49	24.09	23.69	23.42	23.09	22.96	22.51	22.05	21.46	21.06	20.66	20.25	
1	110	104	110	110	94	125	94	94	94	94	123	94	94	125	192	83	83	
2	104	110	104	115	125	110	122	182	182	182	125	189	192	182	163	94	192	
3	127	147	115	125	109	94	110	189	163	189	94	182	163	116	83	192	165	
4	147	128	125	104	182	123	125	109	189	125	192	125	182	81	189	182	106	
5	115	129	116	94	110	116	116	116	125	122	122	123	83	94	93	116	107	
6	129	115	147	147	116	182	123	83	80	81	182	122	125	80	92	125	163	
7	128	127	123	116	189	124	189	125	123	123	189	163	123	123	191	123	191	
8	103	103	129	123	123	115	115	123	93	192	116	192	189	189	94	189	92	
9	126	142	124	124	122	109	124	81	81	163	83	80	80	82	183	122	158	
10	102	126	142	182	81	122	109	192	183	80	124	81	116	122	185	109	93	
k	**19.75**	**18.36**	**17.76**	**17.32**	**16.79**	**16.34**	**15.94**	**15.55**	**14.76**	**14.16**	**13.19**	**12.69**	**12.27**	**11.87**	**11.47**	**11.07**	**9.45**	**9.05**
1	83	83	159	83	159	106	106	163	163	92	106	106	191	92	106	159	191	192
2	163	192	107	106	107	107	192	92	183	163	92	192	183	192	107	106	183	163
3	192	106	106	192	106	192	191	192	93	106	107	107	163	83	159	107	162	191
4	92	191	162	107	162	159	92	191	190	93	83	92	93	163	92	162	163	93
5	158	162	191	108	165	83	83	183	191	183	93	191	92	93	192	165	106	92
6	94	163	92	159	83	92	107	83	192	191	108	93	190	106	191	108	92	183
7	182	183	192	165	192	191	163	93	182	192	192	163	192	185	163	92	192	83
8	93	107	165	92	108	163	159	106	92	185	163	83	162	191	83	192	107	106
9	165	92	183	163	191	162	93	185	80	107	184	159	185	183	162	83	93	107
10	189	159	163	193	92	93	162	162	123	162	183	183	83	107	93	191	159	159

Dissimilarities for k-closest analogues

k	25.88	25.6	25.19	24.89	24.69	24.49	24.09	23.69	23.42	23.09	22.96	22.51	22.05	21.46	21.06	20.66	20.25	
1	0.542	0.531	0.538	0.557	0.569	0.56	0.544	0.526	0.509	0.575	0.55	0.516	0.437	0.389	0.369	0.564	0.457	
2	0.552	0.556	0.593	0.595	0.606	0.566	0.579	0.605	0.553	0.576	0.55	0.542	0.444	0.407	0.38	0.612	0.507	
3	0.569	0.572	0.594	0.605	0.612	0.569	0.58	0.618	0.575	0.583	0.566	0.564	0.454	0.422	0.403	0.639	0.523	
4	0.57	0.593	0.619	0.62	0.614	0.587	0.589	0.621	0.577	0.587	0.576	0.573	0.466	0.443	0.443	0.645	0.53	
5	0.575	0.597	0.624	0.645	0.62	0.604	0.592	0.634	0.589	0.606	0.584	0.596	0.467	0.444	0.448	0.645	0.554	
6	0.576	0.631	0.638	0.653	0.625	0.613	0.593	0.637	0.612	0.625	0.597	0.599	0.473	0.447	0.453	0.646	0.565	
7	0.593	0.634	0.646	0.665	0.631	0.613	0.609	0.639	0.612	0.627	0.6	0.6	0.475	0.45	0.453	0.661	0.566	
8	0.6	0.649	0.678	0.666	0.635	0.614	0.615	0.645	0.612	0.631	0.6	0.602	0.497	0.462	0.46	0.663	0.57	
9	0.604	0.659	0.678	0.682	0.65	0.619	0.617	0.649	0.613	0.636	0.607	0.609	0.507	0.464	0.471	0.665	0.584	
10	0.63	0.664	0.684	0.682	0.663	0.637	0.627	0.658	0.614	0.642	0.611	0.625	0.508	0.476	0.484	0.668	0.587	
k	**19.75**	**18.36**	**17.76**	**17.32**	**16.79**	**16.34**	**15.94**	**15.55**	**14.76**	**14.16**	**13.19**	**12.69**	**12.27**	**11.87**	**11.47**	**11.07**	**9.45**	**9.05**
1	0.467	0.506	0.375	0.419	0.385	0.384	0.452	0.459	0.418	0.487	0.327	0.448	0.376	0.395	0.415	0.356	0.457	0.437
2	0.488	0.509	0.415	0.449	0.448	0.41	0.471	0.469	0.447	0.495	0.347	0.469	0.377	0.396	0.448	0.366	0.469	0.44
3	0.506	0.529	0.422	0.494	0.45	0.426	0.481	0.478	0.47	0.505	0.363	0.474	0.388	0.406	0.449	0.388	0.472	0.449
4	0.513	0.538	0.441	0.506	0.495	0.438	0.486	0.481	0.514	0.517	0.412	0.478	0.42	0.408	0.455	0.492	0.482	0.451
5	0.517	0.559	0.48	0.525	0.549	0.439	0.489	0.489	0.518	0.519	0.421	0.479	0.423	0.43	0.467	0.516	0.487	0.474
6	0.526	0.56	0.505	0.527	0.558	0.454	0.49	0.494	0.526	0.521	0.424	0.485	0.449	0.43	0.477	0.52	0.493	0.486
7	0.54	0.561	0.513	0.55	0.565	0.473	0.493	0.499	0.529	0.534	0.428	0.488	0.45	0.446	0.482	0.526	0.5	0.494
8	0.55	0.566	0.526	0.56	0.58	0.475	0.499	0.501	0.531	0.539	0.429	0.491	0.478	0.451	0.492	0.539	0.502	0.509
9	0.553	0.567	0.531	0.584	0.595	0.492	0.518	0.519	0.548	0.545	0.445	0.503	0.482	0.469	0.497	0.549	0.508	0.513
10	0.557	0.569	0.542	0.588	0.613	0.494	0.521	0.545	0.549	0.552	0.483	0.526	0.528	0.479	0.51	0.565	0.511	0.527

Tab. 6.4 Results of the AM technique for benthic foraminifera, with the 10 closest modern analogues for each fossil sample. The first four analogs, used for the interpretation of assemblages, are colored in accordance with biofacies presented in chapter 5.

k-closest analogues

k	25.88	25.6	24.69	23.69	22.51	21.46	21.06	20.25	18.36	17.32	16.34	12.27	11.47	11.07	9.05
1	138	138	138	138	138	162	83	83	83	83	80	162	162	162	162
2	104	98	98	139	98	101	80	106	171	118	83	95	95	181	95
3	130	104	101	98	139	98	139	171	139	171	192	181	181	188	181
4	139	139	139	101	104	80	138	139	106	132	190	188	80	92	80
5	171	101	104	142	101	138	192	138	138	106	162	80	188	190	92
6	142	142	162	104	142	142	98	118	132	131	82	96	190	80	190
7	128	110	142	83	135	190	97	132	131	139	139	89	92	95	188
8	103	97	135	162	162	81	132	131	97	170	138	92	96	96	89
9	170	83	83	97	83	135	142	97	80	97	98	190	89	192	96
10	98	162	80	171	110	86	171	130	118	138	84	192	192	83	163

Dissimilarities for k-closest analogues

k	25.88	25.6	24.69	23.69	22.51	21.46	21.06	20.25	18.36	17.32	16.34	12.27	11.47	11.07	9.05
1	0.24	0.371	0.383	0.364	0.384	0.399	0.21	0.237	0.24	0.248	0.24	0.587	0.477	0.416	0.495
2	0.248	0.379	0.389	0.384	0.398	0.404	0.283	0.26	0.306	0.299	0.257	0.693	0.571	0.45	0.589
3	0.259	0.383	0.399	0.387	0.404	0.408	0.285	0.272	0.309	0.302	0.313	0.699	0.595	0.454	0.616
4	0.264	0.394	0.401	0.394	0.41	0.412	0.287	0.284	0.311	0.306	0.329	0.729	0.596	0.468	0.62
5	0.265	0.403	0.405	0.411	0.411	0.422	0.295	0.293	0.314	0.315	0.333	0.738	0.621	0.469	0.638
6	0.269	0.409	0.408	0.413	0.435	0.424	0.301	0.295	0.318	0.317	0.34	0.738	0.625	0.469	0.643
7	0.272	0.413	0.417	0.413	0.438	0.425	0.307	0.299	0.329	0.33	0.345	0.738	0.63	0.473	0.644
8	0.277	0.431	0.426	0.416	0.439	0.431	0.308	0.304	0.331	0.341	0.346	0.756	0.631	0.475	0.655
9	0.279	0.434	0.427	0.433	0.446	0.431	0.309	0.316	0.334	0.342	0.353	0.757	0.635	0.496	0.655
10	0.281	0.44	0.44	0.434	0.455	0.432	0.313	0.317	0.341	0.348	0.365	0.758	0.638	0.508	0.668

Tab. 6.5 Results of the AM technique for ostracoda, with the 10 closest modern analogues for each fossil sample. The first four analogs, used for the interpretation of assemblages, are colored in accordance with biofacies presented in chapter 5.

7. THREE-FOLD NATURE OF THE PO PLAIN HIGHSTAND SUCCESSION

7.1 Manuscript II

Three-fold nature of coastal progradation during the Holocene eustatic highstand, Po Plain, Italy—close correspondance of stratal character with distribution patterns*

Alessandro Amorosi, Giulia Barbieri, Luigi Bruno, Bruno Campo, Tina M. Drexler, Wan Hong, Veronica Rossi, Irene Sammartino, Daniele Scarponi, Stefano Claudio Vaiani and Kevin M. Bohacs

*****Submitted to **Sedimentology**

Alessandro Amorosi[1], Giulia Barbieri[1], Luigi Bruno[1], Bruno Campo[1], Tina M. Drexler[2], Wan Hong[3], Veronica Rossi[1], Irene Sammartino[4], Daniele Scarponi[1], Stefano Claudio Vaiani[1] and Kevin M. Bohacs[5]

Three-fold nature of coastal progradation during the Holocene eustatic highstand, Po Plain, Italy—close correspondance of stratal character with distribution patterns

1. Department of Biological, Geological and Environmental Sciences, University of Bologna, Via Zamboni 67, 40126 Bologna, Italy
2. ExxonMobil Development Company, 22777 Springwoods Village Parkway, Spring, TX 77389, USA
3. KIGAM Korea Institute of Geoscience and Mineral Resources, 92 Gwahangro, Yuseong-gu, Daejeon Metropolitan City, Korea
4. Geologic consultant, Bologna, Italy
5. ExxonMobil Upstream Research Company, 22777 Springwoods Village Parkway, Spring, TX 77389, USA; retired

ABSTRACT

Although general trends in transgressive to highstand sedimentary evolution are well known, the details of the turnaround from retrogradational (typically estuarine) to aggradational-progradational (typically coastal/deltaic) stacking patterns are not fully resolved. Following eustatic stabilization, around 7.7 cal ky BP, the middle-late Holocene sedimentary evolution of the Po Delta records a complex pattern of delta upbuilding and 60 km of coastal progradation. Distinctive sedimentological, paleoecological (benthic foraminifers, ostracods, mollusks) and compositional features were used to distinguish facies associations and sediment-dispersal pathways within a radiocarbon-date chronologic framework.

A three-stage progradation model was reconstructed for the Holocene eustatic highstand succession (HST): 1) Just as eustasy achieved highstand (7.7-7.0 cal ky BP), rapid bay-head delta progradation (~5 m/yr), fed mostly by the Po River, took place within a mixed, freshwater and brackish estuarine environment. 2) A dominantly aggradational parasequence set in the lower HST (7.0-2.0 cal ky BP) records the development of a shallow, wave-dominated shoreline fed alongshore, with slow coastal progradation (~2.5 m/yr). 3) The final stage of the eustatic highstand (<2 cal ky BP) saw the upbuilding of faster prograding (~15 m/yr), river-dominated Po delta lobes into significantly deeper (30 m) waters (upper HST).

This study documents the close correspondence of stratal character with sediment distribution patterns within the HST. The major shift from a dominantly aggradational (lower HST) to a fully progradational (upper HST) stacking occurs at a surface named the "A-P surface". This surface demarcates remarkable changes in sediment characteristics, paleoenvironments and direction of sediment transport that reflect the transition from a wave-dominated to a river-dominated deltaic system. Identifying the A-P surface through detailed paleoecologic and compositional data can help guide interpretation of the rock record, especially in mudstone-dominated systems, where facies assemblages and their characteristic geometries are difficult to discern from physical sedimentary structures alone.

Keywords: Progradation, Delta, Paleoecology, Sediment provenance, Holocene, Po Plain

INTRODUCTION

According to conventional sequence stratigraphic models, aggradational to progradational stacking patterns typify prograding deltas and shorelines within the highstand systems tract (HST – Posamentier and Vail, 1988; Van Wagoner et al., 1990; Posamentier and Allen, 1999; Neal and Abreu, 2009). Below the HST, retrogradational parasequence sets (i.e., transgressive systems tracts - TST) comprise backstepping barrier-lagoon-estuary depositional systems on top of fluvial and coastal-plain strata, typically deposited as base level rises (Dalrymple et al., 1992; Allen and Posamentier, 1993; Cattaneo and Steel, 2003; Catuneanu et al., 2009). Criteria for systems tract recognition and for identifying the boundary between TST and HST (maximum flooding surface or MFS) are well established: in seismic stratigraphy, this key stratigraphic surface corresponds with a prominent downlap surface. On a basin scale, the MFS marks the change from retrogradational to aggradational and progradational stacking patterns. On vertical (outcrop or core) profiles, the MFS represents the turnaround from deepening-upward to shallowing-upward trends. In downdip cross-sections, characteristic convex up shoreline trajectories are diagnostic of highstand normal regression, i.e. decelerating base-level rise (Catuneanu et al., 2009).

Although general trends in transgressive to highstand sedimentation are known to reflect the balance between accommodation and sediment supply (‘A/S ratio’, Muto and Steel, 1997), there is a limited awareness of how retrogradational (typically estuarine) trends are succeeded by aggradational-progradational (typically coastal/deltaic) stacking patterns on a detailed depositional system scale (Milli et al., 2013; Aschoff et al., 2018). In addition, the factors that control the dynamics of coastal progradation still need to be understood and acknowledged. The major sources of uncertainty, especially for subsurface sedimentary successions, include: (i) poor facies characterization of prograding sediment bodies, (ii) challenging reconstructions of sediment dispersal systems, (iii) lack of information about the magnitude of depositional hiatuses and stratigraphic condensation recorded at parasequence boundaries. Mudstone-dominated systems, in particular, are central components of modern hydrocarbon exploration (Schieber, 1998; 2016; Macquaker and Bohacs, 2007; Macquaker et al., 2010; Wilson and Schieber, 2014). In these seemingly homogeneous depositional systems, the presence of subtle heterogeneities has been widely overlooked and only few studies have focused on detailed measured sections (Bohacs et al., 2014; Plint, 2014; Lazar et al., 2015; Kietzmann et al., 2016; Birgenheier et al., 2017).

Several historical papers have outlined the general features of middle to late Holocene highstand progradation (Curray and Moore, 1964; Oomkens, 1970; Frazier, 1974; Demarest and Kraft, 1987; Stanley and Warne, 1994), but only few recent studies have framed Holocene successions into chronologically constrained stratigraphic reconstructions, through hundreds of radiocarbon dates (Tanabe et al., 2015; Amorosi et al., 2017). None of these studies, however, has examined in detail the sedimentological features of highstand depositional systems through careful paleoecological investigation and sediment provenance reconstructions.

The goal of this study is to provide a robust model for complex, Holocene highstand coastal development and evolution based on a chronologically well-constrained and cored example—the Po Delta system, northern Italy (Amorosi et al., 2017). Our specific objective is to examine the potential of a carefully integrated paleontologic and geochemical approach for the reliable interpretation of mud-dominated prograding successions, where subtle heterogeneities can be difficult to decipher based on sedimentologic data alone.

.

GEOLOGICAL BACKGROUND

The Po Plain, northern Italy, is bounded by the Alps to the north, the Apennines to the south, and opens to the Adriatic Sea to the east (Fig. 1). The Po River, 652 km in length, flows from W to E across the Po Plain into the Adriatic Sea, where it forms the Po Delta.

Throughout the Middle-Late Pleistocene, alternating continental and shallow-marine deposits record a series of transgressive-regressive cycles on ca. 100 ka timescales (Amorosi et al., 2004). A weakly developed paleosol related to the Younger Dryas cold reversal demarcates the transition from Late Pleistocene alluvial deposits into the Holocene transgressive-regressive cycle (Amorosi et al., 2016). Detailed stratigraphic correlations based on ~150 radiocarbon dates have recently resulted in the identification of a series of millennial-scale Holocene parasequences (Amorosi et al., 2017; Bruno et al., 2017). Early Holocene parasequences record alternating periods of rapid flooding and gradual shoaling, and are stacked in a retrogradational pattern. Conversely, middle to late Holocene parasequences record a complex pattern of coastal progradation and delta upbuilding. For detailed paleogeographic reconstructions of transgressive parasequence architecture, the reader is referred to Bruno et al. (2017). This paper expands on previous work and focus on the highstand prograding succession (HST).

The Holocene highstand succession is a siliciclastic, mud-rich deltaic depositional system up to 30-m thick (Campo et al., 2017). It comprises an aggradational to progradational parasequence set (Amorosi et al., 2005, 2017) that laps down onto a prominent, fossiliferous condensed section (Fig. 2; Scarponi et al., 2013; 2017a). The component parasequences (coarsening-upward successions) likely reflect shoreline and delta progradation (Rizzini, 1974; Amorosi et al., 1999; Stefani and Vincenzi, 2005). Progradation was dominantly controlled by distributary channel avulsion and delta lobe switching, which led to the development of five parasequences of limited areal extent (parasequences 4 to 8 in Amorosi et al., 2017)

The study area, between the city of Ferrara and the Adriatic Sea (Fig. 1), represents the almost flat coastal portion of the Po Plain. This region formed starting circa 7.7 cal ky BP, when the shoreline was about 30 km inland of its present position (Rizzini, 1974; Amorosi et al., 1999). The HST onshore is genetically related to the rapidly deposited mud wedge that accumulated on the shelf for 600 km along the Adriatic Coast of Italy (Trincardi et al., 1996; Cattaneo et al., 2003; Campo et al., 2017).

The toe of the modern Po Delta has been observed at 25-30 m water depth (Correggiari et al., 2005a), and the dynamics of recent delta progradation have been outlined in detail by Correggiari et al. (2005b). Along the mud-dominated Adriatic coastline, inner-shelf mud belts are typically elongated downdrift of the Po River mouth, and the whole modern Po delta system shows a marked asymmetry that reflects prevailing sediment dispersal to the south (Cattaneo et al., 2003; 2007). The modern Po Delta dates back to the early 17th century, when massive hydraulic works ("Porto Viro cut or bypass" – Ninfo et al., 2018) formed one of the largest anthropogenic deltas in the world (Maselli and Trincardi, 2013). Unlike the majority of modern deltaic systems, which have been subjected to fast degradation and shoreline retreat due to the post-1950 marked reduction in sediment supply (Blum and Roberts, 2009; Syvitski et al., 2009), the Po Delta has resumed progradation in the last decade (Ninfo et al., 2018).

METHODS

Fifteen cores were investigated through detailed sedimentologic and paleontologic investigations. These cores were acquired between the city of Ferrara and the modern Po Delta (Fig. 1). Each core data set evaluated in this study spans approximately 25-35 m, i.e. the thickness of the Holocene succession. A total of 140 core descriptions from the Regione Emilia-Romagna stratigraphic database were made available for study (Fig. 1).

Facies analysis was carried out on a centimeter scale. Graphic logs of cores include description of lithology, grain size, primary sedimentary structures, lamination styles, bioturbation levels, and accessory components. The paleoecological characterization of facies assemblages was based upon benthic foraminifers, ostracods, and mollusks. Benthic foraminifer and ostracod analyses were performed on a total of 80 samples from four cores (EM5, EM11, EM13, 187-S6 in Fig. 1), to provide detailed paleoenvironmental information in terms of salinity oscillations, vegetation coverage, riverine organic-matter content and oxygen concentration. These data were integrated with previously published micropaleontological data from cores 205-S5, 205-S7, Core 1, and Core 7 (187-S7 in Fig. 1) (Amorosi et al., 2005; Rossi and Vaiani, 2008; Barbieri et al., 2017).

Core samples were analyzed following the standard procedure reported in Amorosi et al. (2014a) and autochtonous *vs.* allochtonous fossil assemblages were distinguished on the basis of the test preservation state. Three categories of relative abundance (abundant: >30%, common: 30-10%, scarce: <10%) were adopted (Table 1). Taxa identification and autoecological data were based on reference papers, including Bonaduce et al. (1975), Jorissen (1988), Athersuch (1989), Sgarrella and Montcharmont-Zei (1993), Fiorini and Vaiani (2001), and Milker and Schmiedl (2012). Paleoenvironmental interpretations of microfossil assemblages are supported by the recent distribution of taxa in the Northern Adriatic Sea (Colalongo, 1969; D'Onofrio, 1969; Breman, 1975, Jorissen, 1988; Donnici and Serandrei Barbero, 2002) and by comparison with assemblages from other Holocene coastal to shallow-marine successions of the Mediterranean area (e.g., Di Bella and Casieri, 2011; Amorosi et al., 2013; Di Bella et al., 2013; Dinelli et al., 2013; Rossi et al., 2017).

As for mollusks, 8 cores were investigated (205-S2, 205-S4, 205-S5, 205-S6, 205-S7, 205-S9, 205-S10 and EM5 in Fig. 1 – see also Wittmer et al., 2014; Kowalewski et al., 2015) and 151 samples, each representing a ca. 5 or 10-cm core interval, were selected for paleoenvironmental inferences. These samples are typically dominated by extant mollusks with well-understood biology and ecology. In addition, standardized volumes of samples allowed us to track changes in fossil abundance (average density and interquartile range or IQR) and dominant taxa across the sedimentary succession.

A total of 112 core samples and 31 river sediment samples were analyzed for bulk-sediment geochemistry. Modern river sediments were collected from exposed bars or subaqueous channel beds, and all grain sizes, from coarse sand to mud, were considered. Geochemical analyses were performed at University of Bologna. Samples were oven dried at 50°C, powdered and homogenized in an agate mortar and analyzed by X-ray fluorescence (XRF) spectrometry using a Philips PW 1480 spectrometer. The matrix correction methods of Franzini et al. (1972), Leoni and Saitta (1976), and Leoni et al. (1982) were followed. The estimated precision and accuracy for trace-element determinations was 5%. For elements with low concentrations (<10 ppm), the accuracy was 10%.

The Po Basin is a multi-sourced foreland basin system with strongly heterogeneous compositional signatures, where exclusive catchment lithologies can be used to delineate basin-wide markers of sediment provenance and trace detrital signatures across downdip segments of the sediment dispersal system (Amorosi and Sammartino, 2018). It has been documented that trace metals hosted preferentially in mafic and ultramafic rocks, such as Cr, can carry clear provenance signals even in distal segments of the routing system (von Eynatten et al., 2003; Amorosi, 2012; Garzanti, 2016). The original provenance signal can be confounded by changes in grain size, but alumina is effective as a normalization factor (Covelli and Fontolan, 1997; Menon et al., 1998; Liaghati et al., 2004): Cr/Al_2O_3, in particular, has been tested successfully in Po Plain sediments for the discrimination of mafic/ultramafic versus non-mafic/ultramafic source-rock composition (Amorosi et al., 2002; Curzi et al., 2006; Amorosi, 2012; Di Giuseppe et al., 2016). The best proxy for carbonate (dolostone) versus siliciclastic contribution based on single ratios was obtained by MgO/Al_2O_3 (Amorosi et al., 2002, 2007; Curzi et al, 2006; Greggio et al., 2018), which in this area closely reflects the abundance of dolomite in the sediment (Marchesini et al., 2000). Comparison of whole-rock geochemistry from cored samples with composition of modern soil sediments demonstrates that the effects of weathering and post-depositional diagenesis on geochemical element distribution in Holocene deposits are negligible (Amorosi et al., 2014b).

MIDDLE TO LATE HOLOCENE STRATIGRAPHIC ARCHITECTURE

The middle-late Holocene succession of the Po Delta forms an aggradational to progradational parasequence set (Amorosi et al., 2017) made up of discrete delta lobes with significantly different characteristics (Fig. 2). In general, the coastal depositional system follows a proximal-distal trend of finer grain size. The sand to mud ratio decreases at successively eastward positions, and individual clinothems, i.e. distinct delta lobes, thin out in the same, seaward direction. Thus, coastal progradation dynamics are well portrayed by depositional dip-oriented (SW-NE) cross-sections (Fig. 2).

Based on stratal patterns and facies stacking relative to key bounding surfaces, the middle-late Holocene succession of the Po delta area was subdivided into three intervals (uppermost TST, lower HST, and upper HST – units 1–3 in Fig. 2), each of which contains characteristic depositional systems with distinct paleontologic and compositional attributes (Figs. 4, 6). These three stratigraphic intervals are described in chronological order, with a special emphasis on the deltaic facies (Fig. 3).

Uppermost TST (~7.7-7.0 cal ky BP)

Description

The topmost unit of backstepping (TST) estuarine deposits consists of a laterally continuous, <5 m-thick sand body which transitions basinwards to a thin, predominantly muddy unit (Fig. 2). The sand body is bounded below, above, and proximally by soft clays with relatively high organic matter content. It is 4-5 m thick, extends about 5 km down dip (Fig. 2) and correlates 9 km along strike (Bruno et al., 2017). Above an erosional surface, sand-sized sediment is coarse to fine-grained, and exhibits a generally fining-upward (FU) trend, although coarsening-upward (CU) successions are also encountered. Vegetal remains and wood fragments are abundant.

Rare microfossils are present in the sandy lithofacies (Fig. 4A): they are represented by abraded or broken ostracod valves of the euryhaline *Cyprideis torosa*, locally accompanied by freshwater-hypohaline *Ilyocypris* spp. The macrofaunal content shows variable fossil density (average 49 spec./dm^3; IQR 6-202; Fig. 5); the most commonly observed taxa are *A. segmentum*, *Lentidium mediterraneum* and hydrobiids (see Fig. 6A and Table 1).

The muddy facies is dominated by soft clay and silty clay, with faint lamination due to clay-silt alternations, a few mm to cm-thick. This lithofacies assemblage has homogeneous gray color, and only local abundance of plant and wood fragments. Microfossils are abundant and consist of well-preserved foraminifers and ostracods. Foraminiferal assemblages are dominated by *Ammonia parkinsoniana* and *Ammonia tepida* with the common occurrence of *Haynesina germanica* and *Cribroelphidium granosum*. In contrast, the ostracod fauna is of low diversity, being mainly composed of *Cyprideis torosa* and, subordinately, of *Loxoconcha elliptica* and *Leptocythere* species (Fig. 4B and Table 1). The most abundant mollusk species are the brackish bivalves *Abra segmentum* and *Cerastoderma glaucum* (Fig. 6B; Scarponi et al., 2017b). Continental mollusks were also encountered. In less confined areas, the small nearshore corbulid *Lentidium mediterraneum* and the grazer gastropod *Bittium* spp. are also present (Bruno et al., 2017).

Sediment composition from 9 sand samples revealed Cr/Al_2O_3 values between about 9.5 and 14, and low MgO/Al_2O_3 ratios (generally <0.4; Fig. 7). The overall carbonate content is very low, and CaO ranges between about 4% and 8.5%, with a median value of 5.1% (Fig. 5). Elevated levels of elemental sulfur, commonly in the range of 500-2000 mg/kg, are an additional diagnostic feature of this facies tract.

Interpretation

The muddy portion of this facies association likely accumulated in an outer estuarine environment subject to short-lived salinity fluctuations, as documented by micro- and macrofossil assemblages with dominant opportunistic and euryhaline species, such as *A. tepida, C. torosa* (Pint and Frenzel, 2017) and bivalve species *A. segmentum* and *C. glaucum*. This interpretation is also supported by the presence of taxa tolerant of restricted conditions and high organic matter content (*A. parkinsoniana, C. granosum, H. germanica, L. elliptica*). The formation of a wave-dominated estuary during the early Holocene and its backstepping evolution under transgressive conditions have been detailed by Bruno et al. (2017).

Estuarine muds can be linked stratigraphically upstream to proximally equivalent sand bodies, which lie at the boundary between freshwater and brackish environments (Fig. 2). Given the small-scale (~5 m) clinoform and mixed, freshwater-brackish fossil content, these sands are interpreted to have been deposited dominantly by river processes at the head of the estuary, thus representing bay-head deltas within a back-barrier environment (Aschoff et al., 2018). The poor preservation state of ostracods is consistent with continuous reworking under high-energy conditions. Sand bodies with erosional base and marked FU trends are attributable to distributary channels, whereas CU successions are more likely to have formed at bay-head delta mouths.

Based on bulk-sediment geochemistry, the Po River represented the fluvial feeder system of most bay-head delta sands (Fig. 7). Relatively high Cr/Al_2O_3 and very low MgO/Al_2O_3 and CaO% fall very close to the compositional field of modern Po River sediments (Fig. 7). The elevated elemental sulfur concentrations are consistent with sulfate-containing environments, typically wetlands, estuaries or lagoons (Gerardi and Lytle, 2015).

Lower HST (~7.0-2.0 cal ky BP)

Description

The lower HST exhibits a distinctive aggradational to slightly progradational stacking pattern of facies (Fig. 2). Proximal, coarse-grained lithofacies forms an amalgamated sediment body, 5 to 10 m thick, that consists predominantly of very fine to coarse sand (Fig. 2). Silt admixed with very fine sand is more abundant basinwards. On vertical profiles, silt interlamination frequency and thickness increase upwards. Individual sand layers are faintly laminated, with low-angle lamination and gently curved surfaces that possibly reflect hummocky cross-stratification (Harms et al., 1975).

Microfossils are represented by broken or abraded tests of the foraminifer *Ammonia beccarii* (Fig. 4C); well preserved miliolids and other *Ammonia* species are locally present at basinward locations (Table 1). The macrofaunal content of the sandy lithofacies is characterized by high fossil density (average 215 spec/dm^3; IQR 21-438; Fig. 5). Nearshore bivalves *Lentidium mediterraneum*, *Chamelea gallina,* and *Spisula subtruncata* are the most abundant species in at least 50% of examined samples (Fig. 6C, Table 1).

The fine-grained lithofacies, mostly developed in the outer portion of this facies tract (Fig. 2), is up to 10-m thick, and may have a homogenous or mottled texture. Sand-mud alternations and muds are moderately to heavily bioturbated (Fig. 3A-C). Where high bioturbation levels are present, only remnant primary sedimentary structures, such as small wave ripples, are visible (Fig. 3C). Clinoform height as deduced from the stratigraphic panel is <15 m (Fig. 2), and individual lobes become thinner in a basinward direction.

Muds show a markedly different and more diversified microfossil content than the sandy lithofacies (Table 1). The foraminiferal assemblage is characterized by variable amounts of *A. parkinsoniana*, *A. tepida*, *Aubignyna perlucida*, *C. granosum*, and a variety of miliolids, accompanied by subordinate *Nonionella turgida* and hyaline epiphytic taxa. The ostracod fauna includes large amounts of *Semicytherura* spp. and *Loxoconcha* gr. *rhomboidea*, along with *Palmoconcha turbida*, *Pontocythere turbida* and *Sagmatocythere* spp. (Fig. 4D). The muddy lithofacies is typified by more dispersed macrofossil assemblages, dominated by *Corbula gibba*, *Chamelea gallina,* and *Turritella communis* species (Fig. 6D). The average fossil density is less than half of the sandy lithofacies (average 104 spec/dm^3; IQR 35-176; Fig. 5).

Major- and trace-element compositions of 34 core samples from this stratigraphic interval show variable Cr/Al_2O_3 ratios (9–14; Fig. 5), but invariably high MgO/Al_2O_3 ratios (up to 2.4, with median value of 0.7; Figs. 5 and 7). The overall carbonate content is also remarkably high, as indicated by very high CaO values (median value is 14.4%; Fig. 5).

Interpretation

The general abundance of sand and of coastal microfossils reflects deposition above storm-wave base. The progressively lower levels of fossil preservation in a landward direction is considered to reflect higher hydrodynamic conditions. Remnant lamination in the sandy lithofacies indicates active currents in a high-energy regime. Reworking by storms waves is supported by the presence of sand beds showing faint hummocky cross-stratification and oscillation ripples. Intense bioturbation clearly indicates biogenic activity during fair-weather periods under conditions of very low sedimentation rates. In the distal parts of the system, the paucity of sand, dominance of silt and higher bioturbation levels indicate a lower energy depositional regime relative to the updip wave-influenced deposits. The diversified meiofauna points to a shallow marine environment with a dense vegetation cover, as shown by several ostracod species (*Loxoconcha* gr. *rhomboidea*, *Pontocythere turbida*, *Sagmatocythere napoliana*, *Sagmatocythere versicolor*) and selected foraminifers (miliolid and hyaline epiphytic taxa). The relative abundance of *A. parkinsoniana*, *A. tepida*, *A. perlucida*, *C. granosum* and *Palmoconcha turbida* indicates a variable riverine influence.

Ecological traits of the most abundant mollusk taxa within the lower HST clearly depict a shallowing-upward trend. The dominance of mollusk species that commonly peak in abundance at less than 15-m water depth (Wittmer et al., 2014) supports the hypothesis of coastal/deltaic progradation in shallow waters. In addition, the relatively high average density of fossil remains may reflect low sedimentary inputs, although changes in the production rates of skeletal remains may have also played a role in forming such fossil-rich deposits.

The vertical organization of facies, which is typically reflected by the CU succession, and the development of extensive sheet sands are interpreted to reflect the outbuilding of wave-influenced (Bhattacharya and Giosan, 2003) to wave-dominated (arcuate) delta systems, with local development of strandplains shaped by the longshore drift.

Geochemical compositions of cored samples plot far from the field of modern Apennine rivers (Fig. 7), but also display scarce overlap with the Po River end-member (Fig. 7). In contrast, bulk-sediment geochemistry exhibits closer affinity with the MgO-rich compositions typical of sediments derived from Eastern Alpine source rocks (Fig. 7). A sediment provenance from limestone and dolostone source rocks is also supported by very high CaO contents (Fig. 5). As geochemical data from both sands and muds clearly suggest a mixed sediment contribution of Po River and Eastern Alpine end-members, it is argued that sand was partly transported by longshore currents, whereas mud was probably resuspended by storms and wave action above storm wave base, and advected alongshore by geostrophic currents for long distances along the paleoshelf. In the relatively deeper parts of the delta, a partial control on sedimentation by current-enhanced or wave-enhanced sediment gravity flows cannot be ruled out (Macquaker et al., 2010; Birgenheier et al., 2017).

Upper HST (< 2.0 cal ky BP)

Description

A strong progradational stratigraphic motif and a large proportion of mud characterize the upper HST interval in the study area (Fig. 2). The proximal part of this facies tract consists of amalgamated sand bodies, 5 to 10 m thick. Grain size ranges from very fine to coarse sand. Sand is structureless to cross-stratified, with abundant allochthonous plant material and rare foraminifers (Fig. 4E), including well preserved *A. parkinsoniana* and *A. tepida*, along with poorly preserved specimens of planktonic and benthic taxa, such as *Globigerina, Globigerinoides*, *Orbulina*, *Cassidulina*, and *Bulimina* (Table 1). The macrofauna includes relatively low density (average 43 spec./dm^3, IQR 15-118; Fig. 5) and oligotypic *L. mediterraneum* assemblages (Fig. 6E, Table 1).

Basinwards, this facies tract consists of interlayered, millimeter- to centimeter-thick silt to clay couplets (sand proportion is <2%) that typically exhibit normal grading with locally scoured bases (Fig. 3D). The deposit is largely devoid of burrowing (Fig. 3D-F). Rare sand layers show flat-to-undulating lamination (Fig. 3E). Current-generated (asymmetric) ripples are present, whereas wave-modified current ripples are also common. The meiofauna consists of several opportunistic species, such as *A. tepida*, *N. turgida, A. perlucida, Haynesina* spp., *Palmoconcha turbida*, *Leptocythere ramosa* and, to a lesser extent, *Pontocythere turbida* (Fig. 4F). The muddy lithofacies is commonly barren in macrofauna or represented by low density (7 spec./dm^3, IQR 0-43) and variable suites of species (Fig. 6F). Of the three most abundant taxa, none is present in at least 50% of all samples (Table 1).

XRF analysis of 69 core samples, from coarse sand to clay reveals a very narrow range of compositions, with generally high Cr/Al_2O_3 values (Figs. 5 and 7) and remarkably low MgO/Al_2O_3 ratios (<0.4 in Figs. 5 and 7). The overall geochemical composition of the upper HST is similar to sediment composition from the uppermost TST, and the CaO content is invariably lower than in the lower HST, with scarce or no overlap (median value is 8.3%; Fig. 5).

Interpretation

Low bioturbation intensities and a predominance of graded beds are interpreted as indicators of fluvially-dominated delta-front units (Bhattacharya and MacEachern, 2009). Abundant plant material suggests derivation from a terrestrial source (e.g., Bohacs et al., 2014). Current features, such as scours and low-angle lamination indicate tractional flow. Normal grading records waning flow conditions. Sand-silt couplets are interpreted to reflect river-generated hyperpycnal flows, in a prodeltaic environment (Mulder and Syvitski, 1995; Mulder et al., 2003, Bhattacharya and MacEachern, 2009; Schieber, 2016). Hyperpycnal plumes were related to times of elevated river discharge during floods. Rapid sediment deposition in the prodelta environment led to significant soft-sediment deformation, testified by the abundance of dewatering structures (Bohacs et al., 2014; Birgenheier et al., 2017).

Paucity of fossil recovery and low diversity benthic assemblages are attributed to the very high-energy depositional regime and to deposition rates that exceeded colonization rates by benthic communities. Sparse bioturbation is consistent with high physical and chemical stresses in hyperpycnal environments (Bhattacharya and MacEachern, 2009).

The most abundant mollusk taxa retrieved in both sandy and muddy lithofacies are commonly indicative of a highly stressed regime characterized by high net sedimentation rates (Scarponi and Angeletti, 2008) or frequent changes in environmental conditions. Diluted microfossil concentrations of *A. parkinsoniana* and *A. tepida* in sandy intervals are consistent with a river-influenced, shallow-marine depositional environment, close to a river outlet (mouth bar). Poorly preserved foraminifers from a variety of water depths are interpreted to reflect transport from adjacent environments and/or reworking from older units. Small numbers of *Ammonia*, locally accompanied by planktonics are observed in proximity of modern Po River mouths, at water depths <15 m (D'Onofrio, 1969). In contrast, the remarkable amount of opportunistic species tolerant to high organic matter contents within the distal facies indicates high concentration of riverine organic matter, locally inducing a decrease in oxygen concentration at the sea bottom, as testified by the abundance of *N. turgida* and *Palmoconcha turbida*. In the modern Po prodelta, comparable assemblages strongly influenced by riverine inputs are recorded in 15–30-m-deep waters (Breman, 1975; Jorissen, 1988; Donnici & Serandrei Barbero, 2002).

An almost exclusive sediment contribution from the Po River accounts for the geochemical composition of both sandy and muddy deltaic lithofacies, typified in particular by Cr/Al_2O_3 and MgO/Al_2O_3 ratios very similar to modern Po River sediments, with only slightly higher MgO/Al_2O_3 values (Fig. 7). These latter likely reflect a very minor local contribution to the sediment budget by Alpine sources, via longshore drift.

DISCUSSION

Three-fold nature of Holocene coastal progradation

The evolutionary scenario of highstand coastal progradation reflects significant along margin variability of the nearshore/deltaic/shelf system (Olariu and Steel, 2009). Three distinct phases of coastal evolution (A-C in Fig. 8) were reconstructed, based upon detailed sedimentological and paleontological examination of the succession, integrated with sediment provenance analysis: 1) uppermost TST: an initial phase of bay-head delta progradation in a shallow estuarine embayment (7.7-7.0 cal ky BP); 2) lower HST: a subsequent phase of wave-dominated coastal/deltaic progradation with extensive bay/lagoons in shallow (<15 m), open-marine waters (7.0-2.0 cal ky BP); and 3) upper HST: a final phase of river-dominated, deltaic progradation (with minimal bay/lagoons or mainland attached shorelines) in relatively deeper (15-30 m) water (<2.0 cal ky BP).

Phase 1, uppermost TST

The early phase of coastal progradation, between 7.7 and 7.0 cal ky BP, took place in very shallow waters (<5 m), with an extensive mixed, freshwater and brackish back-barrier environment (Fig. 8A). This phase saw the rapid advancing of fluvial mouths into shallow embayments, with a mean progradation rate of ~5 m/yr, which resulted in more or less coalescing bay-head delta lobes at the head of a wave-dominated estuary (Fig. 8A). Owing to the shifting of distributary channels, separate, small-volume bay-head delta systems, each consisting of multiple terminal distributary channels (Olariu and Bhattacharya, 2006), spread laterally across the estuary (Bruno et al., 2017). In dip-oriented cross-sections (Fig. 2), the bay-head delta sand body is up to 5 km long, reflecting the approximate distance between the fluvial mouths and the beach-barrier complex. The large size of the 7.7-7.0 ky BP, coalescing bay-head deltas is due to the relatively long time available for progradation at the turnaround from transgression to regression, in response to decelerating eustatic rise, which favored the complete filling of back-barrier accommodation (Milli et al., 2013; Aschoff et al., 2018). Compositional data indicate that the Po River was the feeder system of most bay-head delta sands (Fig. 7). This implies that between 7.7 and 7.0 cal ky BP, Po River sands were trapped in the estuary and did not contribute significantly to beach-barrier formation (Fig. 8A). Sediment-supply rates might have increased starting at the base of the uppermost TST, which coincided with the transition from Boreal (relatively dry) to Atlantic (more humid) northern Europe climate phase (Mangerud et al., 1974; see Table 2).

Phase 2, lower HST

This phase of relatively weak progradation (~2.5 m/yr) was characterized by delta and shoreline upbuilding into relatively shallow (<15 m), open marine waters (Fig. 8B), on fairly gentle slopes. Delta front-prodelta couplets extended a long way basinwards (~10 km; Fig. 2). Mixed macrofaunal assemblages from a variety of sub-environments characterize this period (Scarponi et al., 2017a). The diverse meiofauna indicates a vegetated sea bottom with variable riverine organic matter concentrations, possibly induced by the combined effect of fluvial avulsions and longshore drift (Rossi and Vaiani, 2008).

Between the Bronze Age and the Roman Age (5,000-2,000 y BP), the Po Delta occupied a broad stretch of the coastal system between Ravenna and Adria, and its discharge was dispersed through several, more or less coeval distributary outlets (Fig. 8B) that nourished cuspate and arcuate (wave-dominated) deltas (Correggiari et al., 2005b). Shallow-water depths facilitated nearshore sediment accumulation, which limited the expansion of the flow and enhanced repeated channel avulsion and shifting in the loci of deposition.

Sedimentologic, paleontologic, and compositional data suggest that delta initiation took place under a mixed fluvial-wave dispersal. Less steep offshore slopes and shallower water depths may have had the effect that a significant proportion of sediment accumulated above fair weather/storm wave base. This resulted in a higher potential for greater effects of wave energy on the shallow offshore area and sediment dispersal by longshore currents and waves. A generally high hydrodynamic energy is also consistent with the poor preservation state of the meiofauna, consisting predominantly of nearshore foraminifers.

Given the general counter-clockwise oceanic circulation pattern (Zavatarelli et al., 1998; Ravaioli et al., 2003), the Eastern Alps represented a key sediment delivery system for wave-influenced deltas in the Adriatic Sea (Fig. 1). Sources of sediment to the Po Plain during this phase were the Triassic platforms and build-ups in the Dolomite Mountains of the Eastern Alps (Amorosi et al., 2002), where thick limestone and dolostone successions are drained by major Eastern Alpine rivers. Strike-elongate sand bodies developed in this period, following temporary Po River avulsion to more southern positions (Fig. 8B). Beach-ridge sands have a litharenite composition, with abundant extrabasinal (limestone and dolomite) carbonate grains (Marchesini et al., 2000). High MgO and CaO concentrations are interpreted to reflect erosion and transport of detrital dolomite and carbonate material from the Eastern Alpine river catchments across all grain-size grades (Marchesini et al., 2000; Ravaioli et al., 2003; Curzi et al., 2006; Spagnoli et al., 2014; Amorosi and Sammartino, 2018; Greggio et al., 2018). During the lower HST, eustasy was relatively stable, whereas regional climate appears to have varied (Hormes et al., 2001; Wirth et al., 2013; Mangerud et al., 1974; see Table 2).

Phase 3, upper HST

During phase 2, delta progradation was limited to relatively landward locations (Fig. 8B). Due to trapping of most coarse-grained sediment nearshore, distal, prodelta areas underwent strong sediment condensation (Amorosi et al., 2017), testified by significant ecological and time condensation of macrobenthic remains (Scarponi et al., 2013; 2017a; Nawrot et al., 2018). The delta system responded to the dominance of sediment supply over accommodation focusing sediment accumulation around the river mouth and along the nearshore. Within the upper HST, the meiofauna is very similar to that of the modern prodelta (Breman, 1975; Jorissen, 1988), and indicates the occurrence of muddy bottoms with remarkable contents of riverine organic matter.

The river-dominated Po Delta is more protrusive than its wave-dominated counterparts (Fig. 8), with an average rate of progradation of ~15 m/yr. In this period, the delta shore varied significantly along strike. The poor correlation of highstand parasequences alongstrike is consistent with data from high-resolution CHIRP-sonar profiles in the adjacent Adriatic Sea, where prodelta lobes overlap laterally and can be traced along-strike as identifiable seismic-stratigraphic units only over relatively short (10-20 km) distances (Correggiari et al., 2005b).

Predominant fluvial dispersal with mouth-bar accretion and minor reworking into beach-ridge complexes is documented by sediment composition of sub-recent delta front sand bodies. Sand supplied during this period to the river mouth was mostly arkosic and rich in metamorphic rock fragments, thus reflecting a Po River parent material (Marchesini et al., 2000). The muddy prodelta units have, as well, remarkably high Cr and Ni concentrations, reflecting sediment contribution from the western Po River catchment (Amorosi, 2012; Amorosi and Sammartino, 2018).

Accommodation was continuously generated under relatively stable eustatic highstand conditions by: (i) tectonic subsidence, due to the flexure of the Adriatic plate beneath the Tyrrhenian plate (Carminati and Di Donato, 1999), augmented by (ii) sediment compaction (Teatini et al., 2011). Modern subsidence rates for the Po Delta area are in the range of 3-4 mm/yr, with substantially different values laterally as a function of subsurface lithology (Vitagliano et al., 2017).

Sediment supply rates also varied due to changing climatic conditions: increased flood activity in the southern Alps between 1.3 and 0.1 ky BP, northern European climate change from Sub-Atlantic to the Little Ice Age (0.4 ky BP), and Alpine glaciers advance and retreat throughout interval (Mangerud et al., 1974; Hormes et al., 2001; Wirth et al., 2013; see Table 2). Following the Porto Viro cut, in the XVII Century (ca. 400 cal. yr BP), the evolution of the delta was no longer a natural process, and progradation took place under considerable anthropogenic influence (Correggiari et al., 2005b).

Applications beyond the Po Plain: Correlation and prediction

The outstanding spatial and temporal resolution available in the Po coastal plain enabled us to construct a detailed model for the coevolution of shoreline sandy and offshore muddy depositional systems under varying accommodation.

Several studies have raised questions concerning the expected evolution of shoreline types as a function of systems-tract architecture. According to Posamentier and Vail (1988), estuarine/tidal depositional systems would be mostly concentrated in the lowstand systems tract (LST), whereas wave-dominated and river-dominated depositional systems are typically observed within TST and HST, respectively. A contrasting model, by Dalrymple et al. (1992), first introduced the concept of estuarine, tidal-dominated depositional systems as typically developed in the TST, as opposed to mostly wave-dominated, mainland-attached shorelines in the HST.

Our view based on the Quaternary example of the Po Plain is that back-stepping, wave-dominated estuaries with barrier bars are typical features of the TST (cf. Dalrymple et al., 1992; Zaitlin et al., 1994), but extensive bay-head delta sand bodies are likely to develop in the uppermost TST, when the rate of increase of coastal accommodation slows significantly, which causes progradation to start.

Contrary to existing sequence-stratigraphic models, significant differences are expected within the HST, at the boundary between the dominantly aggradational (and weakly progradational) stacking that characterizes the lower HST and the strongly progradational stacking of the upper HST. This stratigraphic surface, here named the “A-P surface”, is marked by remarkable changes in sediment characteristics, paleoenvironments and direction of sediment transport that reflect the transition from a wave-dominated to a river-dominated coastal system. The lower HST, in particular, would be characterized by wave-dominated shorelines, with moderate bay/lagoons, whereas the upper HST would be suggestive of river-dominated shorelines with minimal bay/lagoon development.

Broadly similar and coeval dynamics of coastal progradation have been outlined for other Holocene coastal systems, irrespective of their tectonic, climatic, or oceanographic regimes. The change around 7-8 cal ky BP from a funnel-shaped, estuarine morphology, with bay-head delta progradation, to straight, wave-influenced, river mouth morphologies (Figs. 2 and 8) has been reconstructed in coastal systems with high sediment supply, such as the Rhine-Meuse Delta (Hijma et al., 2009), the Song Hong River (Tanabe et al., 2006), and the Tiber River Delta (Milli et al., 2013; 2016). Comparatively low progradation rates (1 m/yr) characterized wave-influenced deltas in the lower HST (Milli et al., 2013). The chronologically well constrained example from the Po Plain, thus, provides an improved model for Holocene delta development and evolution that can be crucial to a predictive understanding of similar river- and wave-influenced systems.

Forcing mechanisms

Extrinsic factors

The spatial and temporal resolution of this data set also enabled investigation of forcing mechanisms. Table 2 summarizes the three-fold stratigraphic record of the middle to late Holocene of the Po River plain in terms of time spans, systems tracts, and components of accommodation and sediment supply. In general, eustasy appears to have been more influential in the TST, whereas subsidence and compaction dominated the HST. Sediment supply varied from the Po River in the uppermost TST, to the eastern Alps in the lower HST, and back to the Po River in the upper HST. Meltwater pulses (and associated eustatic rises) were fundamental controlling factors of TST architecture, contrasting with changing flood activity and glacier advances and retreats in the Alps during HST deposition (Table 2 and Fig. 9). In summary, the degree of influence of extrinsic factors recorded by changes in stratal architecture and distribution varies substantially at the systems-tract scale.

Although Table 2 shows some correspondence between the stratigraphic units and extrinsic allogenic forcing mechanisms in general, closer examination does not reveal any correspondence in detail for the HST. Figure 9 compares the stratal architecture of the last 11 ky with the components of sediment supply and accommodation. Components illustrated are eustasy, flood activity in the Alpine realm, globally recognized cold events and glacial advances. In the TST, there is close correspondence between the ages of the upper two parasequences and eustatic rises associated with glacial melt events mwp-1c and mwp-1d. The overall base of the TST corresponds to MWP-1B (Amorosi et al., 2017; Bruno et al., 2017). In the HST, eustasy was essentially stable (Vacchi et al., 2016, and references therein), and the age of the boundaries of the lower and upper HST do not correspond with Alpine flood activity, cold events, or glacial advances/retreats. Although Alpine flood activity increased overall in the HST, the most abrupt increase in frequency and variation occurred in the middle of the lower HST. The magnitude and frequency of cold events generally decreased, but again, the sharpest decrease was within the upper part of the lower HST. Half of the Bond events (3, 2 and 0 in Fig. 9) occur in the middle of parasequences and half (4 and 2 in Fig. 9) near parasequence boundaries (Bond et al., 2001). Global glacial advances spanned many centuries across parasequence boundaries within the lower HST and were within parasequences in the upper HST.

In summary, the TST appears to have been strongly influenced by eustasy, whereas the HST shows no direct relation to allogenic influences at any reasonable level of confidence. The ‘A-P’ surface, in particular, falls within a period of climate stability, which coincides with a remarkable change in soil use (Late Bronze Age, Early Iron Age), and which could record, in part at least, the impact of anthropogenic activities on sediment discharge (Maselli and Trincardi, 2013). Increasing human influence, especially over the last 3000 years, has been an important driver of changes in sediment supply, strongly modulating worldwide deltaic development (Wang et al., 2011; Maselli and Trincardi, 2013; Anthony et al., 2014).

Intrinsic factors

Such a lack of detailed correspondence of the stratigraphic response to coeval allogenic climate and eustatic influences in the HST is not unexpected, given the character and intrinsic response times of the Po River system. In such systems, fluvial processes tend to 'shred' allogenic input signals (Jerolmack and Paola, 2010, Kim et al., 2006; Li et al., 2015). A periodic input signal can be dispersed ("shredded") over the range of autogenic time scales to the point of being irretrievable at the downstream end of the sediment-transport system (Jerolmack and Paola, 2010). This "shredding" destroys the input signal through sediment storage–release processes that act over a wide range of spatial and temporal scales (Kim et al., 2006). In such cases, the allogenic input signal cannot be recovered by filtering because it is not merely obscured by noise, but no longer present. Such "shredding" is most likely in systems that meet two fundamental conditions: 1) the allogenic input signal must vary more frequently than the longest-period autogenic episode, and 2) the magnitude of the allogenic input volume must be less than the magnitude of the largest autogenic episode (Frette et al., 1996). For the Po River system, these two fundamental conditions were estimated and found both in the range to enable signal "shredding".

Time scale: The autogenic response time was calculated using three approaches—all indicate a longest-period autogenic episode length of about 5000 years. Sheets et al. (2002) suggest estimating such a characteristic timescale (T_i) as $T_i = h/\sigma$ (where h = distributary channel depth, σ = mean subsidence rate). Their formula was applied using an average value of h = 4 m and a long-term subsidence rate based on the depth of the MIS 5e coastal body (0.6-0.9 mm/yr in Amorosi et al., 2004). This results in T_i = 4444 to 6666 yr; using long-term topset accumulation rates, T_i ranges between 800 and 4000 yr. The measured durations of the HST parasequences and delta lobes were used as an estimate of response time; for this approach, T_i = 500 to 1800 yr. The allogenic input signal was calculated using Wirth et al's (2013) spectrum of Alpine climate cycles which ranged from 87 to 3000 yrs and their reports of periods of high flood occurrence that ranged from 200 to 1800 yrs long. Signal shredding is therefore expected because the allogenic signal (climate/flooding) was faster than the longest period autogenic variability (~4000–6000 yr), and mostly shorter than the longest duration HST parasequence.

Volume scale: The magnitude of allogenic input signal, in terms of sediment flux, also appears to have been significantly less than the magnitude of the largest autogenic event. Based on Amorosi et al. (2017), the volume of the largest parasequence in the lower HST is approximately 14.4 km^3. The magnitude of the largest allogenic input signal was calculated based on the 1,800 yr-long periods of increased flood activity in the southern Alps reported by Wirth et al. (2013) and the estimates of bedload and suspended flux volumes of the Po River system in the Holocene by Kettner and Syvitski (2009; suspended flux =18.8 Mt/yr, bedload flux = 0.53 Mt/yr). These values result in an estimated sediment flux volume of a period of increased flood activity of 2.9 km^3. This influx volume is only 20% of the volume of the largest parasequence/delta lobe, indicating that the second criterion for signal "shredding" (magnitude of the allogenic input volume must be less than the magnitude of the largest autogenic episode) was satisfied. Thus, with these parameters, according to Li et al., (2015), the Po River system is unlikely to allow source-to-sink propagation of climate signals through the delta system, where avulsion is the largest-scale process in time and space.

Although there appears to be no detailed correspondence between extrinsic forcing factors and the stratigraphic record of the Po River HST, there does appear to have been some relation in the LST (Pellegrini et al., 2017) and TST (Amorosi et al., 2017). In the LST and TST, there is a close correspondence of the ages of many parasequence boundaries with eustatic or climatic events. In addition, the time scale of allogenic variation appears to have been longer than the characteristic response time of the depositional system in most of the TST and about half of the LST (Pellegrini et al., 2017; Amorosi et al., 2017).

In summary, the stratigraphic architecture of the modern Po River delta does not record uniquely any one particular allogenic forcing (climate or eustasy). The strata are the integrated record of the system response to these forcing factors mediated through landscape evolution and autogenic processes.

CONCLUSIONS

The stratigraphic architecture of the modern Po Delta comprises a middle-late Holocene aggradational to progradational parasequence set that depicts recurrent events of channel avulsion and delta lobe construction under eustatic highstand conditions. Using mollusks, benthic foraminifera, and ostracods as refined indicators of depositional sub-environments, the detailed character of Holocene coastal progradation was reconstructed along a 70-km stretch of coast. Compositional data on sands and muds were used to infer sediment transport pathways from a variety of sources, and indirectly to infer depositional processes.

A threefold progradational model was reconstructed comparing the stratigraphic architecture of the uppermost TST, lower HST, and upper HST. At the top of a retrogradational parasequence set, interpreted to reflect the rapid landward migration of a barrier-lagoon-estuary system under the influence of eustatic rise, the uppermost TST is dominated by an aggradational to progradational internal bedset-scale stacking pattern that reflects bay-head delta development into brackish waters, with a rate of progradation of ~5 m/yr. The lower HST is defined by an aggradational parasequence set with minor coastal regression (~2.5 m/yr) into shallow marine waters, under locally significant wave-influence. Finally, the upper HST has the highest sedimentation rates and is typically identified with a river-dominated progradational parasequence set, associated with rapid regression (15 m/yr).

Fossil assemblages and sediment composition provide diagnostic criteria for depositional processes and environment recognition across the HST with an unprecedented level of detail. The boundary between the lower and upper HST, here termed the “A-P (aggradation-progradation) surface”, marks an abrupt shift in depositional systems configuration and sediment dispersal pathways that cannot be deciphered based on physical sedimentary structures alone. The integrated approach used in this work can provide, in particular, predictive power for process regime changes in mud-dominated, deltaic successions across the transgressive to regressive turnaround. This interpretational framework of prograding coastal successions can be applied to the ancient record to unravel facies complexity and reservoir heterogeneity. It also provides practical guidance for correlation and mapping of sandstone and mudstone hydrocarbon reservoirs, shallow marine seal-prone rocks, and coastal system aquifers, aquitards, and aquicludes.

ACKNOWLEDGMENTS

This study was supported by ExxonMobil Upstram Research Company and NSF grant no. EAR-1559196 “Stratigraphic Paleobiology and Historical Ecology of Po Basin”.

Figure captions

Fig. 1. Study area, with location of cores used for paleontologic (green) and geochemical (red) analyses. Core descriptions (grey dots) and shallow cores sampled for geochemical analysis (red crosses) are also indicated. The dashed line indicates the section trace of Figure 2.

Fig. 2. Stratigraphy of the Holocene aggradational to progradational succession of the Po coastal plain (modified after Amorosi et al., 2017) and its subdivision into uppermost transgressive systems tract (1), lower highstand systems tract (2) and upper highstand systems tract (3). The direction of the cross-section (see Fig. 1, for location) coincides roughly with the depositional-dip direction in the area. The eastern end of the cross-section provides a transition from dip- to strike-oriented delta lobe, as documented by the reduction of the apparent dip of the beds to horizontal. A: aggradation, R: retrogradation, AP: aggradation to progradation, P: progradation.

Fig. 3. Representative core photographs of wave-dominated (lower HST) versus river-dominated (upper HST) deltaic sand-mud alternations and mud-prone lithofacies assemblages. The differences are subtle and best resolved by integrating physical, biogenic, and chemical observations. Core EM13 (see Fig. 1, for location). Core width is about 10 cm.

Fig. 4. Diagnostic microfossil assemblages of the middle-late Holocene prograding succession: bay-head delta (A) and back-barrier/outer estuarine (B) deposits (uppermost TST); wave-dominated, delta front (C) and prodelta (D) facies (lower HST); river-dominated, delta front (E) and prodelta (F) facies (upper HST). Assemblages from core EM5, -14.90 m (A); core 205 S5, -15.90 m (B); core EM 11, -9.50 m (C); core EM13, -24.70 m (D); Core 7 at -7.55 m (E) and Core 1 at -23.45 m (F). Scale bar is 250 µm long. Abbreviations for benthic foraminifers: Abe – *A. beccarii*; Apt – *A. parkinsoniana, A. tepida*; Ape – *A. perlucida*; Cri – *Cribroelphidium* spp.; Hge – *H. germanica*; mil – miliolids; Ntu – *N. turgida*; epiphytic taxa mainly include Ast – *Asterigerinata* spp., Nte – *Neoconorbina terquemi*, Ros – *Rosalina* spp.; pl – planktonic foraminifers. Abbreviations for ostracods: Ctor – *C. torosa*; Lel – *L. elliptica*; Lept – *Leptocythere* spp.; Lrh – *Loxoconcha* gr. *rhomboidea*; Pat – *Palmoconcha turbida*; Pnt – *Pontocythere turbida*; Sgm – *Sagmatocythere* spp.; Sem – *Semicytherura* spp.

Fig. 5. Box-and-whiskers plots, summarizing major paleontologic (A) and geochemical (B-D) attributes of uppermost TST, lower HST, and upper HST. Box plots span the interquartile range. The white segment inside the rectangle shows the median, and "whiskers" above and below the box show the location of the minimum and maximum. Fossil density in species/dm^3.

Fig. 6. Macrofossil assemblages and relevant mollusk taxa retrieved along the depositional profile and across cores in Fig. 1: Bay-head delta sands (A) and back-barrier muds (B) facies (uppermost TST); wave-dominated delta front (C) and prodelta (D) facies (lower HST); river-dominated, delta front (E) and prodelta (F) facies (upper HST). Abbreviations: As - *Abra segmentum;* Cc - *Chamelea gallina;* Cg - *Corbula gibba;* h - *hydrobiids;* Lm - *Lentidum mediterraneum; Ss - Spisula subtruncata;* Tt - *Turritella communis.*

Fig. 7. Scatterplots of MgO/Al_2O_3 versus Cr/Al_2O_3, showing consistent changes in sediment composition across the middle-late Holocene succession, and comparison with modern stream sediment composition, including the Po River, Romagna (Ravenna) Apennines rivers, and selected Eastern Alpine rivers. Uppermost TST and upper HST are interpreted to be dominated by Po-River input, whereas lower HST is influenced by Eastern Alpine stream input. (SA: Sarca, MI: Mincio, AD: Adige, BR: Brenta, PI: Piave, and LI: Livenza – for location, see Fig. 1).

Fig. 8. Middle-late Holocene evolution of the Po coastal system, based upon stratigraphic architecture, paleontologic content and geochemical composition. A: uppermost TST, B: lower HST, C: upper HST. Left: Planview geometry of depositional environments. Right: schematic cross-section. The boundary between lower and upper HST ("A-P" surface") separates dominantly aggradational from progradational stacking patterns and demarcates an abrupt change in sediment characteristics, paleoenvironments and direction of sediment transport.

Fig. 9. Key global and regional events during the Holocene. a) Parasequence stacking patterns; b) Stratigraphic phases, Po River system; c) Age (ky BP); d) Eustasy (after Liu et al., 2004); e) Glacial retreat events, central Alps (Hormes et al., 2001); f) Cold events (Wanner et al., 2011); g) Global glacial advances (Denton and Karién, 1973); h) Iceberg discharge rates and Bond events (Bond et al., 1997); i) Enhanced flood activity in the southern Alpine realm (Wirth et al., 2013); j) Parasequence

number (Amorosi et al., 2017); light pink bars are periods of enhanced flood activity in the general Alpine realm (Wirth et al., 2013).

Table 1. Summary table of paleontologic attributes of facies associations recognized in this study.

Table 2. Summary of systems tracts and key influences. TST: transgressive systems tract, HST: highstand systems tract, blue line: transgressive surface, green line: maximum flooding surface.

REFERENCES

Allen, G.P. and **Posamentier, H.W.** (1993) Sequence stratigraphy and facies model of an incised valley fill: the Gironde Estuary, France. *J. Sed. Petr.*, **63,** 378–391.

Amorosi, A. (2012) Chromium and nickel as indicators of source-to-sink sediment transfer in a Holocene alluvial and coastal system (Po Plain, Italy). *Sed. Geol.*, **280**, 260–269.

Amorosi, A. and **Sammartino, I.** (2018) Shifts in sediment provenance across a hierarchy of bounding surfaces: A sequence-stratigraphic perspective from bulk-sediment geochemistry. *Sed. Geol.*, **375**, 145–156.

Amorosi, A., Colalongo, M.L., Pasini, G. and **Preti, D.** (1999) Sedimentary response to Late Quaternary sea-level changes in the Romagna coastal plain (northern Italy). *Sedimentology*, **46**, 99–121.

Amorosi, A., Centineo, M.C., Dinelli, E., Lucchini, F. and **Tateo, F.** (2002) Geochemical and mineralogical variations as indicators of provenance changes in Late Quaternary deposits of SE Po Plain. *Sed. Geol.*, **151**, 273–292.

Amorosi, A., Colalongo, M.L., Fiorini, F., Fusco, F., Pasini, G., Vaiani, S.C. and **Sarti, G.** (2004) Palaeogeographic and palaeoclimatic evolution of the Po Plain from 150-ky core records. *Global Planet. Change*, **40**, 55–78.

Amorosi, A., Centineo, M.C., Colalongo, M.L. and **Fiorini, F.** (2005) Millennial-scale depositional cycles from the Holocene of the Po Plain, Italy. *Mar. Geol.*, **222–223**, 7–18.

Amorosi, A., Colalongo, M.L., Dinelli, E., Lucchini, F. and **Vaiani, S.C.** (2007) Cyclic variations in sediment provenance from late Pleistocene deposits of the eastern Po Plain, Italy. In: *Sedimentary Provenance and Petrogenesis* (Eds J. Arribas, S. Critelli and M.J. Johnsson), *Geol. Soc. Am. Spec. Pap.*, 420, 13–24.

Amorosi, A., Rossi, V. and **Vella, C.** (2013) Stepwise postglacial transgression in the Rhône Delta area as revealed by high-resolution core data. *Palaeogeogr. Palaeoclimatol. Palaeoecol.*, **374**, 314–326.

Amorosi, A., Rossi, V., Scarponi, D., Vaiani, S.C. and **Ghosh, A.** (2014a) Biosedimentary record of postglacial coastal dynamics: high-resolution sequence stratigraphy from the northern Tuscan coast (Italy). *Boreas*, **43**, 939–954.

Amorosi, A., Guermandi, M., Marchi, N. and **Sammartino, I.** (2014b) Fingerprinting sedimentary and soil units by their natural metal contents: A new approach to assess metal contamination. *Sci. Total Environ.*, **500–501**, 361–372.

Amorosi, A., Maselli, V. and **Trincardi, F.** (2016) Onshore to offshore anatomy of a late Quaternary source-to-sink system (Po Plain–Adriatic Sea, Italy). *Earth-Sci. Rev.*, **153**, 212–237.

Amorosi, A., Bruno, L., Campo, B., Morelli, A., Rossi, V., Scarponi, D., Hong, W., Bohacs, K.M. and **Drexler, T.M.** (2017) Global sea-level control on local parasequence architecture from the Holocene record of the Po Plain, Italy. *Mar. Petrol. Geol.,* **87**, 99–111.

Anthony, E.J., Marriner, N. and **Morhange, C.** (2014) Human influence and the changing geomorphology of Mediterranean deltas and coasts over the last 6000 years: from progradation to destruction phase? *Earth-Sci. Rev.*, **139**, 336–361.

Aschof, J.L., Olariu, C. and **Steel, R.J.** (2018) Recognition and significance of bayhead delta deposits in the rock record: A comparison of modern and ancient systems. *Sedimentology*, **65**, 62–95.

Athersuch, J., Horne, D.J. and **Whittaker, J.E.** (1989) Marine and brackish water ostracods (Superfamilies Cypridacea and Cytheracea). In: *Synopsis of the British Fauna* (Eds D.M. Kermack and R.S.K. Barnes), *New Series*, 43, 1–343. Brill E.J., Leiden.

Barbieri, G., Amorosi, A. and **Vaiani, S.C.** (2017) Benthic foraminifera as a key to delta evolution: A case study from the late Holocene succession of the Po River Delta. *Micropaleontology*, **63**, 27–41.

Bhattacharya, J.P. and **Giosan, L.** (2003) Wave-influenced deltas: Geomorphological implications for facies reconstruction. *Sedimentology,* **50**, 187–210.

Bhattacharya, J.P. and **MacEachern, J.A.** (2009) Hyperpycnal rivers and prodeltaic shelves in the Cretaceous Seaway of North America. *J. Sed. Res.,* **79**, 184–209.

Birgenheier, L.P., Horton, B., McCauley, A.D., Johnson, C.L., and **Kennedy, A.** (2017) A depositional model for offshore deposits of the lower Blue Gate Member, Mancos Shale, Uinta Basin, Utah, USA. *Sedimentology*, **64**, 1402–1438.

Blum. M.D. and Roberts, H. (2009) Drowning of the Mississippi Delta due to insufficient sediment supply and global sea-level rise. *Nature Geoscience*, **2**, 488-491.

Bohacs, K.M., Lazar, O.R. and **Demko, T.M.** (2014) Parasequence types in shelfal mudstone strata—Quantitative observations of lithofacies and stacking patterns, and conceptual link to modern depositional regimes. *Geology,* **42**, 131–134.

Bonaduce, G., Ciampo, G. and **Masoli, M.** (1975) Distribution of Ostracoda in the Adriatic Sea. *Pubblicazioni della Stazione Zoologica di Napoli*, 40, 304 pp.

Bond, G., Showers, W., Cheseby, M., Lotti, R., Almasi, P., Priore, P., Cullen, H., Hajdas, I. and **Bonani, G.** (1997) A pervasive millennial-scale cycle in North Atlantic Holocene and glacial climates. *Science*, **278,** 1257–1266.

Bond, G., Kromer, B., Beer, J., Muscheler, R., Evans, M.N., Showers, W., Hoffmann, S., Lotti-Bond, R., Hajdas, I. and **Bonani, G.** (2001) Persistent solar influence on North Atlantic climate during the Holocene. *Science*, **294,** 2130–2136.

Breman, E. (1975) The distribution of ostracodes in the bottom sediments of the Adriatic Sea. Ph.D Thesis, Vrije Universiteit, Amsterdam.

Bruno, L., Bohacs, K.M., Campo, B., Drexler, T.M., Rossi, V., Sammartino, I., Scarponi, D., Hong, W. and **Amorosi, A.** (2017) Early Holocene transgressive palaeogeography in the Po coastal plain (northern Italy). *Sedimentology,* **64**, 1792–1816.

Campo, B., Amorosi, A. and **Vaiani, S.C.** (2017) Sequence stratigraphy and late Quaternary paleoenvironmental evolution of the Northern Adriatic coastal plain (Italy). *Palaeogeogr. Palaeoclimatol. Palaeoecol.,* **466**, 265–278.

Carminati, E. and **Di Donato, G.** (1999) Separating natural and anthropogenic vertical movements in fast subsiding areas: the Po plain (N. Italy) case. *Geophys. Res. Lett.*, **26**, 2291–2294.

Cattaneo, A. and **Steel, R.J.** (2003) Transgressive deposits: a review of their variability. *Earth-Sci. Rev.*, **62**, 187–228.

Cattaneo, A., Correggiari, A., Langone, L. and **Trincardi, F.** (2003) The late-Holocene Gargano subaqueous delta, Adriatic shelf: sediment pathways and supply fluctuations. *Mar. Geol.*, **193**, 61–91.

Cattaneo, A., Trincardi, F., Asioli, A. and **Correggiari, A.** (2007) The Western Adriatic shelf clinoform: energy-limited bottomset. *Cont. Shelf Res.,* **27**, 506–525.

Catuneanu, O., Abreu, V., Bhattacharya, J.P., Blum, M.D., Dalrymple, R.W., Eriksson, P.G., Fielding, C.R., Fisher, W.L., Galloway, W.E., Gibling, M.R., Giles, K.A., Holbrook, J.M., Jordan, R., Kendall, C.G.St.C., Macurda, B., Martinsen, O.J., Miall, A.D., Neal, J.E., Nummedal, D., Pomar, L., Posamentier, H.W., Pratt, B.R., Sarg, J.F., Shanley, K.W., Steel, R.J., Strasser, A., Tucker, M.E. and **Winker, C.** (2009) Towards the standardization of sequence stratigraphy. *Earth-Sci. Rev.,* **92,** 1–33.

Colalongo, M.L. (1969) Ricerche sugli Ostracodi nei fondali antistanti il delta del Po. *Giorn. Geol.*, **36**, 335–362.

Correggiari, A., Cattaneo, A. and **Trincardi, F.** (2005a) Depositional patterns in the Late-Holocene Po delta system. In: *River Deltas–Concepts, Models and Examples* (Eds. J.P. Bhattacharya and L. Giosan)*, SEPM Spec. Publ.*, 83, 365–392.

Correggiari, A., Cattaneo, A. and **Trincardi, F.** (2005b) The modern Po Delta system: lobe switching and asymmetric prodelta growth. *Mar. Geol.*, **222**, 49–74.

Covelli, S. and **Fontolan, G.** (1997) Application of a normalization procedure in determining regional geochemical baselines. *Environ. Geol.*, **30**, 34–45.

Curray, J.R. and **Moore, D.G.** (1964) Pleistocene deltaic progradation of continental terrace, Costa de Nayarit, Mexico. In: *Deltaic and Shallow Marine Deposits* (Ed. L.M.J.U. Van Straaten), pp. 193-214. Elsevier, Amsterdam.

Curzi, P.V., Dinelli, E., Lucchi, M.R. and **Vaiani, S.C.** (2006) Palaeoenvironmental control on sediment composition and provenance in the late Quaternary deltaic successions: a case study from the Po delta area (Northern Italy). *Geol. J.*, **41**, 591–612.

Dalrymple, R.W., Zaitlin, B.A. and **Boyd, R.** (1992) Estuarine facies models, conceptual basis and stratigraphic implications. *J. Sed. Petrol.*, **62**, 1130–1146.

Demarest, J.M. and **Kraft, J.C.** (1987) Stratigraphic record of Quaternary sea levels: implications for more ancient strata. In: *Sea Level Fluctuation and Coastal Evolution* (Eds D. Nummedal, O.H. Pilkey and S.D. Howard), *SEPM Spec. Publ.*, 41, 223–239.

Denton, G.H. and **Karlén, W.** (1973) Holocene climatic variations—their pattern and possible cause. *Quat. Res.*, **3,** 155-205.

Di Bella, L. and **Casieri, S.** (2011) Paleoenvironmental reconstruction of Late Quaternary succession by foraminiferal assemblages of three cores from the San Benedetto del Tronto coast (central Adriatic Sea, Italy). *Quatern. Int.*, **241**, 169–183.

Di Bella, L., Bellotti, P. and **Milli, S.** (2013) The role of foraminifera as indicators of the Late Pleistocene–Holocene palaeoclimatic fluctuations on the deltaic environment: The example of Tiber delta succession (Tyrrhenian margin, Italy). *Quatern. Int.*, **303**, 191–209.

Di Giuseppe, D., Tessari, U., Faccini, B., Coltorti, M., Vaccaro, C. and **Marin, E.** (2016) Multiple X-ray approaches to discriminate the origin of liquefied sand erupted during the 2012 Emilia Romagna earthquake. *X-Ray Spectrom.*, **45**, 19–27.

Dinelli, E., Ghosh, A., Rossi, V., and **Vaiani, S.C.** (2013) Multiproxy reconstruction of Late Pleistocene-Holocene environmental changes in coastal successions: microfossil and geochemical evidences from the Po Plain (Northern Italy). *Stratigraphy*, **9**, 153–167.

Donnici, S. and **Serandrei Barbero, R.** (2002) The benthic foraminiferal communities of the northern Adriatic continental shelf. *Mar. Micropaleontol.*, **44**, 93–123.

D'Onofrio, S. (1969) Ricerche sui Foraminiferi nei fondali antistanti il Delta del Po. *Giorn. Geol.*, **36**, 283–334.

Fiorini, F. and **Vaiani, S.C.** (2001) Benthic foraminifers and transgressive-regressive cycles in the Late Quaternary subsurface sediments of the Po Plain near Ravenna (Northern Italy). *Boll. Soc. Paleontol. Ital.*, **40**, 357–403.

Franzini, M., Leoni, L. and **Saitta, M.** (1972) A simple method to evaluate the matrix effects in X-ray fluorescence analysis. *X-ray Spectrom.*, **1**, 151–154.

Frazier, D.E. (1974) Depositional episodes: their relationship to the Quaternary stratigraphic framework in the northwestern portion of the Gulf basin. Bureau of Economic Geology, University of Texas at Austin, *Geological Circular*, **74**, 1–28.

Frette, V., Christensen, K., Malthe-Sørenssen, A., Feder, J., Jøssang, T. and **Meakin, P.** (1996) Avalanche dynamics in a pile of rice. *Nature*, **379**, 49.

Garzanti, E. (2016) From static to dynamic provenance analysis—Sedimentary petrology upgraded. *Sed. Geol.*, **336**, 3–13.

Gerardi, M.H. and **Lytle, B.** (2015) Biology and Troubleshooting of Facultative Lagoons. Wiley-Liss, New Jersey, Hoboken.

Greggio, N., Giambastiani, B.M., Campo, B., Dinelli, E. and **Amorosi, A.** (2018) Sediment composition, provenance, and Holocene paleoenvironmental evolution of the Southern Po River coastal plain (Italy). *Geol. J.*, **53**, 914–928.

Harms, J.C., Southard, J.B., Spearing, D.R. and **Walker, R.G. (**1975) Depositional environments as interpreted from primary sedimentary structures and stratification sequences. *SEPM Short Course 2,* 161.

Hijma, M.P., Cohen, K.M., Hoffmann, G., Van der Spek, A.J.F. and **Stouthamer, E.** (2009) From river valley to estuary: the evolution of the Rhine mouth in the early to middle Holocene (western Netherlands, Rhine-Meuse delta). *Netherlands Journal of Geosciences – Geologie en Mijnbouw*, **88**, 13–53.

Hormes, A., Müller, B.U. and **Schlüchter, C.** (2001) The Alps with little ice: evidence for eight Holocene phases of reduced glacier extent in the Central Swiss Alps. *Holocene*, **11**, 255–265.

Jerolmack, D.J. and **Paola, C.** (2010) Shredding of environmental signals by sediment transport. *Geophys. Res. Lett.*, **37**, L19401. https://doi.org/10.1029/2010GL044638.

Jorissen, F.J. (1988) Benthic foraminifera from the Adriatic Sea; principles of phenotypic variation. *Utrecht Micropaleontol. Bull.*, 37, 1–176.

Kettner, A.J. and **Syvitski, J.P.M.** (2009) Fluvial responses to environmental perturbations in the Northern Mediterranean since the Last Glacial Maximum. *Quatern. Sci. Rev.*, **28**, 2386–2397.

Kietzmann, D.A., Ambrosio, A.L., Suriano, J., Alonso, M.S., Tomassini, F.G., Depine, G. and **Repol, D.** (2016) The Vaca Muerta-Quintuco system (Tithonian-Valanginian) in the Neuquen Basin, Argentina: a view from the outcrops in the Chos Malal fold and thrust belt. *AAPG Bull.*, **100**, 743–771.

Kim, W., Paola, C., Swenson, J.B. and **Voller, V.R.** (2006) Shoreline response to autogenic processes of sediment storage and release in the fluvial system. *J. Geophys. Res.*, **111**, F04013. https://doi.org/10.1029/2006JF000470.

Kowalewski, M., Wittmer, J.M., Dexter, T.A., Amorosi, A. and **Scarponi, D.** (2015) Differential responses of marine communities to natural and anthropogenic changes. *Proc. R. Soc. B,* 20142990. https://doi.org/10.1098/rspb.2014.2990

Lazar, O.R., Bohacs, K.M., MacQuaker, J.H.S., Schieber, J. and **Demko, T.M.** (2015) Capturing key attributes of finegrained sedimentary rocks in outcrops, cores and thin sections—nomenclature and description guidelines. *J. Sed. Res.*, **85**, 230–246.

Leoni, L. and **Saitta, M.** (1976) X-ray fluorescence analysis of 29 trace elements in rock and mineral standards. *Rend. Soc. Ital. Mineral. Petrol.*, **32**, 497–510.

Leoni, L., Menichini, M. and **Saitta, M.** (1982) Determination of S, Cl and F in silicate rocks by X-ray fluorescence analyses. *X-Ray Spectrom.*, **11**, 156–158.

Li, Q., Yu, L. and **Straub, K.M.** (2015) Storage thresholds for relative sea-level signals in the stratigraphic record. *Geology*, **44**, 179–182.

Liaghati, T., Preda, M. and **Cox, M.** (2004) Heavy metal distribution and controlling factors within coastal plain sediments, Bells Creek catchment, southeast Queensland, Australia. *Environ. Int.*, **29**, 935–948.

Liu, J.P., Milliman, J.D., Gao, S. and **Cheng, P.** (2004) Holocene development of the Yellow River's subaqueous delta, North Yellow Sea. *Mar. Geol.,* **209,** 45–67.

Macquaker, J.H.S. and **Bohacs, K.M**. (2007) On the accumulation of mud. *Science,* **318**, 1734–1735.

Macquaker, J.H.S., Bentley, S.J. and **Bohacs, K.M.** (2010) Wave-enhanced sediment-gravity flows and mud dispersal across continental shelves: reappraising sediment transport processes operating in ancient mudstone successions. *Geology*, **38**, 947–950.

Mangerud, J.A.N., Andersen, S.T., Berglund, B.E. and **Donner, J.J.** (1974) Quaternary stratigraphy of Norden, a proposal for terminology and classification. *Boreas*, **3**, 109–126.

Marchesini, L., Amorosi, A., Cibin, U., Zuffa, G.G., Spadafora, E. and **Preti, D.** (2000) Sand composition and sedimentary evolution of a Late Quaternary depositional sequence, northwestern Adriatic Coast, Italy. *J. Sed. Res.*, **70**, 829–838.

Maselli, V. and **Trincardi, F.** (2013) Large-scale single incised valley from a small catchment basin on the western Adriatic margin (central Mediterranean Sea). *Global Planet. Change*, **100**, 245–262.

Menon, M.G., Gibbs, R.J. and **Phillips, A.** (1998) Accumulation of muds and metals in the Hudson River estuary turbidity maximum. *Environ. Geol.*, **34**, 214–222.

Milker, Y. and **Schmiedl, G.** (2012) A taxonomic guide to modern benthic shelf foraminifera of the western Mediterranean Sea. *Palaeontol. Electron.*, **15**, 134 pp.

Milli, S., D'ambrogi, C., Bellotti, P., Calderoni, G., Carboni, M.G., Celant, A., Di Bella, L., Di Rita, F., Frezza, V., Magri, D., Pichezzi, R.M. and **Ricci, V.** (2013) The transition from wave-dominated estuary to wave-dominated delta: The Late Quaternary stratigraphic architecture of Tiber deltaic succession (Italy). *Sed. Geol.*, **284-285**, 159–180.

Milli, S., Mancini, M., Moscatelli, M., Stigliano, F., Marini, M. and **Cavinato, G.P.** (2016) From river to shelf, anatomy of a high-frequency depositional sequence: the Late Pleistocene to Holocene Tiber depositional sequence. *Sedimentology*, **63**, 1886-1928.

Mulder, T. and **Syvitski, J.P.M.** (1995) Turbidity currents generated at river mouths during exceptional discharge to the world's oceans. *J. Geol.,* **103**, 285–298.

Mulder, T., Syvitski, J.P., Migeon, S., Faugeres, J.C. and **Savoye, B.** (2003) Marine hyperpycnal flows: initiation, behavior and related deposits. A review. *Mar. Petrol. Geol.*, **20**, 861–882.

Muto, T. and **Steel, R.J.** (1997) Principles of regression and transgression: the nature of the interplay between accommodation and sediment supply. *Journal Sediment. Res.*, **67**, 994–1000.

Nawrot, R., Scarponi, D., Azzarone, M., Dexter, T.A., Kusnerik, K.M., Wittmer, J.M., Amorosi, A. and **Kowaleski, M.** (2018) Stratigraphic signatures of mass extinctions: ecological and sedimentary determinants. *Proc. Roy. Soc. B*, (in press.). http://dx.doi.org/10.1098/rspb.2018.1191.

Neal, J. and **Abreu, V.** (2009) Sequence stratigraphy hierarchy and the accommodation succession method. *Geology*, **37**, 779–782.

Ninfo, A., Ciavola, P. and **Billi, P.** (2018) The Po Delta is restarting progradation: geomorphological evolution based on a 47-years Earth Observation dataset. *Sci. Rep.,* **8**, 3457.

Olariu, C. and **Bhattacharya, J.P.** (2006) Terminal distributary channels and delta front architecture of river-dominated delta systems. *J. Sed. Res.*, **76**, 212–233.

Olariu, C. and **Steel, R.J.** (2009) Influence of point-source sediment-supply on modern shelf-slope morphology: implications for interpretation of ancient shelf margins. *Basin Res.*, **21**, 484–501.

Oomkens, E. (1970) Depositional sequences and sand distribution in the postglacial Rhone delta complex. In: *Deltaic Sedimentation Modern and Ancient* (Ed. J.P. Morgan), *SEPM Spec. Publ.*, 15, 198–212.

Pellegrini, C., Maselli, V., Gamberi, F., Asioli, A., Bohacs, K.M., Drexler, T.M. and **Trincardi, F.** (2017) How to make a 350-m-thick lowstand systems tract in 17,000 years: The Late Pleistocene Po River (Italy) lowstand wedge. *Geology*, **45**, 327–330.

Pint, A. and **Frenzel, P.** (2017) Ostracod fauna associated with Cyprideis torosa – an overview. *J. Micropalaeontol.,* **36**, 113–119.

Plint, A.G. (2014) Mud dispersal across a Cretaceous prodelta: Storm-generated wave-enhanced sediment gravity flows inferred from mudstone microtexture and microfacies. *Sedimentology*, **61**, 609–647.

Posamentier, H.W. and **Allen, G.P.** (1999) Siliciclastic sequence stratigraphy - concepts and applications. *SEPM Concepts Sedimentol. Paleontol.,* 7, Tulsa, 212 pp.

Posamentier, H.W. and **Vail, P.R.** (1988) Eustatic controls on clastic deposition II-Sequence and systems tract models. In: *Sea-Level Changes: an Integrated Approach* (Eds C.K. Wilgus, B.S. Hastings, C.G.St.C. Kendall, H.W. Posamentier, C.A. Ross and J.C. VanWagoner), *Spec. Publ. Soc. Econ. Paleont. Miner.*, 42, 125–154.

Ravaioli, M., Alvisi, F. and **Vitturi, L.M.** (2003) Dolomite as a tracer for sediment transport and deposition on the northwestern Adriatic continental shelf (Adriatic Sea, Italy). *Cont. Shelf Res.*, **23**, 1359–1377.

Rizzini, A. (1974) Holocene sedimentary cycle and heavy mineral distribution, Romagna-Marche coastal plain, Italy. *Sed. Geol.*, **11**, 17–37.

Rossi, V. and **Vaiani, S.C.** (2008) Benthic foraminiferal evidence of sediment supply changes and fluvial drainage reorganization in Holocene deposits of the Po Delta. *Mar. Micropaleontol.*, **69**, 106–118.

Rossi, V., Amorosi, A., Sarti, G. and **Mariotti, S.** (2017) Late Quaternary multiple incised valley systems: An unusually well-preserved stratigraphic record of two interglacial valley-fill successions from the Arno Plain (northern Tuscany, Italy). *Sedimentology*, **64**, 1901–1928.

Scarponi, D. and **Angeletti, L.** (2008) Integration of palaeontological patterns in the sequence stratigraphy paradigm: a case study from Holocene deposits of the Po Plain (Italy). *GeoActa*, **7**, 1-13.

Scarponi, D., Kaufman, D., Amorosi, A. and **Kowalewski, M.** (2013) Sequence stratigraphy and the resolution of the fossil record. *Geology*, **41**, 239–242.

Scarponi, D., Azzarone, M., Kusnerik, K., Amorosi, A., Bohacs, K.M., Drexler, T.M. and **Kowalewski, M.** (2017a) Systematic vertical and lateral changes in quality and time resolution of the macrofossil record: Insights from Holocene transgressive deposits, Po coastal plain, Italy. *Mar. Petrol. Geol.,* **87**, 128–136.

Scarponi, D., Azzarone, A., Kowalewski, M. and **Huntley, J.W.** (2017b) Surges in trematode prevalence linked to centennial-scale flooding events in the Adriatic. *Sci. Rep.*, **7**, 5732.

Schieber, J. (1998) Deposition of mudstones and shales: overview, problems and challenges. In: *Shales and Mudstones* vol. 1, (Eds J. Schieber, W. Zimmerle and P. Sethi), pp. 131-146. E. Schweizerbart'sche Verlagsbuchhandlung, Stuttgart, Germany.

Schieber, J. (2016) Mud re-distribution in epicontinental basins–Exploring likely processes. *Mar. Petrol. Geol*, **71**, 119-133.

Sgarrella, F. and **Moncharmont Zei, M.** (1993) Benthic foraminifera of the Gulf of Naples (Italy): systematics and autoecology. *Boll. Soc. Paleontol. Ital.*, **32**, 145–264.

Sheets, B.A., Hickson, T.A. and **Paola, C.** (2002) Assembling the stratigraphic record: depositional patterns and time-scales in an experimental alluvial basin. *Basin Res.,* **14**, 287–301.

Spagnoli, F., Dinelli, E., Giordano, P., Marcaccio, M., Zaffagnini, F. and **Frascari, F.** (2014) Sedimentological, biogeochemical and mineralogical facies of Northern and Central Western Adriatic Sea. *J. Mar. Syst.*, **139**, 183–203.

Stanley, D.J. and **Warne, A.G.** (1994) Worldwide initiation of Holocene marine deltas by deceleration of sea-level rise. *Science*, **265**, 228–231.

Stefani, M. and **Vincenzi, S.** (2005) The interplay of eustasy, climate and human activity in the late Quaternary depositional evolution and sedimentary architecture of the Po Delta system. *Mar. Geol.*, **222-223**, 19–48.

Syvitski, J.P., Kettner, A.J., Overeem, I., Hutton, E.W., Hannon, M.T., Brakenridge, G.R., Day, J., Vörösmarty, C., Saito, Y., Giosan, L. and **Nicholls, R.J.** (2009) Sinking deltas due to human activities. *Nat. Geosc.*, **2**, 681.

Tanabe, S., Saito, Y., Vu, Q.L., Hanebuth, T.J., Ngo, Q.L. and **Kitamura, A.** (2006) Holocene evolution of the Song Hong (Red River) delta system, northern Vietnam. *Sed. Geol.*, **187**, 29-61.

Tanabe, S., Nakanishi, T., Ishihara, Y. and **Nakashima, R.** (2015) Millennial-scale stratigraphy of a tide-dominated incised valley during the last 14 kyr: Spatial and quantitative reconstruction in the Tokyo Lowland, central Japan. *Sedimentology*, **62**, 1837–1872.

Teatini, P., Tosi, L. and **Strozzi, T.** (2011) Quantitative evidence that compaction of Holocene sediments drives the present land subsidence of the Po Delta, Italy. *J. Geophys. Res.*, **116**, B08408. https://doi.org/10.1029/2010JB008122.

Trincardi, F., Cattaneo, A., Asioli, A., Correggiari, A. and **Langone, L.** (1996) Stratigraphy of the Late-Quaternary deposits in the central Adriatic basin and the record of short term climatic events. *Mem. Istit. Ital. Idrobiol.*, **55**, 39–70.

Vacchi, M., Marriner, N., Morhange, C., Spada, G., Fontana, A. and **Rovere, A.** (2016) Multiproxy assessment of Holocene relative sea-level changes in the western Mediterranean: sea-level variability and improvements in the definition of the isostatic signal. *Earth-Sci. Rev.*, **155**, 172–197.

Van Wagoner, J.C., Mitchum, R.M., Campion, K.M. and **Rahmanian, V.D.** (1990) Siliciclastic sequence stratigraphy in well logs, cores, and outcrops: concepts for high-resolution correlation of time and facies. *AAPG Methods Explor. Ser.,* 7, Tulsa, 55 pp.

Vitagliano, E., Di Maio, R., Scafetta, N., Calcaterra, D. and **Zanchettin, D.** (2017) Wavelet analysis of remote sensing and discharge data for understanding vertical ground movements in sandy and clayey terrains of the Po Delta area (Northern Italy). *J. Hydrol.*, **550**, 386–398.

von Eynatten, H., Barceló-Vidal, C. and **Pawlowsky-Glahn, V.** (2003) Composition and discrimination of sandstones: a statistical evaluation of different analytical methods. *J. Sed. Res.*, **73**, 47–57.

Wang, H.J., Saito, Y.., Zhang, Y., Bi, N.S., Sun, X.X. and **Yang, Z.S.** (2011) Recent changes of sediment flux to the western Pacific ocean from major rivers in east and southeast Asia. *Earth Sci. Rev.*, **108**, 80–100.

Wanner, H., Solomina, O., Grosjean, M., Ritz, S.P. and **Jetel, M.** (2011) Structure and origin of Holocene cold events. *Quat. Sci. Rev.*, **30**, 3109-3123.

Wilson, R.D. and **Schieber, J.** (2014) Muddy hyperpycnites in the Lower Genesee Group of Central New York, USA: implications for mud transport in epicontinental seas. *J. Sed. Res.*, **84**, 866–874.

Wirth, S.B., Glur, L., Gilli, A. and **Anselmetti, F.S.** (2013) Holocene flood frequency across the Central Alps–solar forcing and evidence for variations in North Atlantic atmospheric circulation. *Quat. Sci. Rev.*, **80**, 112–128.

Wittmer, J.M., Dexter, T.A., Scarponi, D., Amorosi, A. and **Kowalewski, M.** (2014) Quantitative bathymetric models for late Quaternary transgressive–regressive cycles of the Po Plain, Italy. *J. Geol.*, **122**, 649–670.

Zaitlin, B.A., Dalrymple, R.W. and **Boyd, R.** (1994) The stratigraphic organization of incised-valley systems associated with relative sea-level change. In: *Incised-Valley Systems: Origin and Sedimentary Sequences* (Eds R.W. Dalrymple, R. Boyd and B.A. Zaitlin), *SEPM Spec. Publ.*, 51, 45–60.

Zavatarelli, M., Raicich, F., Bregant, D., Russo, A. and **Artegiani, A.** (1998) Climatological biogeochemical characteristics of the Adriatic Sea. *J. Mar. Syst.*, **18**, 227–263.

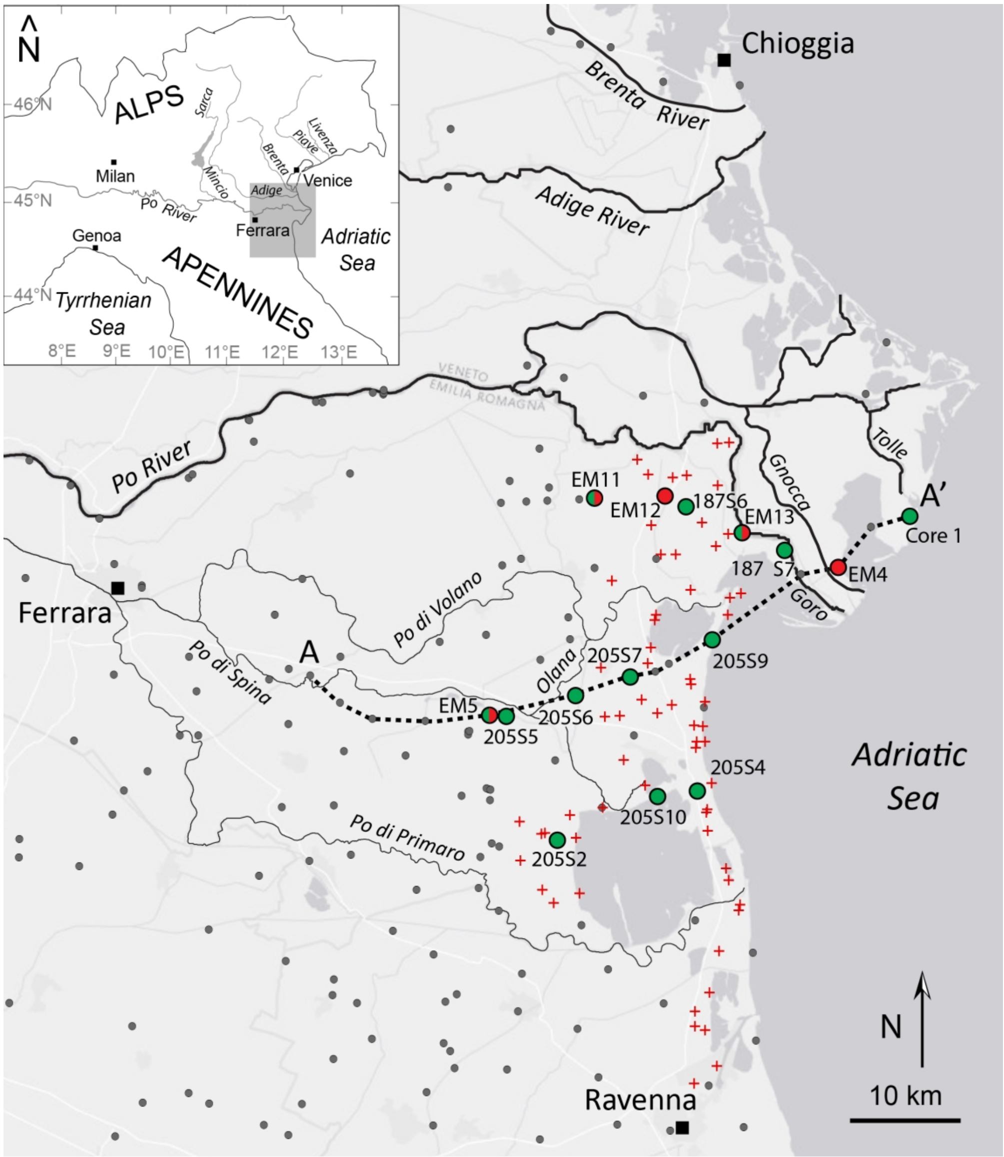

Fig. 1. Study area, with location of cores used for paleontologic (green) and geochemical (red) analyses. Core descriptions (grey dots) and shallow cores sampled for geochemical analysis (red crosses) are also indicated. The dashed line indicates the section trace of Figure 2.

193x223mm (300 x 300 DPI)

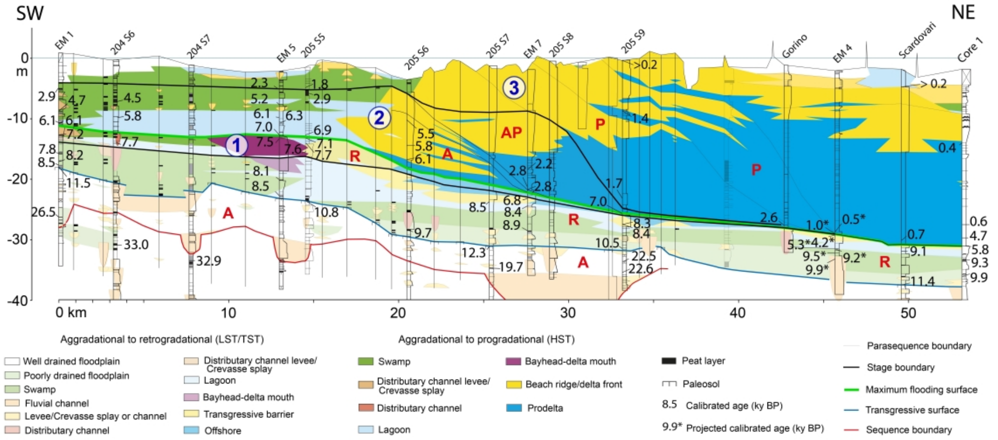

Fig. 2. Stratigraphy of the Holocene aggradational to progradational succession of the Po coastal plain (modified after Amorosi et al., 2017) and its subdivision into uppermost transgressive systems tract (1), lower highstand systems tract (2) and upper highstand systems tract (3). The direction of the cross-section (see Fig. 1, for location) coincides roughly with the depositional-dip direction in the area. The eastern end of the cross-section provides a transition from dip- to strike-oriented delta lobe, as documented by the reduction of the apparent dip of the beds to horizontal. A: aggradation, R: retrogradation, AP: aggradation to progradation, P: progradation.

588x264mm (300 x 300 DPI)

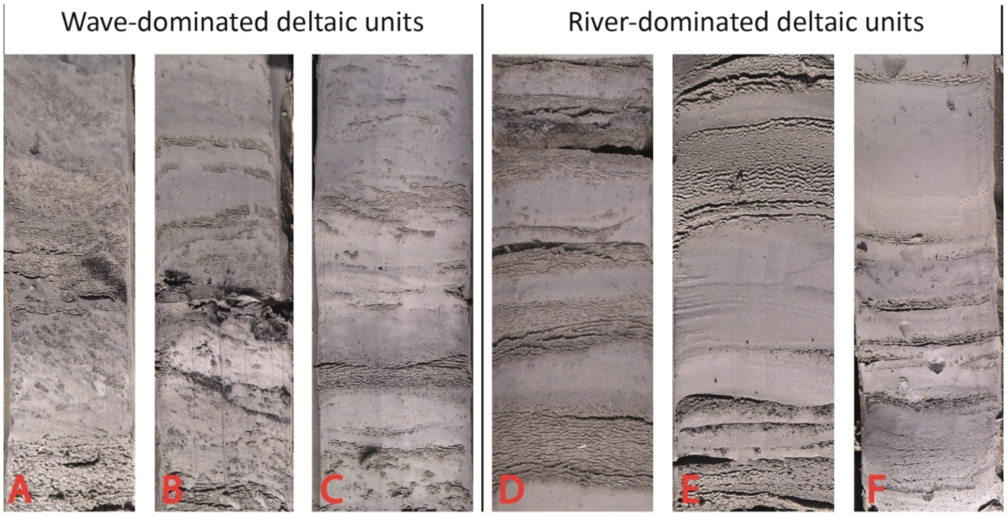

Fig. 3. Representative core photographs of wave-dominated (lower HST) versus river-dominated (upper HST) deltaic sand-mud alternations and mud-prone lithofacies assemblages. The differences are subtle and best resolved by integrating physical, biogenic, and chemical observations. Core EM13 (see Fig. 1, for location). Core width is about 10 cm.

188x96mm (300 x 300 DPI)

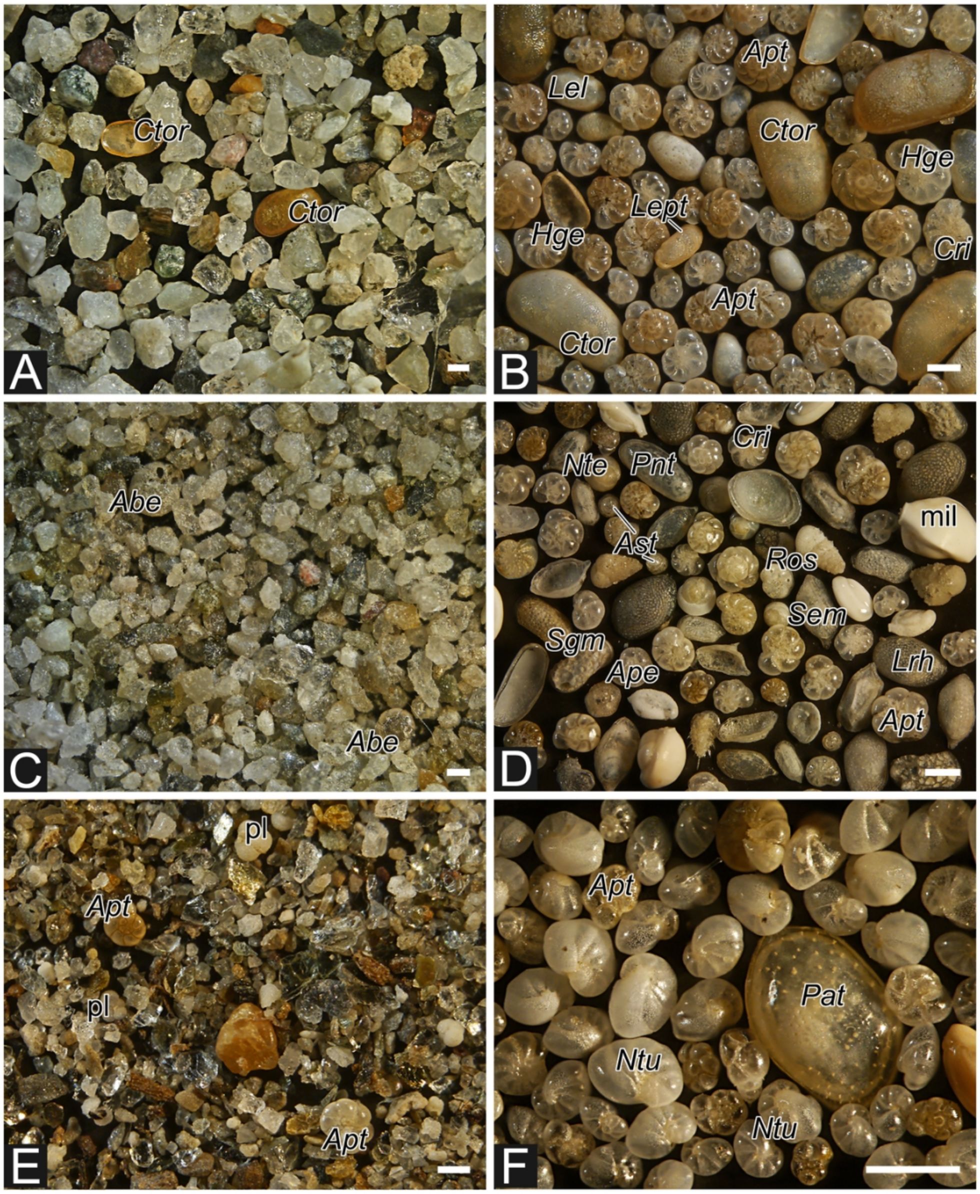

Fig. 4. Diagnostic microfossil assemblages of the middle-late Holocene prograding succession: bay-head delta (A) and back-barrier/outer estuarine (B) deposits (uppermost TST); wave-dominated, delta front (C) and prodelta (D) facies (lower HST); river-dominated, delta front (E) and prodelta (F) facies (upper HST). Assemblages from core EM5, -14.90 m (A); core 205 S5, -15.90 m (B); core EM 11, -9.50 m (C); core EM13, -24.70 m (D); Core 7 at -7.55 m (E) and Core 1 at -23.45 m (F). Scale bar is 250 ☐m long. Abbreviations for benthic foraminifers: Abe – A. beccarii; Apt – A. parkinsoniana, A. tepida; Ape – A. perlucida; Cri – Cribroelphidium spp.; Hge – H. germanica; mil – miliolids; Ntu – N. turgida; epiphytic taxa mainly include Ast – Asterigerinata spp., Nte – Neoconorbina terquemi, Ros – Rosalina spp.; pl – planktonic foraminifers. Abbreviations for ostracods: Ctor – C. torosa; Lel – L. elliptica; Lept – Leptocythere spp.; Lrh – Loxoconcha gr. rhomboidea; Pat – Palmoconcha turbida; Pnt – Pontocythere turbida; Sgm – Sagmatocythere spp.; Sem – Semicytherura spp.

107x130mm (300 x 300 DPI)

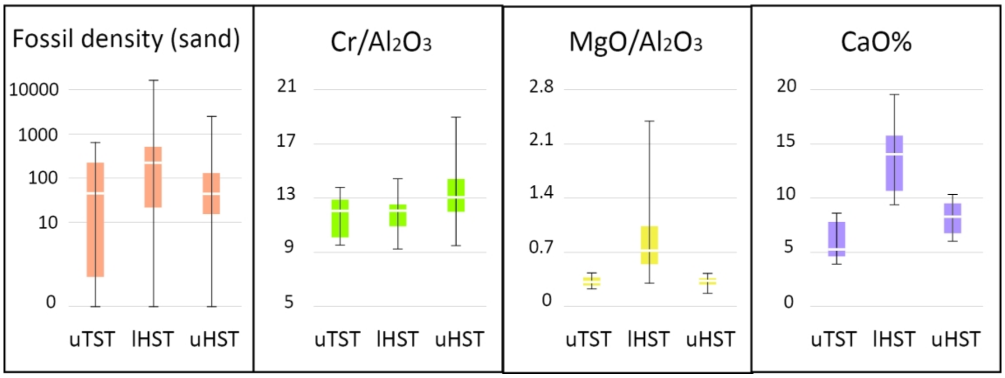

Fig. 5. Box-and-whiskers plots, summarizing major paleontologic (A) and geochemical (B-D) attributes of uppermost TST, lower HST, and upper HST. Box plots span the interquartile range. The white segment inside the rectangle shows the median, and “whiskers” above and below the box show the location of the minimum and maximum. Fossil density in species/dm3.

175x75mm (300 x 300 DPI)

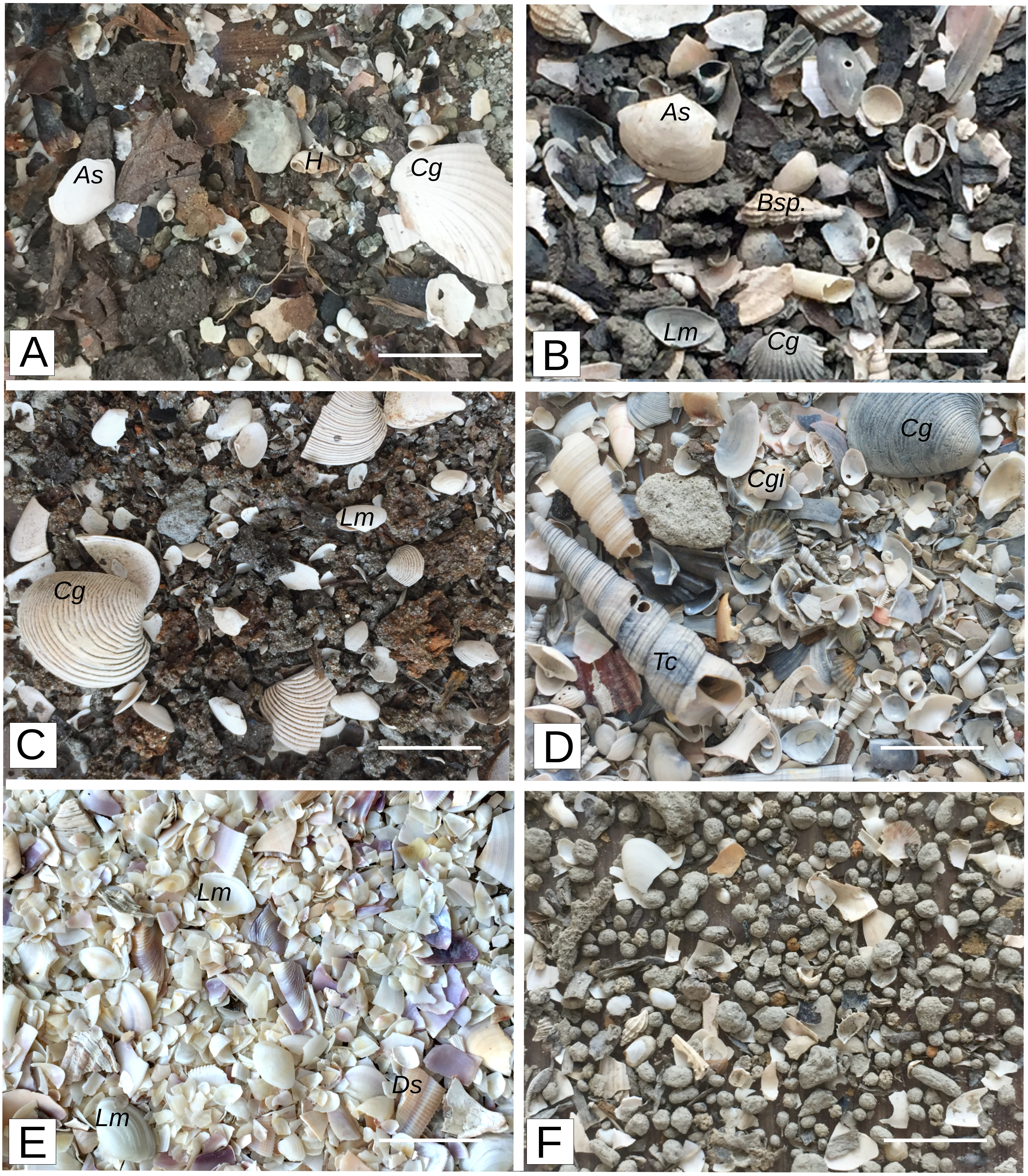
H
As
Cg
A
As
Bsp.
Lm
Cg
B
Lm
Cg
C
Cg
Cgi
Tc
D
Lm
Ds
Lm
E
F

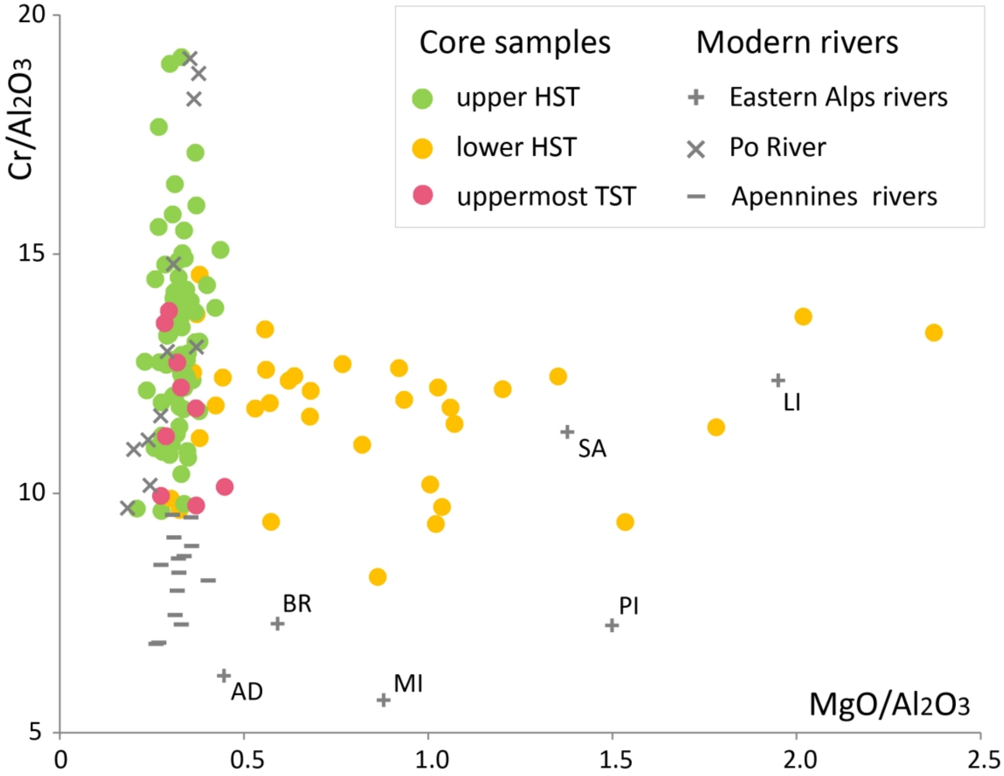

Fig. 7. Scatterplots of MgO/Al2O3 versus Cr/Al2O3, showing consistent changes in sediment composition across the middle-late Holocene succession, and comparison with modern stream sediment composition, including the Po River, Romagna (Ravenna) Apennines rivers, and selected Eastern Alpine rivers. Uppermost TST and upper HST are interpreted to be dominated by Po-River input, whereas lower HST is influenced by Eastern Alpine stream input. (SA: Sarca, MI: Mincio, AD: Adige, BR: Brenta, PI: Piave, and LI: Livenza – for location, see Fig. 1).

179x139mm (300 x 300 DPI)

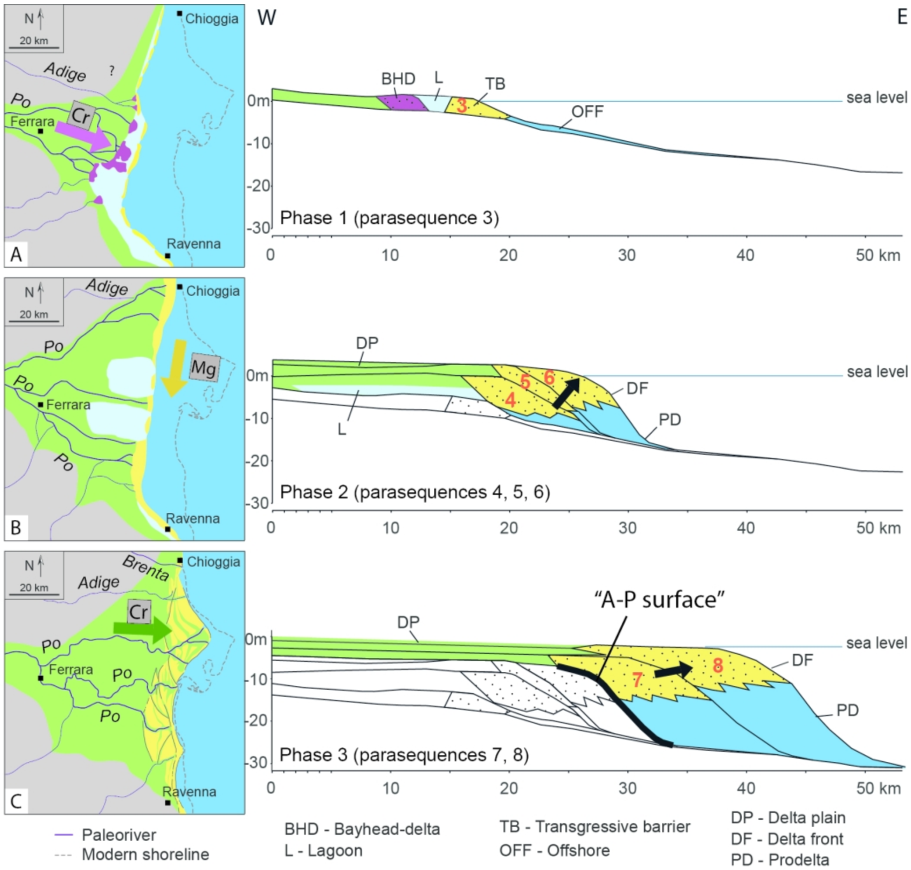

Fig. 8. Middle-late Holocene evolution of the Po coastal system, based upon stratigraphic architecture, paleontologic content and geochemical composition. A: uppermost TST, B: lower HST, C: upper HST. Left: Planview geometry of depositional environments. Right: schematic cross-section. The boundary between lower and upper HST ("A-P" surface") separates dominantly aggradational from progradational stacking patterns and demarcates an abrupt change in sediment characteristics, paleoenvironments and direction of sediment transport.

170x147mm (300 x 300 DPI)

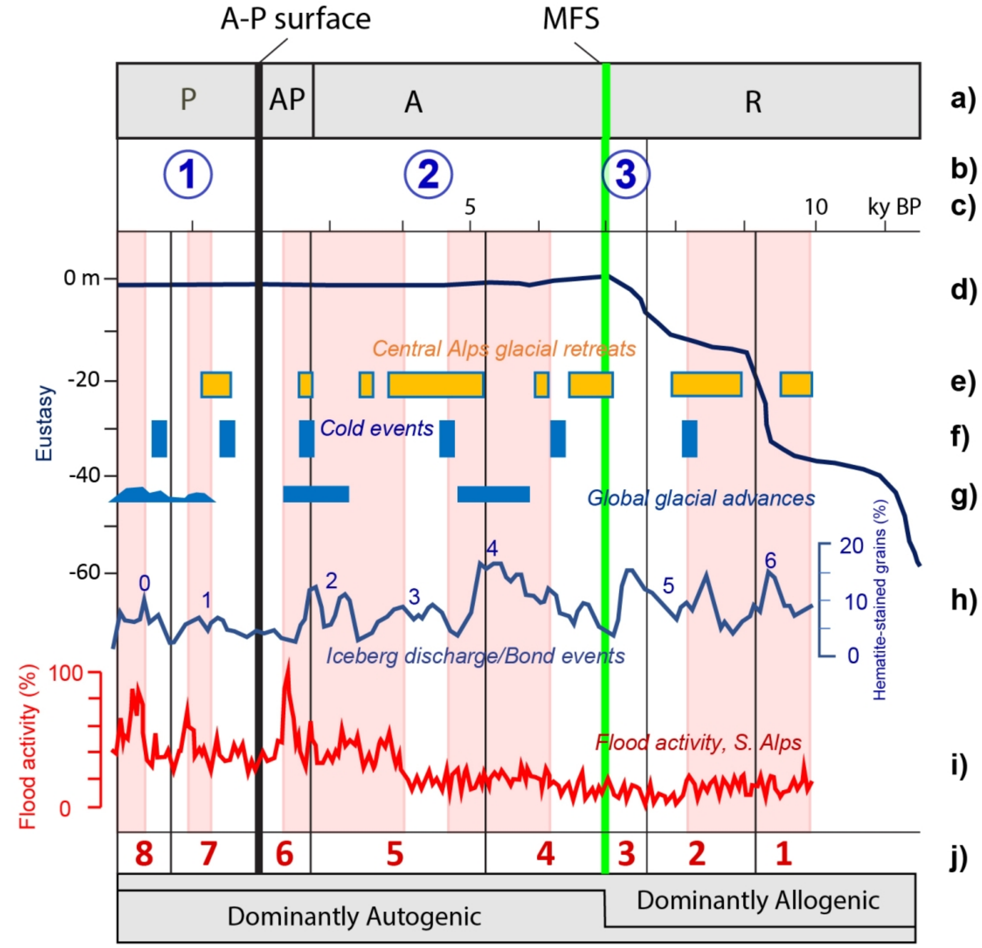

Fig. 9. Key global and regional events during the Holocene. a) Parasequence stacking patterns; b) Stratigraphic phases, Po River system; c) Age (ky BP); d) Eustasy (after Liu et al., 2004); e) Glacial retreat events, central Alps (Hormes et al., 2001); f) Cold events (Wanner et al., 2011); g) Global glacial advances (Denton and Karlén, 1973); h) Iceberg discharge rates and Bond events (Bond et al., 1997); i) Enhanced flood activity in the southern Alpine realm (Wirth et al., 2013); j) Parasequence number (Amorosi et al., 2017); light pink bars are periods of enhanced flood activity in the general Alpine realm (Wirth et al., 2013).

130x128mm (300 x 300 DPI)

		Foraminiferal assemblage	**Ostracod assemblage**	**Mollusk key taxa**	**Biofacies**
Upper HST	Delta front	Rare, well preserved *Ammonia parkinsoniana* and *Ammonia tepida,* and poorly preserved planktonic and benthic taxa (i.e. *Globigerina, Globigerinoides, Orbulina, Bulimina and Cassidulina*)	Absent	*Lentidium mediterraneum*	Opportunistic foraminifers tolerant to high amounts of riverine organic matter in association with transported or reworked taxa. Mainly monotaxic assemblages of the shallow burrower *L. mediterraneum* .
	Prodelta	Abundant to common *Ammonia parkinsoniana* , *Ammonia tepida* and *Nonionella turgida;* common to scarce *Aubignyna perlucida* and *Cribroelphidium granosum;* scarce *Haynesina germanica* and *Quinqueloculina seminulum*	Abundant to common *Palmoconcha turbida;* locally common *Leptocythere ramosa, Pontocythere turbida*	No species meets the requirements	Opportunistic meiofauna tolerant to high amounts of riverine organic matter and, to a lesser extent, oxygen deficiency. Barren of molluscs or scattered macrobenthic remains charachterized by species that are tolerant to a wide range of environmental disturbances
Lower HST	Delta front	Poorly preserved *Ammonia beccarii,* locally associated with well preserved miliolids and other *Ammonia* species	Absent	*Lentidium mediterraneum, Chamelea gallina* and *Spisula subtruncata*	Transported nearshore foraminifers in basinward transition to autochtonous shallow-marine assemblages. Infaunal, low-diversity mollusc assemblages typical of energetical dynamic settings.
	Prodelta	Diversified assemblage with common *Ammonia parkinsoniana, Ammonia tepida* , *Aubignyna perlucida* , *Cribroelphidium granosum* and miliolids; scarce *Nonionella turgida* , other *Cribroelphidium* and epiphytic taxa (such as *Asterigerinata, Neoconorbina, Rosalina*)	Diversified assemblage with common *Loxoconcha* gr. *rhomboidea, Sagmatocythere versicolor* and *Semicytherura* spp.; scarce *Palmoconcha turbida, Pontocythere turbida* and *Sagmatocythere napoliana*	*Corbula gibba, Chamelea. gallina* and *Turritella communis*	Shallow marine meiofauna including both epiphytic taxa and species tolerant to riverine organic matter. Mollusc assemblages dominated by infaunal taxa with high tollerance to torbidity plumes or sedimentation pulses in silty to muddy bottoms.
TST/HST transition	Bay-head delta	Absent	Poorly-preserved *Cyprideis torosa,* locally associated with *Ilyocypris* spp.	*Abra segmentum* , *Lentidium mediterraneum* and hydrobiids	Transported euryhaline and freshwater ostracods. Brackish mollusc assemblages characterized by simplified macrobenthic assemblages and transported freshwater taxa
	Back-barrier	Abundant *Ammonia parkinsoniana* and *Ammonia tepida;* common *Cribroelphidium granosum* and *Haynesina germanica;* scarce *Aubignyna perlucida, Elphidium* and other *Cribroelphidium* species	Abundant *Cyprideis torosa;* common *Loxoconcha elliptica* and *Leptocythere* spp.	*Abra segmentum* , *Cerastoderma glaucum*	Autochtonous brackish meiofauna. Low richness and low equitability macrobenthic assemblages dominated by brackish species

Time span (ky)	***Systems Tract***	***Accommodation***	***Sediment Source***	***Climate and eustatic events***
2.0 – 0.0	upper HST	Subsidence/compaction > eustasy	Po River	S. Alp increased flood activity: 1.3- 0.1 ky BP; N. Europe climate phase change Sub-Atlantic to Little Ice Age (~0.4 ky BP); global and Alpine glacier advances and retreats throughout interval.
7.0 – 2.0	lower HST	Subsidence/compaction > eustasy	E. Alps, alongshore, Po River	S. Alp increased flood activity: 6-5, 3.4-2.4 ky BP; N. Europe climate phase changes: Atlantic to Sub-Boreal (~5.2 ky BP) to Sub-Atlantic (~2.8 ky BP); global and Alpine glacier advances and retreats throughout interval
7.7 – 7.0	Uppermost TST	Eustasy > subsidence/compaction	Po River	Base of interval coincides with glacial melt event mwp-1d
11.5 – 7.7	lower TST	Eustasy >> subsidence/compaction		Base of interval coincides with glacial melt events: MWP-1B

8. BENTHIC FORAMINIFERA: A KEY TOOL IN RIVER-DOMINATED SUCCESSIONS

8.1 Manuscript III

Benthic foraminifera as a key to delta evolution: a case study from the late Holocene succession of the Po River Delta*

Giulia Barbieri, Alessandro Amorosi and Stefano Claudio Vaiani

*Published in **Micropaleontology**

Benthic foraminifera as a key to delta evolution: A case study from the late Holocene succession of the Po River Delta

Giulia Barbieri, Alessandro Amorosi and Stefano Claudio Vaiani
[1] *Dipartimento di Scienze Biologiche, Geologiche e Ambientali,*
University of Bologna, Via Zamboni 67, 40127 Bologna, Italy
email: giulia.barbieri21@unibo.it

ABSTRACT: Benthic foraminifera from stratigraphically expanded, late Quaternary prodelta successions of the Po Delta plain reveal small-scale paleoenvironmental variations within lithologically homogeneous deposits formed under conditions of rapid sedimentation (ca. 6 cm/yr). A detailed paleoenvironmental reconstruction was obtained comparing benthic foraminifera with shallow-water assemblages from the modern Po Delta. The integration with sediment geochemistry and radiocarbon dates was also tested to detect short time-scale delta dynamics controlled by autogenic factors.

Core 7 records the development of an inner-shelf environment (interval A), replaced by a prodelta with strong fluvial influence, shown by the sharp increase in *Ammonia tepida* and *Ammonia parkinsoniana* (interval B). These taxa are replaced by *Aubignyna perlucida* (interval C) which indicates a major mouth shift (Ficarolo avulsion). Subsequent abrupt increases in *A. tepida* and *A. parkinsoniana* document a step-like progradation of the Po di Goro delta lobe (intervals D and E). In the seaward Core 1, possible minor mouth shifts are recorded by a sharp increase in *A. tepida* and *A. parkinsoniana*, paralleled by Cr/Al_2O_3 depletion. The upper portion of both prodelta successions includes stacked flood layers formed near the river mouth, as indicated by scarce *A. tepida* and *A. parkinsoniana*.

INTRODUCTION

Benthic foraminifera have been extensively studied in river-influenced shelves, highlighting the relationships between species distribution and environmental parameters (Jorissen 1988; Blackwelder et al. 1996; Osterman 2003; Duchemin et al. 2008; Frontalini et al. 2011; Barras et al. 2014; Dessandier et al. 2016). In these settings, foraminiferal assemblages are mostly influenced by fluvial discharge products, in terms of the amount and type of organic matter, sedimentary features, depositional rates and oxygen availability (e.g., Van der Zwaan and Jorissen 1991; Jorissen et al. 1992; Mojtahid et al. 2009; Goineau et al. 2011).

Over the last decades, the Po River Delta, one of the major river-dominated deltas in the Mediterranean area, has been the subject of a number of studies focused on foraminiferal distribution (D'Onofrio 1969; Fregni 1978, 1980; Jorissen 1987, 1988; Jorissen et al. 1992; Donnici and Serandrei Barbero 2002), which led to the identification of peculiar shallow-water (ca. 8–20 m) assemblages. Based on these studies, *Ammonia tepida* (Cushman 1926) and *Ammonia parkinsoniana* (d'Orbigny 1839) were recognized as dominant taxa near river outlets, where sedimentation rates, organic matter and oxygen contents are extremely variable. Episodic sedimentation of thick river flood layers determines foraminiferal assemblages with few specimens of *A. tepida* and *A. parkinsoniana* in front of the main fluvial mouths (D'Onofrio 1969; Wheatcroft et al. 2006; Tesi et al. 2008). At comparable depths, but away from river outlets, these species are associated with *Nonionella turgida* (Williamson 1858) (text-fig. 1). At deeper locations (20–30 m water depth), where surface currents concentrate fluvial organic matter in clay sediments and episodes of anoxia regularly occur (the shallow "mud belt" of Van der Zwaan and Jorissen 1991), *N. turgida* is abundant, whereas *A. tepida* and *A. parkinsoniana* become scarce (Jorissen 1988; Donnici and Serandrei Barbero 2002). Finally, foraminiferal assemblages dominated by *A. tepida* and *A. parkinsoniana,* including high percentages of *Aubignyna perlucida* (Heron-Allen & Earland 1913) and commonly associated with *Cribroelphidium granosum* (d'Orbigny 1846), occupy shallow-water areas (ca. 13 m water depth) less enriched in organic matter south of the main river outlets (text-fig. 1; Jorissen 1988). All these assemblages are controlled by the combined effect of river discharge, distance from fluvial outlets and current circulation patterns of the North Adriatic, which govern the distribution of riverine material (Jorissen 1988; Donnici and Serandrei Barbero 2002).

The modern distribution of benthic foraminifera in the Po River delta area has been used as a "modern analogue" for the stratigraphic interpretation of subsurface sedimentary successions. Specifically, previous studies have focused on the role of sea-level rise and the subsequent onset of the Po Delta from the Last Glacial Maximum to the present, under a sequence-stratigraphic framework (Amorosi et al. 2008) or on the micropaleontological record of the fossil Po mud belt below the modern delta plain (Rossi and Vaiani 2008). Geomorphology, core stratigraphy and seismic profiles have also shown that eustatic sea-level rise exerted a major control on stratigraphic architecture during the early Holocene, whereas from the Bronze Age a strong autogenic control took place (Ciabatti 1966; Correggiari et al. 2005b; Stefani and Vincenzi 2005). Local (autogenic) factors, such as river mouth migration, delta lobe switching, and river floods highly influenced deltaic sedimentation during historical times (e.g., Stefani and Vincenzi 2005). High sediment discharge from river mouths resulted in the local deposition of expanded prodelta sediment successions

(Correggiari et al. 2005a), which are potentially suitable to examine short-term deltaic evolution. Specifically, radiometric dating of selected cores shows remarkably high sedimentation rates of deltaic units during the last centuries (about 4 to 6 cm/yr from the late Middle Age; Roveri et al. 2001; Rossi and Vaiani 2008). On such short-term timescales, bathymetric variations related to eustasy or subsidence might be negligible, and most likely reflect changes in sediment supply.

These previous studies provide morphological and stratigraphic evidences for the substantial role of autogenic factors in the deltaic evolution and form the framework of this work mainly focused on the response of benthic foraminifera to past autogenic events. In details, local factors that may influence prodelta sedimentation, such as mouth migrations and floods can hardly be assessed by conventional core facies analysis. However, they produce variations in fluvial discharge, sediment supply and amount of continental organic matter, that can be recorded by benthic foraminifera, which are extremely sensitive to even subtle changes in river-influenced, marine environmental conditions (e.g., Jorissen 1988; Jorissen et al. 1992).

This study focuses on foraminiferal distribution from the expanded prodelta succession of Core 7 (text-fig. 1), recovered in the southern part of the modern Po Delta plain and is integrated by the review of data from the more distal Core 1 (Amorosi et al. 2008; Rossi and Vaiani, 2008; text-fig. 1) in order to recognize the foraminiferal evidences of past autogenic events in a seaward position.

Specific aims of this paper are: (i) to test the ability of benthic foraminifera to record short paleoenvironmental variations induced by autogenic deltaic processes, strictly constrained in time and space, such as avulsion and flood events, and (ii) to provide insights on the overall dynamics of river-dominated deltas under stable eustatic conditions, when autogenic control prevails over allogenic factors.

HOLOCENE STRATIGRAPHY AND DEVELOPMENT OF THE PO RIVER DELTA

Above a thick package of Late Pleistocene alluvial plain deposits, the Holocene succession in the subsurface of the Po River Delta consists of a transgressive-regressive sedimentary wedge made up of coastal to shallow-marine deposits (e.g., Rizzini 1974; Amorosi et al. 1999, 2017 – text-fig. 1b). These two units are separated by the transgressive surface (TS in text-fig. 1b). The superposition of transgressive barrier sands and inner-shelf clays onto back-barrier facies (text-fig. 1b) reflects the backstepping of a barrier-lagoon-estuary system during the early Holocene eustatic rise (transgressive systems tract – TST). The shallowing-upward succession of prodelta, delta front, and delta plain deposits of Middle to Late Holocene age (text-fig. 1b) has been interpreted to reflect delta (and strandplain) progradation during the following sea-level highstand (highstand systems tract – HST – Amorosi et al., 2003).

Po Delta initiation occurred at the onset of sea-level highstand conditions, ca. 5.5 ka BP (Piva et al. 2008; Amorosi et al. 2016). As revealed by several comprehensive reviews (e.g. Ciabatti 1966; Nelson 1970; Correggiari et al. 2005a, b; Stefani and Vincenzi 2005), HST development was controlled by the interplay of climate change, autogenic factors and anthropic activity. Subtle "transgressive" events, followed by localized progradation and bay infilling, characterized the early sea-level highstand (Stefani and Vincenzi, 2005). From the late Bronze Age to the Middle Ages (ca 3000-1200 cal yr BP), a complex network of distributary channels developed south of Adria under a dominant wave activity.

In the middle of the XII Century, a major avulsion event historically reported as "Rotta di Ficarolo" (A.D. 1152-1192; 798-758 yr BP) caused a substantial northward shift of the Po Delta (Veggiani 1990), with abandonment of the southern mouths. At first, Po di Goro (text-fig. 1a) was the main outlet (Ciabatti 1966), producing the last cuspate delta of the Po River (XII-XVI Century). Gradually, Po delle Fornaci (i.e., the modern Po di Levante in text-fig. 1a) became the most active channel, generating the first lobate delta. In order to prevent the infilling of the Venice Lagoon by the northern migration of the delta, the Venice Republic operated the "Porto Viro" cut in A.D. 1600-1604 (350-346 yr BP), which deviated Po delle Fornaci into the Goro Lagoon. The Fornaci branch was progressively abandoned, and the construction of the modern input-dominated Po Delta started with the development of several delta lobes fed by recent distributary channels (text-fig. 1a).

The offshore sedimentary evolution of the Po Delta is recorded by seismic profiles from the modern prodelta area, which reveal the same history reconstructed onshore on the basis of geomorphological features (Correggiari et al. 2005a). The delta lobes that followed the Ficarolo avulsion, between A.D. 1200 and 1600, have been recovered in the subsurface of the modern delta plain and consist of stratigraphically expanded prodelta successions (Roveri et al. 2001; Amorosi et al. 2008).-

MATERIALS AND METHODS

Foraminiferal analyses were carried out on Core 7, stratigraphically described by Stefani and Vincenzi (2005; listed as 187-S7) and compared with previously published data from Core 1 (text-fig. 1; Rossi and Vaiani 2008). Core 7, 55 m-long, was recovered by wire-line perforation in the Po di Goro delta lobe (ca. 800-350 cal. yr BP; Stefani and Vincenzi 2005). Micropaleontological analyses were undertaken in the upper 37 m of the succession. A total of 89 samples of approximately 80 g of dry weight, collected every 50-30 cm, were treated following the procedures reported for Core 1 in Rossi and Vaiani (2008), to facilitate comparison of paleontological data between the two cores. Specifically, sediment samples were (i) dried at 60 °C for 24 hours; (ii) soaked in water or water plus hydrogen peroxide (35% vol.); (iii) washed through 63 µm sieves (240 mesh); (iv) dried again for 24 hours. Treated samples were observed under a binocular microscope to perform a qualitative analysis of the foraminiferal assemblage. After that, 48 samples containing well preserved and abundant foraminifera were chosen for quantitative analysis, divided into small portions including at least 300 specimens in the size fraction >125 µm with a microsplitter and then counted (11 of these samples contained fewer than 300 specimens in the whole >125µm sediment; details in Appendix 1). The other 41 samples are barren in foraminifera or show only very rare and poorly preserved specimens.

Foraminiferal taxa were identified on the basis of original microfossil descriptions (Ellis and Messina 1940) and several key papers (Jorissen 1988; Albani and Serandrei Barbero 1990; Cimerman and Langer 1991; Fiorini and Vaiani 2001; Sgarrella and Moncharmont Zei 1993; Rasmussen 2005).

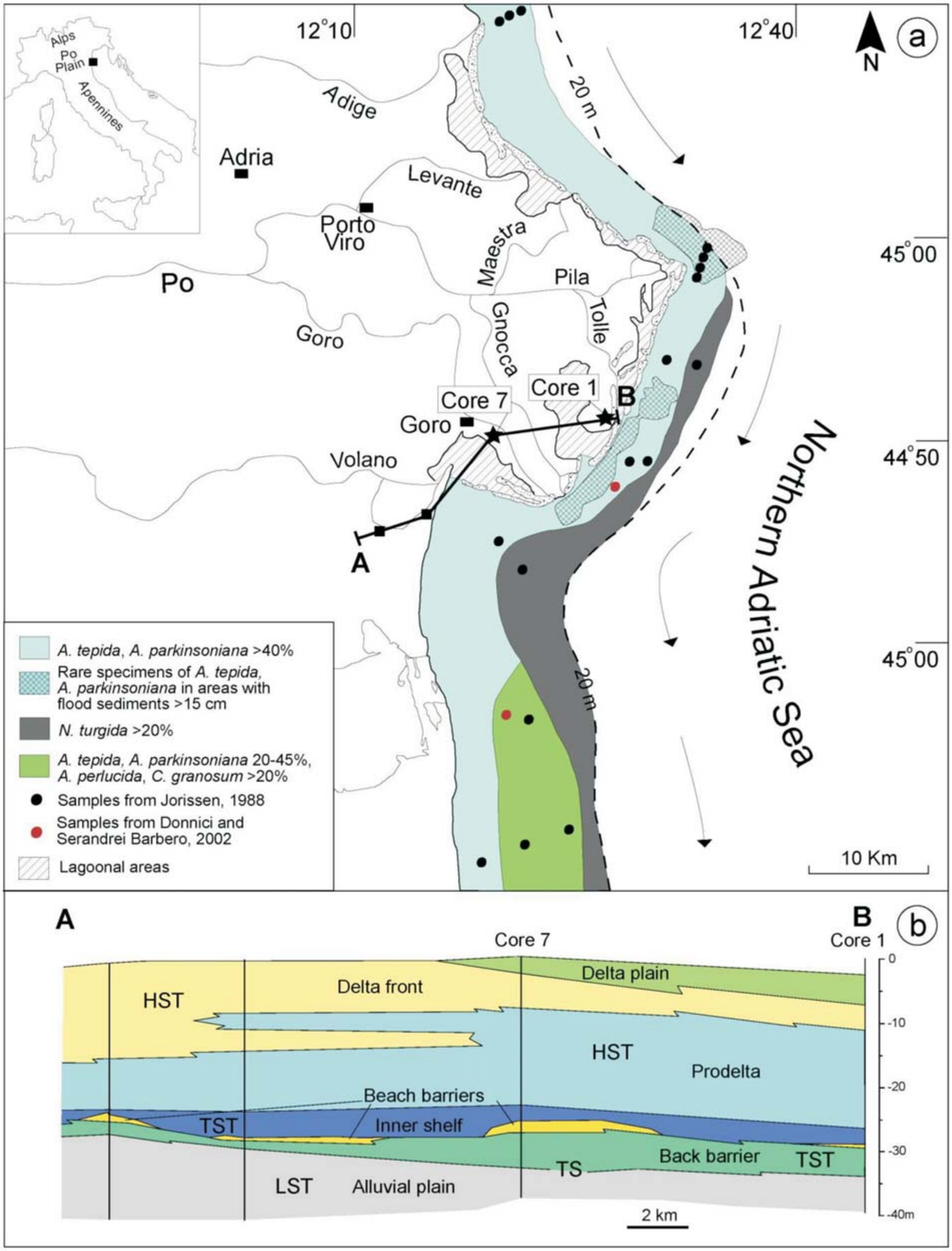

TEXT-FIGURE 1
a) Location of cores 1 and 7. Colored areas correspond to benthic foraminiferal assemblages recorded in the shallow Po prodelta at <20 m water depth (Jorissen 1988; Donnici and Serandrei Barbero 2002). Cross-line filled areas: distribution of sediments with thickness >15 cm related to the A.D. 2000 Po river flood (Wheatcroft et al. 2006), corresponding to samples with scarce fauna reported by D'Onofrio (1969). Arrows: main North Adriatic longshore current. Black thick line: trace of section reported in text-figure 1b. b) Facies architecture beneath the modern Po Delta and Romagna coastal plain (modified after Amorosi et al. 2003). LST: lowstand systems tract, TST: transgressive systems tract, HST: highstand systems tract, TS: transgressive surface.

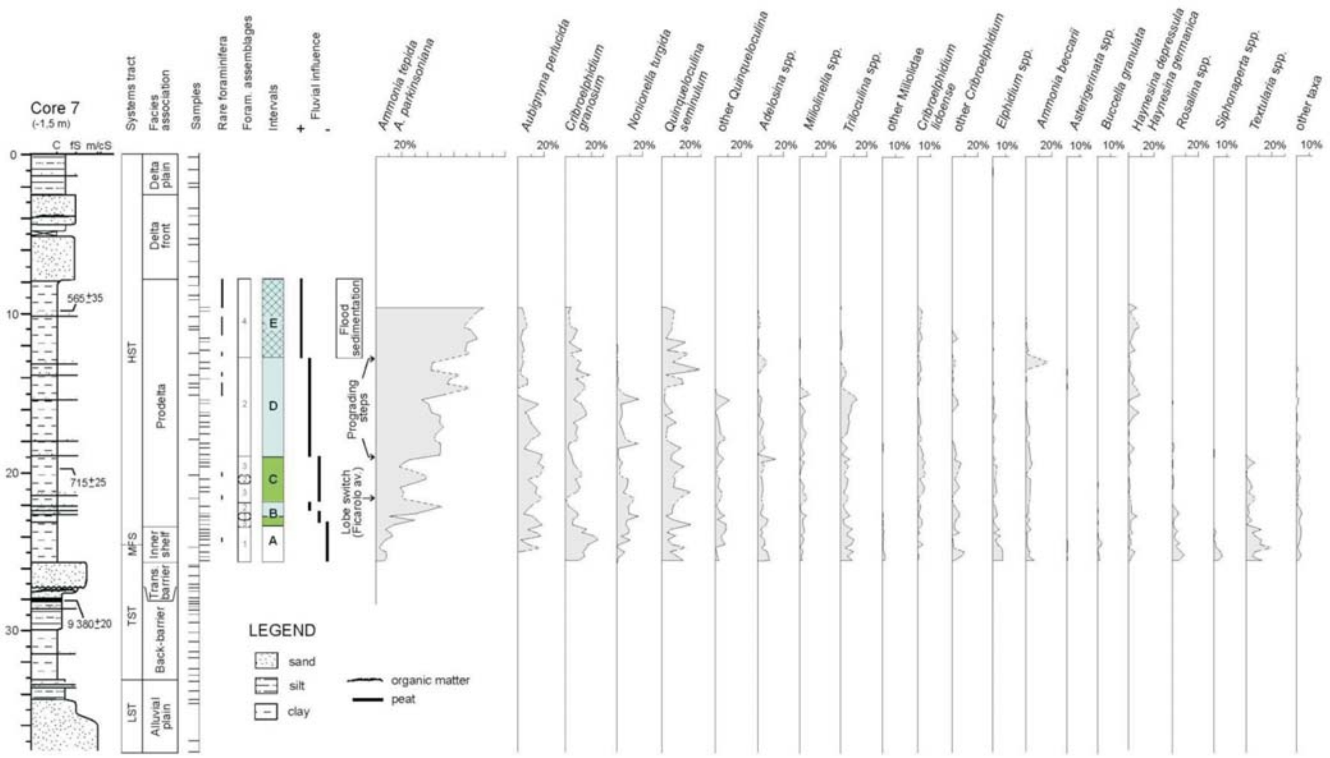

TEXT-FIGURE 2
Stratigraphy and vertical distribution of foraminiferal assemblages within Core 7. Letters atop of core log indicate sediment grain size (C, clay; fS, fine sand; mS, medium sand; cS, coarse sand). Ages are reported as calibrated years BP. Samples analysed for benthic foraminiferal assemblages with >300 specimens included in the data matrix on the right side, samples containing <300 specimens or not included in the data matrix on the left side. Rare foraminifera indicate samples containing <300 specimens of benthic foraminifera. Colored intervals refer to the environmental distribution of foraminiferal assemblages (text-fig. 1). Fluvial influence is assessed by the environmental significance of fossil foraminiferal assemblages, as evidenced also by the nMDS analysis (text-fig. 5).

In order to define foraminiferal assemblages and the main trends of foraminiferal faunas, multivariate statistical analyses were performed using the PAST software (PAleontological STatistic, ver. 3.10, Hammer et al. 2001), specifically designed for paleontological purposes. Only samples with >300 specimens (a total of 68 samples) were used for statistical analyses. In addition to samples of Core 7, samples from Core 1 were included in the data matrix (37 samples from Core 7 and 31 samples from Core 1), to compare the trend in microfossil assemblages of the study area. The data matrix included non-standardized percentage data of taxa (up to genera level; Davis 1986), in accordance with other studies on shallow-marine environments (Jorissen 1988; Donnici and Serandrei Barbero 2002; Frezza and Carboni 2009; Mojtahid et al. 2009; Goineau et al. 2011). Groups of taxa up to genera level include a wide number of species with low frequencies and similar ecological significance, typically found within subsurface sedimentary successions of the Po Delta (Fiorini and Vaiani 2001). Taxa were grouped in accordance with Rossi and Vaiani (2008), in order to compare the microfossil fauna of cores 7 and 1. Eighteen taxa with abundance >4% observed in both cores were included in the data matrix for multivariate analyses. Q-mode cluster analysis (Unweighted Pair-group Method with Arithmetic mean – UPGMA algorithm) based on Bray-Curtis distance was applied to obtain groups of samples with similar foraminiferal content. In order to detect the taxa responsible for the variability among groups of samples defined by Q-mode cluster analysis, a Similarity Percentage Analysis (SIMPER) was performed. In the end, the application of a non-Metric Multidimensional Scaling (nMDS) allowed us to understand the distribution of samples related to the main paleoenvironmental gradient. The acceptable value of stress (<0.20) resulted from nMDS performed in two dimensions.

The paleoenvironmental interpretation of foraminiferal assemblages relies upon a series of specific papers about recent foraminiferal distribution in the Po Delta and other Mediterranean coastal systems (D'Onofrio 1969; Jorissen 1987, 1988; Van der Zwaan and Jorissen, 1991; Barmawidjaja et al. 1992; Bellotti et al. 1994; Donnici and Serandrei Barbero 2002; Murray 2006; Frezza and Carboni 2009; Mojtahid et al. 2009; Goineau et al. 2011, 2012, 2015). Fossil foraminiferal assemblages were compared with total assemblages of Jorissen (1988) and Donnici and Serandrei Barbero (2002), which represent reliable modern analogue faunas. The use of total assemblages is particularly important, because taphonomical (transport, test disintegration, mixing) and biological factors (population dynamics) may alter the composition of dead foraminiferal assemblages from the original living ones, particularly in river-dominated shelves (Murray 1991; Jorissen and Wittling 1999; Mendes et al. 2013; Goineau et al. 2015). Relationships between river flood sedimentation and foraminiferal fauna were reconstructed through correlation of flood sediment distribution (Wheatcroft et al. 2006) with foraminiferal assemblages in this area (D'Onofrio 1969; Jorissen 1988).

The chronological framework of the cored succession relies on three calibrated AMS ^{14}C dates (Table 1). Conventional radiocarbon dates were calibrated using software OxCal Ver. 3.10 and the dataset of Reimer et al. (2004). The marine calibration curve and the Northern Adriatic ΔR (-61±50) were applied to dated mollusks.

RESULTS

Stratigraphy of Core 7

The stratigraphy of Core 7 includes a succession of upper Pleistocene, lowstand (LST) alluvial facies overlain by Holocene, transgressive-regressive (TST+HST) deposits (text-fig. 2). The sedimentological features of Core 7 have been described at length by Stefani and Vincenzi (2005), and will not be reiterated here. On the other hand, micropaleontological criteria were used in this paper to identify the maximum flooding surface (MFS in text-fig. 2). This key stratigraphic surface, at the boundary between TST and HST, commonly occurs within seemingly homogeneous shallow-marine muds and has poor sedimentological expression. For this reason, the analysis of foraminiferal assemblages from Core 7 was focused on shallow-marine deposits between 25.50 and 7.95 core depth (text-fig. 2).

Definition of foraminiferal assemblages by statistical analysis

Q-mode cluster analysis allowed the identification of three main clusters with a cut-off level of 0.47, and additional sub-clusters within cluster 2 (text-fig. 3). Contribution of foraminiferal species to each cluster is shown by SIMPER analysis (Table 2).

Five major taxa that contribute for >60% of the total difference between groups are *A. tepida – A. parkinsoniana*, *N. turgida*, *A. perlucida* and *C. granosum*. Contribution of taxa is equally distributed in cluster 1, where the main taxa are *C. granosum* (16%) and *A. perlucida* (12.2%). The major contribution of *Textularia* (4.4%), *Rosalina* (2.5%), *Siphonaperta* (1.5%) and *Buccella granulata* (Di Napoli Alliata 1952) (0.6%) is recorded in this cluster, which includes the lowermost samples of both cores (assemblage 1, Text-figures 3, 4a). Cluster 2 is characterized by high percentages of *A. tepida – A. parkinsoniana*. These taxa account for 47% in the composition of sub-cluster 2.1 (assemblage 2), whereas they show a frequency of 20.9% in sub-cluster 2.2, with relatively high abundance of *A. perlucida* (17.6%), *Quinqueloculina seminulum* (Linnaeus, 1758) (12.2%) and *C. granosum* (9.4%), which define assemblage 3 (text-fig. 4b). The relative contribution of *A. tepida – A. parkinsoniana* reaches its maximum in the uppermost samples of both cores in sub-cluster 2.3, thus foraminiferal assemblage 4 is strongly dominated by these taxa (83.4%) and *N. turgida, A. perlucida, C. granosum* and *Q. seminulum* become very rare (text-fig. 4c). Assemblage 5 includes the remaining samples of cluster 3, from 25.08 to 20.65 m depth of Core 1, where the main contributor is *N. turgida* (45.6%), with the slight occurrence of *A. tepida – A. parkinsoniana* (17.4%) (text-fig. 4d).

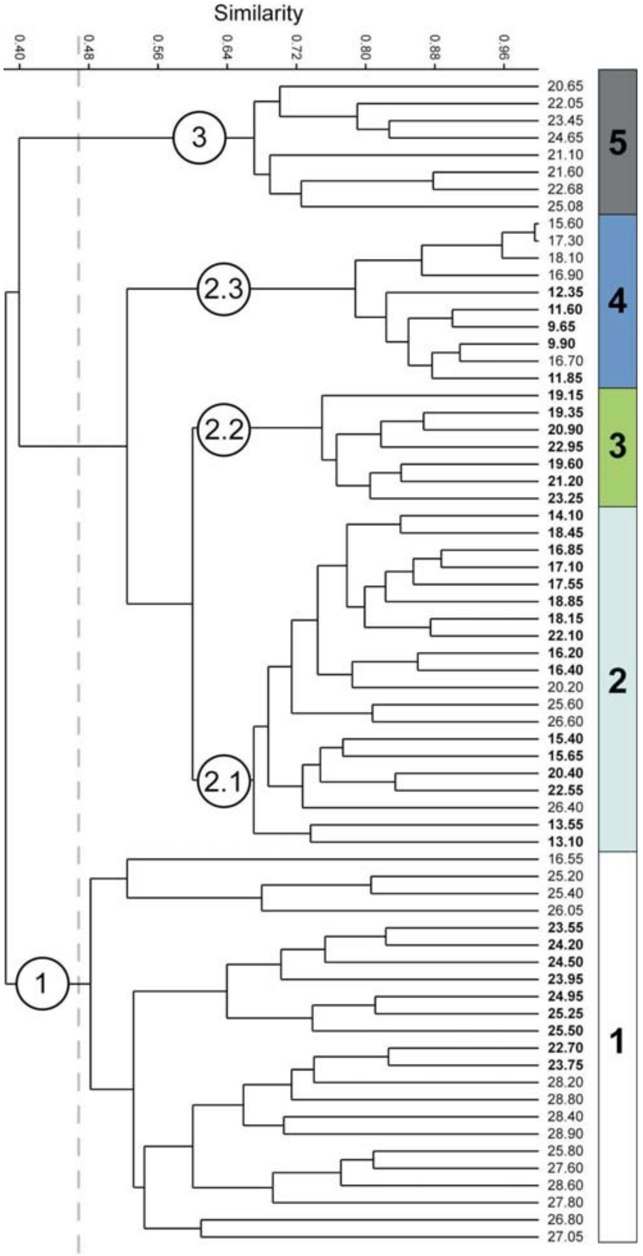

TEXT-FIGURE 3
Q-mode cluster analysis (UPGMA, Bray Curtis distance) for the 18 most abundant taxa (>4%) of benthic foraminifera >125 ìm from fine-grained sediment successions of cores 7 and 1. Core 7 samples are shown in bold. Clusters and sub-clusters' numbers are circled. Each of them represents a fossil assemblages, indicated in the column on the right side.

Stratigraphic distribution of foraminiferal assemblages

Following the definition of foraminiferal assemblages through Q-mode cluster, five intervals were identified on Core 7 based on the distribution of foraminiferal assemblages.

Interval A, between 25.50 and 23.40 m core depth, includes samples of assemblage 1. A strong faunal change is recorded upwards in interval B, which is characterized by assemblage 3 up to 22.80 m core depth, overlain by assemblage 2. An isolated

TEXT-FIGURE 4
Benthic foraminiferal assemblages from selected samples of cores 7 and 1. a: Foraminiferal assemblage 1 (diversified fauna); Core 7, interval A, 24.50 m depth; b: foraminiferal assemblage 3 (common *A. tepida*, *A. parkinsoniana*, *A. perlucida*, *C. granosum* and *Q. seminulum*); Core 7, interval C, 19.60 m depth; c: foraminiferal assemblage 4 (dominated by *A. tepida* and *A. parkinsoniana*); Core 7, interval E, 9.90 m depth; d: foraminiferal assemblage 5 (dominated by *N. turgida*); Core 1 interval 2, 21.60 m depth. Scale bar: 200 µm.

sample within this interval (22.70 m core depth) belongs to assemblage 1. Interval C is determined by the presence of assemblage 3 from 21.65 to 19.00 m core depth, with only one sample at 20.40 m core depth attributed to assemblage 2. This part of the succession (19.80 core depth) was dated to 715±25 cal. yr BP. The overlying interval D is defined by assemblage 2, up to 12.70 m core depth, whereas the uppermost interval E is identified by assemblage 4 and the common occurrence of samples with low amount of specimens dominated by *A. tepida* and *A. parkinsoniana* (rare foraminifera in text-fig. 2). The radiocarbon date performed at 9.90 m depth revealed an age of 565±35 cal. yr BP.

In order to make a comparison with the new data from Core 7, statistical analyses were performed also within samples from Core 1. The distribution of foraminiferal assemblages within Core 1 is substantially comparable with the previous work of Rossi and Vaiani (2008). In particular, assemblage 1 is recorded from 28.90 to 25.15 m core depth, excluding some scattered samples assigned to assemblage 2 (26.60, 26.40 and 25.60 m core depths). Foraminiferal assemblage 5 dominates between 25.10 and 20.50 m core depth, and is overlain by just one sample attributed to assemblage 2. The upper portion of the succession includes foraminiferal assemblage 4 and samples with a scarce fauna dominated by *A. tepida* and *A. parkinsoniana*. Among these, sample at 16.55 m core depth is included in cluster 1 (text-fig. 3).

Foraminiferal assemblages in the nMDS

The nMDS ordination of all samples allows the identification of the general trend of benthic foraminiferal assemblages from cores 7 and 1 (text-fig. 5).

Samples are regularly distributed along axis 1 of the ordination plot. Assemblage 1 is placed in the right part of the diagram, with remarkable positive loadings on axis 1. Foraminiferal as-

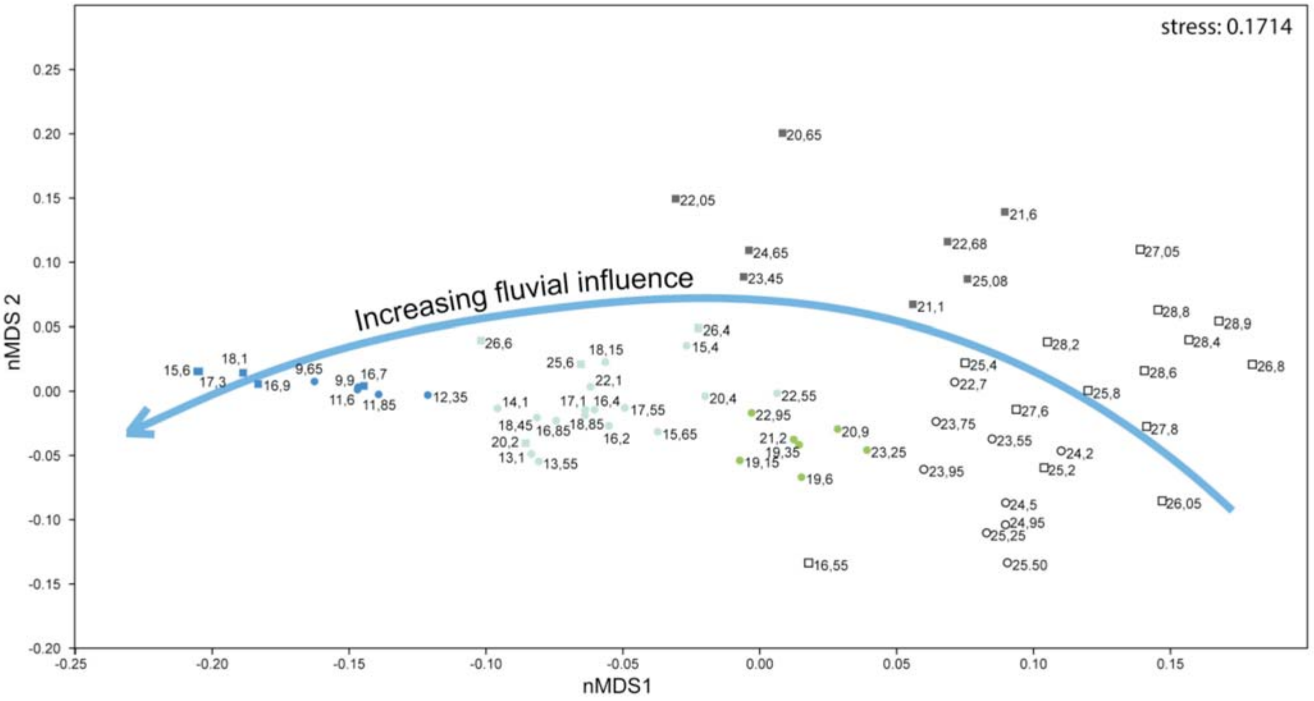

TEXT-FIGURE 5
Non-Metric Multidimensional Scaling (nMDS) based on Bray-Curtis distance. Projection of the 68 samples from cores 7 and 1. Circles: samples from Core 7; squares: samples from Core 1. Arrow indicates the increasing fluvial influence, responsible for the distribution of foraminiferal assemblages on the plot.

semblages 5 and 3 show similar values for axis 1, but assemblage 5 is positively correlated with axis 2, whereas assemblage 3 has slightly negative loadings. Samples of assemblage 2 are placed in the central-left part of the diagram, but the most negative values of axis 1 are related to foraminiferal assemblage 4, in the extreme left portion of the plot.

DISCUSSION

Paleoecological significance of benthic foraminiferal assemblages

Results of cluster and SIMPER analyses define five main foraminiferal assemblages, related to specific benthic environments. Ecological features of major contributor taxa and the comparison with modern foraminiferal assemblages near the Po Delta (Jorissen 1988; Donnici and Serandrei Barbero 2002) provide detailed information about paleoenvironmental conditions recorded by foraminiferal assemblages.

Foraminiferal assemblage 1 includes taxa typical of shallow-marine environments with vegetated and oxygenated bottoms, like *Textularia, Buccella*, *Rosalina* and *Asterigerinata* (Blanc-Vernet 1969; Jorissen 1988; Sgarrella and Montcharmont Zei 1993; Goineau et al. 2011). *Quinqueloculina seminulum* is reported from inner shelves to lagoons (Murray 2006), and it is also common in prodelta environments (Bellotti et al. 1994; Donnici and Serandrei Barbero 2002). *Cribroelphidium granosum* and *A. perlucida* typically live in river influenced environments on clayey bottoms enriched in organic matter, and reach maximum frequencies at <20 m water depth, south of the modern Po Delta (Jorissen 1988). Benthic foraminiferal assemblage 1 reflects an inner-shelf environment with low fluvial discharge. Local high concentrations of *A. perlucida* or *C. granosum* suggest transition to the prodelta.

Assemblage 2 shows frequencies of *A. tepida* and *A. parkinsoniana* (40–50%) comparable to those recorded near the Po Delta outlets, at ca. 10 m water depth (Jorissen 1988; text-fig. 1). These taxa are able to thrive in environments with strong fluctuations in sediment and organic matter inputs (Jorissen 1988; Mojtahid et al. 2009; Frontalini et al. 2011).

The high frequency of *A. perlucida* and *C. granosum* indicative of assemblage 3 is consistent with a shallow prodelta environment. Amounts of *A. tepida* and *A. parkinsoniana* (26%), *A. perlucida* and *C. granosum* (24% considered together) comparable to those resulting from SIMPER analysis have been found ca. 30 km south of the Po Delta, at 17 m water depth (Jorissen 1988; text-fig. 1). Assemblage 3 includes also significant concentrations of *Q. seminulum*, a species recorded with its highest frequencies in proximity of the Po River outlets (Donnici and Serandrei Barbero 2002). The considerable amounts of *A. perlucida*, *C. granosum* and *Q. seminulum* are consistent with a shallow prodelta environment with high organic matter content and slight oxygen deficiency at the bottom.

Ammonia tepida and *A. parkinsoniana* strongly dominate assemblage 4, as in the modern Po Delta, where these taxa are dominant (>50%) in front of the main river outlets, at 9–15 m water depth, being typically associated with low amounts of *A.*

TABLE 1
Radiocarbon dates from Core 7.

Core ID	Core depth (m)	Material	Conventional age (yr BP)	Calibrated age (cal yr BP)	Laboratory	Reference
Core 7	9.90	Mollusk shells	820±30	565±35	KIGAM (Korea)	This paper
Core 7	19.80	Mollusk shells	1050±30	715±25	KIGAM (Korea)	This paper
Core 7	28.10	Peat	8150±100	9380±20	Beta analytic (FL, USA)	Cibin and Stefani, 2009

perlucida and *C. granosum* (Jorissen 1988). These zones are subject to remarkable sediment discharge, especially during flood events (Wheatcroft et al. 2006; text-fig. 1). Similarly, in the shallow Rhône prodelta (24 m water depth), Goineau et al. (2012) observed assemblages almost entirely composed of *A. tepida* (94% within the uppermost 5 cm of a flood layer in the >150 μm size fraction) few weeks after a river flood that produced unstable conditions with massive sediment input and high organic matter supply. The observed amounts of *A. tepida* and *A. parkinsoniana* and the distribution of subordinate species reflect a strongly river-influenced environment, very close to the fluvial mouth.

Assemblage 5 is dominated by the stress-tolerant taxon *N. turgida*, which typically thrives in mud belt areas, where high amounts of fine-grained fluvial sediments enriched in organic matter are deposited (Van der Zwaan and Jorissen 1992; Mojtahid et al. 2009). This species is also able to proliferate under spring bloom conditions, with strong inputs of fresh phytodetritus promoted by upwelling or a supply of riverine sediments (Gustafsson and Nordberg 2001; Diz et al. 2006; Duchemin et al. 2008; Goineau et al. 2012). In the Northern Adriatic Sea, this species dominates modern assemblages of the mud belt located some km seaward from river mouths, at less than 20 m water depth (Jorissen 1988; Donnici and Serandrei Barbero 2002; text-fig. 1). The degradation of organic matter provided by the Po River plume and seasonal algal blooms promote the development of anoxic conditions in this area (Van der Zwaan and Jorissen 1992; Barmawidjaja et al. 1995).

Based on the paleoecological significance of benthic foraminiferal assemblages, their distribution in the nMDS diagram can be related to a main paleoenvironmental gradient, that reflects a progressive increase of fluvial influence (text-fig. 5), as it was documented also for the Rhône prodelta by Mojtahid et al. (2009). In this context, fluvial influence is intended as the combination of vicinity to river outlets and amount of fluvial discharge (i.e., freshwater, sediment and organic matter inputs provided by rivers), which leads to stressful conditions in the bottom sediments. The right portion of the nMDS plot is occupied by inner shelf assemblages with the least fluvial influence, whereas higher fluvial influenced conditions are reflected by foraminiferal assemblages 3 and 5 in the central area of the diagram. Abundant *A. perlucida* and *C. granosum* characteristic of assemblage 3 are common a few km south of the Po Delta, whereas assemblage 5 dominated by *N. turgida* is typical of the North Adriatic mud belt located some km away from fluvial outlets (Jorissen 1988; Donnici and Serandrei Barbero 2002). These assemblages indicate high fluvial influence in areas supplied by high amount of sediments enriched in organic matter from the Po River, with slight (assemblage 3) or high (assemblage 5) oxygen deficiency. Moving towards the left side of the nMDS, assemblage 2 is related to a further increase in fluvial influence that reaches its maximum with assemblage 4, with the overwhelming dominance of *A. tepida* and *A. parkinsoniana* close to the river mouths (Goineau et al. 2012).

A similar variation in fluvial influence has also been documented in the modern Rhône prodelta by dead foraminiferal assemblages (Goineau et al. 2015). In that setting, the most stressful and fluvial influenced conditions are recorded near the fluvial mouths by foraminiferal faunas dominated by *A. tepida*; assemblages with abundant *N. turgida* are found few km further, under relatively less stressful conditions, whereas more stable and less fluvial influenced conditions are reflected in high-diversity assemblages of the continental shelf. In our samples plotted on the nMDS diagram we observe a succession of analogous foraminiferal assemblages, from inner shelf (mixed riverine/marine influence in Goineau et al. 2015) to mud belt (river plume) and then river mouth faunas, interpreted to reflect increasing fluvial influence. However, variations in the main foraminiferal taxa within cores 7 and 1 are abrupt (text-fig. 6), suggesting sudden paleoenvironmental changes.

Shallow-marine to prodelta evolution of Core 7

Foraminiferal assemblage 1 from interval A is indicative of an inner-shelf environment and the local abundance of *C. granosum* and *A. perlucida*, mainly in the upper part of the interval, suggests transition to a river influenced (prodelta) environment. The highest concentration of open-marine taxa (*Asterigerinata* spp.*, Buccella granulata, Siphonaperta aspera, Textularia* spp.) and the lowest abundance of euryhaline species (*A. tepida* and *A. parkinsoniana*) at 24.50 m depth, thus, are considered indicative of the maximum flooding surface (MFS in text-fig. 2), according to the criteria described in Amorosi and Colalongo (2005) and applied to various subsurface successions of the Po Delta (e.g., Amorosi et al. 2008; Rossi and Vaiani 2008). After peak transgression, sediment supply prevailed over the reduced sea-level rise, inducing progradation of the coastal system (Amorosi et al. 1999).

The high frequencies of *A. perlucida* and *C. granosum* recorded by assemblage 3 at the base of interval B are consistent with a shallow prodelta environment. One sample (22.70 m core depth) from assemblage 1 is present within this interval, which suggests unstable environmental conditions. The superposition of assemblages 3 and 2 is indicative of increasing fluvial influence related to an approaching river mouth (i.e., deltaic progradation).

The abrupt change in foraminiferal assemblages from interval B to C is consistent with a sudden decrease in fluvial influence, attributed to a river avulsion in the delta plain (lobe switch in text-fig. 2), with no substantial bathymetric variations. Based on the radiocarbon age from the middle portion of interval C (715±25 cal. yr BP), this paleoenvironmental change at the interval B-C boundary is related to the Ficarolo avulsion, which occurred between 798 and 758 yr BP (1152 – 1192 A.D.; Ciabatti 1966). Before this event, Po di Volano was one of the

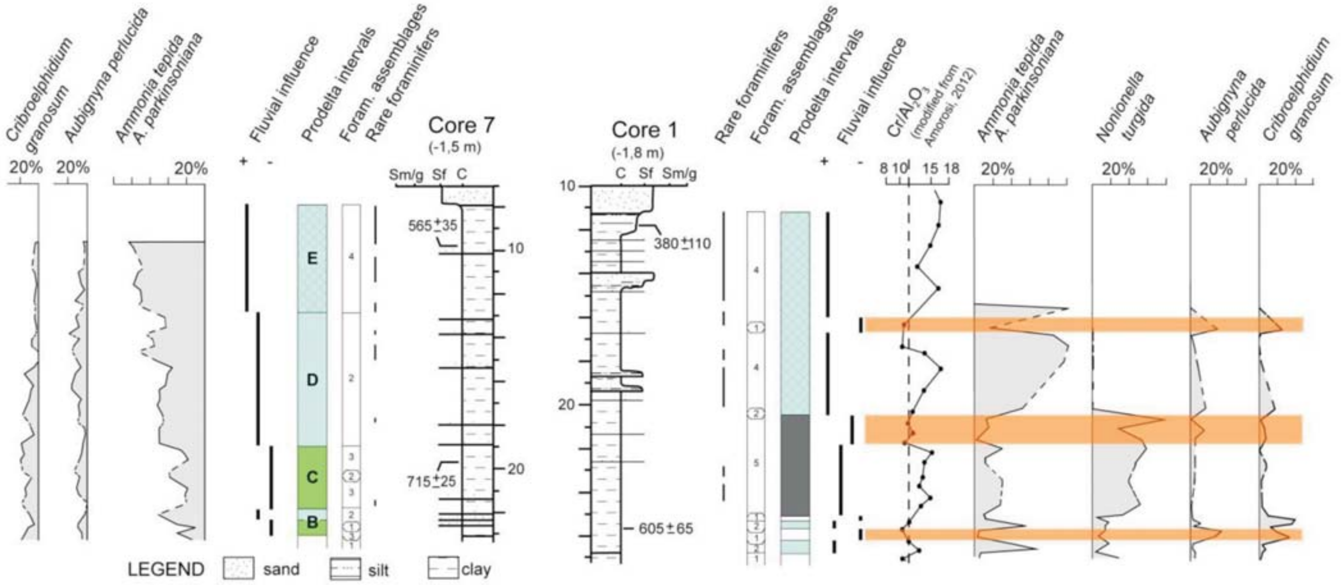

TEXT-FIGURE 6
Core stratigraphy, foraminiferal assemblages, fluvial influence and frequency of river-influenced taxa in the prodelta successions of cores 7 and 1. Colored intervals defined by foraminiferal assemblages; colors refer to the foraminiferal distribution reported in text-figure 1. Profile of Cr/Al$_2$O$_3$ from Core 1 indicative of Po River provenance for values >11.5 (dashed line) (from Amorosi 2012). Transverse bars in Core 1: decreased Po River influence recorded by samples with Cr/Al$_2$O$_3$<11.5 and/or low fluvial-influenced foraminiferal assemblages.

most active Po River branches (Correggiari et al. 2005b) and its maximum discharge phase is recorded by interval B. The Ficarolo avulsion shifted the most active river mouths to a more northern position, defining Po di Goro and Po delle Fornaci (nowadays known as Po di Levante) as the main outlets (Ciabatti 1966). This event induced a major phase of drainage reorganization with limited delta outbuilding (Veggiani 1990; Correggiari et al. 2005b), recorded by foraminiferal assemblages of interval C, when the core area was poorly affected by riverine sedimentation.

Foraminiferal assemblage 2 within interval D indicates a substantial increase in fluvial influence, consistent with a prograding delta. The sharp increase in *A. tepida – A. parkinsoniana* at the base of this interval records the approach of the Po di Goro river mouth during its phase of maximum activity (Ciabatti 1966).

The topmost part of prodelta deposits (interval E) shows a further increase in *A. tepida* and *A. parkinsoniana* (assemblage 4), indicative of substantial proximity to the fluvial outlet, and often includes low amount of foraminifera, mainly near the transition to delta front sands. Samples with rare foraminifera are ascribed to the massive sediment input discharged by river floods, similar to modern thick flood layers, which are locally barren in foraminifera or include low number of specimens (D'Onofrio 1969). The deposition of thick flood layers produces sediment reworking in the uppermost cms of the bottom layer (Wheatcroft 1990) where most of the foraminifera live (Jorissen et al. 1992; Murray 2006), thus creating foraminiferal assemblages with scarce specimens dispersed in the sediment. In this respect, interval E represents a thick succession of flood layers (text-fig. 2), similar to the ones observed close to the present Po outlets (Wheatcroft et al. 2006). The presence of abundant foraminifera of assemblage 4 records lower sediment supply among the flood events. Increases in *A. tepida* and *A. parkinsoniana* at the base of intervals D and E suggest rapid transition to more riverine-influenced conditions. Specifically, the step-like distribution superposed onto the overall increasing trend of taxa indicative of fluvial influence (i.e., *A. tepida* and *A. parkinsoniana*) provides evidence for irregular deltaic progradation (text-fig. 2). A radiocarbon date from interval E (565±35 yr BP) indicates that the deposition of this interval preceded the Porto Viro cut, which occurred between 350 and 346 yr BP, thus the prodelta succession was deposited in ca. 150 years, with an average sedimentation rate of 6.6 cm/yr.

Recent Po Delta evolution as revealed by cores 1 and 7

The observed evolution of the Po di Goro delta lobe is consistent with the chronology and foraminiferal distribution recognized in more seaward position (Core 1; Text-figures 1, 6). At this location, prodelta sedimentation started about 600 yr BP (Rossi and Vaiani 2008; text-fig. 6) and rapid delta progradation led to deposition of a 14 m-thick succession in about 225 years, between the Ficarolo and Porto Viro avulsions, with an overall shallowing-upward trend (from about 18 to 8-10 m depth – Rossi and Horton 2009).

The alternation of foraminiferal assemblages 2 and 1 in the basal part of the prodelta succession is attributed to unstable environmental conditions (text-fig. 6; Rossi and Vaiani 2008). Samples with very low amounts of *A. tepida – A. parkinsoniana* have been included in assemblage 1, which indicates inner shelf conditions with possible low fluvial influence, as suggested by local abundant *C. granosum* and *A. perlucida*. These samples were previously grouped by Rossi and Vaiani (2008) into a separate assemblage, indicative of a prodelta without oxygen deficiency in the bottom sediments. High percentages of *C. granosum* in the Adriatic Sea are recorded from 17.5 m water depth within clayey bottoms enriched in organic matter

TABLE 2
Similarity percentage (SIMPER) analysis for benthic foraminiferal assemblages defined by cluster analysis (Fig. 3), including taxa with occurrence >4% in at least one sample of the two cores. Overall average dissimilarity: 57.47.

Taxon	Average dissimilarity	Contribution %	Cumulative %	Cluster 1	Cluster 2.1	Cluster 2.2	Cluster 2.3	Cluster 3
Ammonia tepida. A. parkinsoniana	20.20	35.14	35.14	6.41	47.00	20.90	83.40	17.40
Nonionella turgida	8.53	14.84	49.98	9.92	6.11	4.44	0.37	45.60
Aubignyna perlucida	5.15	8.97	58.95	12.20	8.26	17.60	1.89	3.88
Criboelphidium granosum	4.63	8.05	67.00	16.00	8.58	9.36	3.25	4.93
Quinqueloculina seminulum	3.30	5.74	72.74	6.11	7.55	12.20	5.60	6.57
Triloculina spp.	1.79	3.12	75.85	3.96	3.86	3.37	0.22	0.78
other Quinquelocuilina	1.66	2.89	78.74	4.30	2.79	3.68	0.07	2.41
Adelosina spp.	1.65	2.87	81.61	3.21	2.63	5.57	1.84	1.52
Textularia spp.	1.57	2.73	84.34	4.36	0.59	2.97	0.00	0.62
Haynesina depressula. H. germanica	1.47	2.56	86.90	2.94	2.09	3.27	1.74	0.86
Elphidium spp.	1.41	2.45	89.35	4.39	0.82	1.62	0.06	1.00
other Criboelphidium	1.28	2.23	91.57	2.01	2.06	4.21	0.40	1.18
Ammonia beccarii	1.19	2.07	93.64	2.09	2.30	2.81	0.22	0.91
Miliolinella spp.	1.16	2.02	95.66	3.08	1.23	1.82	0.032	0.28
Criboelphidium lidoense	0.98	1.70	97.36	1.08	1.63	3.94	0.92	1.33
Rosalina spp.	0.83	1.44	98.80	2.45	0.35	0.40	0.00	0.00
Siphonaperta spp.	0.48	0.83	99.63	1.46	0.043	0.00	0.00	0.041
Buccella granulata	0.21	0.37	100.00	0.62	0.043	0.074	0.00	0.00

(Jorissen 1988), but they are coupled with common *A. tepida* – *A. parkinsoniana* and *A. perlucida* only near the Po Delta. The low percentages of *A. tepida* and *A. parkinsoniana* recorded in samples of Core 1 point to low fluvial-influenced conditions relatively far from river mouths, but the remarkable presence of *A. perlucida* and *C. granosum* suggests high organic matter content. Similar assemblages could reflect transitional conditions between inner shelf and prodelta, in a slightly fluvial-influenced environment, with high organic matter and no remarkable oxygen deficiency. The repeated superposition of assemblages 1 and 2 could be linked to the transition from inner shelf (i.e., without or very low fluvial influence) to prodelta (i.e., more fluvially-influenced) environments, recording the first influence of the prograding Po di Goro lobe after the Ficarolo avulsion.

The abrupt change (25.08 m core depth) to assemblage 5 (text-fig. 6) documents the onset of a shallow mud belt (Van der Zwaan and Jorissen 1991), where fluvial organic matter was concentrated by the North Adriatic currents, a few km away from the river outlets. According to the radiocarbon age of 605±65 cal. yr BP at 25.70 m core depth, this mud belt was formed two centuries after the Ficarolo avulsion (Rossi and Vaiani 2008). Assemblages dominated by *N. turgida* are absent in Core 7, indicating that a mud belt did not developed at this location. The shallow Po mud belt grew in response to the Ficarolo event, which determined an increased sediment supply in the Core 1 area (Rossi and Vaiani 2008). At the same time, comparable conditions are not recorded in Core 7 due to its closer position to the river mouths, reflected in foraminiferal assemblages dominated by near-fluvial mouth species (*A. tepida* and *A. parkinsoniana*) of interval D (text-fig. 1).

Upsection, the foraminiferal assemblage 2 occurs at 20.20 m core depth, overlain by foraminiferal assemblage 4 also with low numbers of specimens (rare foraminifera, text-fig. 6). Similar to Core 7, such a sharp change in the foraminiferal assemblage suggests flood sedimentation near the river mouth and records a step-like deltaic progradation. Sample at 16.55 m depth shows a dramatic decrease of *A. tepida* and *A. parkinsoniana*, replaced by *A. perlucida* and *C. granosum* (Rossi and Vaiani 2008). This sample is included in assemblage 1 (text-fig. 3) and it is placed near assemblage 3 in the nMDS diagram (text-fig. 5). This strong faunal turnover is diagnostic of decreasing fluvial influence, and can be related to minor river mouth migration or to a period of reduced flood activity.

To summarize, the superposition of different foraminiferal assemblages in the prodelta succession of Core 1 indicates irregular deltaic progradation with an overall increase in fluvial influence, related to approaching river outlets. The observed paleoenvironmental reconstruction is substantially consistent with that of Core 7, however it shows some local features, such as the development of the mud belt related to its seaward position, or the possible river mouth migration at 16.55 m core depth not recorded in Core 7.

This paleoenvironmental evolution is also consistent with trace-metal distribution (text-fig. 6). In particular, chromium represents an efficient indicator of sediment source composition for the late Holocene deposits of the Po Plain (Amorosi et al. 2014): high chromium concentrations (Cr/Al_2O_3 >11.5 in text-fig. 6) are characteristic of sediment supplied from Alpine (ophiolite-rich) sources drained by the Po River, whereas lower chromium values indicate sediment provenance from the Apennines (Amorosi et al. 2002; Amorosi 2012).

Within the prodelta succession of Core 1, changes in sediment geochemistry are paralleled by the distribution of *A. tepida* and *A. parkinsoniana* (text-fig. 6). In detail, high amounts of *A. tepida* and *A. parkinsoniana*, which are indicative of high fluvial influence and proximity to fluvial outlets, are associated with high Cr values, supporting the hypothesis of direct sediment supply from the Po River mouth. In contrast, the decrease of these taxa and concomitant lower Cr values indicate diminished Po River influence, in response to (i) a local shift of the fluvial mouth or (ii) decreased river input due to reduced flood activity (orange bars in text-fig. 6). After the onset of Po sedimentation, the first low-Cr event is recorded at 26.10-25.80 m core depth, paralleled by the occurrence of assemblage 1 with very low *A. tepida* – *A. parkinsoniana* concentrations. The unstable environmental conditions recorded by benthic foraminifera are confirmed by geochemical values, which point to an oscillating fluvial influence from the Po River. The second and third low-Cr events respectively correspond to oscillating *N. turgida* and an increase in *A. perlucida* and *C. granosum*, both with very low *A. tepida* – *A. parkinsoniana*. A decreased fluvial influence is recorded mainly by geochemical values in the upper part of the mud belt, where foraminiferal assemblage 5 indicates stable environmental conditions. The third event is recorded both in micropaleontological (assemblage 1) and geochemical data.

In the very short interval of time involved (about two centuries), eustatic sea-level change and subsidence were negligible, and changes in sediment provenance are inferred to represent minor variations in the depositional environment under a predominantly autogenic control. Increasing distance from river mouths or decreasing Po River discharge resulted in mixing of fluvial deposits with sediment supplied from different sources by the basin circulation pattern. Such changes can be recorded by benthic foraminiferal assemblages or by sediment geochemistry and a detailed record of short-term deltaic events can be obtained if these proxies are used together.

CONCLUSIONS

We examined a thick prodelta succession spanning less than 300 years (from the Late Middle Ages) by micropaleontological analysis of two closely spaced cores from the modern Po Delta plain. In this short interval of time, deltaic evolution was controlled by autogenic factors and bathymetric changes most likely reflect variations in sediment supply, whereas subsidence and eustatic changes were negligible.

Modern shallow-water benthic foraminiferal assemblages from the Po shelf reflect specific environmental conditions, controlled by fluvial discharge, sediment supply, the amount of continental organic matter and are mainly related to the distance from river outlets. Identification of these assemblages within late Holocene, expanded prodelta successions reveals small-scale paleoenvironmental variations that developed in response to local events, such as mouth migration and river floods, superposed onto an overall shallowing-upward trend. Above a basal interval that records the historical Ficarolo avulsion, i.e., the onset of the Po Delta in the study area, the superposition of *A. tepida* and *A. parkinsoniana* – dominated assemblages are ascribed to the step-like progradation of the Po di Goro delta lobe during its phase of maximum activity. At a more seaward location, foraminiferal assemblages and chromium vertical profiles document occasional changes in fluvial (Po River) input, consistent with river mouth shifting or changes in the frequency and amount of flood deposition. Upper prodelta deposits in both cores show the vertical stacking of flood layers, deposited near the river mouths.

The ability of benthic foraminifera to detect subtle variations in environmental parameters allowed the recognition of high-frequency (centennial scale) paleoenvironmental changes within a prodelta succession. These changes, mostly related to autogenic factors, can be used to assess natural delta dynamics on river-influenced shelves.

ACKNOWLEDGMENTS

Radiocarbon analyses were performed at Korea Institute of Geoscience and Mineral Resources (KIGAM, Republic of Korea). We are indebted to Regione Emilia-Romagna – RER – Geological, Seismic and Soil Survey for providing access to Core 7. We thank F.J. Jorissen, M.A. Kaminski and an anonymous reviewer for the constructive comments on an early version of the manuscript. We are grateful to Veronica Rossi, Luigi Bruno and Bruno Campo for their useful comments and help with the calibration of the radiocarbon dates.

REFERENCES

ALBANI, A. and SERANDREI BARBERO, R., 1990. I Foraminiferi della Laguna e del Golfo di Venezia. *Memorie di Scienze Geologiche Padova*, 42: 271–341.

AMOROSI, A., BRUNO, L., CAMPO, B., ROSSI, V., SCARPONI, D., HONG, W., BOHACS, K.M. and DREXLER, T.M., 2017. Global sea-level control on local parasequence architecture from the Holocene record of the Po Plain, Italy. *Marine and Petroleum Geology*, 87: 99-111.

AMOROSI, A., CENTINEO, M. C., DINELLI, E., LUCCHINI, F. and TATEO, F., 2002. Geochemical and mineralogical variations as indicators of provenance changes in Late Quaternary deposits of SE Po Plain. *Sedimentary Geology*, 151: 273–292.

AMOROSI, A., CENTINEO, M. C., COLALONGO, M. L., PASINI, G., SARTI, G. and VAIANI, S. C., 2003. Facies architecture and Latest Pleistocene–Holocene depositional history of the Po Delta (Comacchio area). Italy. *The Journal of Geology*, 111: 39–56.

AMOROSI, A., COLALONGO, M. L., PASINI, G. and PRETI, D., 1999. Sedimentary response to Late Quaternary sea-level changes in the Romagna coastal plain (northern Italy). *Sedimentology*, 46: 99–121.

AMOROSI, A., COLALONGO, M. L., FIORINI, F., FUSCO, F., PASINI, G., VAIANI, S. C. and SARTI, G., 2004. Palaeogeographic and palaeoclimatic evolution of the Po Plain from 150-ky core records. *Global and Planetary Change*, 40: 55–78.

AMOROSI, A. and COLALONGO, M. L., 2005. The linkage between alluvial and coeval nearshore marine successions: evidence from the Late Quaternary record of the Po River Plain, Italy. In: Blum, M.D., Marriott, S.B., Leclair, S.F., Eds., *Fluvial Sedimentology VII*, International Association of Sedimentologists. Special Publication, vol. 35. Blackwell Scientific Publications, Oxford: 257–275.

AMOROSI, A., DINELLI, E., ROSSI, V., VAIANI, S. C. and SACCHETTO, M., 2008. Late Quaternary palaeoenvironmental evolution of the Adriatic coastal plain and the onset of Po River Delta. *Palaeogeography, Palaeoclimatology, Palaeoecology*, 268: 80–90.

AMOROSI, A., 2012. Chromium and nickel as indicators of source-to-sink sediment transfer in a Holocene alluvial and coastal system (Po Plain, Italy). *Sedimentary Geology*, 280: 260–269.

AMOROSI, A., GUERMANDI, M., MARCHI, N. and SAMMARTINO, I., 2014. Fingerprinting sedimentary and soil units by their natural metal contents: A new approach to assess metal contamination. *Science of the Total Environment*, 500–501: 361–372.

AMOROSI, A., MASELLI, V. and TRINCARDI, F., 2016. Onshore to offshore anatomy of a late Quaternary source-to-sink system (Po Plain-Adriatic Sea, Italy). *Earth-Science Reviews*, 153: 212–237.

BARMAWIDJAJA, D. M., JORISSEN, F. J., PUSKARIC, S. and VAN DER ZWAAN, G. J., 1992. Microhabitat selection by benthic foraminifera in the northern Adriatic Sea. *Journal of Foraminiferal Research*, 22: 297–317.

BARMAWIDJAJA, D. M., VAN DER ZWAAN, G. J., JORISSEN, F. J. and PUSKARIC, S., 1995. 150 years of eutrophication in the northern Adriatic Sea, evidence from a benthic foraminiferal record. *Marine Geology*, 122: 367–384.

BARRAS, C., JORISSEN, F. J., LABRUNE, C., ANDRAL, B. and BOISSERY, P., 2014. Live benthic foraminiferal faunas from the French Mediterranean Coast: Towards a new biotic index of environmental quality. *Ecological Indicators*, 36: 719–743.

BELLOTTI, P., CARBONI, M. G., DI BELLA, L., PALAGI, I. and VALERI, P., 1994. Benthic foraminiferal assemblages in the depositional sequence of the Tiber Delta. In: Matteucci, R., (Eds.), Studies on Ecology and Paleoecology of Benthic Communities. *Bollettino della Società Paleontologica Italiana*, Spec. Vol. 2: 29–40.

BLACKWELDER, P., HOOD,T., ALVAREZ-ZAFIKIAN, C., NELSENT, T. A. and MCKEE, B., 1996. Benthic foraminifera from the NECOP study area impacted by the Mississippi river plume and seasonal hypoxia. *Quaternary International,* 31: 19–36.

BLANC-VERNET, L., 1969. Contribution à l'étude des foraminifères de Méditerranée. *Travaux de la Station Marine d'Endoume*, Marseille, France.

CIABATTI, M., 1966. Ricerche sull'evoluzione del Delta Padano. *Giornale di Geologia,* 34: 381–406.

CIBIN, U. and STEFANI, M., 2009. Carta Geologica d'Italia alla scala 1:50.000 – Codigoro Foglio 187. ISPRA - Servizio Geologico d'Italia, Roma.

CIMERMAN, F. and LANGER, M. R., 1991. *Mediterranean Foraminifera*. Academia Scientiarum et Artium Slovenica Classis IV 30, Ljubljana.

CORREGGIARI, A., CATTANEO, A. and TRINCARDI, F., 2005a. The modern Po delta system: lobe switching and asymmetric prodelta growth. *Marine Geology*, 222–223: 49–74.

———, 2005b. Depositional patterns in the Holocene Po Delta system. In: Bhattacharya, J.P., Giosan, L., Eds., River Deltas: Concepts, Models and Examples. SEPM Special Publication, 83: 365–392.

D'ONOFRIO, S., 1969. Ricerche sui Foraminiferi nei fondali antistanti il Delta del Po. *Giornale di Geologia*, 36: 283–334.

DAVIS, J.C., 1986. *Statistics and Data Analysis in Geology*, 2nd ed. John Wiley and Sons, New York. 289 pp.

DESSANDIER, P.-A., BONNIN, J., KIM, J.-H., BICHON, S., DEFLANDRE, B., GRÉMARE, A. and SINNINGHE DAMSTÉ, J.S., 2016. Impact of organic matter source and quality on living benthic foraminiferal distribution on a river-dominated continental margin: A study of the Portuguese margin. *Journal of Geophysical Research: Biogeosciences*, 121: 1689–1714.

DIZ, P., FRANCÉS, G. and ROSÓN, G., 2006. Effects of contrasting upwelling–downwelling on benthic foraminiferal distribution in the Ría de Vigo (NW Spain). *Journal of Marine Systems*, 60: 1–18.

DONNICI, S. and SERANDREI BARBERO, R., 2002. The benthic foraminiferal communities of the northern Adriatic continental shelf. *Marine Micropaleontology*, 44: 93–123.

DUCHEMIN, G., JORISSEN, F. J., LE LOC'H, F., ANDRIEUX-LOYER, F., HILY, C. and THOUZEAU, G., 2008. Seasonal variability of living benthic foraminifera from the outer continental shelf of the Bay of Biscay. *Journal of Sea Research*, 59: 297–319.

ELLIS, B. F. and MESSINA, A. R., 1940. *Catalogue of Foraminifera*. New York: Micropaleontology Press.

FIORINI, F., 2004. Benthic foraminiferal associations from Upper Quaternary deposits of southeastern Po Plain, Italy. *Micropaleontology*, 50: 45–58.

FIORINI, F. and VAIANI, S. C., 2001. Benthic foraminifers and transgressive–regressive cycles in the Late Quaternary subsurface sediments of the Po Plain near Ravenna (Northern Italy). *Bollettino della Società Paleontologica Italiana*, 40: 357–403.

FREGNI, P., 1978. I foraminiferi recenti della piattaforma continentale tra Ancona e Ravenna. In: Colantoni, P., Gallignani, P., Eds., *Ricerche sulla piattaforma continentale dell'Alto Adriatico*. Consiglio Nazionale delle Ricerche, Quaderno 1, Bologna: 45–56.

———, 1980. I Foraminiferi della piattaforma continentale Adriatica tra Ravenna e Chioggia. In: Colantoni, P., Gallignani, P., Eds., *Ricerche sulla piattaforma continentale dell'alto Adriatico*. Consiglio Nazionale delle Ricerche, Quaderno 2, Bologna: 43–53.

FREZZA, V. and CARBONI, M. G., 2009. Distribution of recent foraminiferal assemblages near the Ombrone River mouth (Northern Tyrrhenian Sea, Italy). *Revue de Micropaléontologie*, 52: 43–66.

FRONTALINI, F., SEMPRUCCI, F., COCCIONI, R., BALSAMO, M., BITTONI, P. and COVAZZI-HARRIAGUE, A., 2011. On the quantitative distribution and community structure of the meio and macrofaunal communities in the coastal area of the Central Adriatic Sea (Italy). *Environmental Monitoring and Assessment*, 180: 325–344.

GOINEAU, A., FONTANIER, C., JORISSEN, F. J., LANSARD, B., BUSCAIL, R., MOURET, A., KERHERVÉ, P., ZARAGOSI, S., ERNOULT, E., ARTÉRO, C., ANSCHUTZ, P., METZGER, E. and RABOUILLE, C., 2011. Live (stained) benthic foraminifera from the Rhône prodelta (Gulf of Lion, NW Mediterranean): Environmental controls on a river-dominated shelf. *Journal of Sea Research*, 65: 58–75.

GOINEAU, A., FONTANIER, C., JORISSEN, F. J., BUSCAIL, R., KERHERVÉ, P., CATHALOT, C., PRUSKI, A. M., LANTOINE, F., BOURGEOIS, S., METZGER, E., LEGRAND, E. and RABOUILLE, C., 2012. Temporal variability of live (stained) benthic foraminiferal faunas in a river-dominated shelf: faunal response to rapid changes of the river influence (Rhône prodelta, NW Mediterranean). *Biogeosciences*, 9: 1367–1388.

GOINEAU, A., FONTANIER, C., MOJTAHID, M., FANGET, A.-S., BASSETTI, M.-A., BERNÉ, S. and JORISSEN F., 2015. Live–dead comparison of benthic foraminiferal faunas from the Rhône prodelta (Gulf of Lions, NW Mediterranean): Development of a proxy for palaeoenvironmental reconstructions. *Marine Micropaleontology*, 119: 17–33.

GUSTAFSSON, M. and NORDBERG, K., 2001. Living (stained) benthic foraminiferal response to primary production and hydrography in the deepest part of the Gullmar Fjord, Swedish West Coast, with comparison to Höglund's 1927 material. *Journal of Foraminiferal Research*, 31: 2–11.

HAMMER, Ø., HARPER, D. A. T. and RYAN, P. D., 2001. Past: palaeontological statistics software package for education and data analysis. *Palaeontologia Electronica* 4, 9.

JORISSEN, F. J., 1987. The distribution of benthic foraminifera in the Adriatic Sea. *Marine Micropaleontology*, 12: 21–48.

———, 1988. Benthic foraminifera from the Adriatic Sea; principles of phenotypic variation. *Utrecht Micropaleontological Bulletins*, 37: 1–174.

JORISSEN, F. J., BARMAWIDJAJA, D. M., PUSKARIC, S. and VAN DER ZWAAN, G. J., 1992. Vertical distribution of benthic foraminifera in the northern Adriatic Sea: the relation with the organic flux. *Marine Micropaleontology*, 19: 131–146.

JORISSEN, F. J. and WITTLING, I., 1999. Ecological evidence from live–dead comparisons of benthic foraminiferal faunas off Cape Blanc (Northwest Africa). *Palaeogeography, Palaeoclimatology, Palaeoecology*, 149: 151–170.

MENDES, I., DIAS, J. A., SCHÖNFELD, J., FERREIRA, Ó., ROSA, F. and LOBO, F. J., 2013. Living, dead and fossil benthic foraminifera on a river dominated shelf (northern Gulf of Cadiz) and their use for paleoenvironmental reconstruction. *Continental Shelf Research*, 68: 91–111.

MOJTAHID, M., JORISSEN, F., LANSARD, B., FONTANIER, C., BOMBLED, B. and RABOUILLE, C., 2009. Spatial distribution of live benthic foraminifera in the Rhône prodelta: Faunal response to a continental–marine organic matter gradient. *Marine Micropaleontology*, 70: 177–200.

MURRAY, J. W., 1991. *Ecology and palaeoecology of benthic foraminifera*. London: Longman Scientific & Technical, , 397 pp.

———, 2006. *Ecology and Applications of Benthic Foraminifera*. Cambridge: Cambridge University Press, 426 pp.

NELSON, B. W., 1970. Hydrography, sediment dispersal, and recent historical development of the Po river delta, Italy. In: Morgan, J.P., Ed., *Deltaic Sedimentation: Modern and Ancient*. SEPM Special Publication, vol. 15: 152–184.

OSTERMAN, L. E., 2003. Benthic foraminifers from the continental shelf and slope of the Gulf of Mexico: an indicator of shelf hypoxia. Estuarine, *Coastal and Shelf Science*, 58: 17–35.

PIVA, A., ASIOLI, A., TRINCARDI, F., SCHNEIDER, R. R. and VIGLIOTTI, L., 2008. Late Holocene climate variability in the Adriatic Sea (Central Mediterranean). *The Holocene*, 18: 153–167.

RASMUSSEN, T. L., 2005. Systematic paleontology and ecology of benthic foraminifera from the Plio–Pleistocene Kallithea Bay Section, Rhodes, Greece. In: Thomsen, E., Ed., *Lagoon to deep–water foraminifera and ostracods from the Plio–Pleistocene Kallithea bay section, Rhodes, Greece*. Cushman Foundation Special Publication, vol. 39, Washington DC: 53–157.

REIMER, P. J., BAILLIE, M. G. L., BARD, E., BAYLISS, A., BECK, J. W., BERTRAND, C. J. H., BLACKWELL, P. G., BUCK, C. E., BURR, G. S., CUTLER, K. B., DAMON, P. E., EDWARDS, R. L., FAIRBANKS, R. G., FRIEDRICH, M., GUILDERSON, T. P., HOGG, A. G., HUGHEN, K. A., KROMER, B., MCCORMAC, F. G., MANNING, S. W., RAMSEY, C. B., REIMER, R. W., REMMELE, S., SOUTHON, J. R., STUIVER, M., TALAMO, S., TAYLOR, F. W., VAN DER PLICHT, J. and WEYHENMEYER, C. E., 2004. IntCal04 terrestrial radiocarbon age calibration. *Radiocarbon*, 46: 1029–1058.

RIZZINI, A., 1974. Holocene sedimentary cycle and heavy mineral distribution, Romagna–Marche coastal plain, Italy. *Sedimentary Geology*, 11: 17–37.

ROSSI, V. and HORTON, B. P., 2009. The application of a subtidal foraminiferal-based transfer function to reconstruct the Holocene paleobathymetry of the Po Delta, Northern Adriatic Sea. *Journal of Foraminiferal Research*, 39: 180-190.

ROSSI, V. and VAIANI, S. C., 2008. Microfaunal response to sediment supply changes and fluvial drainage reorganization in Holocene deposits of the Po Delta, Italy. *Marine Micropaleontology*, 69: 106–118.

ROVERI, M., ASIOLI, A., CORREGGIARI, A. and TRINCARDI, F., 2001. Ultra high-resolution marine record of paleoenvironmental changes in the last 5000 years. *Archivio di Oceanografia e Limnologia*, 22: 223–234.

SGARRELLA, F. and MONCHARMONT ZEI, M., 1993. Benthic Foraminifera of the Gulf of Naples (Italy): systematics and autoecology. *Bollettino della Società Paleontologica Italiana*, 32: 145–264.

STEFANI, M. and VINCENZI, S., 2005. The interplay of eustasy, climate and human activity in the late Quaternary depositional evolution and sedimentary architecture of the Po Delta system. *Marine Geology*, 222–223: 19–48.

TESI, T., LANGONE, L., GOÑI, M. A., MISEROCCHI, S. and BERTASI, F., 2008. Changes in the composition of organic matter from prodeltaic sediments after a large flood event (Po River, Italy). *Geochimica et Cosmochimica Acta*, 72: 2100–2114.

VAN DER ZWAAN, G. J. and JORISSEN, F. J., 1991. Biofacial patterns in river-induced shelf anoxia. In: Tyson, R. V., Pearson, T.H., Eds., Modern and Ancient Continental Shelf Anoxia. *Geological Society Special Publication*, vol. 58, pp. 65–82, London.

VEGGIANI, A., 1990. Fluttuazioni climatiche e trasformazioni ambientali nel territorio imolese dall'alto medioevo all'età moderna. In: Mancini, F., Gioberti, M., Veggiani, A., Eds., *Imola nel Medioevo*, pp. 41–102, Imola.

WHEATCROFT, R. A., 1990. Preservation potential of sedimentary event layers. *Geology*, 18: 843–845.

WHEATCROFT, R. A., HUNT, L., STEVENS, A. and LEWIS, R., 2006. The large-scale distribution and internal geometry of the fall 2000 Po River flood deposit: evidence from digital X-radiography. *Continental Shelf Research*, 26: 499–516.

APPENDIX 1
Benthic foraminiferal count of Core 7. List of taxa is the same as reported in text-fig. 2.

Sample depth (m)	9.65		9.90		10.25		10.85		11.05		11.60		11.85		12.35	
	Tot	%	Tot	%	Tot	%	Tot	%	Tot	%	Tot	%	Tot	%	Tot	%
Ammonia tepida, A. parkinsoniana	253	83.2%	239	78.4%	0	0.0%	96	67.6%	57	73.1%	254	78.2%	222	70.5%	224	68.9%
Ammonia beccarii	0	0.0%	0	0.0%	0	0.0%	1	0.7%	0	0.0%	0	0.0%	1	0.3%	6	1.8%
Aubignyna perlucida	9	3.0%	13	4.3%	0	0.0%	10	7.0%	3	3.8%	6	1.8%	10	3.2%	15	4.6%
Nonionella turgida	0	0.0%	0	0.0%	0	0.0%	0	0.0%	0	0.0%	0	0.0%	0	0.0%	3	0.9%
Criboelphidium granosum	12	3.9%	8	2.6%	0	0.0%	5	3.5%	7	9.0%	20	6.2%	9	2.9%	40	12.3%
Criboelphidium lidoense	1	0.3%	10	3.3%	0	0.0%	3	2.1%	1	1.3%	11	3.4%	4	1.3%	3	0.9%
other Criboelphidium	0	0.0%	0	0.0%	0	0.0%	0	0.0%	0	0.0%	13	4.0%	0	0.0%	0	0.0%
Elphidium spp.	0	0.0%	0	0.0%	0	0.0%	1	0.7%	0	0.0%	0	0.0%	0	0.0%	2	0.6%
Haynesina depressula, H. germanica	19	6.3%	4	1.3%	0	0.0%	12	8.5%	4	5.1%	8	2.5%	4	1.3%	16	4.9%
Quinqueloculina seminulum	9	3.0%	30	9.8%	0	0.0%	11	7.7%	6	7.7%	11	3.4%	57	18.1%	14	4.3%
other Quinquelocuilina	0	0.0%	0	0.0%	0	0.0%	0	0.0%	0	0.0%	0	0.0%	0	0.0%	0	0.0%
Adelosina spp.	0	0.0%	1	0.3%	0	0.0%	3	2.1%	0	0.0%	0	0.0%	3	1.0%	2	0.6%
Siphonaperta spp.	0	0.0%	0	0.0%	0	0.0%	0	0.0%	0	0.0%	0	0.0%	0	0.0%	0	0.0%
Triloculina spp.	1	0.3%	0	0.0%	0	0.0%	0	0.0%	0	0.0%	2	0.6%	4	1.3%	0	0.0%
Miliolinella spp.	0	0.0%	0	0.0%	0	0.0%	0	0.0%	0	0.0%	0	0.0%	1	0.3%	0	0.0%
Textularia spp.	0	0.0%	0	0.0%	0	0.0%	0	0.0%	0	0.0%	0	0.0%	0	0.0%	0	0.0%
Asterigerinata spp.	0	0.0%	0	0.0%	0	0.0%	0	0.0%	0	0.0%	0	0.0%	0	0.0%	0	0.0%
Buccella granulata	0	0.0%	0	0.0%	0	0.0%	0	0.0%	0	0.0%	0	0.0%	0	0.0%	0	0.0%
Rosalina spp.	0	0.0%	0	0.0%	0	0.0%	0	0.0%	0	0.0%	0	0.0%	0	0.0%	0	0.0%
Other Miliolidae	0	0.0%	0	0.0%	0	0.0%	0	0.0%	0	0.0%	0	0.0%	0	0.0%	0	0.0%
Other taxa	0	0.0%	0	0.0%	0	0.0%	0	0.0%	0	0.0%	0	0.0%	0	0.0%	0	0.0%
Total	304	100.0%	305	100.0%	0	0.0%	142	100.0%	78	100.0%	325	100.0%	315	100.0%	325	100.0%

Sample depth (m)	12.55		13.10		13.55		13.85		14.10		14.40		14.65		15.10	
	Tot	%	Tot	%	Tot	%	Tot	%	Tot	%	Tot	%	Tot	%	Tot	%
Ammonia tepida, A. parkinsoniana	48	72.7%	150	43.7%	133	42.6%	99	65.1%	190	57.1%	69	55.2%	133	73.1%	46	51.7%
Ammonia beccarii	0	0.0%	61	17.8%	1	0.3%	0	0.0%	3	0.9%	0	0.0%	0	0.0%	0	0.0%
Aubignyna perlucida	2	3.0%	14	4.1%	7	2.2%	4	2.6%	24	7.2%	9	7.2%	0	0.0%	0	0.0%
Nonionella turgida	0	0.0%	2	0.6%	2	0.6%	1	0.7%	4	1.2%	1	0.8%	1	0.5%	6	6.7%
Criboelphidium granosum	2	3.0%	40	11.7%	27	8.7%	28	18.4%	27	8.1%	17	13.6%	28	15.4%	9	10.1%
Criboelphidium lidoense	0	0.0%	6	1.7%	8	2.6%	1	0.7%	8	2.4%	1	0.8%	0	0.0%	0	0.0%
other Criboelphidium	0	0.0%	9	2.6%	8	2.6%	0	0.0%	5	1.5%	0	0.0%	1	0.5%	1	1.1%
Elphidium spp.	0	0.0%	0	0.0%	0	0.0%	0	0.0%	0	0.0%	1	0.8%	0	0.0%	0	0.0%
Haynesina depressula, H. germanica	0	0.0%	6	1.7%	0	0.0%	4	2.6%	15	4.5%	4	3.2%	11	6.0%	8	9.0%
Quinqueloculina seminulum	14	21.2%	29	8.5%	89	28.5%	5	3.3%	50	15.0%	21	16.8%	5	2.7%	2	2.2%
other Quinquelocuilina	0	0.0%	0	0.0%	5	1.6%	0	0.0%	0	0.0%	0	0.0%	0	0.0%	1	1.1%
Adelosina spp.	0	0.0%	25	7.3%	19	6.1%	0	0.0%	1	0.3%	0	0.0%	0	0.0%	1	1.1%
Siphonaperta spp.	0	0.0%	0	0.0%	0	0.0%	0	0.0%	0	0.0%	0	0.0%	0	0.0%	0	0.0%
Triloculina spp.	0	0.0%	0	0.0%	10	3.2%	7	4.6%	6	1.8%	1	0.8%	1	0.5%	8	9.0%
Miliolinella spp.	0	0.0%	0	0.0%	0	0.0%	0	0.0%	0	0.0%	1	0.8%	0	0.0%	7	7.9%
Textularia spp.	0	0.0%	0	0.0%	0	0.0%	0	0.0%	0	0.0%	0	0.0%	0	0.0%	0	0.0%
Asterigerinata spp.	0	0.0%	0	0.0%	0	0.0%	1	0.7%	0	0.0%	0	0.0%	1	0.5%	0	0.0%
Buccella granulata	0	0.0%	0	0.0%	0	0.0%	0	0.0%	0	0.0%	0	0.0%	0	0.0%	0	0.0%
Rosalina spp.	0	0.0%	0	0.0%	1	0.3%	0	0.0%	0	0.0%	0	0.0%	0	0.0%	0	0.0%
Other Miliolidae	0	0.0%	0	0.0%	0	0.0%	0	0.0%	0	0.0%	0	0.0%	0	0.0%	0	0.0%
Other taxa	0	0.0%	1	0.3%	2	0.6%	2	1.3%	0	0.0%	0	0.0%	1	0.5%	0	0.0%
Total	66	100.0%	343	100.0%	312	100.0%	152	100.0%	333	100.0%	125	100.0%	182	100.0%	89	100.0%

Sample depth (m)	15.40		15.65		16.20		16.40		16.85		17.10		17.55		17.90	
	Tot	%	Tot	%	Tot	%	Tot	%	Tot	%	Tot	%	Tot	%	Tot	%
Ammonia tepida, A. parkinsoniana	118	36.8%	129	40.8%	150	43.1%	161	49.8%	151	49.2%	160	52.1%	145	46.3%	27	45.0%
Ammonia beccarii	0	0.0%	2	0.6%	1	0.3%	2	0.6%	5	1.6%	8	2.6%	9	2.9%	0	0.0%
Aubignyna perlucida	15	4.7%	52	16.5%	19	5.5%	26	8.0%	31	10.1%	39	12.7%	54	17.3%	6	10.0%
Nonionella turgida	49	15.3%	9	2.8%	14	4.0%	13	4.0%	6	2.0%	10	3.3%	17	5.4%	4	6.7%
Criboelphidium granosum	23	7.2%	37	11.7%	55	15.8%	51	15.8%	19	6.2%	28	9.1%	24	7.7%	6	10.0%
Criboelphidium lidoense	1	0.3%	2	0.6%	4	1.1%	5	1.5%	8	2.6%	3	1.0%	3	1.0%	2	3.3%
other Criboelphidium	14	4.4%	16	5.1%	0	0.0%	0	0.0%	0	0.0%	0	0.0%	0	0.0%	0	0.0%
Elphidium spp.	5	1.6%	3	0.9%	1	0.3%	8	2.5%	1	0.3%	0	0.0%	0	0.0%	1	1.7%
Haynesina depressula, H. germanica	2	0.6%	0	0.0%	27	7.8%	15	4.6%	2	0.7%	0	0.0%	2	0.6%	0	0.0%
Quinqueloculina seminulum	8	2.5%	9	2.8%	29	8.3%	8	2.5%	34	11.1%	14	4.6%	11	3.5%	2	3.3%
other Quinquelocuilina	35	10.9%	19	6.0%	0	0.0%	4	1.2%	9	2.9%	10	3.3%	13	4.2%	5	8.3%
Adelosina spp.	8	2.5%	7	2.2%	7	2.0%	3	0.9%	14	4.6%	11	3.6%	5	1.6%	3	5.0%
Siphonaperta spp.	0	0.0%	0	0.0%	0	0.0%	0	0.0%	0	0.0%	0	0.0%	0	0.0%	0	0.0%
Triloculina spp.	39	12.1%	28	8.9%	26	7.5%	19	5.9%	20	6.5%	18	5.9%	15	4.8%	0	0.0%
Miliolinella spp.	0	0.0%	0	0.0%	15	4.3%	6	1.9%	6	2.0%	5	1.6%	15	4.8%	2	3.3%
Textularia spp.	0	0.0%	0	0.0%	0	0.0%	1	0.3%	0	0.0%	1	0.3%	0	0.0%	0	0.0%
Asterigerinata spp.	0	0.0%	0	0.0%	0	0.0%	0	0.0%	0	0.0%	0	0.0%	0	0.0%	0	0.0%
Buccella granulata	0	0.0%	0	0.0%	0	0.0%	0	0.0%	0	0.0%	0	0.0%	0	0.0%	0	0.0%
Rosalina spp.	1	0.3%	0	0.0%	0	0.0%	0	0.0%	0	0.0%	0	0.0%	0	0.0%	0	0.0%
Other Miliolidae	0	0.0%	0	0.0%	0	0.0%	0	0.0%	0	0.0%	0	0.0%	0	0.0%	0	0.0%
Other taxa	4	1.2%	3	0.9%	0	0.0%	1	0.3%	1	0.3%	0	0.0%	0	0.0%	2	3.3%
Total	322	100.0%	316	100.0%	348	100.0%	323	100.0%	307	100.0%	307	100.0%	313	100.0%	60	100.0%

APPENDIX 1
Continued.

Sample depth (m)	18.15		18.45		18.85		19.15		19.35		19.60		20.15		20.40	
	Tot	%	Tot	%	Tot	%	Tot	%	Tot	%	Tot	%	Tot	%	Tot	%
Ammonia tepida, A. parkinsoniana	156	49.8%	154	50.0%	152	49.7%	82	26.5%	66	21.8%	56	18.2%	32	39.0%	119	38.4%
Ammonia beccarii	8	2.6%	8	2.6%	10	3.3%	11	3.5%	14	4.6%	12	3.9%	0	0.0%	11	3.5%
Aubignyna perlucida	25	8.0%	15	4.9%	57	18.6%	53	17.1%	47	15.5%	60	19.5%	14	17.1%	23	7.4%
Nonionella turgida	51	16.3%	4	1.3%	3	1.0%	6	1.9%	13	4.3%	7	2.3%	2	2.4%	27	8.7%
Criboelphidium granosum	9	2.9%	6	1.9%	13	4.2%	16	5.2%	18	5.9%	24	7.8%	11	13.4%	24	7.7%
Criboelphidium lidoense	0	0.0%	8	2.6%	13	4.2%	11	3.5%	17	5.6%	12	3.9%	5	6.1%	5	1.6%
other Criboelphidium	5	1.6%	7	2.3%	11	3.6%	6	1.9%	21	6.9%	18	5.9%	3	3.7%	7	2.3%
Elphidium spp.	1	0.3%	0	0.0%	0	0.0%	6	1.9%	0	0.0%	10	3.3%	2	2.4%	5	1.6%
Haynesina depressula, H. germanica	2	0.6%	13	4.2%	1	0.3%	3	1.0%	5	1.7%	0	0.0%	0	0.0%	2	0.6%
Quinqueloculina seminulum	23	7.3%	45	14.6%	24	7.8%	22	7.1%	32	10.6%	53	17.3%	7	8.5%	32	10.3%
other Quinquelocuilina	10	3.2%	5	1.6%	7	2.3%	20	6.5%	13	4.3%	6	2.0%	1	1.2%	11	3.5%
Adelosina spp.	11	3.5%	17	5.5%	1	0.3%	43	13.9%	10	3.3%	16	5.2%	2	2.4%	10	3.2%
Siphonaperta spp.	0	0.0%	0	0.0%	1	0.3%	0	0.0%	0	0.0%	0	0.0%	0	0.0%	0	0.0%
Triloculina spp.	5	1.6%	15	4.9%	3	1.0%	21	6.8%	9	3.0%	18	5.9%	2	2.4%	17	5.5%
Miliolinella spp.	5	1.6%	4	1.3%	10	3.3%	0	0.0%	10	3.3%	5	1.6%	0	0.0%	0	0.0%
Textularia spp.	1	0.3%	1	0.3%	0	0.0%	8	2.6%	20	6.6%	7	2.3%	0	0.0%	6	1.9%
Asterigerinata spp.	0	0.0%	0	0.0%	0	0.0%	0	0.0%	0	0.0%	0	0.0%	0	0.0%	0	0.0%
Buccella granulata	0	0.0%	0	0.0%	0	0.0%	0	0.0%	0	0.0%	0	0.0%	0	0.0%	0	0.0%
Rosalina spp.	0	0.0%	4	1.3%	0	0.0%	0	0.0%	1	0.3%	1	0.3%	0	0.0%	2	0.6%
Other Miliolidae	0	0.0%	1	0.3%	0	0.0%	0	0.0%	0	0.0%	0	0.0%	0	0.0%	0	0.0%
Other taxa	1	0.3%	1	0.3%	0	0.0%	2	0.6%	7	2.3%	2	0.7%	1	1.2%	9	2.9%
Total	313	100.0%	308	100.0%	306	100.0%	310	100.0%	303	100.0%	307	100.0%	82	100.0%	310	100.0%

Sample depth (m)	20.90		21.20		21.60		22.10		22.55		22.70		22.95		23.25	
	Tot	%	Tot	%	Tot	%	Tot	%	Tot	%	Tot	%	Tot	%	Tot	%
Ammonia tepida, A. parkinsoniana	62	18.8%	67	21.6%	13	20.0%	155	51.3%	95	30.5%	32	10.3%	91	30.1%	47	13.7%
Ammonia beccarii	11	3.3%	10	3.2%	2	3.1%	6	2.0%	6	1.9%	2	0.6%	9	3.0%	3	0.9%
Aubignyna perlucida	48	14.6%	41	13.2%	12	18.5%	29	9.6%	14	4.5%	35	11.2%	43	14.2%	64	18.6%
Nonionella turgida	25	7.6%	15	4.8%	9	13.8%	26	8.6%	29	9.3%	51	16.3%	23	7.6%	24	7.0%
Criboelphidium granosum	36	10.9%	27	8.7%	0	0.0%	7	2.3%	29	9.3%	30	9.6%	17	5.6%	18	5.2%
Criboelphidium lidoense	17	5.2%	14	4.5%	0	0.0%	7	2.3%	3	1.0%	2	0.6%	10	3.3%	11	3.2%
other Criboelphidium	19	5.8%	8	2.6%	0	0.0%	6	2.0%	18	5.8%	17	5.4%	9	3.0%	6	1.7%
Elphidium spp.	8	2.4%	10	3.2%	0	0.0%	5	1.7%	10	3.2%	10	3.2%	1	0.3%	6	1.7%
Haynesina depressula, H. germanica	4	1.2%	1	0.3%	1	1.5%	7	2.3%	8	2.6%	20	6.4%	6	2.0%	5	1.5%
Quinqueloculina seminulum	30	9.1%	68	21.9%	9	13.8%	26	8.6%	25	8.0%	11	3.5%	26	8.6%	77	22.4%
other Quinquelocuilina	7	2.1%	15	4.8%	3	4.6%	3	1.0%	12	3.9%	22	7.1%	5	1.7%	28	8.1%
Adelosina spp.	13	4.0%	12	3.9%	2	3.1%	13	4.3%	7	2.3%	10	3.2%	24	7.9%	22	6.4%
Siphonaperta spp.	0	0.0%	0	0.0%	0	0.0%	0	0.0%	0	0.0%	0	0.0%	0	0.0%	0	0.0%
Triloculina spp.	15	4.6%	7	2.3%	4	6.2%	5	1.7%	16	5.1%	22	7.1%	5	1.7%	10	2.9%
Miliolinella spp.	11	3.3%	6	1.9%	4	6.2%	0	0.0%	4	1.3%	15	4.8%	7	2.3%	7	2.0%
Textularia spp.	16	4.9%	6	1.9%	5	7.7%	5	1.7%	8	2.6%	4	1.3%	14	4.6%	3	0.9%
Asterigerinata spp.	0	0.0%	0	0.0%	0	0.0%	0	0.0%	0	0.0%	0	0.0%	0	0.0%	0	0.0%
Buccella granulata	1	0.3%	0	0.0%	0	0.0%	0	0.0%	1	0.3%	0	0.0%	0	0.0%	1	0.3%
Rosalina spp.	2	0.6%	0	0.0%	0	0.0%	0	0.0%	13	4.2%	15	4.8%	4	1.3%	2	0.6%
Other Miliolidae	0	0.0%	0	0.0%	0	0.0%	0	0.0%	0	0.0%	1	0.3%	0	0.0%	1	0.3%
Other taxa	4	1.2%	3	1.0%	1	1.5%	2	0.7%	13	4.2%	13	4.2%	8	2.6%	9	2.6%
Total	329	100.0%	310	100.0%	65	100.0%	302	100.0%	311	100.0%	312	100.0%	302	100.0%	344	100.0%

Sample depth (m)	23.55		23.75		23.95		24.20		24.50		24.95		25.25		25.50	
	Tot	%	Tot	%	Tot	%	Tot	%	Tot	%	Tot	%	Tot	%	Tot	%
Ammonia tepida, A. parkinsoniana	26	7.6%	37	11.5%	42	13.1%	28	7.5%	13	4.2%	24	8.0%	26	8.3%	20	6.5%
Ammonia beccarii	13	3.8%	2	0.6%	4	1.2%	3	0.8%	3	1.0%	9	3.0%	6	1.9%	20	6.5%
Aubignyna perlucida	26	7.6%	46	14.3%	56	17.4%	8	2.1%	26	8.5%	0	0.0%	0	0.0%	0	0.0%
Nonionella turgida	32	9.3%	29	9.0%	10	3.1%	38	10.1%	2	0.7%	18	6.0%	5	1.6%	1	0.3%
Criboelphidium granosum	55	16.0%	41	12.8%	69	21.5%	93	24.8%	53	17.3%	40	13.3%	46	14.7%	30	9.7%
Criboelphidium lidoense	0	0.0%	5	1.6%	0	0.0%	0	0.0%	12	3.9%	0	0.0%	3	1.0%	0	0.0%
other Criboelphidium	7	2.0%	18	5.6%	0	0.0%	3	0.8%	4	1.3%	29	9.6%	21	6.7%	3	1.0%
Elphidium spp.	17	5.0%	3	0.9%	18	5.6%	8	2.1%	12	3.9%	23	7.6%	24	7.7%	24	7.8%
Haynesina depressula, H. germanica	5	1.5%	10	3.1%	1	0.3%	7	1.9%	6	2.0%	15	5.0%	7	2.2%	4	1.3%
Quinqueloculina seminulum	25	7.3%	14	4.4%	35	10.9%	18	4.8%	25	8.2%	19	6.3%	38	12.2%	51	16.6%
other Quinquelocuilina	28	8.2%	24	7.5%	15	4.7%	19	5.1%	23	7.5%	3	1.0%	5	1.6%	9	2.9%
Adelosina spp.	8	2.3%	13	4.0%	8	2.5%	20	5.3%	17	5.6%	22	7.3%	26	8.3%	28	9.1%
Siphonaperta spp.	0	0.0%	5	1.6%	1	0.3%	0	0.0%	4	1.3%	14	4.7%	20	6.4%	9	2.9%
Triloculina spp.	30	8.7%	17	5.3%	16	5.0%	38	10.1%	25	8.2%	29	9.6%	15	4.8%	27	8.8%
Miliolinella spp.	12	3.5%	11	3.4%	3	0.9%	13	3.5%	4	1.3%	7	2.3%	3	1.0%	5	1.6%
Textularia spp.	40	11.7%	17	5.3%	23	7.2%	45	12.0%	34	11.1%	21	7.0%	15	4.8%	39	12.7%
Asterigerinata spp.	0	0.0%	0	0.0%	0	0.0%	0	0.0%	3	1.0%	2	0.7%	0	0.0%	3	1.0%
Buccella granulata	0	0.0%	0	0.0%	1	0.3%	1	0.3%	13	4.2%	0	0.0%	3	1.0%	5	1.6%
Rosalina spp.	5	1.5%	13	4.0%	6	1.9%	6	1.6%	16	5.2%	17	5.6%	28	9.0%	16	5.2%
Other Miliolidae	0	0.0%	3	0.9%	1	0.3%	2	0.5%	1	0.3%	2	0.7%	6	1.9%	5	1.6%
Other taxa	14	4.1%	13	4.0%	12	3.7%	25	6.7%	10	3.3%	7	2.3%	15	4.8%	9	2.9%
Total	343	100.0%	321	100.0%	321	100.0%	375	100.0%	306	100.0%	301	100.0%	312	100.0%	308	100.0%

9. ACCURACY OF BENTHIC FORAMINIFERA AND OSTRACODA IN BACK-BARRIER SUCCESSIONS

9.1 Manuscript IV

Benthic foraminifera or Ostracoda? Comparing the accuracy of palaeoenvironmental indicators from a Pleistocene lagoon of the Romagna coastal plain (Italy)*

Giulia Barbieri and Stefano Claudio Vaiani

*Published in **Journal of Micropalaeontology**

J. Micropalaeontology, 37, 203–230, 2018
https://doi.org/10.5194/jm-37-203-2018

Journal of
Micropalaeontology
Open Access

Benthic foraminifera or Ostracoda? Comparing the accuracy of palaeoenvironmental indicators from a Pleistocene lagoon of the Romagna coastal plain (Italy)

Giulia Barbieri and Stefano Claudio Vaiani

Dipartimento di Scienze Biologiche, Geologiche e Ambientali, University of Bologna,
via Zamboni 67 Bologna, 40127, Italy

Correspondence: Giulia Barbieri (giulia.barbieri21@unibo.it)

Received: 30 October 2017 – Revised: 29 December 2017 – Accepted: 6 January 2018 – Published: 29 January 2018

Abstract. Integrated analyses of multiple groups of microfossils are frequently performed to unravel the palaeoenvironmental evolution of subsurface coastal successions, where the complex interaction among several palaeoecological factors can be detected with benthic assemblages. This work investigates the palaeoenvironmental resolution potential provided by benthic foraminifera and ostracoda within a Pleistocene lagoonal succession of the Romagna coastal plain (northern Italy). Quantitative approaches and statistical techniques have been applied to both groups in order to understand the main factors that controlled the composition of assemblages and compare the palaeoecological record provided by single fossil groups.

The two faunal groups are characterized by the high dominance of opportunistic species (*Ammonia tepida–Ammonia parkinsoniana* and *Cyprideis torosa*); however, detailed palaeoecological information is inferred from less common taxa. Benthic foraminiferal assemblages are mainly determined by the frequencies of abnormal individuals and species related to high concentrations of organic matter, showing two assemblages: a stressed assemblage, consistent with a brackish-water environment subject to salinity and oxygen fluctuations, and an unstressed assemblage, which indicates more stable conditions. Despite the lower number of species, ostracoda show more significant differences in terms of species composition and ecological structure between their three assemblages, formed in response to a salinity gradient and indicative of inner, central, and outer lagoon conditions. The stratigraphic distribution of ostracod assemblages shows a general transgressive–regressive trend with minor fluctuations, whereas benthic foraminifera highlight the presence of a significant palaeoenvironmental stress.

In this case, the higher abundance along the stratigraphic succession, the higher differentiation of the assemblages, and the well-defined relationship between taxa and ecological parameters determine Ostracoda as the most reliable fossil group for precise palaeoenvironmental reconstructions. Nevertheless, benthic foraminifera indicate palaeoenvironmental stress and can be used to refine the environmental interpretation in the presence of monospecific ostracod assemblages.

1 Introduction

The use of microfossils as palaeoenvironmental proxies is quite common in geological studies since they are sensitive to a great number of ecological factors. Benthic foraminifera and Ostracoda are widely applied for stratigraphic and palaeoecological purposes since both of them have (i) an extremely wide distribution, from continental water bodies to the deep ocean; (ii) a short reproductive cycle that allows them to react quickly to environmental changes; and (iii) a hard shell that guarantees a high preservation potential in sediments (Murray, 2006; Rodriguez-Lazaro and Ruiz-Muñoz, 2012). These characteristics also make them suitable for ecological studies in modern environments, especially in the paralic realm, where benthic foraminifera and ostracoda are particularly abundant. Special attention has been reserved

Published by Copernicus Publications on behalf of The Micropalaeontological Society.

for lagoons because today their fragile equilibrium is endangered by a series of factors, such as anthropogenic pollution and climatic changes. Composition and structure of assemblages have been described in relation to many ecological parameters, allowing the use of recent assemblages as "modern analogues" of fossil associations.

Benthic foraminiferal assemblages are determined by multiple factors, which sometimes create stressed conditions. Benthic foraminifera have been proved to be excellent environmental bio-indicators in paralic environments, such as estuaries and lagoons (Coccioni, 2000; Frontalini et al., 2009; Armynot du Châtelet and Debenay, 2010). Under stressed conditions, these microorganisms modify the community structure and develop a series of peculiar morphological abnormalities of the test (Alve, 1991). Abundant studies have been focused on the response of benthic foraminifera to anthropogenic pollution (Yanko et al., 1994; Alve, 1995; Armynot du Châtelet and Debenay, 2010; Frontalini and Coccioni, 2011), but foraminiferal abnormalities can also occur from natural stresses, such as extreme values of salinity, nutrients, oxygen, or very rapid changes in ecological parameters (Scott and Medioli, 1980; Almogi-Labin et al., 1992; Geslin et al., 2002). High concentrations of aberrant benthic foraminifera also occur in fossil assemblages, even though only a few cases are reported in the literature and are attributed to low or oscillating salinity (Bik, 1964; Bugrova, 1975; Wang et al., 1985). As suggested by Boltovskoy et al. (1991), the presence of highly deformed assemblages in both modern and fossil environments is not related to a single factor, but it may be produced by a series of ecological parameters. Although assessing which is the main ecological factor that led to the creation of deformities is generally difficult, the relative abundance of aberrant benthic foraminifera is a good proxy for palaeoenvironmental stress (Geslin et al., 2002).

Nevertheless, benthic foraminifera could be absent in environments characterized by strong fluctuations in salinity, organic matter, and hydrodynamic conditions (Laut et al., 2016; Pint and Frenzel, 2017). Conversely, ostracoda are abundant from freshwater to hyperhaline environments and guarantee a great continuity of palaeoecological information (Rodriguez-Lazaro and Ruiz-Muñoz, 2012). Even if paralic environments with unstable environmental parameters are often characterized by oligotypic assemblages dominated by opportunistic taxa, rare species provide reliable information (Slack et al., 2000). Salinity is considered one of the major controlling factors affecting the distribution of ostracoda; therefore, this group is often applied for palaeosalinity reconstructions (Gliozzi and Mazzini, 1998; Marco-Barba et al., 2013; Amorosi et al., 2014). However, a combination of factors usually affects benthic assemblages in transitional environments, determining the degree of confinement, defined as the time of renewal for marine waters (Guélorget and Perthuisot, 1983). Ostracod assemblages can be indicative of a wide range of parameters, including the salinity and the degree of isolation from the sea, as it has been recently demonstrated by Salel et al. (2016) in the Gulf of Lion and Ebro Delta (western Mediterranean).

Both benthic foraminifera and ostracoda can provide a wide range of palaeoenvironmental information (type of substrate, salinity, organic matter content, oxygen concentration, etc.), but each group has peculiar characteristics that make it more suitable as a proxy for specific conditions. Within back-barrier sediment successions, the interaction of sediment supply, accommodation space, and eustatic oscillations produces subtle environmental changes detectable by the combined application of benthic foraminifera and ostracoda. However, palaeoenvironmental reconstructions performed on both groups are rarely applied and mostly based on qualitative or semi-quantitative approaches (e.g. Rossi et al., 2011; Trog et al., 2013), whereas quantitative analyses and statistical methods are often applied to only a single fossil group (e.g. Marco-Barba et al., 2013; Vaiani and Pennisi, 2014). Integrated analyses of multiple fossil groups are scarcely available in the literature and they are mostly restricted to the postglacial period (e.g. Cearreta et al., 2003; Amorosi et al., 2014).

The aim of this work is to compare the palaeoenvironmental resolution potential of Foraminifera and Ostracoda through multivariate analysis of fossil assemblages within a Pleistocene short sedimentary succession of the Po River coastal plain. Composition and structure of assemblages have been analysed in detail in order to investigate the ability of each group to highlight specific palaeoecological conditions within the same stratigraphic interval.

2 Geological setting

The Po River coastal plain is the easternmost part of the Po Plain (Fig. 1), a foredeep system bounded by the Alps to the north and the northern Apennines to the south, filled with Pliocene–Quaternary sediments with a maximum thickness of 7 km in the major depocenters (Pieri and Groppi, 1981; Castellarin and Vai, 1986). Geophysical investigations have evidenced that the Po basin is deformed by diffuse north-verging thrusts, but the late Quaternary sediments were deposited under relatively undisturbed conditions (Regione Emilia-Romagna and ENI–AGIP, 1998).

Detailed subsurface studies on the Po coastal plain revealed a cyclic facies architecture of transgressive–regressive (T–R) cycles formed by alternated alluvial and wedge-shaped coastal deposits (Amorosi and Colalongo, 2005). Integrated pollen analyses and radiocarbon dates performed on the three uppermost T–R cycles allowed their attribution from Marine Isotope Stage (MIS) 7 to 1 (Amorosi et al., 1999a, 2004). Specifically, thick alluvial sediments including scarce pollen of non-arboreal taxa are related to cold conditions, whereas abundant deciduous and broadleaved pollens are included within back-barrier and shallow marine deposits formed dur-

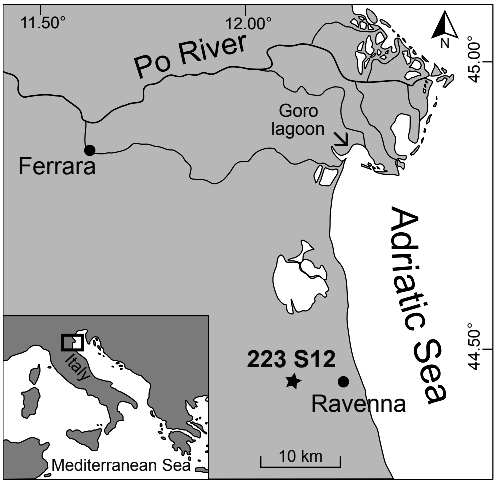

Figure 1. Location map of core 223 S12.

ing interglacial periods (MIS 1, 5, and 7; Amorosi et al., 1999a, 2004). This suggests that T–R cycles were formed in response to glacio-eustatic fluctuations with a frequency of 100 kyr, determined by the Milankovitch eccentricity-driven cycles (Lisiecki and Raymo, 2005).

The two most recent coastal wedges show a retrogradational stacking pattern of coastal plain and littoral facies, interpreted as a landward-migrating barrier–lagoon–estuary system during the transgressive phase, followed by deltaic and coastal progradation related to high stand conditions (Amorosi et al., 2004).

Lagoonal sediments in the subsurface of the Po River coastal plain are commonly developed within back-barrier facies associations. These are generally thin (1–2 m) at the base of Holocene (MIS 1) and Eemian (MIS 5e) transgressive–regressive wedges and are truncated at the top by an erosive ravinement surface that marks the passage to transgressive barrier facies (e.g. Amorosi et al., 2004; Campo et al., 2017). In contrast, well-developed paralic successions are locally present close to the innermost palaeoshoreline position reached at the peak of the MIS 1 and 5e transgressions (Dinelli et al., 2013; Campo et al., 2017) or below the Eemian units, representing the sedimentary response to the MIS 7 sea level variation (Amorosi et al., 1999a; Vaiani and Pennisi, 2014). Specifically, below the two uppermost T–R cycles, coastal and paralic deposits attributed to MIS 7 were recognized at some locations of the Po River coastal plain at more than 140 m core depth (e.g. Fiorini and Vaiani, 2001; Bondesan et al., 2006). The age attribution is supported by the stratigraphic position and the comparison with Mediterranean pollen zones, which limit the deposition of this interval during the late Middle Pleistocene (Amorosi et al., 1999a).

3 Materials and methods

The analysed succession is part of core 223 S12, drilled approximately 14 km inland from the modern shoreline near the city of Ravenna (Fig. 1) by wireline perforation, which guaranteed a continuous and undisturbed core stratigraphy, with recovery percentages higher than 90 %. This core reached a depth of 170 m and includes two paralic to shallow marine intervals formed in response to MIS 1 and 5.5 interglacials and a lagoonal interval attributed to MIS 7; these are alternated by continental deposits formed during glacial periods (Amorosi et al., 1999b, 2004). The detailed distribution of benthic foraminifera in the upper 130 m of this succession, including the MIS 1 and 5.5 interglacials, is reported in Fiorini (2004); this work is focused on the lower portion of this core, between ca. 165 and 160 m core depth, dated to the MIS 7 (Amorosi et al., 1999b), which has not been studied in detail.

Micropalaeontological analyses were performed on 19 sediment samples of ca. 150 g that were treated with a standard method as reported, for instance, in Amorosi et al. (1999b) and in Fiorni and Vaiani (2001): (i) dried for 8 h at 60 °C, (ii) soaked in water, (iii) wet-sieved at 63 µm (240 mesh), and (iv) dried again. The obtained residue was examined under a binocular microscope to qualitatively analyse the meiofauna. Foraminiferal tests were subsequently separated with flotation from 16 samples with abundant fauna, using carbon tetrachloride (CCl_4). Both the light (floated) and the heavy fractions were dry-sieved through a 125 µm sieve to concentrate adult tests and avoid problems of specific attribution on juvenile moults and individuals. The obtained light residue was then split into small proportions containing at least 300 specimens of benthic foraminifera, which were counted and identified. For all samples, the light fraction was then added to the heavy residue, including most of ostracoda, and split into portions including at least 300 ostracod valves for quantitative analyses. At the same time, benthic foraminifera were counted within the same residue to determine the relative proportion of the two groups. The micropalaeontological samples are housed in the Department of Biological, Geological and Environmental Sciences of the University of Bologna.

Identification of taxa was supported by original descriptions (Ellis and Messina, 1940). Furthermore, several reference works focusing on detailed taxonomy of Elphidiidae (Hansen and Lykke-Andersen, 1976; Hayward et al., 1997) and on the Mediterranean benthic foraminifera (e.g. Jorissen, 1988; Cimerman and Langer, 1991; Fiorini and Vaiani, 2001; Milker and Schmiedl, 2012) have been used for specific attribution of benthic foraminifera. Additional taxonomical remarks are reported in Appendix A. Due to the remarkable presence of deformed benthic foraminifera, the foraminiferal abnormality index (FAI, defined as the percentage of aberrant specimens in each sample) was calculated (Frontalini and Coccioni, 2008). Morphological abnormalities of tests were identified following Yanko et al. (1994), Geslin et al. (1998), and Coccioni (2000). Ostracod identification is also supported by works of Bonaduce et al. (1975), Breman (1975), Athersuch et al. (1989), Henderson (1990), and Mazzini et al. (1999). Photographs of specimens were obtained using a scanning electron microscope JEOL JSM 5200 at the Department of Biological, Geological and Environmental Sciences of the University of Bologna. A detailed analysis of the most common benthic foraminifera has been carried out due to their high morphological variability, and selected images are depicted in Plates 1 and 2.

Data matrices for multivariate statistical analyses were produced considering the most abundant taxa, with a frequency $> 1\,\%$ in at least one sample for both groups, in order to reduce background noise produced by rare species. Analyses performed on the full data matrix and with cut-off levels of 3 and 4 % show that the composition of clusters is stable; therefore, a 1 % cut-off level was applied, as suggested by other studies on benthic foraminifera and ostracoda of transitional environments (e.g. Frontalini et al., 2013; Martínez-Garcia et al., 2013). The benthic foraminiferal data matrix included the 14 most common taxa or groups and the relative abundance of deformed specimens (FAI) as an additional variable. A total of 10 species or morphotypes were included in the ostracod data matrix. Specifically, *Cyprideis torosa* was differentiated in noded and un-noded forms because these two morphotypes are related to different environmental conditions, as evidenced by several works (e.g. Keyser and Aladin, 2004; Frenzel et al., 2012; Pint et al., 2012). Prior to statistical analyses, a logarithmic transformation ($\log_{10}(X+1)$, where X is the number of tests or valves) was applied to relative abundance data in order to increase the contribution of less abundant species and to reduce the overwhelming effect of the dominant taxa. One sample including only 277 ostracod valves (163.65 m core depth) was included in the data matrix since it can be considered a significant number for quantitative analysis on ostracod assemblages (Boomer et al., 2003) and it enhances the accuracy of the palaeoenvironmental reconstruction.

A Q-mode cluster analysis, using an unweighted pair group method with arithmetic mean algorithm (UPGMA), was performed in order to group samples with similar fauna. To further evaluate the null hypothesis of no variability in the faunal composition between benthic assemblages, a one-way analysis of similarities (ANOSIM; Clarke, 1993) with 9999 permutations was carried out. This test compares the ranks of distances within groups with ranks of distances between groups: if the dissimilarity between groups is greater than that within groups, p values are < 0.5 and groups are considered to be distinct. A similarity percentage (SIMPER) analysis defined the main taxa responsible for the differences between groups. These analyses were based on the Bray–Curtis dissimilarity, a measure that does not take into account the absence of species, but it focuses on the composition of assemblage and the relative abundances of taxa (Field et al., 1982; Legendre and Legendre, 2012).

To characterize the biodiversity of assemblages, four faunal parameters were calculated: (1) species diversity (S), the number of species in each sample; (2) dominance (D); (3) Shannon–Weaver index (H), a measure of entropy that considers the distribution of taxa among the total individuals (Shannon, 1948); and (4) Pielou's evenness (J), to describe how individuals are divided between taxa (Pielou, 1975). Finally, differences between the structure of assemblages were tested using a Euclidean-based ANOSIM on D, H, and J. In this case, the Euclidean distance was chosen because it retains the mean and variance properties of original data, including the 0 values.

Multivariate statistical analyses and calculation of diversity indices were carried out using the software PAST (PAlaeontological STatistic – version 3.10 by Hammer et al., 2001) as specifically designed for palaeontological analyses.

4 Results

All 16 samples included abundant ostracod valves and were counted for quantitative analysis. Due to the low abundance of benthic foraminifera at the base (163.95–163.50 m core depth) and at the top (160.85–160.55 m core depth) of the studied interval, only 11 samples were quantitatively analysed to determine the benthic foraminiferal fauna.

4.1 Benthic foraminifera diversity and assemblages

A total of 4756 benthic foraminifera, belonging to 36 taxa, have been counted and identified between 163.50 and 160.95 m core depth (Table S1 in the Supplement). The high morphological variability shown by Elphidiidae and *Ammonia* specimens allowed the identification of several taxa, which are described in detail in the taxonomic section (Appendix A) and depicted in Plates 1 and 2.

Species richness (S) varies from 12 (sample at 161.45 m depth) to 23 (163.05 m) (Table 1). Dominance (D) shows a maximum value of 0.33 in the sample at 161.45 m, whereas the minimum corresponds to 0.12 at 163.20 m core depth. The lowest value of Shannon–Weaver index (H) is recorded at 161.45 m core depth (1.42) and the highest is reached at 163.20 m core depth (2.29). Pielou's evenness (J) varies from 0.57 (161.25 and 161.45 m core depth) to 0.79 (163.20 m core depth).

Ammonia parkinsoniana and intermediate *A. tepida*–*A. parkinsoniana* forms generally dominate the foraminiferal fauna (20.54 and 33.03 % on average, respectively), with subordinate *Haynesina germanica* (13.89 %), *Aubignyna perlucida* (7.99 %), *Ammonia tepida* (7.16 %), and *Cribroelphidium granosum* (5.35 %). Lower concentrations of *Haynesina depressula* (2.66 %), *Elphidium* sp. 1 (1.86 %), *Cribroelphidium oceanense* (1.60 %), *Elphidium advenum* (1.40 %), and *Elphidium clavatum* (1.31 %) are recorded.

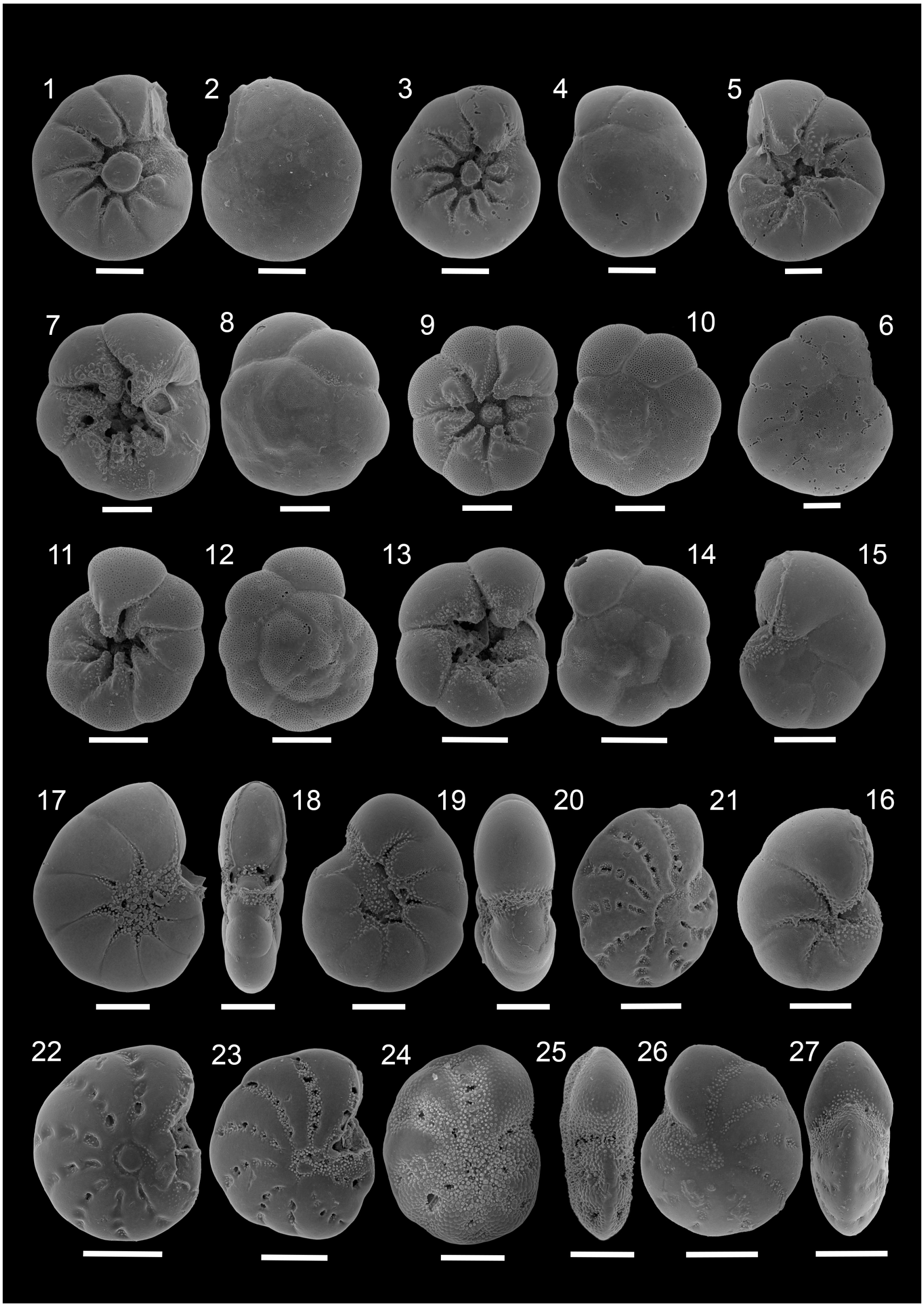

Plate 1. SEM photomicrographs of some of the most common benthic foraminiferal species found in the studied succession. Scale bar = 100 µm. **(1–2)** *Ammonia parkinsoniana* (*sobrina*-type), 162.50 m. **(1)** Umbilical side. **(2)** Spiral side. **(3–4)** *Ammonia parkinsoniana*, 162.50 m. **(3)** Umbilical side. **(4)** Spiral side. **(5–6)** *Ammonia tepida–A. parkinsoniana* intermediate morphotype C, 162.50 m. **(5)** Umbilical side. **(6)** Spiral side. **(7–8)** *Ammonia tepida–A. parkinsoniana* intermediate morphotype B, 162.50 m. **(7)** Umbilical side. **(8)** Spiral side. **(9–10)** *Ammonia tepida–A. parkinsoniana* intermediate morphotype A, 162.50 m. **(9)** Umbilical side. **(10)** Spiral side. **(11–14)** *Ammonia tepida,* 162.50 m. **(11, 13)** Umbilical side. **(12, 14)** Spiral side. **(15–16)** *Aubignyna perlucida*, 163.20 m. **(15)** Spiral side. **(16)** Umbilical side. **(17–18)** *Haynesina depressula*, 162.50 m. **(17)** Side view. **(18)** Peripheral view. **(19–20)** *Haynesina germanica*, 162.50 m. **(19)** Side view. **(20)** Peripheral view. **(21)** *Elphidium advenum*, 162.70 m. Side view. **(22)** *Elphidium clavatum*, 163.05 m. Side view. **(23)** *Elphidium gerthi*, 162.50 m. Side view. **(24–25)** *Elphidium* sp. 1, 163.20 m. **(24)** Side view. **(25)** Peripheral view. **(26–27)** *Elphidium* sp. 2, 161.30 m. **(26)** Side view. **(27)** Peripheral view.

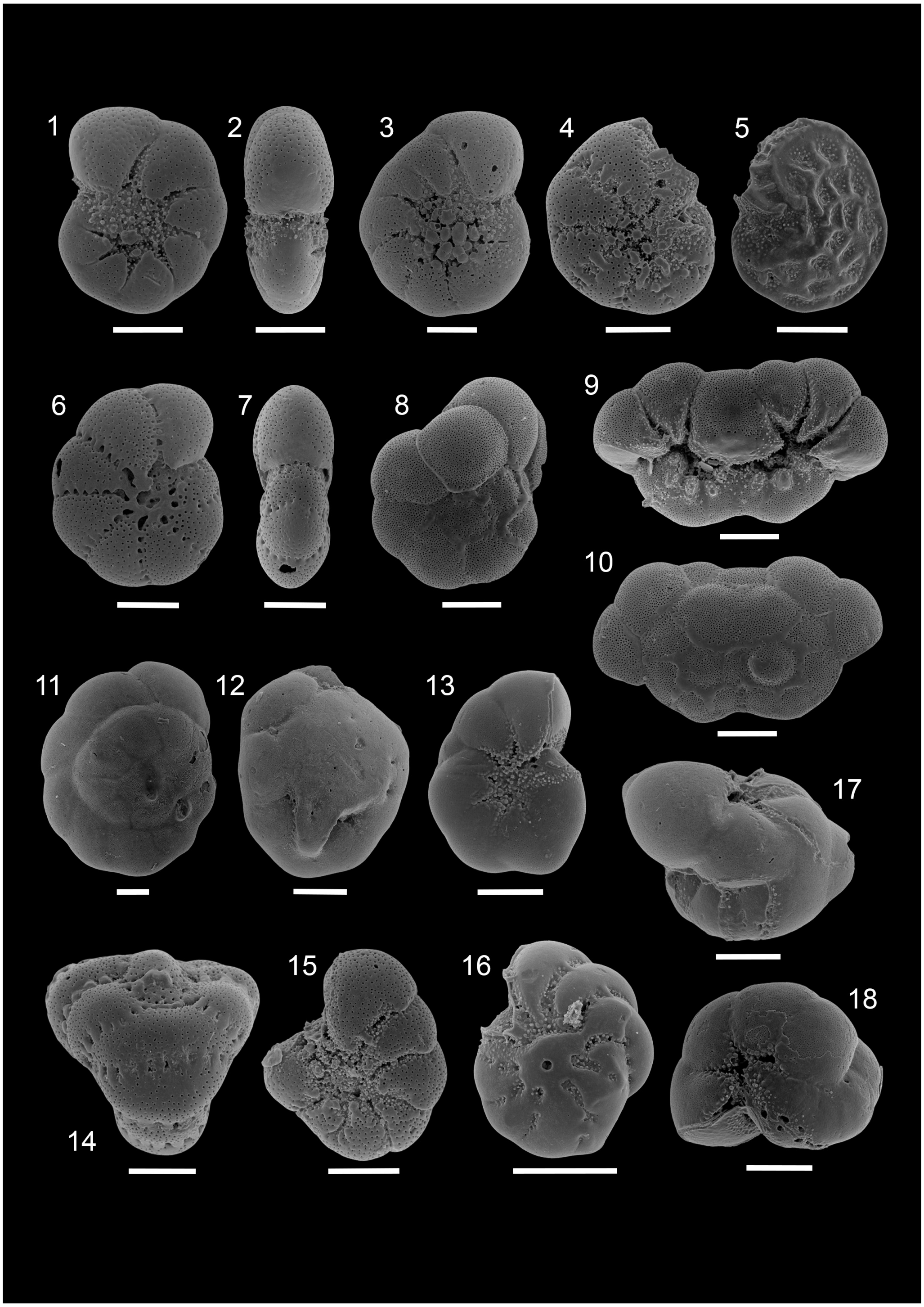

Plate 2. SEM photomicrographs of selected Elphidiidae and individuals affected by morphological abnormalities of the test. Scale bar = 100 µm. **(1–2)** *Cribroelphidium granosum*, 163.05 m. **(1)** Side view. **(2)** Peripheral view. **(3)** *Cribroelphidium lidoense*, 162.50 m. Side view. **(4)** *Cribroelphidium oceanense*, 162.70 m. Side view. **(5)** *Parrellina verriculata*, 161.30 m. Side view. **(6–7)** *Cribroelphidium poeyanum*, 162.50 m. **(6)** Side view. **(7)** Peripheral view. **(8)** *Ammonia tepida–A. parkinsoniana* intermediate morphotype A, 162.50 m. Change in coiling direction. **(9–10)** *Ammonia tepida*, 161.75 m. Twinned tests. **(9)** Umbilical side. **(10)** Spiral side. **(11)** *Ammonia tepida–A. parkinsoniana* intermediate morphotype B, 160.95 m. Change in coiling direction and anomalous protuberances on the spiral side. **(12)** *Ammonia parkinsoniana*, 163.40 m. Non-developed test. **(13)** *Haynesina germanica*, 163.20 m. Change in coiling direction. **(14)** *Cribroelphidium oceanense*, 162.50 m. Complex form. **(15)** *Cribroelphidium oceanense*, 163.20 m. Abnormal protruding chamber. **(16)** *Elphidium clavatum*, 163.20 m. Aberrant chamber shape. **(17)** *Aubignyna perlucida*, 162.50 m. Twinned tests. **(18)** *Haynesina germanica*, 162.50 m. Twinned tests.

Table 1. Diversity indices (species diversity, dominance, Shannon–Weaver, and Pielou's evenness indices) calculated for benthic foraminifera and ostracoda in each sample. The foraminiferal abnormality index (FAI) for benthic foraminifera is included.

Sample depth (m)	160.55	160.70	160.75	160.95	161.25	161.45	161.75	161.90	162.15	162.50	162.70	163.05	163.20	163.40	163.65	163.95
Benthic foraminifera																
FAI				5.58	0.00	0.80	4.33	6.48	5.62	6.13	7.10	1.60	10.09	12.26		
Species diversity (S)				19	15	12	15	20	14	18	20	23	18	14		
Dominance (D)				0.20	0.28	0.33	0.28	0.17	0.22	0.20	0.14	0.18	0.12	0.18		
Shannon–Weaver (H)				1.89	1.55	1.42	1.70	2.18	1.85	1.92	2.28	2.21	2.29	1.94		
Pielou's evenness (J)				0.64	0.57	0.57	0.63	0.73	0.70	0.66	0.76	0.70	0.79	0.73		
Ostracoda																
Species diversity (S)	3	2	2	3	8	9	2	3	3	3	6	10	13	1	1	1
Dominance (D)	0.81	0.99	0.99	0.93	0.29	0.54	0.99	0.97	0.97	0.89	0.86	0.52	0.41	1.00	1.00	1.00
Shannon–Weaver (H)	0.38	0.04	0.04	0.17	1.39	0.95	0.02	0.10	0.09	0.26	0.35	1.05	1.25	0.00	0.00	0.00
Pielou's evenness (J)	0.35	0.05	0.06	0.16	0.67	0.43	0.03	0.09	0.08	0.24	0.19	0.46	0.49	0.00	0.00	0.00

Morphological abnormalities, mainly observed in transitional individuals of *A.tepida–A. parkinsoniana, C. oceanense*, and *H. germanica* (Table S1), have been recorded in all samples, except at 161.25 m core depth. The average value of FAI recorded in the studied succession is 5.45 and reaches the maximum at 163.40 m core depth (12.26). Following the literature (Yanko et al., 1994; Coccioni, 2000), different types of test abnormalities have been recognized: abnormal protruding chambers, abnormal additional chambers, distorted chamber arrangement, change in coiling direction, twinned tests, and non-developed tests. Some individuals exhibit two or even more test abnormalities, resulting in complex forms, sometimes difficult to recognize (Plate 2).

The Q-mode cluster analysis performed on the benthic foraminifera dataset allows us to distinguish two main groups of samples (Fig. 2a). ANOSIM analysis confirms the presence of significant differences in species composition between groups of samples recognized by the Q-mode cluster analysis ($R = 0.982$, $p = 0.0173$; Table 2). SIMPER analysis evidences that more than 50 % of differences between clusters are defined by four major groups of benthic foraminifera (Table 3), with the dominant contribution of the abundance of deformed specimens, followed by *C. granosum*, *C. oceanense*, *E. clavatum*, and other less common species of *Elphidium* and *Cribroelphidium* (*Cribroelphidium lidoense, Elphidium gerthi, Elphidium* sp. 1, and *Elphidium* sp. 2; see the taxonomic section for descriptions). Cluster A is mainly defined by the high occurrence of abnormal individuals and the significant presence of *C. granosum*, *C. oceanense, E. clavatum*, *Cribroelphidium poeyanum*, and other species of *Elphidium* and *Cribroelphidium*. In contrast, cluster B is characterized by a very low occurrence of aberrant specimens, a lower number of Elphidiidae and *A. perlucida* and slightly higher frequencies of Miliolidae (represented by *Adelosina cliarensis, Miliolinella* sp., *Quinqueloculina seminula* , and *Triloculina trigonula*). *Ammonia parkinsoniana*, *A. tepida* (and related morphotypes), and *H. germanica* represent some of the most common taxa in both clusters (Table 4) and they do not substantially contribute to the main differences between them. A very low contribution is also provided by *Asterigerinata mamilla* and *Haynesina depressula*. The one-way ANOSIM performed on diversity indices reveals significant variations in D, H, J, and for crossed diversity indices between assemblages (Table 2).

4.2 Ostracod diversity and assemblages

The 16 samples analysed for Ostracoda included 5013 ostracod valves from 19 taxa (Table S2). Some of the most common or peculiar taxa are reported in Plate 3.

The number of recorded ostracod species per sample (S) ranges from 1 (samples at 163.40, 163.65, and 163.95 m core depth) to 13 (163.20 m depth, Table 1). As a consequence, D shows the maximum value of 1 in samples 163.40, 163.65, and 163.95 m core depth and it reaches a minimum of 0.29

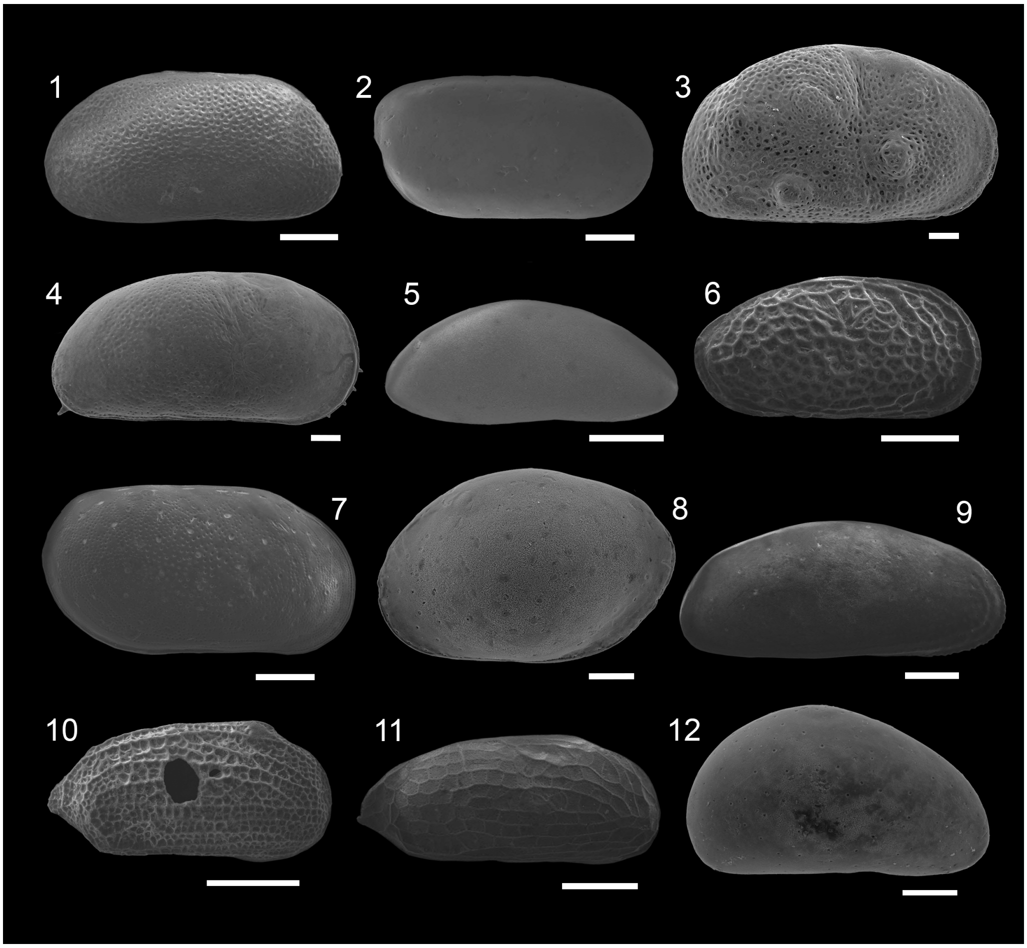

Plate 3. SEM photomicrographs of the most common or peculiar ostracod taxa found in the studied succession. Scale bar = 100 µm. **(1)** *Pseudocandona* sp., juvenile LV, 160.55 m. **(2)** *Basslerites berchoni*, RV, 163.05 m. **(3)** *Cyprideis torosa*, noded RV, 163.65 m. **(4)** *Cyprideis torosa*, un-noded RV, 162.50 m. **(5)** *Cytherois fischeri*, RV, 161.45 m. **(6)** *Leptocythere bacescoi*, RV, 161.25 m. **(7)** *Loxoconcha elliptica*, RV, 160.95 m. **(8)** *Loxoconcha stellifera*, LV, 161.45 m. **(9)** *Pontocythere turbida*, RV, 161.75 m. **(10)** *Semicytherura reticulata*, RV, 161.25 m. **(11)** *Semicytherura* cf. *sulcata*, RV, 163.05 m. **(12)** *Xestoleberis dispar*, RV, 161.25 m.

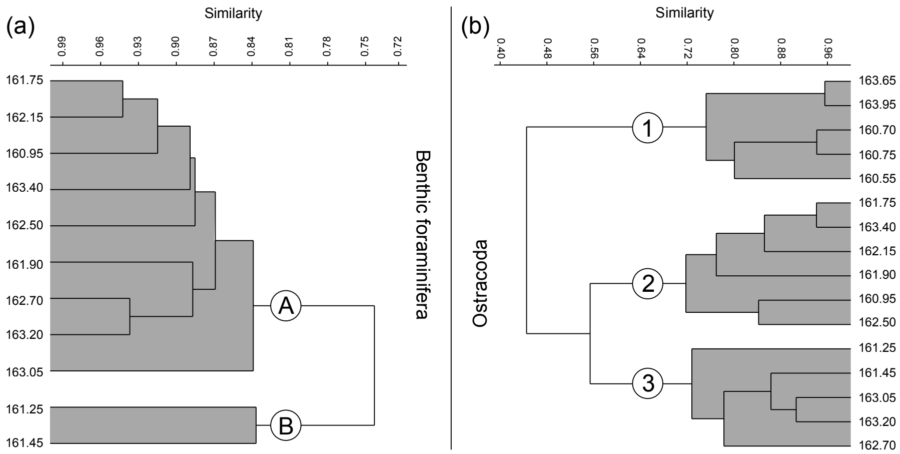

Figure 2. Dendrogram classification from the Q-mode cluster analysis using the Bray–Curtis distance on **(a)** benthic foraminifera and **(b)** ostracoda.

Table 2. Results of the one-way ANOSIM analysis based on diversity indices (Euclidean distance) and faunal composition (Bray–Curtis distance) between the two benthic foraminiferal and the three ostracod assemblages defined by Q-mode cluster analysis (Fig. 2).

	Benthic foraminifera		Ostracoda	
	R	p	R	p
D	0.6982	0.0377^{a}	0.4403	0.0009^{b}
H	0.7072	0.0219^{a}	0.4587	0.0014^{b}
J	0.7237	0.0143^{a}	0.3923	0.0028^{b}
$D \times H \times J$	0.7132	0.0149^{a}	0.4467	0.0008^{b}
Faunal composition	0.982	0.0173^{a}	0.9429	0.0001^{b}

[a] and [b] indicate significant values of $p < 0.05$ and $p < 0.01$, respectively.

Table 3. Similarity percentage (SIMPER) analysis performed on benthic foraminiferal assemblages defined by Q-mode cluster analysis (Fig. 2a). Overall average dissimilarity: 25.7.

Taxon	Average dissimilarity	Contribution (%)	Cumulative (%)	Cluster A	Cluster B
Deformed specimens	3.76	14.63	14.63	1.40	0.30
Cribroelphidium granosum	3.30	12.83	27.46	1.35	0.39
Cribroelphidium oceanense	3.10	12.07	39.53	0.91	0.00
Elphidium clavatum	2.46	9.56	49.09	0.72	0.00
Other *Elphidium*, *Cribroelphidium*	2.10	8.17	57.26	1.01	0.39
Cribroelphidium poeyanum	1.79	6.95	64.21	0.67	0.15
Miliolidae	1.59	6.20	70.41	0.25	0.54
Elphidium advenum	1.22	4.74	75.15	0.78	0.54
Aubignyna perlucida	1.17	4.54	79.69	1.54	1.21
A. tepida–A. parkinsoniana morphotypes	1.00	3.90	83.59	2.07	2.33
Asterigerinata mamilla	0.95	3.70	87.29	0.28	0.00
Haynesina germanica	0.88	3.43	90.72	1.72	1.81
Ammonia tepida	0.88	3.42	94.14	1.46	1.40
Ammonia parkinsoniana	0.82	3.20	97.33	1.87	2.05
Haynesina depressula	0.69	2.67	100.00	1.06	1.08

at 161.25 m core depth. In the same sample, H has the maximum value (1.39), whereas the minimum (0) is recorded in samples with only one species. In samples at 163.40, 163.65 and 163.95 m core depth J has the value of 0, whereas it reaches 0.67 at 161.25 m core depth.

Ostracoda are largely dominated by *Cyprideis torosa* (87.59 % on average). Other species are mainly represented by *Xestoleberis dispar* (6.34 %), *Loxoconcha stellifera* (2.99 %), and *Pontocythere turbida* (1.02 %).

The Q-mode cluster analysis performed on the ostracod fauna reveals the presence of three groups of samples (Fig. 2b) with significantly different faunal composition, as confirmed by ANOSIM ($R = 0.9429$, $p = 0.0001$; Table 2). The SIMPER analysis (Table 5) shows that more than 50 % of the difference between clusters is defined by noded *C. torosa* (25.96 % of relative contribution), *L. stellifera* (18.92 %), and *X. dispar* (18.14 %), followed by lower contributions of *Pontocythere turbida* (10.03 %), un-noded *C. torosa* (6.13 %), *Leptocythere bacescoi* (5.92 %), and *Candona* sp. (5.82 %). Cluster 1 is dominated by noded and un-noded *C. torosa*. Relatively low numbers of *Pseudocandona* sp. and *Candona* sp. are recorded only in this cluster (specifically, within the upper samples at 160.75, 160.70, and 160.55 m core depth). Un-noded *C. torosa* dominates cluster 2, followed by very low frequencies of *X. dispar* and *L. stellifera* recorded in scattered samples. Although cluster 3 is still dominated by un-noded *C. torosa*, it includes high concentrations of several other species, such as *X. dispar, L. stellifera, P. turbida, L. bacescoi*, and *Basslerites berchoni* (Table 6). The results of ANOSIM performed on diversity indices indicate highly significant differences (with $p < 0.01$) in the ostracod assemblages between D, H, J, and crossed indices (Table 2).

4.3 Stratigraphy and distribution of microfossil assemblages

The lower stratigraphic portion of core 223 S12 is composed of finely grained, alluvial deposits completely barren in microfossils with scattered layers of fine sand (Fig. 3; Amorosi et al., 1999b). From 163.95 to 163.50 m core depth, ostracod assemblage 1 occurs and includes very high proportions of

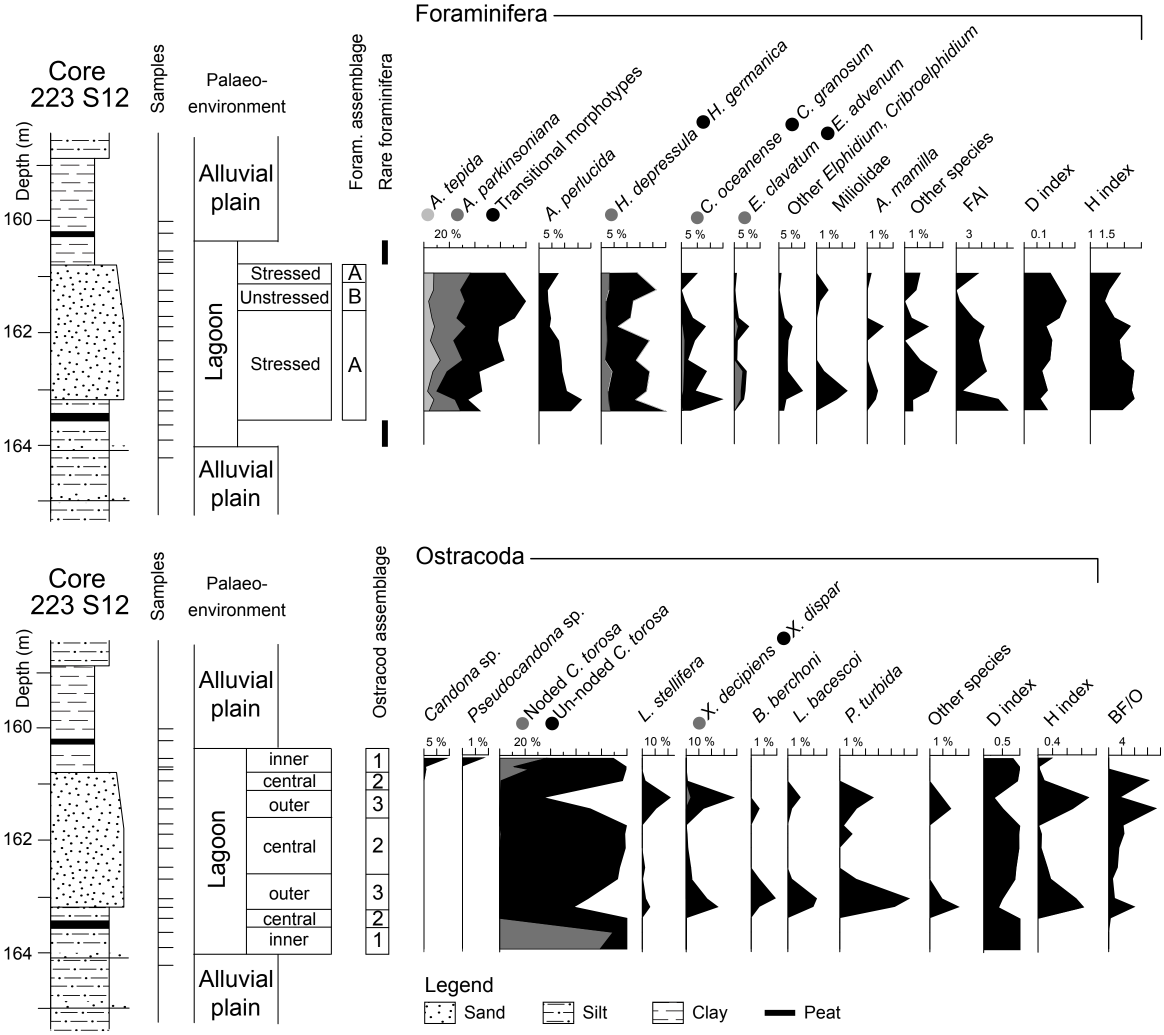

Figure 3. Stratigraphy and vertical distribution of benthic foraminifera and ostracoda in the studied interval of core 223 S12. Curves represent the relative frequency of major benthic foraminiferal and ostracod taxa, FAI index, diversity indices, and the quantitative ratio between benthic foraminifera and ostracoda (BF / O).

noded *C. torosa*, whereas benthic foraminifera are extremely rare and include mainly small specimens of *A. tepida–A. parkinsoniana*. Above this interval, benthic foraminifera become abundant, represented by assemblage A, whereas ostracoda are characterized by assemblage 2, entirely composed of un-noded specimens of *C. torosa*. A major shift in lithology and in the composition of ostracod fauna occurs at 163.30 m core depth, where clayey silt sediments are replaced by fine sands. This interval is characterized by ostracod assemblage 3, which is replaced by ostracod assemblage 2 at 162.60 m core depth. From 161.60 m core depth, both fossil groups mark a change in faunal composition, as benthic foraminifera shifts from assemblage A to assemblage B and ostracoda from assemblage 2 to assemblage 3. Benthic foraminifera of assemblage A and ostracoda of assemblage 2 are recorded again within the following stratigraphic interval, from 161.10 to 160.80 m core depth. Upward, clayey sediments include scattered individuals of *A. tepida–A. parkinsoniana*, whereas ostracoda are abundant and represented by assemblage 1. Above a thick peat layer at 160.50 m core depth, clay and silts of alluvial plain (Amorosi et al., 1999b) are barren in microfossils.

5 Discussion

5.1 Benthic foraminiferal assemblages

Both assemblages are dominated by euryhaline taxa, such as *A. parkinsoniana*, *A. tepida*, and *H. germanica*, which suggest the development of a brackish lagoon environment. These taxa dominate lagoons, coastal lakes, and estuaries, where salinity, oxygen, organic matter, and nutrients rapidly change (Alve and Murray, 1994; Stouff et al., 1999). Specif-

Table 4. Mean values of relative abundances of selected taxa, FAI, and diversity indices for benthic foraminiferal assemblages identified using cluster analysis.

Benthic foraminifera		
Assemblage	A	B
Ammonia parkinsoniana	18.68	24.83
Ammonia tepida	6.96	5.66
A. tepida–A. parkinsoniana morphotypes	27.81	45.94
Asterigerinata mamilla	0.36	0.00
Aubignyna perlucida	8.91	3.36
Cribroelphidium granosum	6.16	0.67
Cribroelphidium lidoense	0.09	0.13
Cribroelphidium oceanense	0.67	0.00
Cribroelphidium poeyanum	1.13	0.13
Elphidium advenum	1.58	0.58
Elphidium clavatum	1.54	0.00
Elphidium gerthi	0.23	0.00
Elphidium sp. 1	2.10	0.13
Elphidium sp. 2	0.09	0.09
Haynesina depressula	2.70	2.47
Haynesina germanica	12.66	14.32
Miliolidae	0.28	0.39
FAI	6.58	0.40
Dominance (D)	0.19	0.31
Shannon–Weaver (H)	2.03	1.49
Pielou's evenness (J)	0.71	0.57

ically, *A. parkinsoniana* is common in the northern Adriatic lagoons of Venice (Coccioni et al., 2009), Marano, and Grado (Melis and Covelli, 2013) and also in the Goro lagoon of the Po River delta (Fig. 1; Coccioni, 2000). *Ammonia tepida* is a widespread species dominant in lagoons, estuaries, and deltaic environments (Jorissen, 1988; Murray, 2006), commonly recorded in central lagoonal assemblages of the Mediterranean associated with *H. germanica* (Debenay et al., 2000). The latter taxon prefers to feed on labile organic matter, such as diatoms, in contrast to *A. tepida*, which is able to consume many food sources, including refractory material (Goldstein and Corliss, 1994; de Nooijer et al., 2007).

The observed foraminiferal distribution is substantially comparable with that present today in the Goro lagoon (Fig. 1; Coccioni, 2000), a brackish-water area with an average depth of ca. 1.5 m, showing remarkable local and seasonal variations in physico-chemical parameters (salinity: 11.7–31 ‰; temperature: 4.2–27.5 °C; oxygen: 3.7–12.4 $\mathrm{mg\,L^{-1}}$) of the bottom water. In this lagoon, the frequencies of *A. parkinsoniana*, *A. tepida*, and related morphotypes (from 16 to 84 % of total assemblage, average 52 %) are not clearly linked with the sample position within the lagoon. A similar pattern is also shown by other abundant species, such as *H. germanica* and *C. oceanense* (listed as *C. gunteri* in Coccioni, 2000). Similar to the assemblages of core 223 S12, foraminifera with morphological abnormalities are common, but their presence in the Goro lagoon is mainly attributed to heavy metal contamination; in the succession analysed, the distribution of these peculiar specimens is the main factor for the distinction of two clusters, defining assemblages A and B (Fig. 2a).

5.1.1 Stressed assemblage (assemblage A)

The concentration of abnormal individuals (FAI) is relatively high (6.58 on average) and exceeds 1 in all samples of the assemblage, which is considered the threshold value between stressed and unstressed populations from literature sources (Alve, 1991; Frontalini and Coccioni, 2008). Benthic foraminifera exposed to extreme values of salinity, oxygen deficiency, high concentrations of nutrients, or contaminants show frequencies of deformed tests always > 1 %, whereas the occurrence of benthic foraminiferal abnormalities under normal conditions is always lower (Stouff et al., 1999; Le Cadre and Debenay, 2006). Therefore, the high FAI recorded in the samples studied can be considered indicative of palaeoenvironmental stress, likely resulting from rapid oscillations in physico-chemical parameters such as salinity and oxygen concentration at the bottom. This is in accordance with other studies performed on benthic foraminiferal assemblages that interpret the high occurrence of abnormal specimens within transitional palaeoenvironments as a consequence of reduced, fluctuating salinity (Bik, 1964; Wang et al., 1985), oxygen depletion (Alve, 1991), or both (Geslin et al., 2002). Nevertheless, the contribution of other adverse ecological parameters could not be excluded since communities with high numbers of deformed tests generally result from the interplay of multiple environmental factors (Scott and Medioli, 1980; Boltovskoy et al., 1991).

Similar values of relatively low dominance (0.19 on average) and high diversity (H value of 2.03 on average) recorded for this assemblage are reported from inner to outer portions of Adriatic and Tyrrhenian brackish-water environments (Carboni et al., 2009; Melis and Covelli, 2013).

The distribution of *H. germanica* and *A. tepida* suggests relatively high nutrient inputs, represented by labile and refractory organic matter. Ample food availability (and possibly low oxygen concentration) is confirmed by the relatively high frequencies of *A. perlucida*, *C. granosum*, and *C. poeyanum*, which typically live in shallow marine environments with substrates enriched in organic matter and limited oxygen deficiency (Jorissen, 1988). These *Cribroelphidium* species are considered stressed and tolerant forms, in contrast to their unstressed counterparts represented by *C. lidoense* and *C. decipiens*, more abundant on substrates with low organic matter content (Jorissen, 1988). In addition to these taxa, a wide variety of *Elphidium* and *Cribroelphidium* species are recorded almost exclusively within this assemblage and greatly contribute to the increase in interspecific diversity. In detail, *Cribroelphidium oceanense* is a brackish-water species, common in shallow Mediterranean lagoons

Table 5. Similarity percentage (SIMPER) analysis for ostracod assemblages defined with Q-mode cluster analysis (Fig. 2b). Overall average dissimilarity: 45.35.

Taxon	Average dissimilarity	Contribution (%)	Cumulative (%)	Cluster 1	Cluster 2	Cluster 3
Noded *C. torosa*	13.41	25.96	25.96	2.08	0.23	0.06
Loxoconcha stellifera	9.77	18.92	44.87	0.00	0.35	1.81
Xestoleberis dispar	9.37	18.14	63.02	0.00	0.48	1.69
Pontocythere turbida	5.18	10.03	73.05	0.00	0.15	0.95
Un-noded *C. torosa*	3.17	6.13	79.18	2.09	2.48	2.28
Leptocythere bacescoi	3.06	5.92	85.10	0.00	0.00	0.59
Candona sp.	3.01	5.82	90.92	0.51	0.00	0.00
Basslerites berchoni	2.51	4.86	95.78	0.00	0.00	0.46
Xestoleberis decipiens	1.32	2.55	98.33	0.00	0.00	0.28
Pseudocandona sp.	0.86	1.67	100.00	0.16	0.00	0.00

Table 6. Mean ostracod assemblages' parameters and relative frequencies of major taxa.

	Ostracoda		
Assemblage	1	2	3
Noded *C. torosa*	47.94	0.43	0.07
Un-noded *C. torosa*	49.66	98.05	65.15
Candona sp.	2.07	0.00	0.00
Pseudocandona sp.	0.33	0.00	0.00
Basslerites berchoni	0.00	0.00	0.78
Loxoconcha stellifera	0.00	0.80	8.59
Leptocythere bacescoi	0.00	0.00	1.17
Xestoleberis decipiens	0.00	0.00	0.86
Xestoleberis dispar	0.00	1.07	19.00
Pontocythere turbida	0.00	0.22	3.00
Semicytherura spp.	0.00	0.00	0.25
Dominance (D)	0.96	0.96	0.52
Shannon–Weaver (H)	0.09	0.11	1.00
Pielou's evenness (J)	0.16	0.12	0.45

and coastal lakes (Debenay et al., 2000; Carboni et al., 2009; Frontalini et al., 2009). This taxon is particularly abundant in eutrophic areas characterized by high concentrations of nutrients and variations in salinity (Melis and Covelli, 2013). *Elphidium advenum* lives in coastal areas and it is recorded in low percentages in the Mediterranean lagoons (Albani and Serandrei Barbero, 1990; Hohenegger et al., 1993). *Elphidium clavatum* and *E. gerthi* are usually found in low-salinity waters, such as estuaries, outer lagoons, and marginal marine environments strongly influenced by fluvial inputs (Murray, 2006). Moreover, *E. clavatum* is an opportunistic species, able to tolerate high sediment and nutrient inputs, also in oxygen-depleted conditions (Linke and Lutze, 1993; Alve and Murray, 1999).

Summarizing, the composition of foraminiferal assemblage A is indicative of a brackish lagoon with substantially stressed conditions, possibly produced by strong variations in salinity and oxygen. This assemblage is considered to reflect a palaeoenvironment comparable with the recent Goro lagoon, probably with higher organic matter and lower oxygen concentration as revealed by the frequencies of species indicative of these conditions (such as *A. perlucida, C. granosum, C. poeyanum*, and *C. oceanense*).

5.1.2 Unstressed assemblage (assemblage B)

This assemblage shows a significantly lower number of aberrant specimens (FAI values < 1); this concentration is in agreement with the number of abnormal individuals naturally present within benthic foraminifera populations, as revealed by laboratory studies (Stouff et al., 1999). Compared with assemblage A, it also includes a lower number of species indicative of high nutrient inputs and low oxygenated bottom water, such as selected *Cribroelphidium*, *Elphidium*, and *A. perlucida*. The substantially lower concentrations of these taxa, mainly replaced by morphotypes of *A. tepida* and *A. parkinsoniana,* are responsible for the differences in faunal composition and community structure between the two assemblages (specifically, higher D and lower H and J values of assemblage B). Therefore, even if assemblage B shows a lower H index, the absence of species related to eutrophic conditions seems to be indicative of a less stressed environment in terms of oxygen conditions.

The palaeoenvironmental interpretation of assemblage B is substantially comparable with that of the previous one; however, the low FAI values are indicative of unstressed conditions in a relatively stable palaeoenvironment, characterized by lower concentrations of organic matter and without oxygen depletion at the bottom.

5.2 Ostracod assemblages

All ostracod assemblages are dominated by *C. torosa*, a widespread, euryhaline taxon, commonly found in transitional environments such as lagoons, estuaries, and inland ponds (Athersuch et al., 1989). It is an opportunistic species, able to live from almost freshwater to hypersaline conditions, irrespective of substratum type, vegetation cover, temperature, and oxygen concentration (Meisch, 2000). This species is recorded with very high frequencies in the major northern Adriatic lagoons of Italy, such as Venice, Marano, and Grado (Montenegro and Pugliese, 1996; Ruiz et al., 2000). In accordance with benthic foraminifera, the ostracod fauna dominated by *C. torosa* reflects the development of a lagoonal basin.

Despite the strong dominance of *C. torosa* in the analysed succession, significant differences in composition and ecological structure of ostracod assemblages could be related to the faunal response to changing palaeoenvironmental conditions. In comparison to benthic foraminifera, ostracod assemblages show more significant differences in the community structure (Table 2), indicating that this group reacted with sharp faunal changes to subtle palaeoenvironmental variations not recorded by the other fossil group.

5.2.1 Inner lagoon assemblage (assemblage 1)

Cyprideis torosa presents two morphotypes with different ornamentation of the valves, and both of them are recorded within this assemblage: noded and un-noded. The formation of nodes in *C. torosa* is related to salinity and concentration of Ca^{2+} in the water (Keyser and Aladin, 2004; Frenzel et al., 2012). There is disagreement about the salinity limits proposed for the presence of noded valves. Some authors reported the occurrence of noded valves in waters with salinity of < 14–15 psu (Marco-Barba, 2010), but it seems that nodes are formed mainly below the switching point of osmotic regulation for *C. torosa* at ca. 8 psu (Aladin, 1993). High frequencies of noded valves are reported for values of salinity below 2 (Frenzel et al., 2010, 2012) or 5 psu (Marco-Barba, 2010). Since ecophenotypes in *C. torosa* are likely determined by multiple factors (Van Harten, 2000; Keyser and Aladin, 2004), palaeosalinity estimation based exclusively on morphological variability in *C. torosa* should be carefully used, but it is a useful proxy to detect palaeoenvironmental trends (Pint et al., 2012).

Pseudocandona and *Candona* are freshwater–mesohaline taxa found only within the uppermost samples, frequent in European ponds and lakes (Meisch, 2000; Pieri et al., 2005).

The very high dominance (0.96 on average), paralleled by the low H and J values (on average 0.09 and 0.16, respectively) suggest restricted palaeoenvironmental conditions.

The co-dominance of noded and un-noded *C. torosa* reflects deposition in a restricted, oligohaline environment, like a low-salinity inner lagoon possibly with oxygen deficiency, where only this opportunistic species is able to thrive. The abundance of noded valves of *C. torosa* is indicative of oligohaline conditions (Frenzel et al., 2012). Un-noded *C. torosa* associated with lower frequencies of noded valves is reported from specific areas of the Venice Lagoon subject to high freshwater inputs from rivers and urban and industrial activities (Ruiz et al., 2000). The presence of *Candona* and *Pseudocandona* in the uppermost samples indicates a consistent contribution of freshwater. Similar ostracod assemblages composed mainly of *C. torosa* and freshwater species are reported from a northern European oligohaline lagoon strongly influenced by river inflows (Pint and Frenzel, 2017).

5.2.2 Central lagoon assemblage (assemblage 2)

Assemblage 2 is dominated by un-noded *C. torosa*, the most widespread morphotype of this species in Mediterranean lagoons. The observed concentrations of un-noded *C. torosa* (> 90 %) are similar to those recorded in the Venice Lagoon, where monospecific assemblages also occur (Ruiz et al., 2000). Very low concentrations of brackish-marine taxa such as *X. dispar* and *L. stellifera* are reported from the northern Adriatic lagoons of Venice, Marano, and Grado and could suggest slight influxes of normal saline water (Montenegro and Pugliese, 1996; Ruiz et al., 2000). Ostracod assemblages dominated by un-noded *C. torosa* are also reported from confined lagoons of the Gulf of Lion characterized by extreme euryhalinity (Salel et al., 2016).

The increasing H index in comparison to assemblage 1 can be related to a higher salinity. Dominance is still very high (paralleled by low J index) and suggests variable physico-chemical parameters.

Ostracod assemblage 2 is consistent with a central lagoonal basin, possibly subject to salinity oscillations. The dramatic decrease in noded *C. torosa*, replaced by the un-noded morphotype and the absence of freshwater taxa, indicates an increasing salinity.

5.2.3 Outer lagoon assemblage (assemblage 3)

The concentration of the euryhaline *C. torosa* decreases and a great number of species appear. One of the most common taxa is *X. dispar*, a phytal, polyhaline–euhaline species commonly recorded along the Italian coasts and in open lagoons greatly influenced by seawater (Bonaduce et al., 1975; Breman, 1975; Arbulla et al., 2004; Aiello et al., 2006). This assemblage also includes relatively high percentages of *L. stellifera*, a shallow-water species that lives from mesohaline to normal saline waters in lagoons, bays, and slightly freshwater-influenced areas along the Adriatic coast, reaching higher concentrations on vegetated substrates (Bonaduce et al., 1975; Arbulla et al., 2004; Aiello et al., 2006). Other species are less common but recorded almost exclusively within assemblage 3. Among them, *P. turbida* typically lives in coastal environments; it is dominant along the Italian shorelines of the Adriatic Sea and also near the fluvial mouths of the Po Delta (Colalongo, 1969; Bonaduce et al., 1975). *Leptocythere bacescoi* is well distributed along the Adriatic coast of Italy, reported also from the Limsky Channel and Marano and Grado lagoons, from polyhaline to euhaline waters (Uffenorde, 1972; Breman, 1975; Montenegro and Pugliese, 1996). Other taxa such as *X. decipiens, B. berchoni*, and *Cytherois fischeri* live in polyhaline–euhaline shallow water environments with vegetated bottoms (Uffenorde, 1972; Bonaduce et al., 1975; Arbulla et al., 2004). Rare specimens of the brackish-water taxon *Loxoconcha elliptica* and some marine species of the genus *Semicytherura* (Athersuch et al., 1989) are exclusively recorded within this assemblage.

The maximum diversity (*H* index), evenness, and decrease in dominance indicate more favourable palaeoenvironmental conditions for the ostracod fauna, in accordance with an increasing salinity due to the influence of seawater.

The composition of this assemblage is considered to reflect a lagoon highly influenced by normal saline waters, possibly an outer lagoonal area. Brackish-marine taxa characterize this assemblage, and the great abundance of phytal species indicates vegetation cover at the bottom. Ostracod assemblages with high frequencies of *C. torosa* and *Xestoleberis* are reported from the Venice Lagoon, behind the sand barriers that divide the lagoon from the northern Adriatic Sea (Ruiz et al., 2000), where macroalgae and low hydrodynamic conditions are present. Ostracod assemblages with higher frequencies of marine taxa such as *P. turbida* and *Semicytherura* spp. are recorded around the tidal inlets (Ruiz et al., 2000) in areas greatly influenced by seawater.

5.3 Evolution of the palaeolagoon: the combined approach of benthic foraminifera and ostracoda

Detailed micropalaeontological analyses performed on benthic foraminifera and ostracoda allow an accurate characterization of the stratigraphic interval. The two microfossil groups provide distinct information, related to specific palaeoenvironmental conditions. The main differences between the benthic foraminiferal assemblages are represented by the FAI and the number of brackish-water species related to high concentrations of nutrients. Accordingly, two assemblages have been defined: (i) a stressed assemblage, formed mainly in response to salinity oscillations accompanied by high organic matter and low oxygen concentrations at the bottom, and (ii) an unstressed assemblage that suggests oxygenated conditions in a more stable palaeoenvironment. Despite the overall lower number of species, ostracod assemblages show higher differences in the community structure and include taxa with specific environmental tolerance ranges, indicative of distinct sub-environments. In this case, the contribution of subordinate freshwater and brackish-marine taxa allowed the definition of inner, central, and outer lagoon assemblages that reflect a distinct salinity gradient.

Above the basal alluvial plain deposits, the great abundance of noded *C. torosa* (assemblage 1) marks the beginning of transgression and the onset of a strong freshwater-influenced inner lagoon, where abundant populations of calcareous foraminifera cannot be developed mainly due to the extremely low salinity. In these settings agglutinated foraminifera are locally present (e.g. Debenay et al., 2000), but these are not observed in this succession, probably for the low preservation potential of their fragile tests. In this respect, previous work on foraminiferal assemblages of subsurface successions of the Po Plain have shown the rare occurrence of agglutinated foraminifera of the inner lagoon, almost entirely represented by *Trochammina inflata,* and observed uniquely in Holocene sediments of the upper 20 m of cored successions (e.g. Amorosi et al., 2004; Fiorini, 2004).

Upward, the superposition of ostracod assemblages 2 and 3 indicates the passage to central and outer lagoon conditions and an increasing salinity. The development of a marine-influenced lagoon is consistent with the landward migration of a back-barrier system driven by MIS 7 transgression, when the sea level reached a maximum of −18 m below the present sea level in the Adriatic area (Dutton et al., 2009). The high occurrence of deformed benthic foraminifera provides evidence for an extremely unstable environment in the palaeolagoon, with thalassic conditions (FAI < 20 %; Pint et al., 2017). The maximum FAI value recorded in the first sample including abundant benthic foraminifera (163.40 m core depth) is indicative of very stressed conditions possibly related to oxygen depletion and salinity variations, considered important environmental parameters that control the development of test deformities in paralic environments (Geslin et al., 2002). This is also consistent with the monospecific ostracod assemblages, represented by the highly opportunistic taxon *C. torosa*. However, other disadvantageous palaeoenvironmental parameters could have contributed to the formation of the stressed foraminiferal assemblage.

A drastic reduction of marine-influenced ostracod species (i.e. the onset of assemblage 2) from 162.60 to 161.60 m core depth is indicative of lower salinity and higher confinement, likely related to a progradation of the lagoon during a reduced rate of sea level rise. The recorded ostracod assemblage with extremely high concentrations (> 90 %) of un-noded *C. torosa* could be indicative of both brackish and hypersaline conditions (Ruiz et al., 2000; Salel et al., 2016; Pint and Frenzel, 2017) in the absence of SEM analysis on sieve pores (Pint et al., 2017); however, the benthic foraminiferal assemblages are consistent with a brackish palaeoenvironment. In detail, hyperhaline environments determine benthic foraminiferal assemblages with a very low diversity, often represented by monospecific populations of *A. tepida* (Almogi-Labin et al., 1992; Engel et al., 2012). The relatively high diversity of benthic foraminifera within this stratigraphic interval and the common occurrence of selected taxa, such as *H. germanica* and *E. clavatum*, indicate the presence of brackish waters. The high rate of deformed tests can be related to unstable environmental parameters, probably oscillations of salinity derived from freshwater inputs. Nevertheless, species related to bottom water enriched in organic matter (*A. perlucida*, *C. granosum*, *C. oceanense*, *E. clavatum*) are still abundant and suggest that the palaeoecological stress could even be provided by slightly reduced oxygen concentrations. As a whole, ostracoda and benthic foraminifera highlight an episode of more restricted conditions in the lagoon, when the interplay between freshwater and marine inputs created an unstable palaeoenvironment.

A new phase of higher salinity, related to a higher influence of seawater, is recorded by ostracod assemblage 3 between 161.60 and 161.10 m core depth. The lower proportions of the opportunistic *C. torosa*, paralleled by the common occurrence of shallow marine ostracoda and the highest value of the ostracod's Shannon and evenness indices at 161.25 m core depth, are inferred to indicate the maximum marine influence. Benthic foraminifera with a FAI < 1 (foraminiferal assemblage B) evidence a phase of relatively stable palaeoenvironmental conditions, recorded only within this interval.

Upward, the presence of ostracod assemblage 2 with the high dominance of un-noded *C. torosa* is considered to reflect a lower influence of seawater. At the same time, stressed foraminiferal assemblages indicate unstable palaeoenvironmental conditions likely related to low salinity, high organic matter content, and low oxygen concentrations typical of the innermost portion of Mediterranean coastal lagoons (Alves Martins et al., 2016). In the following samples, a great faunal turnover to oligohaline ostracod assemblages reveals relevant freshwater inputs in a restricted environment, in proximity to the innermost portion of the lagoon. Here, palaeoenvironmental conditions exceeded the tolerance limit for calcareous foraminifera, which disappeared. The relative regressive trend culminates with the deposition of barren sediments of an alluvial plain.

6 Benthic foraminifera or Ostracoda, the conclusions

Quantitative palaeontological analyses performed on benthic foraminifera and ostracoda from a relatively short stratigraphic interval attributed to MIS 7 allowed a detailed palaeoenvironmental reconstruction. Specifically, the quantitative approach provided information about the environmental resolution potential for each group of fossils.

The combined application of benthic foraminifera and ostracoda indicates the development of a lagoon subject to minor environmental variations, in response to the interplay of freshwater and marine water inputs. A general transgressive–regressive trend is recorded by ostracod assemblages, with the occurrence of a minor relatively regressive phase. Outer lagoonal, unstressed conditions observed by ostracoda and benthic foraminifera are related to the highest marine influence recorded in the succession.

Both fossil groups contributed to the palaeoenvironmental reconstruction; however, the most accurate environmental resolution is commonly shown by the Ostracoda for their (i) abundant occurrence, (ii) higher differences in the ecological structure of assemblages, and (iii) distinct faunal composition in terms of species with precisely defined tolerance ranges. Scarce or rare taxa greatly contribute to the palaeoenvironmental interpretation, even if assemblages are dominated by opportunistic species. The same characteristics are not accomplished by benthic foraminifera, which show more similar assemblages in this succession. In spite of the higher number of species, they are generally not related to distinctive or quantitatively defined environmental ranges, producing a less precise palaeoenvironmental reconstruction. In addition, benthic foraminifera are not present in inner lagoon deposits (probably for the low preservation potential of agglutinated tests). However, when ostracod fauna is composed almost entirely of un-noded *C. torosa*, the distinction between brackish or hyperhaline settings is provided by the benthic foraminifera.

Benthic foraminiferal assemblages are mainly defined by the abundance of specimens with morphological abnormalities. High concentrations of deformed benthic foraminifera are quite rare in fossil assemblages and are here considered to indicate stressed conditions, possibly produced by oxygen depletion, fluctuation of salinity, and, eventually, other factors that typically characterize transitional environments. Therefore, benthic foraminifera also give indications of palaeoenvironmental stress that are not clearly shown by ostracod assemblages.

In conclusion, it is substantially intuitive that the quantitative approach to both (or even multiple) fossil groups should be preferred in palaeoenvironmental studies. However, if a choice is required between ostracoda and foraminifera within lagoonal successions, we would prefer Ostracoda. This group allows us to obtain more detailed palaeoenvironmental reconstructions with the recognition of subenvironments not recorded by the benthic foraminifera. In contrast, foraminifera provide relevant additional information (i.e. environmental stability) and, locally, an unambiguous interpretation of peculiar ostracod assemblages (i.e. entirely represented by un-noded *C. torosa*).

Data availability. All the data analysed in this paper are available in the tables provided within the paper or in the Supplement.

Appendix A: Taxonomic descriptions of some species of benthic foraminifera

Elphidiidae, Rotaliidae, and Nonionidae are some of the most common families of benthic foraminifera reported from modern and fossil coastal deposits, from arctic to tropical areas (Murray, 2006). Due to the high morphological variability among individuals of each group, the specific attribution of a taxon is sometimes difficult. Many studies were performed with the aim of clarifying the classification of these taxa from different geographical zones (e.g. Hansen and Lykke-Andersen, 1976; Hayward et al., 1997).

The contribution of recent studies that combine molecular and morphological data (e.g. Holzmann and Pawlowski, 2000; Darling et al., 2016) is a valuable resource. Previously, attribution of some taxa was controversial due to the uncertainty around formae, subspecies, or species. The genetic characterization of benthic foraminifera with similar morphological features offers solutions for this problem.

Within the studied interval, the high morphological differentiation of the above-mentioned groups led us to a detailed taxonomic analysis, following the classification of Loeblich and Tappan (1987). In the case of uncertain attribution between species, varieties, or formae, the contribution of genetic studies on benthic foraminifera has been taken into consideration, mainly for the taxonomy of selected Elphidiidae (Darling et al., 2016).

Family **Nonionidae** Schultze, 1854

Subfamily **Nonioninae** Schultze, 1854

Genus *Haynesina* Banner and Culver, 1978

Haynesina depressula (Walker and Jacob, 1798)

Plate 1, figs. 17–18

1798 *Nautilus depressulus* Walker and Jacob: p. 641, pl. 14, fig. 33

1976 *Nonion depressulum* (Walker and Jacob); Hansen and Lykke-Andersen, p. 21, pl. 19, figs. 3–6.

1978 *Haynesina depressula* (Walker and Jacob); Banner and Culver, p. 200, pl. 10, figs. 1–8.

1984 *Nonion depressulum* (Walker and Jacob); Sgarrella and Barra, p. 88, pl. 4, fig. 16.

1988 *Nonion depressulum* (Walker and Jacob); Jorissen, p. 23, pl. 2, fig. 7.

1991 *Haynesina depressula* (Walker and Jacob); Cimerman and Langer, p. 81 , pl. 83, figs. 1–4.

1993 *Nonion depressulum* (Walker and Jacob); Sgarrella and Montcharmont-Zei, p. 238, pl. 24, figs. 3–4.

1997 *Haynesina depressula depressula* (Walker and Jacob); Hayward et al., p. 98, pl. 19, figs. 4–7.

2001 *Nonion depressulum* (Walker and Jacob); Fiorini and Vaiani, p. 393, pl. 8, figs. 18–19.

2012 *Haynesina depressula* (Walker and Jacob); Milker and Schmiedl, p. 112, fig. 25, 17–18.

2013 *Haynesina depressula* (Walker and Jacob); Melis and Covelli, p. 449, pl. 1, fig. 25.

2016 *Haynesina depressula* (Walker and Jacob); Darling et al., p. 9, fig. 3, S17.

Description and remarks: Test planispiral, involute, with 8–12 chambers in the last whorl. Rounded to lobate outline, compressed profile, and rounded periphery. Inflated, slightly depressed sutures that gently open near the umbilicus. Relatively wide, star-shaped umbilical area covered by papillae, which are also present in the innermost part of the sutures, along the aperture, and at the base of apertural face. The primary aperture is defined by a row of interiomarginal rounded pores on the last chamber. The test is smooth.

Distribution: It is reported from infralittoral zones of the Mediterranean Sea, in proximity to the river mouths (Sgarrella and Barra, 1984; Jorissen, 1988; Sgarrella and Montcharmont Zei, 1993). This species also occurs in brackish-water environments such as lagoons and coastal lakes (Carboni et al., 2009; Melis and Covelli, 2013).

It is considered not tolerant of heavy metal pollution, preferring clean and sandy substrates (Frontalini and Coccioni, 2008).

Haynesina germanica (Ehrenberg, 1840)

Plate 1, figs. 19–20

1840 *Nonionina germanica* Ehrenberg: p. 23, pl. 2, fig. 1.

1976 *Protoelphidium anglicum* Murray; D'Onofrio et al., p. 273, pl. 19, figs. 1–7.

1976 *Nonion germanicum* (Ehrenberg); Hansen and Lykke-Andersen, p. 21, pl. 19, figs. 7–12.

1978 *Haynesina germanica* (Ehrenberg); Banner and Culver, p. 191, pl. 5, figs. 1–8; pl. 9, figs. 1–11, 15.

2000 *Haynesina germanica* (Ehrenberg); Coccioni, p. 78, fig. 3, 22–23.

2013 *Haynesina germanica* (Ehrenberg); Melis and Covelli, p. 449, pl. 1, fig. 28.

2016 *Haynesina germanica* (Ehrenberg); Darling et al., p. 9, fig. 3, S16.

Description and remarks: Test planispirally enrolled, involute, with 6–12 chambers in the last whorl. The outline is lobulate, profile inflated with parallel sides, periphery broadly rounded. Backward curved, slightly depressed sutures becoming more depressed and wide near the umbilical region. Depressed umbilicus occupied by papillae. Umbilical area, depressed sutures, and base of the apertural face ornamented by papillae. A series of interiomarginal pores at the base of the apertural face forms the aperture. Wall smooth.

Haynesina germanica could seem quite similar to *H. depressula*; however, they differ for some morphological features. In particular, *H. depressula* is laterally more compressed (Plate 1, fig. 18) and has chambers that increase in height more rapidly (Plate 1, fig. 17). Consequently, individuals of *H. depressula* are flatter and more elongated compared to the broader tests of *H. germanica*.

In our samples, *H. germanica* shows some morphological abnormalities, such as abnormal additional chambers, change in coiling or distorted chamber arrangement (Plate 2, fig. 13), and twinned tests (Plate 2, fig. 18).

Distribution: This is one of the dominant species in the inner and central portions of Mediterranean lagoons, usually related to freshwater inputs and high-confinement conditions (Debenay et al., 2000; Carboni et al., 2009). It is very common in a wide range of Italian brackish-water environments, including the Po Delta lagoons (D'Onofrio et al., 1976; Coccioni, 2000). This species usually prefers low-salinity waters, within organic-rich clayey bottoms (Melis and Covelli, 2013).

Haynesina germanica is considered a tolerant species to pollution since high percentages of abnormal individuals are reported from lagoonal areas contaminated by heavy metals or urban wastes (Zampi and D'Onofrio, 1986; Coccioni, 2000).

Family **Trichohyalidae** Saidova, 1981

Genus *Aubignyna* Margerel, 1970

Aubignyna perlucida (Heron-Allen and Earland, 1913)

Plate 1, figs. 15–16

1913 *Rotalia perlucida* Heron-Allen and Earland: p. 139, pl. 13, figs. 7–9.

1988 *Ammonia perlucida* (Heron-Allen and Earland); Jorissen, p. 51, pl. 2, figs. 11–12, pl. 11, figs. 4–5.

1990 *Valvulineria perlucida* (Heron-Allen and Earland); Albani and Serandrei Barbero, p. 312, pl. 4, figs. 11–12.

2000 *Ammonia perlucida* (Heron-Allen and Earland); Coccioni, p. 76, fig. 2, 26–28.

2000 *Aubignyna perlucida* (Heron-Allen and Earland); Murray et al., p. 61, pl. 1, figs. 1–14.

2008 *Aubignyna perlucida* (Heron-Allen and Earland); Frontalini and Coccioni, p. 409, pl. 1, fig. 7.

Description and remarks: Test low trochospiral, spiral side evolute, umbilical side involute with five to six chambers in the final whorl. Lobate to slightly lobate outline, inflated profile with broadly rounded periphery. Backward curved, slightly depressed sutures, more depressed near the umbilical area. Closed, depressed umbilicus. Fine papillae cover the umbilical area and the basal part of the last chambers. The aperture consists of a thin slit in interiomarginal position, often covered by pustules. The test is smooth and finely perforated.

Aberrant tests of *A. perlucida* are not commonly recorded in our samples and include some individuals with distorted coiling or twinned tests (Plate 2, fig. 17).

Distribution: *Aubignyna perlucida* is one of the most common species in the northern Adriatic lagoons, reported from Venice, Goro, Marano, and Grado lagoons (Albani and Serandrei Barbero, 1990; Coccioni, 2000; Melis and Covelli, 2013). It is also recoded south of the Po Delta, where it reaches relatively high concentrations at shallow depths (ca. 15–20 m) (Jorissen, 1988; Donnici and Serandrei Barbero, 2002). This species lives in areas characterized by high organic matter inputs and it shows a limited tolerance for anoxic conditions (Jorissen, 1988).

The common occurrence of deformed specimens of *A. perlucida* within northern Adriatic polluted lagoons suggests that this taxon is quite sensitive to environmental and anthropogenic stress (Coccioni et al., 2009; Melis and Covelli, 2013).

Family **Rotaliidae** Ehrenberg, 1839

Subfamily **Ammoniinae** Saidova, 1981

Genus *Ammonia* Brünnich, 1772

Ammonia parkinsoniana (d'Orbigny, 1839)

Plate 1, figs. 1–4

1839 *Rosalina parkinsoniana* d'Orbigny: p. 99, pl. 4, figs. 25–27.

1988 *Ammonia parkinsoniana* var. *parkinsoniana* (d'Orbigny), morphotype 5; Jorissen, p. 46, pl. 9, figs. 1–2.

1991 *Ammonia parkinsoniana* (d'Orbigny); Cimerman and Langer, p. 76, pl. 87, figs. 7–9.

1993 *Ammonia parkinsoniana* (d'Orbigny); Sgarrella and Montcharmont-Zei, p. 228, pl. 20, figs. 4–5.

2000 *Ammonia* specimen/T9; Holzmann and Pawlowsky, p. 89, pl. 1, fig. 5.

2001 *Ammonia parkinsoniana* (d'Orbigny); Fiorini and Vaiani, p. 384, pl. 6, figs. 14–15.

2008 *Ammonia parkinsoniana* (d'Orbigny); Frontalini and Coccioni, p. 409, pl. 1, fig. 5.

2009 *Ammonia parkinsoniana* (d'Orbigny); Coccioni et al., p. 261, pl. 1, fig. 2.

2012 *Ammonia parkinsoniana* (d'Orbigny); Milker and Schmiedl, p. 119, fig. 27, 3–4.

Description and remarks: Test low trochospiral, spiral side evolute, umbilical side involute with eight to nine chambers in the final whorl. Circular outline, rounded periphery and un-inflated chambers. Backward curved sutures, generally flush with the test but on the last chambers they can be slightly depressed. The umbilicus is relatively closed and provided with a prominent boss. Primary aperture is a thin slit in interiomarginal position, at the base of the last chamber from the umbilicus to the test periphery. Wall smooth.

Individuals with very large umbilical knobs can be linked to the *A. parkinsoniana sobrina* type (*Rotalia beccarii* var. *sobrina* Shupack, 1934) and are considered within the *A. parkinsoniana* species here (e.g. Jorissen, 1988).

Deformed individuals of *A. parkinsoniana* are quite rare in our samples and they mainly show abnormal protruding chambers or non-developed tests (Plate 2, fig. 12).

Distribution: *Ammonia parkinsoniana* is one of the most common species along the Italian coasts, dominating the benthic foraminiferal assemblages from 10 to 20 m water depth in the Adriatic Sea (Jorissen, 1988). It is also common in Mediterranean lagoons and coastal lakes (Carboni et al., 2009; Coccioni et al., 2009).

This species is considered less tolerant to environmental pollution than its counterpart *A. tepida*, preferring clean and less polluted areas (Frontalini and Coccioni, 2008). However, abnormal specimens are still found with relatively low frequencies in polluted brackish-water environments, which indicates a certain tolerance for stressful conditions (Carboni et al., 2009; Melis and Covelli, 2013).

Ammonia tepida (Cushman, 1926)

Plate 1, figs. 11–14

1926 *Rotalia beccarii* (Linné) var. *tepida* Cushman: p. 79, pl. 1.

1987 *Ammonia beccarii tepida* (Cushman); Jorissen, p. 38, pl. 2, fig. 8.

1988 *Ammonia parkinsoniana* (d'Orbigny) var. *tepida* Cushman, morphotypes 1, 2, 3; Jorissen, p. 46, pl. 7, figs. 1–4, pl. 10, fig. 1.

1991 *Ammonia tepida* (Cushman); Cimerman and Langer, p. 76, pl. 87, figs. 10–12.

1993 *Ammonia beccarii* var. *tepida* (Cushman); Sgarrella and Montcharmont-Zei, p. 228, pl. 20, figs. 5–6.

2000 *Ammonia parkinsoniana* (d'Orbigny) forma *tepida* Cushman; Coccioni, p. 76, figs. 2, 1–3, 7–9, 16–18.

2001 *Ammonia tepida* (Cushman); Fiorini and Vaiani, p. 384, pl. 6, figs. 7–8.

2004 *Ammonia tepida* (Cushman); Hayward et al., p. 256, pl. 2, fig. T; pl. 3, fig. T; pl. 4, fig. T.

2008 *Ammonia tepida* (Cushman); Frontalini and Coccioni, p. 409, pl. 1, fig. 6.

2009 *Ammonia tepida* (Cushman); Coccioni et al., p. 261, pl. 1, fig. 1.

Description and remarks: Test low trochospiral, spiral side evolute, six to eight chambers visible in the last whorl of the involute umbilical side. The outline is lobate, with strongly inflated chambers and a broadly rounded periphery. Slightly backward curved sutures, slightly depressed and progressively deeper toward the umbilicus. Open umbilicus without knob. A thin slit in the interiomarginal position defines the primary aperture. The test surface is smooth.

Deformities recorded in *A. tepida* are abnormal protruding chambers, abnormal additional chambers, and twinned tests (Plate 2, figs. 9–10).

Distribution: *Ammonia tepida* is a widespread, euryhaline species that dominates in estuaries, lagoons, and deltaic environments (Debenay et al., 2000; Murray, 2006). In the Mediterranean area, it can be found from the innermost to the outer portion of lagoons and in the vicinity of river mouths (Jorissen, 1988; Debenay et al., 2000). It is recorded in highly fluvially influenced environments, as it dominates in the innermost part of the Venice Lagoon (Albani and Serandrei Barbero, 1990) and in the river channels that flow into the Marano and Grado lagoons (Melis and Covelli, 2013). *Ammonia tepida* is also common in the Po Delta lagoons (D'Onofrio et al., 1976; Coccioni, 2000).

This species is known for its great tolerance of high levels of organic matter, reduced or overwhelming salinity, and environmental pollution; therefore, it is considered the most tolerant species of a variety of environmental and anthropogenic stresses (Yanko et al., 1994; Geslin et al., 1998; Almogi-Labin et al., 1992; Frontalini and Coccioni, 2008).

Ammonia tepida–*Ammonia parkinsoniana* transitional morphotypes

Plate 1, figs. 5–10

Description and remarks: Intermediate morphotypes between *A. tepida* and *A. parkinsoniana* always occur in our samples and they were classified within the "*A. tepida*–*A. parkinsoniana* intermediate morphotypes" group. All of them present a low trochospiral test, evolute on the spiral side, involute on the umbilical side, and backward curved sutures. The aperture consists of a slit in interiomarginal position and the wall is smooth. The discriminant characters of transitional morphologies are provided here.

Morphotype A (Plate 1, figs. 9–10): six to eight chambers in the final whorl, lobate outline, inflated chambers with a boss in the umbilicus.

Morphotype B (Plate 1, figs. 7–8): 7–10 chambers visible in the umbilical side, slightly lobate outline that progressively become lobate at the end of the last whorl; a small knob is often present in the umbilicus.

Morphotype C (Plate 1, figs. 5–6): 7–11 chambers in the last whorl, rounded or very slightly lobate outline, umbilicus without central knob.

Transitional individuals between *A. tepida* and *A. parkinsoniana* are the most commonly deformed taxa in the analysed samples. They show several types of morphological abnormalities of the tests, mainly abnormal protuberances (Plate 2, fig. 11), abnormal additional chambers, distorted chamber arrangement or change in coiling direction (Plate 2, figs. 8, 11), twinned tests, and non-developed tests.

Family **Elphidiidae** Galloway, 1933

Subfamily **Elphidiinae** Galloway, 1933

Genus *Cribroelphidium* Cushman and Brönniman, 1948

Cribroelphidium granosum (d'Orbigny, 1846)

Plate 2, figs. 1–2

1826 *Nonionina granosa* d'Orbigny: p. 128 (*nomen nudum*).

1846 *Nonionina granosa* d'Orbigny: p. 110, pl. 5, figs. 19–20.

1987 *Elphidium granosum* forma *granosum* (d'Orbigny, 1846); Jorissen, p. 47, pl. 2, fig. 1.

1988 *Elphidium granosum* forma *granosum* (d'Orbigny, 1846); Jorissen, p. 104, pl. 2, figs. 1–2, pl. 16, figs. 1–5.

1993 *Elphidium granosum* (d'Orbigny, 1846); Sgarrella and Montcharmont-Zei, p. 229, pl. 21, figs. 1–2

2005 *Elphidium granosum* (d'Orbigny, 1846); Rasmussen, p. 110, pl. 19, fig. 8.

2012 *Elphidium granosum* (d'Orbigny, 1846); Milker and Schmiedl, p. 121, fig. 27, 17–18.

Description and remarks: Test planispiral, involute, with six to eight chambers in the last whorl. Lobate or slightly lobate outline, convex profile with flattened sides, broadly rounded periphery. The sutures are backward curved, slightly depressed, and open towards the umbilical area. Umbilicus slightly depressed covered by papillae. Primary aperture at the base of the last chamber, formed by a row of small openings. Test coarsely perforated, apertural face imperforate. Pustules are present at the base of the last chamber, near the aperture and in the whole umbilical area, including the inner portion of the sutures.

Distribution: In the Mediterranean, this species is reported from lagoonal to infralittoral environments and it is abundant near the river mouths (Sgarrella and Barra, 1984; Zampi and D'Onofrio, 1986; Sgarrella and Montcharmont Zei, 1993). In the Adriatic Sea, it is common in a narrow belt between 17.5 and 30 m water depth, on clayey bottoms enriched in organic matter (Jorissen, 1988). It is one of the most common species in the northern Adriatic and in the adjacent Venice Lagoon, from the innermost to the outer lagoonal areas (Albani and Serandrei Barbero, 1990).

Cribroelphidium lidoense (Cushman, 1936)

Plate 2, fig. 3

1936 *Elphidium lidoense* Cushman: p. 86, pl. 15, fig. 6.

1976 *Elphidium tuberculatum* (d'Orbigny); Hansen and Lykke-Andersen, p. 14, pl. 12, figs. 1–4.

1987 *Elphidium granosum* forma *lidoense* Cushman; Jorissen, p. 38, pl. 2, fig. 3.

1988 *Elphidium granosum* forma *lidoense* Cushman; Jorissen, p. 105, pl. 17, figs. 1–5.

2013 *Elphidium granosum* forma *lidoense* Cushman; Melis and Covelli, p. 449, pl. 1, fig. 21.

2016 *Elphidium lidoense* Cushman; Darling et al., p. 10 , fig. 3, S13.

Description and remarks: Test planispirally enrolled, involute, with 8–12 chambers in the last whorl. Rounded to moderately lobate outline, convex profile with flattened sides, periphery broadly rounded. Backward curved, slightly depressed sutures. Slightly depressed umbilicus occupied by distinct flat-topped knobs, surrounded by pustules. The primary aperture is formed by a series of rounded openings in the interiomarginal position. The test is coarsely perforated, except to the apertural face, which is imperforate. Papillae are present in the umbilical region and at the base of the last chamber.

Cribroelphidium granosum has often been confused with *C. lidoense*, but they can be distinguished by a series of features (Jorissen, 1988): (i) *C. granosum* has a lower number of chambers (6–8) than *C. lidoense* (8–12); (ii) the umbilicus of *C. granosum* is occupied only by pustules or, if any, very small knobs, whereas several prominent bosses are present in *C. lidoense*; (iii) sutures that open towards the centre of the test are typical of *C. granosum*, in contrast to thin sutures of *C. lidoense*; and (iv) the test outline of *C. granosum* is usually more lobate than the rounded one of *C. lidoense*. Intermediate morphotypes of these end-members are commonly recorded in the Adriatic Sea (Jorissen, 1988).

Results of recent genetic studies (Darling et al., 2016) performed on benthic foraminifera with a morphology comparable to *C. lidoense* reveal that this is a distinct species and it was classified as *Elphidium lidoense*. However, genetic sequencing of *C. granosum* was not performed; therefore, a study on this species is needed to understand if it can be regarded as a form or a separated species.

Distribution: This species is reported from infralittoral and circalittoral zones of the Mediterranean (Blanc-Vernet, 1969) and it reaches high concentrations in the shallowest part of the Adriatic Sea (Jorissen, 1988). It also occurs in the outer lagoons, with low frequencies (Melis and Covelli, 2013).

Cribroelphidium oceanense (d'Orbigny in Fornasini, 1904)

Plate 2, fig. 4

1826 *Polystomella oceanensis* d'Orbigny: p. 285 (*nomen nudum*).

1904 *Polystomella oceanensis* d'Orbigny; Fornasini, p. 13, pl. 3, fig. 10.

1976 *Elphidium gunteri* Cole; Hansen and Lykke-Andersen, p. 12, pl. 8, figs. 10–12, pl. 9, figs. 1–3.

1997 *Elphidium gunteri* Cole; Hayward et al., p. 80, pl. 11, figs. 13–15.

2000 *Cribroelphidium gunteri* (Cole); Coccioni, p.78, fig. 3, 5–6.

2009 *Cribroelphidium oceanensis* (d'Orbigny); Coccioni et al., p. 261, pl. 1, fig. 8.

2013 *Elphidium gunteri* (Cole); Melis and Covelli, p. 449, pl. 1, fig. 24.

2016 *Elphidium oceanense* (d'Orbigny) Darling et al., p. 8, fig. 3, S3.

Description and remarks: Test planispiral, involute, with 8–11 chambers in the final whorl. Outline slightly lobulate to clearly lobulate, profile inflated, periphery broadly rounded. The sutures are depressed, straight to backward curved. The ponticuli are present, irregular in number, generally broad and slightly raised from the sutures. The umbilicus is depressed and provided by irregular flat-topped knobs. Sutures, umbilical region, and the base of the apertural face are occupied by papillae. The aperture consists of a series of rounded openings arranged in a single row at the base of the apertural face. The wall is densely and coarsely perforated.

Cribroelphidium oceanense and *Cribroelphidium gunteri* show similar morphological features, but the latter species presents more chambers (about 14) in the last whorl. Specimens recorded in the studied succession always show a low number of chambers in the final whorl, consistent with the attribution to *C. oceanense*.

Our individuals often have a low number of sutural bridges, especially in the first chambers, where they may be only partially developed. This species commonly presents individuals affected by various types of deformation of the test: abnormal protruding chambers (Plate 2, fig. 15), distorted chambers, change in coiling direction, and also complex forms (Plate 2, fig. 14).

Distribution: This species is very common in the Mediterranean lagoons (Debenay et al., 2000). It occurs in the Venice (Coccioni et al., 2009) and Santa Gilla lagoons (Frontalini et al., 2009). It is recorded with relatively high abundances from the Marano and Grado (Melis and Covelli, 2013), Goro (Coccioni, 2000), and Orbetello lagoons (Zampi and D'Onofrio, 1986), reported as *Elphidium* or *Cribroelphidium gunteri*. It typically lives at shallow depths, thriving in the organic-rich innermost and intertidal parts of the lagoons and it is also present, with lower concentrations, in the outer lagoons.

It characterizes oligotypic benthic foraminiferal assemblages in areas subject to high freshwater inputs and industrial discharges (Frontalini et al., 2009). It also shows a great tolerance for high concentrations of nutrients and heavy metals (Coccioni, 2000; Melis and Covelli, 2013).

Cribroelphidium poeyanum (d'Orbigny, 1839)

Plate 2, figs. 6–7

1839 *Polystomella poeyana* d'Orbigny: p. 55, pl. 8, figs. 25–26.

1930 *Elphidium poeyanum* (d'Orbigny); Cushman, p. 25, pl. 10, figs. 4–5.

1976 *Elphidium kugleri* (Cushmand and Brönnimann); Hansen and Lykke-Andersen, p. 12, pl. 9, figs. 4–8.

1976 *Elphidium poeyanum* (d'Orbigny); Hansen and Lykke-Andersen, p. 13, pl. 9, figs. 9–12, pl. 10, figs. 1–5.

1983 *Cribrononion sp.*; Sgarrella et al., p. 92, pl. 3, fig. 7.

1987 *Elphidium poeyanum* forma *poeyanum* (d'Orbigny); Jorissen, p. 38, pl. 2, fig. 4.

1988 *Elphidium poeyanum* (d'Orbigny); Jorissen, p. 116, pl. 2, fig. 4a–b, pl. 22, fig. 3a–b, pl. 23, fig. 3.

2001 *Elphidium poeyanum* (d'Orbigny); Fiorini and Vaiani, p. 392, pl. 8, figs. 8–9.

Description and remarks: Test planispiral, involute, with six to eight chambers in the last whorl. Outline slightly lobulate to lobulate, profile slightly inflated, periphery broadly rounded. Sutures slightly depressed, increasingly backward curved in the last whorl. The ponticuli are short. The umbilical region can be depressed and it is covered by a flap-like projection of the last chamber. A row of interiomarginal openings at the base of the apertural face forms the primary aperture. The test is smooth, finely perforated by small pores. Ponticuli, flap projections on the umbilicus and apertural face, are imperforate.

Cribroelphidium poeyanum differs from *Cribroelphidium decipiens* (Costa, 1856) by the lower number of chambers and the more lobate test, but the latter species is not present in our samples.

Distribution: In the Adriatic Sea, *C. poeyanum* lives in shallow areas influenced by the fluvial run-off, with relatively high concentrations of organic matter, but it shows only a little tolerance for oxygen deficiency (Jorissen, 1988). This species is also recorded north of the Po Delta and in the Venice Lagoon (Albani and Serandrei Barbero, 1990).

Genus *Elphidium* de Montfort, 1808

Elphidium advenum (Cushman, 1922)

Plate 1, fig. 21

1922 *Polystomella advena* Cushman: p. 56, pl. 9, figs. 11, 12.

1930 *Elphidium advenum* (Cushman); Cushman, p. 25, pl. 10, figs. 1–2.

1976 *Elphidium advenum* (Cushman); Hansen and Lykke-Andersen, p. 7, pl. 2, figs. 10–11.

1988 *Elphidium advenum* (Cushman); Jorissen, p. 22, pl. 2, figs. 9–10.

1990 *Cribrononion advenum* (Cushman); Albani and Serandrei Barbero, p. 316, pl. 4, fig. 16.

1993 *Elphidium advenum* (Cushman); Hohenegger et al., p. 81, pl. 1, fig. 9.

1993 *Elphidium punctatum* (Terquem); Sgarrella and Montcharmont-Zei, p. 230, pl. 21, figs. 3–4.

2001 *Elphidium advenum* (Cushman); Fiorini and Vaiani, p. 388, pl. 7, figs. 10, 12–13.

2005 *Elphidium advenum* (Cushman); Rasmussen, p. 108, pl. 18, figs. 13–15.

2012 *Elphidium advenum* (Cushman); Milker and Schmiedl, p. 119, fig. 27, 7–8.

2013 *Elphidium gerthi* van Voorthuysen; Melis and Covelli, p. 449, pl. 1, fig. 22.

Description and remarks: Planispiral, involute test with 10–14 chambers in the final whorl. Circular to very slightly lobulate outline, slightly biconvex profile and acute, keeled periphery. The sutures are slightly depressed and backward curved. Sutural bridges are relatively numerous, raised from the sutures, and flush with the chamber wall. The umbilicus is occupied by a flat, circular boss. Chambers overlap near the umbilical area. Small papillae are present along the sutures, at the base of the apertural face, and within a small collar rim near the last chambers. A series of rounded openings in the apertural face defines the aperture. The wall is smooth.

Distribution: This species is widespread in the Mediterranean, reported especially from the infralittoral and circalittoral zones (Blanc-Vernet, 1969; Milker and Schmiedl, 2012). *Elphidium advenum* is commonly recorded in the Adriatic Sea and it is considered tolerant to low salinity and pollution (Jorissen, 1988). It is also reported from the Venice, Marano, and Grado lagoons and from the Gulf of Trieste (Albani and Serandrei Barbero, 1990; Hohenegger et al., 1993; Melis and Covelli, 2013). This species has also been found near the inlets of the Fogliano and Lungo coastal lakes, strongly related to sandy bottoms (Carboni et al., 2009).

Elphidium clavatum (Cushman, 1930)

Plate 1, fig. 22

1930 *Elphidium incertum* var. *clavatum* Cushman: p. 20, pl. 7, fig. 10.

1953 *Elphidium clavatum* Cushman; Loeblich and Tappan, p. 98, pl. 19, figs. 8–10.

1982 *Elphidium excavatum* (Terquem) forma *clavata* Cushman; Miller et al., p. 124, pl. 1, figs. 5–6, pl. 3, figs. 3–8, pl. 4, figs. 2–6, pl. 4, figs. 4–8.

1997 *Elphidium excavatum clavatum* Cushman; Hayward et al., p. 76, pl. 8, figs. 14–17, pl. 9, figs. 1–5.

2016 *Elphidium clavatum* Cushman; Darling et al., p. 9, fig. 3, S2.

Description and remarks: Test planispiral, involute, with 9 to 13 slightly inflated chambers in the last whorl. Rounded to slightly lobulate outline, subacute profile. Slightly depressed, moderately arched sutures that close before reaching the umbilicus, forming a ring-shaped area. The ponticuli are moderately short. The umbilicus presents an elevated knob, surrounded by an umbilical collar. Sutures and umbilical collar can be ornamented by papillae. The aperture is formed by a row of small circular openings at the base of the last chamber. Wall thin and translucent.

This species was originally considered by Cushman (1930) as a variety of *E. incertum,* then it was elevated to species rank by Loeblich and Tappan (1953), but some authors continued to consider it as a variety or a subspecies. Recent genetic studies (Pillet et al., 2013; Darling et al., 2016) revealed that the morphotype traditionally assigned to *E. excavatum clavatum* is a distinct species and therefore the taxonomic name *Elphidium clavatum* should be applied.

Only rare deformed specimens of this taxon have been found in our samples, with distorted chambers (Plate 2, fig. 16).

Distribution: This species is found from Arctic to temperate shallow water environments, from normal to reduced salinity waters (Miller and Lohmann, 1982; Darling et al., 2016). It is also reported from brackish to marginal marine environments of New Zealand, where it dominates benthic foraminiferal assemblages of middle estuaries (Hayward et al., 1997). Direct observations revealed that *E. excavatum* is a motile species able to shift from infaunal to elevated epifaunal in response to oxygen and nutrient concentrations; therefore, it is considered highly adaptable to changing environmental conditions (Linke and Lutze, 1993).

Elphidium gerthi van Voorthuysen, 1957

Plate 1, fig. 23

1957 *Elphidium gerthi* van Voorthuysen: p. 32, pl. 23, fig. 12.

1976 *Elphidium gerthi* van Voorthuysen; Hansen and Lykke-Andersen, p. 10, pl. 5, figs. 7–12.

1991 *Elphidium gerthi* van Voorthuysen; Cimerman and Langer, p. 78, pl. 91, figs. 1–2.

Description and remarks: Test planispiral, involute, with 10–12 chambers in the final whorl. Outline from moderately rounded to slightly lobulate, test profile compressed and acutely rounded periphery. Depressed, backward curved sutures. Sutural bridges are variable in number, slightly raised from the sutures. The umbilicus is depressed and provided with a prominent knob. Chambers are fused near the umbilical area, forming an almost complete ring-shaped area around the umbilicus, which is interrupted by longer, distinct sutures of the last chambers. Pustules cover the sutures and the depressed umbilical area around the knob. A row of openings at the base of the last chamber form the aperture. The wall has a smooth surface.

In our individuals, ponticuli are less evident in the last chambers, where they are often covered by pustules.

Only one specimen with an aberrant chamber shape has been found in our samples.

Distribution: *Elphidium gerthi* is reported from shallow, strong fluvially influenced waters of the Baltic Sea, the British Channel, and the Gulf of Cádiz, usually related to sandy or vegetated bottoms (Murray, 2006; Mendes et al., 2012). Hansen and Lykke-Andersen (1976) report the presence of this species from the shallow Kattegat Sea.

Elphidium sp. 1

Plate 1, figs. 24–25

Test planispirally enrolled, involute, with 7–10 chambers in the last whorl. Outline perfectly rounded to slightly lobulate, profile compressed with acutely rounded and carinate periphery. Backward curved and depressed sutures, usually quite deep especially among the last chambers. Sutural bridges are evident, thick, and broad. Umbilicus slightly depressed or flush with the chambers, without knobs. The primary aperture is formed by a series of openings at the base of the apertural face. Abundant, evident pustules and pseudospines cover sutures, ponticuli, border of chambers, umbilical area, and the base of the apertural face. The central part of the chambers is ornamented with slightly or well-developed pustules, but it can be also smooth, especially in the last chambers.

This species differs from *Elphidium margaritaceum* (Cushman, 1930) by the more compressed profile, the lower number of ponticuli and the coverage of pustules, which is not complete in our individuals.

Only rare aberrant individuals attributed to this taxon, mainly with a distorted chamber arrangement, are present in our assemblages.

Elphidium sp. 2

Plate 1, figs. 26–27

Test planispiral, involute, with approximately 9–10 chambers in the last whorl. Rounded outline, profile biconvex with flat sides, slightly rounded to acutely rounded periphery. Sutures backward curved, slightly or almost not depressed. A few, short ponticuli that tend to disappear in the last chambers. The umbilicus is slightly depressed. Small openings in the interiomarginal position at the base of the apertural face form the primary aperture, which is partially covered by pustules or pseudo-spines. Papillae are also present on the sutures and on the umbilical area. The wall is generally smooth, except for the area covered by pustules.

Subfamily **Notorotaliinae** Hornibrook, 1961

Genus *Parrellina* Thalmann, 1951

Parrellina verriculata (Brady, 1881)

Plate 2, fig. 5

1881 *Polystomella verriculata* Brady: p. 66.

1991 *Elphidium* sp. 5; Cimerman and Langer, p. 80, pl. 91, figs. 8–10.

1993 *Parrellina verriculata* (Brady); Sgarrella and Montcharmont Zei, p. 232, pl. 21, fig. 7.

2012 *Parrellina verriculata* (Brady); Milker and Schmiedl, p. 122, fig. 27, 27–28.

Description and remarks: Test planispiral, involute, with eight to nine chambers in the final whorl. Rounded to slightly lobulated outline, acute and carinate periphery. Sutures backward curved, occupied by large ponticuli that form subrectangular fossettes. Septal ridges and ponticuli are raised, thick, and form a network on the test. The apertural face is occupied by pustules. The aperture consists of a row of interiomarginal rounded openings. Sutures and umbilicus are ornamented with pustules.

Distribution: This species is recorded in the Mediterranean Sea and reported from *Posidonia* prairies and the upper circalittoral zone (Blanc-Vernet, 1969; Sgarrella and Montcharmont Zei, 1993).

The Supplement related to this article is available online at https://doi.org/10.5194/jm-37-203-2018-supplement.

Author contributions. Both authors defined the design of the work and carried out benthic foraminiferal analyses, whereas the ostracod analyses and statistical elaborations were performed by GB. Interpretation of fossil data and preparation of the paper was contributed to by both authors.

Competing interests. The authors declare that they have no conflict of interest.

Acknowledgements. We are grateful to Regione Emilia-Romagna – RER – Geological, Seismic and Soil Survey for providing core material. Thanks are due to Maria Roberta Randi for the SEM assistance. We warmly thank the editor Thomas M. Cronin, Virgilio Frezza, and the anonymous reviewer for their constructive comments that greatly improved the quality of the work.

Edited by: Thomas M. Cronin
Reviewed by: Virgilio Frezza and one anonymous referee

References

Aiello, G., Barra, D., Coppa, M. G., Valente, A., and Zeni, F: Recent infralittoral Foraminiferida and Ostracoda from the Porto Cesareo Lagoon (Ionian Sea, Mediterranean), B. Soc. Paleontol. Ital., 45, 1–14, 2006.

Aladin, N. V.: Salinity tolerance, morphology and physiology of the osmoregulation organs in Ostracoda with special reference to Ostracoda from the Aral Sea, in: Ostracoda in the Earth and Life Sciences, edited by: Jones, P. and McKenzie, K., A. A. Balkema, Rotterdam, 387–403, 1993.

Albani, A. and Serandrei Barbero, R.: I Foraminiferi della Laguna e del Golfo di Venezia, Memorie di Scienze Geologiche, 42, 271–341, 1990.

Almogi-Labin, A., Perelis-Grossovicz, L., and Raab, M.: Living *Ammonia* from a hypersaline inland pool, Dead Sea area, Israel, J. Foramin. Res., 22, 257–266, 1992.

Alve, E.: Benthic foraminifera in sediment cores reflecting heavy metal pollution in Sørfjord, Western Norway, J. Foramin. Res., 21, 1–19, 1991.

Alve, E.: Benthic foraminiferal responses to estuarine pollution: a review, J. Foramin. Res., 25, 190–203, 1995.

Alve, E. and Murray, J. W.: Ecology and taphonomy of benthic foraminifera in a temperate mesotidal inlet, J. Foramin. Res., 24, 18–27, 1994.

Alve, E. and Murray, J. W.: Marginal marine environments of the Skagerrak and Kattegat: a baseline study of living (stained) benthic foraminiferal ecology, Palaeogeogr. Palaeocl., 146, 171–193, 1999.

Alves Martins, M. V., Helali, M. A., Zaaboub, N., Boukef-BenOmrane, I., Frontalini, F., Reis, D., Portela, H., Martins Matos Moreira Clemente, I., Nogueira, L., Pereira, E., Miranda, P., El Bour, M., and Aleya, L.: Organic matter quantity and quality, metals availability and foraminiferal assemblages as environmental proxy applied to the Bizerte Lagoon (Tunisia), Mar. Pollut. Bull., 105, 161–179, 2016.

Amorosi, A. and Colalongo, M. L.: The linkage between alluvial and coeval nearshore marine successions: evidence from the Late Quaternary record of the Po River Plain, Italy, in: Fluvial Sedimentology VII, edited by: Blum, M. D., Marriott, S. B., and Leclair, S. F., Blackwell Publishing Ltd., Oxford, 257–275, 2005.

Amorosi, A., Colalongo, M. L., Fusco, F., Pasini, G., and Fiorini, F.: Glacio-eustatic control of continental-shallow marine cyclicity from Late Quaternary deposits of the southeastern Po Plain (Northern Italy), Quaternary Res., 52, 1–13, 1999a.

Amorosi, A., Colalongo, M. L., Pasini, G., and Preti, D.: Sedimentary response to Late Quaternary sea-level changes in the Romagna coastal plain (northern Italy), Sedimentology, 46, 99–121, 1999b.

Amorosi, A., Colalongo, M. L., Fiorini, F., Fusco, F., Pasini, G., Vaiani, S. C., and Sarti, G.: Palaeogeographic and palaeoclimatic evolution of the Po Plain from 150-ky core records, Global Planet. Change, 40, 55–78, 2004.

Amorosi, A., Rossi, V., Scarponi, D., Vaiani, S. C., and Ghosh, A.: Biosedimentary record of postglacial coastal dynamics: high-resolution sequence stratigraphy from the northern Tuscan coast (Italy), Boreas, 43, 939–954, 2014.

Arbulla, D., Pugliese, N., and Russo, A.: Ostracods from the National Park of La Maddalena Archipelago (Sardinia, Italy), B. Soc. Paleontol. Ital., 43, 91–99, 2004.

Armynot du Châtelet, E. and Debenay, J. P.: Anthropogenic impact on the western French coast as revealed by foraminifera: a review, Revue de Micropaléontologie, 53, 129–137, 2010.

Athersuch, J., Horne, D. J., and Whittaker, J. E.: Marine and brackish water ostracods, in: Synopses of the British Fauna (New Series), 43, edited by: Kermack, D. M. and Barnes, R. S. K., Brill E.J., Leiden, 345 pp., 1989.

Banner, F. T. and Culver, S. J.: Quaternary *Haynesina* n. gen. and Paleogene *Protelphidium* Haynes; their morphology, affinities and distribution, J. Foramin. Res., 8, 177–207, 1978.

Bik, A.: An aberrant Nonionid from the Miocene of the Mayence basin, Notizblatt des Hessischen Landesamtes für Bodenforschung zu Wiesbaden, 92, 68–74, 1964.

Blanc-Vernet, L.: Contribution à l'étude des foraminifères de Méditerranée, Travaux de la Station Marine d'Endoume, Marseille, France, 1969.

Boltovskoy, E., Scott, D. B., and Medioli, F. S.: Morphological variations of benthic foraminiferal tests in response to changes in ecological parameters: a review, J. Paleontol., 65, 175–185, 1991.

Bonaduce, G., Ciampo, G., and Masoli, M.: Distribution of Ostracoda in the Adriatic Sea, Pubblicazioni della Stazione Zoologica di Napoli, 40, 304 pp., 1975.

Bondesan, M., Cibin, U., Colalongo, M. L., Pugliese, N., Stefani, M., Tsakiridis, E., Vaiani, S. C., and Vincenzi, S.: Benthic communities and sedimentary facies recording late Quaternary environmental fluctuations in a Po Delta subsurface succession (Northern Italy), in: Proceedings of the Second and Third Italian Meeting of Environmental Micropaleontology, edited by: Coccioni, R., Lirer, F., and Marsili, A., The Grzybowski Foundation Special Publication, 11, 21–31, 2006.

Boomer, I., Horne, D. J., and Slipper, J.: The use of ostracods in palaeoenvironmental studies, or what can you do with an ostracod shell?, in: Bridging the gap: Trends in the Ostracode Biological and Geological Sciences, edited by: Park, L. E. and Smith, A. J., The Paleontological Society Papers, 9, 153–179, 2003.

Brady, H. B.: Notes on some reticularian Rhizopoda of the “Challenger” expedition, Part 3, Q. J. Microsc. Sci., 21 , 31–71, 1881.

Breman, E.: The distribution of Ostracodes in the bottom sediments of the Adriatic Sea, PhD thesis, Free University of Amsterdam, the Netherlands, 1975.

Brünnich, M. T.: Zoologiæ fundamenta Prælectionibus Academicis Accommodata – Grunde i dyrlæren, Hafniæ et Lipsiæ, 253 pp., 1772.

Bugrova, E. M.: Morfologicheskij oblik rakovin foraminifer kak pokasatel’ uslovij ihk obitanij (The morphology of foraminiferal tests as indicator of their environment), in: Obraz zhisni i zakonomernosti rasselenija sovremennoj i iskopaemoj mikrofauny (Mode of Life and Mechanisms of Settling of Recent and Fossil Microfauna), edited by: Furssenko, A. V., Trudy Instituta Geologii i Geofiziki, Akademija Nauk SSSR, Sibirskoe otdelenie, 333, 439 pp., 1975.

Campo, B., Amorosi, A., and Vaiani, S. C.: Sequence stratigraphy and late Quaternary paleoenvironmental evolution of the Northern Adriatic coastal plain (Italy), Palaeogeogr. Palaeocl., 466, 265–278, 2017.

Carboni, M. G., Succi, M. C., Bergamin, L., Di Bella, L., Frezza, V., and Landini, B.: Benthic foraminifera from two coastal lakes of southern Latium (Italy). Preliminary evaluation of environmental quality, Mar. Pollut. Bull., 59, 268–280, 2009.

Castellarin, A. and Vai, G. B.: South alpine versus Po Plain apenninic arcs, in: The Origin of Arcs, Development in Geotectonics, 20, edited by: Wezel, F. C., Elsevier, Amsterdam, 253–280, 1986.

Cearreta, A., Cachão, M., Cabral, M. C., Bao, R., and Ramalho, M. J.: Lateglacial and Holocene environmental changes in Portuguese coastal lagoons: 2. Reconstruction of the Santo André coastal area (SW Portugal) during the last 14,000 years based on microfossil multiproxy evidence, Holocene, 13, 449–460, 2003.

Cimerman, F. and Langer, M. R.: Mediterranean Foraminifera, Academia Scientiarum et Artium Slovenica, Classis IV, 30, Ljubljana, 118 pp., 1991.

Clarke, K. R.: Non-parametric multivariate analyses of changes in community structure, Aust. J. Ecol., 18, 117–143, 1993.

Coccioni, R.: Benthic foraminifera as bioindicators of heavy metal pollution – a case study from the Goro Lagoon (Italy), in: Environmental micropaleontology: the application of microfossils to environmental geology, edited by: Martin, R. E., Kluwer Academic/Plenum Publishers, New York, 71–103, 2000.

Coccioni, R., Frontalini, F., Marsili, A., and Mana, D.: Benthic foraminifera and trace element distribution: A case-study from the heavily polluted lagoon of Venice (Italy), Mar. Pollut. Bull., 59, 257–267, 2009.

Colalongo, M. L.: Ricerche sugli Ostracodi nei fondali antistanti il delta del Po, Giornale di Geologia, 36, 335–362, 1969.

Costa, O. G.: Paleontologia del regno di Napoli contenente la descrizione e figura di tutti gli avanzi organici fossili racchuisi nel suolo di questo regno, Napoli, 512 pp., 1856.

Cushman, J. A.: Results of the Hudson Bay Expedition, 1920 – 1, The foraminifera, Contributions to Canadian Biology, for 1921, 135–147, 1922.

Cushman, J. A.: Recent Foraminifera from Porto Rico, Publications of the Carnegie Institution of Washington, 344 pp., 1926.

Cushman, J. A.: The foraminifera of the Atlantic Ocean, Part 7: Nonionidae, Camerinidae, Peneroplidae and Alveolinellidae, Bulletin of the United States National Museum, 104, 1–79, 1930.

Cushman, J. A.: Some new species of *Elphidium* and related genera, Contributions from the Cushman Laboratory for Foraminiferal Research, 12, 78–91, 1936.

Cushman, J. A. and Brönnimann, P.: Some new genera and species of foraminifera from brackish water of Trinidad, Contributions from the Cushman Laboratory for Foraminiferal Research, 24, 15–21, 1948.

Darling, K. F., Schweizer, M., Knudsen, K. L., Evans, K. M., Bird, C., Roberts, A., Filipsson, H. L., Kim, J. H., Gudmundsson, G., Wade, C. M., Sayer, M. D. J., and Austin, W. E. N.: The genetic diversity, phylogeography and morphology of Elphidiidae (Foraminifera) in the Northeast Atlantic, Mar. Micropaleontol., 129, 1–23, 2016.

Debenay, J. P., Guillou, J. J., Redois, F., and Geslin, E.: Distribution trends of foraminiferal assemblages in paralic environments: a base for using foraminifera as bioindicators, in: Environmental micropaleontology: the application of microfossils to environmental geology, edited by: Martin, R. E., Kluwer Academic/Plenum Publishers, New York, 39–67, 2000.

de Montfort, D.: Conchyliologie Systematique et Classification Methodique des Coquilles, F. Schoell, Paris, 1808.

de Nooijer, L. J., Duijnstee, I. A. P., and van der Zwaan, G. J.: Spatial distribution of intertidal benthic foraminifera in the Dutch Wadden Sea, Geologica Ultraiectina, 272, 21–32, 2007.

Dinelli, E., Ghosh, A., Rossi, V., and Vaiani, S. C.: Multiproxy reconstruction of Late Pleistocene-Holocene environmental changes in coastal successions: microfossil and geochemical evidences from the Po Plain (Northern Italy), Stratigraphy, 9, 153–167, 2013.

Donnici, S. and Serandrei Barbero, R.: The benthic foraminiferal communities of the northern Adriatic continental shelf, Mar. Micropaleontol., 44, 93–123, 2002.

D’Onofrio, S., Marabini, F., and Vivalda, P.: Foraminiferi di alcune lagune del delta del Po, Giornale di Geologia, 40, 267–276, 1976.

d’Orbigny, A.: Tableau Methodique de la Classe des Cephalopodes, Ann. Sci. Nat. Zool., 7, 96–314, 1826.

d’Orbigny, A.: Foraminiféres, in: Histoire physique, politique et naturelle de L’ile de Cuba, edited by: De la Sagra, R. M., Bertrand A., Paris, 1839.

d’Orbigny, A.: Foraminiféres fossils du bassin tertiarie de Vienne (Autriche) (Die fossilen Foraminiferen des tertiaeren Beckens von Wien), Gide et Comp., Paris, 110 pp., 1846.

Dutton, A., Bard, E., Antonioli, F., Esat, T. M., Lambeck, K., and McCulloch, M. T.: Phasing and amplitude of sea-level and climate change during the penultimate interglacial, Nat. Geosci., 2, 355–359, 2009.

Ehrenberg, C. G.: Über die Bildung der Kreidefelsen und des Kreidemergels durch unsichtbare Organismen, Abhandlungen der Königlichen Akademie der Wissenschaften in Berlin 1838, 60–148, 1839.

Ehrenberg, C. G.: Eine weitere Erläuterung des Organismus mehrerer in Berlin lebend beobachteter Polythalamien der Nordsee, K. Preuss. Akad. Wiss., Berlin, 18–23, 1840.

Ellis, B. F. and Messina, A. R.: Catalogue of Foraminifera, Micropaleontology Press, New York, 1940.

Engel, M., Brückner, H., Pint, A., Wellbrock, K., Ginau, A., Voss, P., Grottker, M., Klasen, N., and Frenzel, P.: The early Holocene humid period in NW Saudi Arabia – evidence from sediments, microfossils and palaeo-hydrological modelling, Quaternary Int., 266, 131–141, 2012.

Field, J. G., Clarke, K. R., and Warwick, R. M.: A practical strategy for analyzing multispecies distribution patterns, Mar. Ecol.-Prog. Ser., 8, 37–52, 1982.

Fiorini, F.: Benthic foraminiferal associations from Upper Quaternary deposits of southeastern Po Plain, Italy, Micropaleontology, 50, 45–58, 2004.

Fiorini, F. and Vaiani, S. C.: Benthic foraminifers and transgressive–regressive cycles in the Late Quaternary subsurface sediments of the Po Plain near Ravenna (Northern Italy), B. Soc. Paleontol. Ital., 40, 357–403, 2001.

Fornasini, C.: Illustrazione di specie orbignyane di foraminiferi istituite nel 1826, Memorie della Reale Accademia delle Scienze dell'Istituto di Bologna, series 6(I), 1904.

Frenzel, P., Keyser, D., and Viehberg, F. A.: An illustrated key and (palaeo)ecological primer for recent to postglacial Ostracoda (Crustacea) of the Baltic Sea, Boreas, 39, 567–575, 2010.

Frenzel, P., Schulze, I., and Pint, A.: Noding of *Cyprideis torosa* valves (Ostracoda) – a proxy for salinity? New data from field observations and a long-term microcosm experiment, Int. Rev. Hydrobiol., 97, 314–329, 2012.

Frontalini, F. and Coccioni, R.: Benthic foraminifera for heavy metal pollution monitoring: a case study from the central Adriatic Sea coast of Italy, Estuar. Coast. Shelf S., 76, 404–417, 2008.

Frontalini, F. and Coccioni, R.: Benthic foraminifera as bioindicators of pollution: a review of Italian research over the last three decades, Revue de Micropaléontologie, 54, 115–127, 2011.

Frontalini, F., Buosi C., Da Pelo, S., Coccioni, R., Cherchi, A., and Bucci C.: Benthic foraminifera as bio-indicators of trace element pollution in the heavily contaminated Santa Gilla lagoon (Cagliari, Italy), Mar. Pollut. Bull., 58, 858–877, 2009.

Frontalini, F., Margaritelli, G., Francescangeli, F., Rettori, R., Armynot du Châtelet, E., and Coccioni, R.: Benthic Foraminiferal Assemblages and Biotopes in a Coastal Lake: The Case Study of Lake Varano (Southern Italy), Acta Protozool., 52, 147–160, 2013.

Galloway, J. J.: A Manual of Foraminifera, Principia Press, Bloomington, 483 pp., 1933.

Geslin, E., Debenay, J. P., and Lesourd, M.: Abnormal wall textures and test deformation in *Ammonia beccarii* (hyaline foraminifer), J. Foramin. Res., 28, 148–156, 1998.

Geslin, E., Debenay, J. P., Duleba, W., and Bonetti, C.: Morphological abnormalities of foraminiferal tests in Brazialian environments: comparison between polluted and non-polluted areas, Mar. Micropaleontol., 45, 151–168, 2002.

Gliozzi, E. and Mazzini, I.: Palaeoenvironmental analysis of Early Pleistocene brackish marshes in the Rieti and Tiberino intrapenninic basins (Latium and Umbria, Italy) using ostracods (Crustacea), Palaeogeogr. Palaeocl., 140, 325–333, 1998.

Goldstein, S. T. and Corliss, B. H.: Deposit feeding in selected deep-sea and shallow-water benthic foraminifera, Deep-Sea Res. Pt. I, 41, 229–241, 1994.

Guelorget, O. and Perthuisot, J. P.: Le domaine paralique: expressions géologiques, biologiques et économiques du confinement, Travaux du laboratoire de Géologie, 16, Paris, 136 pp., 1983.

Hammer, Ø., Harper, D. A. T., and Ryan, P. D.: PAST: Paleontological Statistics Software Package for Education and Data Analysis, Palaeontol. Electron., 4, 1–9, 2001.

Hansen, H. J. and Lykke-Andersen, A.-L.: Wall structure and classification of fossil and recent elphidiid and nonionid Foraminifera, Fossils and Strata, 10, 1–37, 1976.

Hayward, B. W., Hollis, C. J., and Grenfell, H. R.: Recent Elphidiidae (Foraminiferida) of the South-west Pacific and fossil Elphidiidae of New Zealand, Institute of Geological & Nuclear Sciences monograph, 16, Lower Hutt, New Zealand, 170 pp., 1997.

Henderson, P. A.: Freshwater ostracods, in: Synopses of the British Fauna (New Series), 42, edited by: Kermack, D. M. and Barnes, R. S. K., Brill E.J., Leiden, 228 pp., 1990.

Heron-Allen, A. and Earland, A.: Clare Island Survey; Part 64 – The foraminifera of the Clare Island District, Co. Mayo, Ireland, P. Roy. Irish Acad., 31, 1–188, 1913.

Hohenegger, J., Piller, W. E., and Baal, C.: Horizontal and vertical spatial microdistribution of foraminifers in the shallow subtidal Gulf of Trieste, Northern Adriatic Sea, J. Foramin. Res., 23, 79–101, 1993.

Holzmann, M. and Pawlowski, J.: Taxonomic relationships in the genus *Ammonia* (Foraminifera) based on ribosomal DNA sequences, J. Micropalaeontol., 19, 85–95, 2000.

Hornibrook, de B. N.: Tertiary Foraminifera from Oamaru District (N.Z). Part 1-Systematics and Distibution, New Zealand Geological Survey Paleontological Bulletin, 34, 1–194, 1961.

Jorissen, F. J.: The distribution of benthic foraminifera in the Adriatic Sea, Mar. Micropaleontol., 12, 21–48, 1987.

Jorissen, F. J.: Benthic Foraminifera from the Adriatic Sea; principles of phenotypic variation, Utrecht Micropaleontological Bulletins, 37, 176 pp., 1988.

Keyser, D. and Aladin, N.: Noding in *Cyprideis torosa* and its causes, Studia Quaternaria, 2, 19–24, 2004.

Laut, L. L. M., Clemente, I. M. M. M., Belart, P., Martins, M. V. A., Frontalini, F., Laut, V. M., Gomes, A., Boski, T., Lorini, M. L., Fortes, R. R., and Rodrigues, M. A. C.: Multiproxies (benthic foraminifera, ostracods and biopolymers) approach applied to identify the environmental partitioning of the Guadiana River Estuary (Iberian Peninsula), Journal of Sedimentary Environments, 1, 184–201, 2016.

Le Cadre, V. and Debenay, J. P.: Morphological and cytological responses of *Ammonia* (foraminifera) to copper contamination: implication for the use of foraminifera as bioindicators of pollution, Environ. Pollut., 143, 304–317, 2006.

Legendre, P. and Legendre, L.: Numerical Ecology, 3rd Edn., Elsevier B.V., Amsterdam, the Netherlands, 2012.

Linke, P. and Lutze, G. F.: Microhabitat preferences of benthic foraminifera a static concept or a dynamic adaptation to optimize food acquisition?, Mar. Micropaleontol., 20, 215–234, 1993.

Lisiecki, L. E. and Raymo, M. E.: A Pliocene-Pleistocene stack of 57 globally distributed benthic δ^{18}O records, Paleoceanography, 20, PA1003, https://doi.org/10.1029/2004PA001071, 2005.

Loeblich, A. R. and Tappan, H.: Studies of Arctic foraminifera, Smithsonian Miscellaneous Collections, 12, 150 pp., 1953.

Loeblich, A. R. and Tappan, H.: Foraminiferal Genera and Their Classification, Van Nostrand Reinhold, New York, 970 pp., 1987.

Marco-Barba, J.: Freshwater ostracods ecology and geochemistry as paleoenvironmental indicators in marginal marine ecosystems: a case of study, the Albufera of Valencia, PhD thesis, Universidad de Valencia, 2010.

Marco-Barba, J., Holmes, J. A., Mesquita-Joanes, F., and Miracle, M. R.: The influence of climate and sea-level change on the Holocene evolution of a Mediterranean coastal lagoon: Evidence from ostracod palaeoecology and geochemistry, Geobios, 46, 409–421, 2013.

Margerel, J. P.: *Aubignyna*, noveau genre de foraminifères du Pliocène du Bosq d'Aubigny (Manche), Revue de Micropaléontologie, 13, 58–64, 1970.

Martínez-García, B., Pascual, A., Rodríguez-Lázaro, J., Martín-Rubio, M., and Rofes, J.: The Ostracoda (Crustacea) of the Tina Menor estuary (Cantabria, southern Bay of Biscay): Distribution and ecology, J. Sea Res., 83, 111–122, 2013.

Mazzini, I., Anadón, P., Barbieri, M., Castorina, F., Ferreli, L., Gliozzi, E., Mola, M., and Vittori, E.: Late Quaternary sea–level changes along the Tyrrhenian coast near Orbetello (Tuscany, Central Italy): paleoenvironmental reconstruction using ostracods, Mar. Micropaleontol., 37, 289–311, 1999.

Meisch, C.: Freshwater Ostracoda of Western and Central Europe, in: Süsswasserfauna von Mitteleuropa 8/3, Schwoerbel, J. and Zwick, P., Spektrum Akademischer Verlag, Heidelberg, Berlin, 522 pp., 2000.

Melis, R. and Covelli, S.: Distribution and morphological abnormalities of recent foraminifera in the Marano and Grado Lagoon (North Adriatic Sea, Italy), Mediterr. Mar. Sci., 14, 432–450, 2013.

Mendes, I., Dias, J. A., Schönfeld, J., and Ferreira, O.: Distribution of living benthic foraminifera on the northern Gulf of Cadiz continental shelf, J. Foramin. Res., 42, 18–38, 2012.

Milker, Y. and Schmiedl, G.: A taxonomic guide to modern benthic shelf foraminifera of the western Mediterranean Sea, Palaeontol. Electron., 15, 134 pp., 2012.

Miller, K. and Lohmann, G.: Environmental distribution of Recent benthic foraminifera on the northeast United States continental slope, Geol. Soc. Am. Bull., 93, 6–200, 1982.

Montenegro, M. E. and Pugliese, N.: Autecological remarks on the ostracod distribution in the Marano and Grado Lagoons (Northern Adriatic Sea Italy), B. Soc. Paleontol. Ital., 3, 123–132, 1996.

Murray, J. W.: Ecology and applications of benthic foraminifera, Cambridge University Press, Cambridge, 426 pp., 2006.

Murray, J. W., Whittaker, J. E., and Alve, E.: On the type species of *Aubignyna* and a description of *A. hamblensis*, a new microforaminifer from temperate shallow waters, J. Micropalaeontol., 19, 61–67, 2000.

Pielou, E. C.: Ecological Diversity, John Wiley, New York, 165 pp., 1975.

Pieri, M. and Groppi, G.: Subsurface geological structure of the Po Plain, Italy, Pubblicazione del Progetto Finalizzato Geodinamica, 414, 1–23, 1981.

Pieri, V., Martens, K., Meisch, C., and Rossetti, G.: An annotated checklist of the Recent non-marine ostracods (Ostracoda: Crustacea) from Italy, Zootaxa, 3919, 271–305, 2005.

Pillet, L., Voltski, I., Korsun, S., and Pawlowski, J.: Molecular phylogeny of Elphidiidae (foraminifera), Mar. Micropaleontol., 103, 1–14, 2013.

Pint, A. and Frenzel, P.: Ostracod fauna associated with *Cyprideis torosa* – an overview, J. Micropalaeontol., 36, 113–119, 2017.

Pint, A., Frenzel, P., Fuhrmann, R., Scharf, B., and Wennrich, V.: Distribution of *Cyprideis torosa* (Ostracoda) in: Quaternary athalassic sediments in Germany and its application for palaeoecological reconstructions, Int. Rev. Hydrobiol., 97, 330–355, 2012.

Pint, A., Engel, M., Melzer, S., Frenzel, P., Plessen, B., and Brückner, H.: How to discriminate athalassic and marginal marine microfaunas: foraminifera and other fossils from an early Holocene continental lake in northern Saudi Arabia, J. Foramin. Res., 47, 175–187, 2017.

Rasmussen, T. L.: Systematic paleontology and ecology of benthic foraminifera from the Plio-Pleistocene Kallithea Bay Section, Rhodes, Greece, in: Lagoon to deepwater foraminifera and ostracods from the Plio-Pleistocene Kallithea bay section, Rhodes, Greece, edited by: Thomsen, E., Cushman Foundation Special Publication, 39, 53–157, 2005.

Regione Emilia-Romagna and ENI–AGIP: Riserve idriche sotterranee della Regione Emilia-Romagna, S.EL.CA, Firenze, 1998.

Rodriguez-Lazaro, J. and Ruiz-Muñoz, F.: A General Introduction to ostracods: morphology, distribution, fossil record and applications, in: Ostracoda as proxies for Quaternary climate change, edited by: Horne, D. J., Holmes, J. A., Rodriguez-Lazaro, J., and Viehberg, F., Developments in Quaternary Science, 17, Elsevier, 1–14, 2012.

Rossi, V., Amorosi, A., Sarti, G., and Potenza, M.: Influence of inherited topography on the Holocene sedimentary evolution of coastal systems: An example from Arno coastal plain (Tuscany, Italy), Geomorphology, 135, 117–128, 2011.

Ruiz, F., González-Regalado, M. L., Baceta, J. I., Menegazzo-Vitturi, L., Pistolato, M., Rampazzo, G., and Molinaroli, E.: Los ostrácodos actuales de la laguna de Venecia (NE de Italia), Geobios, 33, 447–454, 2000.

Saidova, K. M.: On an up-to-date system of supraspecific taxonomy of Cenozoic benthonic foraminifera, Institut Okeanologii P.P.Shirshova, Akademiya Nauk, SSSR, Moscow, 73 pp., 1981 (in Russian).

Salel, T., Bruneton, H., and Lefèvre, D.: Ostracods and environmental variability in lagoons and deltas along the north-western Mediterranean coast (Gulf of Lions, France and Ebro delta, Spain), Revue de Micropaléontologie, 59, 425–444, 2016.

Scott, D. B. and Medioli, F. S.: Quantitative studies of marsh foraminiferal distributions in Nova Scotia: implications for sea level studies, Cushman Foundation for Foraminiferal Research Special Publication, 17, 1–58, 1980.

Schultze, M. S.: Über den Organismus der Polythalamien (Foraminiferen) nebst Bemerkungen über die Rhizopoden im Allgemeinen, Engelmann, Leipzig, 1854.

Sgarrella, F. and Barra, D.: Distribuzione dei foraminiferi bentonici nel Golfo di Salerno (Basso Tirreno, Italia), Bollettino della società dei naturalisti di Napoli, 93, 51–110, 1984.

Sgarrella, F. and Moncharmont Zei, M.: Benthic Foraminifera of the Gulf of Naples (Italy): systematics and autoecology, B. Soc. Paleontol. Ital., 32, 145–264, 1993.

Sgarrella, F., Barra, D., and Improta, A.: The benthic foraminifers of the Gulf of Policastro (Southern Tyrrhenian Sea, Italy), Bollettino della società dei naturalisti di Napoli, 92, 77–114, 1983.

Shannon, C. E.: A mathematical theory of communication, Bell Syst. Tech. J., 27, 379–423, 1948.

Shupack, B.: Some Foraminifera from western Long Island and New York Harbor, Am. Mus. Novit., 737, 1–12, 1934.

Slack, J. M., Kaesler, R. L., and Kontrovitz, M.: Trend, signal and noise in the ecology of Ostracoda: information from rare species in low-diversity assemblages, Hydrobiologia, 419, 181–189, 2000.

Stouff, V., Geslin, E. G., Debenay, J. P., and Lesourd, M.: Origin of morphological abnormalities in *Ammonia* (foraminifera): studies in laboratory and natural environments, J. Foramin. Res., 29, 152–170, 1999.

Thalmann, H. E.: Mitteilungen über Foraminiferen, Eclogae Geol. Helv., 43, 221–225, 1951.

Trog, C., Höfer, D., Frenzel, P., Camacho, S., Schneider, H., and Mäusbacher, R.: A multi-proxy reconstruction and comparison of Holocene palaeoenvironmental changes in the Alvor and Alcantarilha estuaries (southern Portugal), Revue de Micropaléontologie, 56, 131–158, 2013.

Uffenorde, H.: Okologie und jahreszeitliche Verteilung rezenter benthonischer Ostracoden des Limski kanal bei Rovinj (nördliche Adria) [Ecology and seasonal distribution of Recent benthonic Ostracodes from the Limski kanal near Rovinj (northern Adriatic Sea)], Göttinger Arbeiten zur Geologie und Paläontologie, 13, Göttingen, 136 pp., 1972.

Vaiani, S. C. and Pennisi, M.: Tracing freshwater provenance in palaeo-lagoons by boron isotopes and relationship with benthic foraminiferal assemblages. A comparison from late Quaternary subsurface successions in Northern and Central Italy, B. Soc. Paleontol. Ital., 53, 55–66, 2014.

van Harten, D.: Variable noding in *Cyprideis torosa* (Ostracoda, Crustacea): an overview, experimental results and a model from Catastrophe Theory, Hydrobiologia, 419, 131–139, 2000.

van Voorthuysen, J. H.: Foraminiferen aus dem Eemien (Riss-Würm-Interglazial) in der Bohrung Amersfoort I (Locus typicus), Geologische Stichting, Meded., 11, Haarlem, the Netherlands, 1957.

Walker, G. and Jacob, E.: Essays on the Microscope, 2nd Edn., edited by: Adams, G., Dillon and Keating, London, 712 pp., 1798.

Wang, P., Min, Q., and Bian, Y.: On marine continental transitional faunas in Cenozoic deposits of East China, in: Marine Micropaleontology of China, edited by: Wang, P., China Ocean Press, Springer-Verlag, Berlin, New York, 15–33, 1985.

Yanko, V., Kronfeld, J., and Flexer, A.: Response of benthic foraminifera to various pollution sources: implications for pollution monitoring, J. Foramin. Res., 24, 1–17, 1994.

Zampi, M. and D'Onofrio, S.: I foraminiferi della Laguna di Levante (Orbetello, Grosseto), Atti della Società Toscana di Scienze Naturali, Memorie Serie A, 93, 101–127, 1986.

10. MODERN MEIOFAUNA OF THE LAGOON OF BELLOCCHIO

10.1 Introduction

Transitional environments represent sites of great interest due to their sensitivity to coastal dynamics coupled with economic importance, since they host human activities since historical times. They are subject to the influence of marine and freshwater, and characterized by strong environmental gradients even at short spatial scales (Debenay and Guillou, 2002). In this context, benthic foraminifera and ostracoda are considered valuable proxies for the environmental characterization of transitional settings, as well as to detect the presence of natural and anthropogenic pressure (Frontalini and Coccioni, 2011; Armynot du Châtelet and Debenay, 2010).

The distribution of benthic foraminifera and ostracoda was investigated in a wide number of transitional environments of the Mediterranean Sea (Ruiz et al., 2000, 2006; Carboni et al., 2009; Melis and Covelli, 2013; Ferraro et al., 2016; El Kateb et al., 2018), with a specific emphasis on the employment of benthic foraminifera as tracers of pollution (e.g., Frontalini et al., 2009, 2010). Some studies were performed also on the coastal lagoons of the Po Plain, however they exclusively treated benthic foraminifera and they mostly deal with the anthropogenic influence on assemblages (Coccioni, 2000) or they include data with a low level of detail on sparse samples (D’Onofrio et al., 1976). A model for the distribution of meiofauna in the coastal lagoons of the Po Plain is currently lacking; moreover, the construction of a modern reference set would represent a valuable tool for palaeoenvironmental reconstructions in the same study area (Horton and Edwards, 2006).

This chapter shows some preliminary results about the distribution of ostracoda and living benthic foraminifera in the coastal lagoon of Bellocchio. This site was selected because it is a protected area which should be representative of natural conditions. Aims of the project include: i) the definition of benthic foraminiferal biotopes and ostracod biofacies and their relationship with environmental parameters; ii) the comparison between living and dead assemblages of benthic foraminifera to understand the effect of taphonomic processes in this setting and remove the effect of seasonal variations on benthic populations; iii) the construction of a modern reference set for the late Quaternary transitional successions of the Po Plain. This project is a collaboration between University of Bologna (Dr. Veronica Rossi and Giulia Barbieri), University of Urbino (Dr. Fabrizio Frontalini), CNR (National Research Council) Pisa (Dr. Simone Da Prato), CNR Rome (Dr. Ilaria Mazzini) and University of Lille for the geochemical characterization of the sediment and organic material (Dr. Eric Armynot du Châtelet).

10.2 Study area

The study area is represented by a coastal lagoon located south of the Po Delta and it is formally divided into *"Sacca di Bellocchio I"* (southern portion) and *"Sacca di Bellocchio II"* (northern portion). They are included within the complex named "*Vene del Bellocchio"*, a system of coastal wetlands and lagoons developed from the Reno River mouth to Porto Garibaldi (Fig. 10.1). The study area represents the southern portion of the complex, it is bounded by the Reno River towards the south and the *Canale Logonovo* towards the north (Fig. 10.2). Its western limit is connected with the Comacchio wetlands through the artificial channel *Canale Gobbino*. The lagoon is divided from the Adriatic Sea by a littoral sand bar to the east. This area is a protected natural reserve included in the Po Delta Regional Park.

Fig. 10.1 Location of the lagoon of Bellocchio.

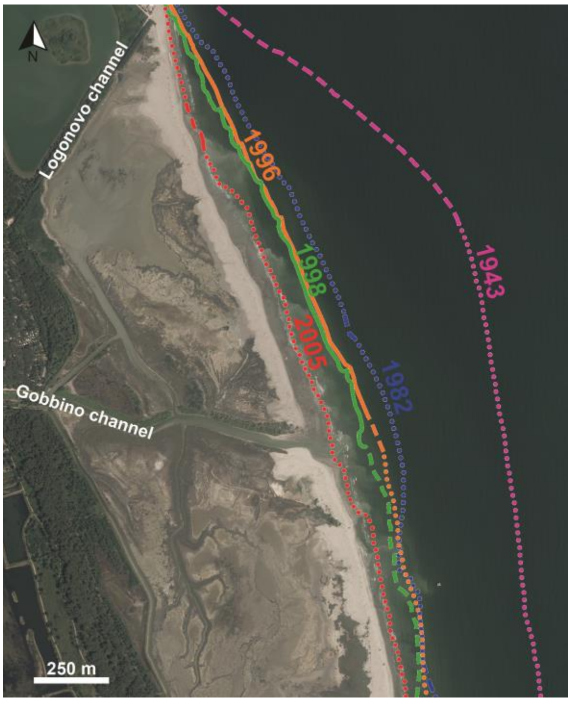

Fig. 10.2 Variation of the coastline in the study area.

The northern portion of the lagoon is permanently inundated, with a maximum measured water depth of ca. 50 cm, whereas perennial or seasonal-dry ponds and creeks are developed south of the Gobbino channel. Most of the water inputs are provided by the Comacchio wetlands, which are artificially regulated for aquaculture activities, as well as from channels that drain the surrounding agricultural lands (Migani et al., 2015). The connection to the sea is nowadays obstructed due to the marked longshore current and sediment overwash. Therefore, the only inputs of saline water derive from saltwater intrusion (Perini and Calabrese, 2010).

The coast facing the lagoon of Bellocchio is one of the few traits of the Emilia-Romagna coast in natural conditions and the first anthropic structure on the shoreline is the jetty of Porto Garibaldi, ca. 5 km north of the study site (fig. 10.1). This coastal area underwent to a strong shoreline retreat (Fig. 10.2; ca. 5-11 m/year), and the almost total loss of the humid areas of the *Vene di Bellocchio* is forecasted for the year 2090 (Calabrese et al., 2010). The area suffers from severe anthropogenic subsidence, with a rate of 4-7.5 mm/year, as well as natural subsidence (0.3

mm/year; Preti et al., 2009). The sediment flux reaching the coastline is negligible due to the anthropogenic alteration of the channels and inland areas.

10.3 Results

At the moment, I have determined living benthic foraminifera and ostracoda within 16 samples out of the 64 surface samples that form the database of the lagoon of Bellocchio. Seven samples (15A-18A, 12B-14B) were retrieved from the permanently submerged portion of the lagoon, at ca. 20-40 cm water depth, three samples from the washover fan (15-17B), five samples from minor tidal channels (12-14C, 16-17C) and one at the border of the Gobbino channel in proximity of the closed inlet (18C; Fig. 10.3). The remaining 48 samples are divided among the other institutions that take part into the project.

10.3.1 Benthic foraminifera

A total of 22 taxa were identified from the analyzed samples, mostly represented by calcareous taxa (11 taxa), subordinately by porcelaneous (6 species) and agglutinated (5 species) taxa (Table 10.1, Table 10.2).

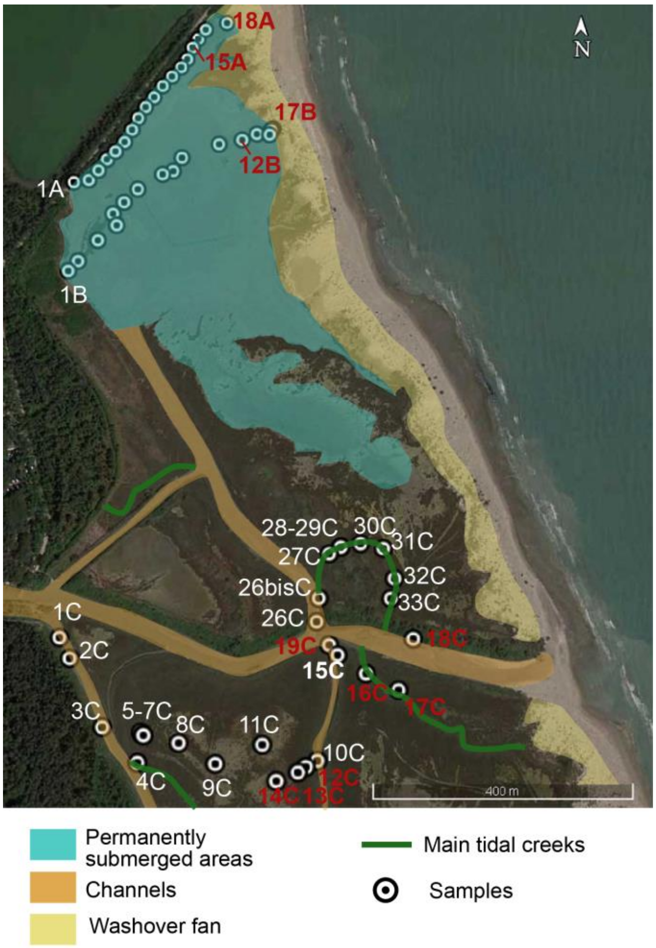

Fig. 10.3 Distribution of samples collected from the lagoon of Bellocchio and main geomorphological features. Data presented in this chapter refer to samples evidenced in red.

Samples of transects A and B from the northern portion of the lagoon are characterized by relatively abundant *Ammonia tepida* (24.4-54.8%), associated to lower frequencies of *Haynesina germanica* (9.0-33.2%) and *Ammonia parkinsoniana* (8.3-29.9%). A wide number of scarce to rare taxa occur. Among calcareous taxa, *Cribroelphidium* spp. (likely juvenile individuals of *Cribroelphidium oceanense* that will be determined with the help of SEM images) occur (up to 7.3%), associated to *C. oceanense* (up to 8.3%). *Ammotium salsum* is the most representative species among agglutinated taxa (2.5-14.3%), associated to rare *Trochammina inflata* and *Ammobaculites foliaceus* (≤1%). Among Milioloidea, *Quinqueloculina* cf. *seminula* (up to 7%) and *Quinqueloculina laevigata* (0.7-2.3%) are the most common species in this sector of the lagoon. Samples recovered on the washover fan, at the sediment-water interface include few tests of living *A. tepida* and *H. germanica*, as well as transported shallow marine taxa and reworked planktonic and benthic foraminifera.

On the southern portion of the study area, samples of transect C are dominated by *H. germanica* (55.4-68.8%) with subordinate *A. tepida* (14.0-39.3%). *Aubignyna perlucida* locally reaches frequencies of >11%, whereas other species such as *Haynesina depressula, P. granosum, C. oceanense* are very rare (≤2%). Among agglutinants, *T. inflata* is relatively more abundant (1.3-2.6%) within samples from this portion of the lagoon, even though it is still rare. Milioloidea are very scarce and mostly represented by *Q. laevigata* and *Quinqueloculina* cf. *seminula*. Samples of the innermost portion of the tidal inlet, at very low water depth (1-2 cm) are almost barren in benthic foraminifera.

10.3.2 Ostracoda

The ostracod fauna of the analyzed samples is low diversified and include a total of 10 taxa (Table 10. 3, Table 10. 4). Assemblages are strongly dominated by *Cyprideis torosa* (64.8-100%), associated to lower abundances of *Loxoconcha elliptica* (up to 13%). Samples 16C, 17C and 18C include low frequencies of freshwater species (*Ilyocypris* cf. *monstrifica*, *Candona neglecta*). Specifically, sample 18C is the most diversified sample and includes a mixture of freshwater, brackish water and marine taxa. Rare living ostracoda or single valves are recorded from sandy sediments of the washover fan.

10.4 Interpretation

Benthic foraminifera and ostracoda of the lagoon of Bellocchio are dominated by species that typically thrive in brackish water settings of the Mediterranean area, tolerant to fluctuating environmental conditions. Among benthic foraminifera, *A. tepida* is an opportunistic species that lives from deltaic environments to inner lagoons at the transition with river mouths (Murray, 2006; Melis and Covelli, 2013; Jorissen et al., 2018). *Ammonia parkinsoniana* is considered less opportunistic and it is common in the northern Adriatic lagoons (Coccioni, 2000; Coccioni et al., 2009). *Haynesina germanica* is common in the Mediterranean lagoons with an intermediate degree of confinement (Debenay and Guillou, 2002). The dominant ostracod *C. torosa* is an opportunist, euryhaline, widespread species that thrives on a wide range of environmental settings (estuaries, lagoons, coastal lakes, sabhka, etc.) irrespective of the physical and geochemical characteristics of the substrate (Athersuch et al., 1989; Pint and Frenzel, 2017). *Loxoconcha elliptica* is a oligohaline-polyhaline species common in the inner portion of the North Adriatic lagoons (Montenegro and Pugliese, 1996; Ruiz et al, 2000).

The northern portion of the lagoon is characterized by scarce water circulation and salinity of ca. 30‰ from inland to seaward locations. Salinity is considered one of the most important controlling factors on the distribution of benthic foraminifera and ostracoda in back-barrier environments (e.g. Debenay and Guillou, 2002; Frenzel and Boomer, 2005). Nevertheless, the extremely scarce freshwater inputs from inland sources and the permanent saltwater intrusion determine almost stable salinity levels in Bellocchio lagoon, as it was shown by in-situ measurements. Conversely, the southern portion of the lagoon could be affected by salinity oscillations due to the evaporation of water in seasonal dry ponds and creeks. Benthic foraminifera in the northern sector of the lagoon are dominated by *A. tepida, H. germanica*, *A. parkinsoniana* and *C. oceanense*, which suggest high food availability in terms of both labile and refractory organic matter, as similarly recorded in other Mediterranean lagoons (Hohenegger et al., 1989; Melis and Covelli, 2013). *Ammotium salsum* found on this part of the lagoon is typical of sub-tidal settings, suggesting that substrates of this area are not subject to subaerial exposure (Scott and Medioli, 1980; Kemp et al., 2009). Conversely, assemblages dominated by *H. germanica* are found in the southern portion of the lagoon, characterized by seasonal dry ponds and creeks where the water depth is very shallow. The abundance of this species is consistent with an intertidal environment subject to strong oscillations of environmental parameters, since this taxon is abundant on intertidal areas with high fluctuations of nutrients and salinity (Coccioni et al., 2009; Melis and Covelli, 2013). This is confirmed by the higher numbers of *T. inflata,* typical of middle marsh settings (Kemp et al., 2009).

On the other hand, ostracoda are less diversified and assemblages are dominated by *C. torosa* and *L. elliptica*. Both species tolerate fluctuations in salinity and therefore are able to colonize the whole lagoonal area, both the northern side with stable conditions, as well as southern sites along the tidal creek where environmental parameters can fluctuate. Similar assemblages are found in the innermost portions of the lagoons of Venice, Marano and Grado subject to strong oscillations of salinity in proximity to river outlets (Montenegro and Pugliese, 1996; Ruiz et al., 2000). Freshwater species in the southern sites 16C and 17C (along a minor tidal creek) and 18C (behind the sand bar that obstructs the main inlet of the lagoon) can be transported from the inland humid areas by the Gobbino channel, even though local lowered salinities cannot be excluded. Shallow marine taxa within sample 18C are likely transported from the nearby marine environment due to overwash processes. In fact, tests of marine ostracoda such as the euhaline *Pontocythere turbida* or the polyhaline-euhaline *Leptocythere ramosa* are thick and locally abraded.The paucity of meiofauna within washover sands suggests that these organisms are not able to colonize such energetic environment.

10.5 Conclusions and future perspectives

Preliminary results about the composition of living benthic foraminiferal and ostracod fauna from the lagoon of Bellocchio reveal that:

- Benthic foraminifera seem to be represented by two assemblages: one in the northern area under stable environmental conditions (*A. tepida, H. germanica, C. oceanense*), the second in the southern portion of the lagoon subject to intertidal oscillations (*H. germanica, A. tepida, T. inflata*).

- Ostracoda show a single assemblage, dominated by *C. torosa* with subordinate *L. elliptica*. The presence of freshwater taxa along small tidal creeks suggests transport processes from inland waters.
- Washover deposits include rare individuals of benthic foraminifera and ostracoda; among ostracoda, transported shallow marine taxa are also recorded.

After the completion of the meiofaunal database, data about ostracoda and living benthic foraminifera will be integrated with abiotic data (sediment grain-size and geochemistry) in order to delineate a possible connection between the meiofauna and environmental parameters. Faunal parameters such as density of living individuals and diversity indices will be calculated, since the structure of the assemblage is considered a sensitive indicator of stressed conditions. The results will be organized in a manuscript that will be submitted to a peer-review journal. Afterwards, the construction of the modern reference set will be performed on dead benthic foraminiferal assemblages and ostracoda on the sediment fraction >125 µm to keep the data comparable to fossil samples of the Po Plain sediment succession.

10.6 Supplementary tables

LIVING BENTHIC FORAMINIFERA														
Taxa/Sample	**15A**	**%**	**16A**	**%**	**17A**	**%**	**18A**	**12B**	**13B**	**14B**	**%**	**15B**	**16B**	**17B**
								Scarce tests of living *A. tepida* and *A. perlucida.* Very rare *Q. costata* and *Q. seminula*	Scarce tests of living *A. tepida* and *A. perlucida.* Very rare *Q. seminula*			Rare tests of reworked planktonic and benthic foraminifera; rare tests of transported benthic foraminifera (*Ammonia beccarii, Elphidium crispum*). Rare, well-preserved tests of *A. tepida*	Rare tests of reworked benthic and planktonic foraminifera	Rare tests of reworked benthic and planktonic foraminifera
Trochammina inflata	2	0.7%		0.0%	3	1.0%	Rare living individuals of *H. germanica*				0.0%			
Ammobaculites foliaceus		0.0%		0.0%	1	0.3%					0.0%			
Ammotium salsum	12	4.0%	8	2.7%	44	14.3%				8	2.5%			
Textularia earlandi	1	0.3%		0.0%	1	0.3%					0.0%			
Ammonia tepida	166	54.8%	107	35.5%	75	24.4%				164	51.1%			
Ammonia parkinsoniana	25	8.3%	28	9.3%	46	15.0%				96	29.9%			
Aubignyna perlucida	1	0.3%		0.0%	1	0.3%					0.0%			
Cribroelphidium oceanense	10	3.3%	25	8.3%	14	4.6%				1	0.3%			
Cribroelphidium granosum		0.0%		0.0%	1	0.3%					0.0%			
Cribroelphidium spp.	22	7.3%	34	11.3%	16	5.2%				3	0.9%			
Haynesina germanica	41	13.5%	63	20.9%	102	33.2%				29	9.0%			
Haynesina spp.	4	1.3%	1	0.3%		0.0%					0.0%			
Bolivina seminuda		0.0%	1	0.3%		0.0%					0.0%			
Quinqueloculina costata	1	0.3%	1	0.3%	1	0.3%				9	2.8%			
Quinqueloculina bosciana		0.0%		0.0%		0.0%					0.0%			
Quinqueloculina laevigata	14	4.6%	11	3.7%	1	0.3%				10	3.1%			
Quinqueloculina cf. *seminula*	4	1.3%	14	4.7%		0.0%					0.0%			
Miliolinella webbiana		0.0%	8	2.7%	1	0.3%				1	0.3%			
TOTAL	303	100.0%	301	100.0%	307	100.0%				321	100.0%			

Table 10.1 Total and percentage abundance of benthic foraminifera within analyzed samples of transects A and B (northern portion of the lagoon). Samples with <300 tests include a qualitative description of the assemblage.

LIVING BENTHIC FORAMINIFERA									
Taxa/Sample	**12C**	**13C**	**14C**	**16C**	**%**	**17C**	**%**	**18C**	**%**
	Few tests of living *A. tepida* and *H. germanica*	Barren	Barren						
Trochammina inflata				7	2.3%	8	2.6%	4	1.3%
Entzia macrescens					0.0%		0.0%	1	0.3%
Ammonia tepida				42	14.0%	119	39.3%	61	19.6%
Ammonia parkinsoniana				3	1.0%		0.0%	4	1.3%
Aubignyna perlucida				12	4.0%	1	0.3%	37	11.9%
Cribroelphidium oceanense				1	0.3%		0.0%	3	1.0%
Cribroelphidium granosum					0.0%	1	0.3%		0.0%
Cribroelphidium lidoense					0.0%	1	0.3%		0.0%
Haynesina germanica				207	68.8%	168	55.4%	187	60.1%
Haynesina depressula					0.0%		0.0%	5	1.6%
Haynesina spp.					0.0%	3	1.0%		0.0%
Quinqueloculina costata					0.0%		0.0%	1	0.3%
Quinqueloculina laevigata				7	2.3%	2	0.7%	5	1.6%
Quinqueloculina cf. *seminula*				21	7.0%		0.0%	2	0.6%
Miliolinella elongata				1	0.3%		0.0%	1	0.3%
TOTAL				301	100.0%	303	100.0%	311	100.0%

Table 10.2 Total and percentage abundance of benthic foraminifera within analyzed samples of transect C (southern portion of the lagoon). Samples with <300 tests include a qualitative description of the assemblage.

OSTRACODA									
Taxa/sample	**15A**	**%**	**16A**	**%**	**17A**	**%**	**18A**		
							Rare carapaces of dead and living *C. torosa*		
Cyprideis torosa	281	90.9%	277	88.8%	282	88.4%			
Loxoconcha elliptica	28	9.1%	35	11.2%	37	11.6%			
Leptocythere sp.		0.0%		0.0%		0.0%			
TOTAL	309	100.0%	312	100.0%	319	100.0%			

	OSTRACODA								
Taxa/sample	**12B**	**%**	**13B**	**%**	**14B**	**%**	**15B**	**16B**	**17B**
							Rare *C. torosa* , very rare *L. elliptica*	Barren	Barren
Cyprideis torosa	420	87.0%	284	91.0%	328	97.3%			
Loxoconcha elliptica	63	13.0%	26	8.3%	9	2.7%			
Leptocythere sp.		0.0%	2	0.6%		0.0%			
TOTAL	483	100.0%	312	100.0%	337	100.0%			

Table 10. 3 Total and percentage abundance of ostracoda within analyzed samples of transects A and B (northern portion of the lagoon). Samples with <300 valves include a qualitative description of the assemblage.

OSTRACODA												
Taxa/Sample	**12C**	**%**	**13C**	**%**	**14C**	**%**	**16C**	**%**	**17C**	**%**	**18C**	**%**
Ilyocypris cf. *monstrifica*		0.0%		0.0%		0.0%	3	1.0%	2	0.5%	6	2.0%
Candona neglecta		0.0%		0.0%		0.0%	1	0.3%		0.0%	2	0.7%
Candona sp.		0.0%		0.0%		0.0%		0.0%	8	2.0%	49	16.3%
Cyprideis torosa	377	99.2%	547	98.2%	382	100.0%	277	92.0%	362	89.4%	195	64.8%
Leptocythere spp.		0.0%		0.0%		0.0%		0.0%	1	0.2%	11	3.7%
Leptocythere ramosa		0.0%		0.0%		0.0%		0.0%		0.0%	4	1.3%
Loxoconcha elliptica	2	0.5%	10	1.8%		0.0%	19	6.3%	28	6.9%	28	9.3%
Loxoconcha stellifera	1	0.3%		0.0%		0.0%		0.0%		0.0%		0.0%
Loxoconcha sp.		0.0%		0.0%		0.0%		0.0%		0.0%	2	0.7%
Pontocythere turbida		0.0%		0.0%		0.0%	1	0.3%	4	1.0%	4	1.3%
TOTAL	380	100.0%	557	100.0%	382	100.0%	301	100.0%	405	100.0%	301	100.0%

Table 10. 4 Total and percentage abundance of ostracoda within analyzed samples of transect C (southern portion of the lagoon). Samples with <300 valves include a qualitative description of the assemblage.

11. CONCLUSIONS

The application of benthic foraminifera and ostracoda as proxies for present-day and past environmental conditions is widespread from continental to deep-ocean settings. The Po Plain represents a great laboratory for the study of late Quaternary microfossil assemblages, since the high natural subsidence and the relatively low tectonic deformation allowed an exceptional preservation of the deposits. Benthic foraminifera and ostracoda were applied in the last years with the aim of determining the palaeoenvironmental evolution of the Po Plain in a sequence stratigraphic perspective. Even though the geological history of the Po Plain in relationship with the last climatic-eustatic cycles is well known, depositional dynamics at short-time scales under the influence of autogenic processes are relatively unexplored, as well as those occurred at the turnaround from different eustatic conditions. In these contexts, benthic foraminifera and ostracoda would provide a valuable tool for the interpretation of the sedimentary record.

This project shows the importance of integrating benthic foraminifera and ostracoda in present-day and fossil settings, focusing on the nature of (palaeo)ecological information provided by each benthic group. To achieve this goal, my Ph.D. project focused on both present-day environments and the late Quaternary sediment succession of the Po Plain, from shallow marine to transitional (i.e., back-barrier) settings. Two study cases presented here represent modern analogs of the late Quaternary depositional systems of the subsurface of the Po Plain, which were investigated in the remaining four study cases. Multivariate analyses and statistical techniques represented a useful instrument to assess the contribution of environmental drivers on modern assemblages and to detect shift in meiofaunal composition within fossil successions.

1. The first study case (chapter 5) investigates and compares the zonation of benthic foraminifera and ostracoda of the shallow (<40 m water depth) North Adriatic shelf, subject to a strong river influence in a deltaic progradational context. Due to its vicinity to the Po Plain, this can be considered the most reliable modern analogue for the late Quaternary shallow marine succession. We show that the faunal turnover of each benthic group is driven by distinct environmental parameters: organic matter for benthic foraminifera, grain size for ostracoda and, secondary for both groups, bathymetry. The integration of the five benthic foraminiferal biofacies and the seven ostracod biofacies allows the identification of five depositional environments with a specific position with respect to the main source of riverine material (i.e., the Po Delta). We identify three sectors of the North Adriatic Shelf with a specific coastal to offshore sequence of depositional environments, that transposed in the stratigraphic record would allow to obtain detailed palaeogeographical reconstructions.

2. Results of the first study case were used as base for the interpretation of the shallow marine succession of core EM13, recovered on the Po Delta plain (chapter 6). The record of benthic foraminifera and ostracoda provides distinct lines of evidence for the palaeoecological characterization of this succession, in relationship with the well-known evolutive phases of the Po Delta. Preliminary results seem to indicate that benthic foraminifera are a proxy for organic matter palaeofluxes and give indications about the distance from a river mouth. The signal provided by ostracoda seems to be indicative of amounts of sediment input in relationship with depositional processes (wave-dominated vs. river-dominated settings).

3. In the third study case (chapter 7), the combination of sedimentological, geochemical and palaeontological (benthic foraminifera, ostracoda, mollusks) proxies allow to define a three-stage progradation model for the Holocene high-stand succession of the Po Plain. In this context, benthic foraminifera and ostracoda represent useful proxies for the palaeoecological characterization of fine- and coarse-grained deposits and identify characteristic facies associations: a) bay-head delta and estuary in the uppermost TST (7.7-7.0 cal. kyr BP); b) shallow marine environment subject to low river influence in the lowermost HST (7.0-2.0 cal. kyr BP); c) prodelta subject to high sediment input and local oxygen deficiency in the uppermost HST (2.0 cal. kyr BP- present).

4. Benthic foraminifera are tested as indicators of autogenic deltaic processes specifically focusing on the uppermost HST in the fourth study case (chapter 8). Here, we show that benthic foraminifera from expanded prodelta successions record short time-scale, local palaeoenvironmental variations induced by autogenic deltaic processes and river floods. Changes in riverine inputs, related to variations in sediment supply or mouth shifting, are simultaneously marked by benthic foraminifera and sediment geochemistry.

5. The palaeoenvironmental resolution provided by benthic foraminifera and ostracoda is tested in the fifth study case, where a Pleistocene back-barrier succession was investigated (chapter 9). In this case as well, benthic foraminifera and ostracoda are related to distinct palaeoecological conditions: the former indicates stressed/unstressed conditions, the latter inner/central/outer lagoon conditions under different degrees of salinity. In a stratigraphic perspective, ostracoda seem to be more useful in this case, because the succession of assemblages clearly indicates a general transgressive-regressive trend with minor fluctuations of salinity, likely related to minor regressive phases.

6. In the last study case (chapter 10), I present preliminary results about the meiofauna of the lagoon of Bellocchio, a natural coastal lagoon that would represent a modern analog for the late Holocene back-barrier successions of the Po Plain. Benthic foraminifera from the

analyzed samples are gathered in two assemblages: in the northern sector of the lagoon, brackish water species typical of nutrient-rich settings dominate; in the southern sector, taxa of intertidal zones subject to environmental fluctuations are abundant. On the other hand, ostracoda are dominated by opportunistic taxa tolerant to fluctuating salinity within all study sites. The future correlation with environmental parameters will allow to test the presence of specific environmental drivers on the benthic fauna of transitional environments of the Po Plain.

In conclusion, this research tested the integrated application of benthic foraminifera and ostracoda in different (palaeo)environmental settings and evidenced that each group provides a distinct (palaeo)ecological signal. Therefore, it should be preferable to combine both for the characterization of modern environments as well as fossil successions, especially on river-influenced settings where it is difficult to detect variations of single environmental parameters.

12. REFERENCES

AGIP, 1982. Foraminiferi Padani (Terziario e Quaternario): Plate I–LII. AGIP, Milano.

Aguzzi, M., Amorosi, A., Colalongo, M.L., Ricci Lucchi, M., Rossi, V., Sarti, G., Vaiani, S.C., 2007. Late Quaternary climatic evolution of the Arno coastal plain (Western Tuscany, Italy) from subsurface data. Sediment. Geol. 202, 211–229.

Albani, A., and Serandrei Barbero, R., 1982. A foraminiferal fauna from the Lagoon of Venice, Italy. J. Foramin. Res., 12, 234–241.

Albani, A., and Serandrei Barbero, R.. 1990. I Foraminiferi della Laguna e del Golfo di Venezia. Memorie di Scienze Geologiche, 42, 271–341.

Albani, A., Serandrei Barbero, R., and Donnici, S., 2007. Foraminifera as ecological indicators in the Lagoon of Venice, Italy. Ecol. Indic., 7, 239–253.

Alve, E., 1995. Benthic foraminiferal responses to estuarine pollution: a review. J. Foramin. Res. 25, 190–203.

Alvisi, F., Giani, M., Ravaioli, M., and Giordano, P., 2013. Role of sedimentary environment in the development of hypoxia and anoxia in the NW Adriatic shelf (Italy). Estuar. Coast. Shelf S., 128, 9–21.

Amorosi, A., Colalongo, M. L., Fusco, F., Pasini, G., and Fiorini, F, 1999a. Glacio-eustatic control of continental-shallow marine cyclicity from Late Quaternary deposits of the southeastern Po Plain (Northern Italy). Quaternary Res., 52, 1–13.

Amorosi, A., Colalongo, M. L., Pasini, G., and Preti, D., 1999b. Sedimentary response to Late Quaternary sea-level changes in the Romagna coastal plain (northern Italy). Sedimentology, 46, 99–121.

Amorosi, A., Centineo, M. C., Colalongo, M. L., Pasini,G., Sarti, G., and Vaiani, S. C., 2003. Facies architecture and Latest Pleistocene–Holocene depositional history of the Po Delta (Comacchio area), Italy. J. Geol., 111, 39–56.

Amorosi, A., Colalongo, M. L., Fiorini, F., Fusco, F., Pasini, G., Vaiani, S. C., and Sarti, G., 2004. Palaeogeographic and palaeoclimatic evolution of the Po Plain from 150-ky core records. Global Planet. Change, 40, 55–78.

Amorosi, A., Centineo, M.C., Colalongo, M.L., Fiorini, F., 2005. Millennial-scale depositional cycles from the Holocene of the Po Plain, Italy. Marine Geology 222–223, 7–18.

Amorosi, A., Dinelli, E., Rossi, V., Vaiani, S. C., and Sacchetto, M., 2008. Late Quaternary palaeoenvironmental evolution of the Adriatic coastal plain and the onset of Po River Delta. Palaeogeo., Palaeocl., Palaeoecol., 268, 80–90.

Amorosi, A., Bruno, L., Rossi, V., Severi, P., and Hajdas, I., 2014a. Paleosol architecture of a late Quaternary basin-margin sequence and its implications for high-resolution, non-marine sequence stratigraphy. Glob. Planet. Change 112, 12–25.

Amorosi, A., Rossi, V., Scarponi, D., Vaiani, S.C., and Ghosh, A., 2014b. Biosedimentary record of postglacial coastal dynamics: high-resolution sequence stratigraphy from the northern Tuscan coast (Italy). Boreas 43, 939–954.

Amorosi, A., Maselli, V. and Trincardi, F., 2016a. Onshore to offshore anatomy of a late Quaternary source-to-sink system (Po Plain-Adriatic Sea, Italy). Earth-Sci. Rev., 153, 212–237.

Amorosi, A., Bracone, V., Campo, B., D'Amico, C., Rossi, V., and Rosskopf, C.M., 2016b. A late Quaternary multiple paleovalley system from the Adriatic coastal plain (Biferno River, Southern Italy). Geomorphology, 254, 146–159.

Amorosi, A., Bruno, L., Campo, B., Morelli, A., Rossi, V., Scarponi D., Hong, W., Bohacs, K.M. and Drexler, T., 2017. Global sea-level control on local parasequence architecture from the Holocene record of the Po Plain, Italy. Mar. Petrol. Geol. 87, 99–111.

Angue Minto’o, C.M., Bassetti, M.-A., Jouet, G., and Toucanne, S., 2013. Distribution of modern ostracoda and benthic foraminifera from the Golo margin (East-Corsica). Revue de Paléobiologie 32 (2), 607–628.

Angue Minto'o, C.M., Bassetti, M.A., Morigi, C., Ducassou, E., Toucanne, S., Jouet, G., and Mulder, T., 2015. Levantine intermediate water hydrodynamic and bottom water ventilation in the northern Tyrrhenian Sea over the past 56,000 years: New insights from benthic foraminifera and ostracods. Quatern. Int., 357, 295–313.

Antonellini, M., Mollema, P., Giambastiani, B., Banzola, E., Bishop, K., Caruso, L., La Penna, E., Mischio, A., Pellegrini, L., Rizzo, E., Sabia, M., Ulazzi, E., and Gabbianelli, G., 2006. Saltwater intrusion in the coastal aquifer of the southern Po plain. What Future is There for Our Coastal Freshwater? ADRIA 2006 International Geological Congress on the Adriatic area, Urbino (IT) 19–20 June 2006, pp. 23–24.

Antonellini, M., Giambastiani, B.M.S., Greggio, N., Bonzi, L., Calabrese, L., Luciani, P., Perini, L., and Severi, P., 2019. Processes governing natural land subsidence in the shallow coastal aquifer of the Ravenna coast, Italy. Catena, 172, 76–86.

Armynot du Châtelet, E., and Debenay, J.-P., 2010. Anthropogenic impact on the western French coast as revealed by foraminifera: a review. Revue de Micropaléontologie, 53, 129–137.

Athersuch, J., Horne, D. J., and Whittaker, J. E., 1989. Marine and brackish water ostracods In: Kermack, D. M. and Barnes, R. S. K., (Eds.), Synopses of the British Fauna (New Series), 43. Brill E.J., Leiden, 345 pp.

Barmawidjaja, D.M., Jorissen, F.J., Puskaric, S., and Van Der Zwaan, G.J., 1992. Microhabitat selection by benthic foraminifera in the northern Adriatic Sea. J. Foramin. Res., 22, 297–317.

Bassetti, M.A., Carbonel, P., Sierro, F.J., Perez-Folgado, M., Jouët, G., and Berné, S., 2010. Response of ostracods to abrupt climate changes in the Western Mediterranean (Gulf of Lions) during the last 30 kyr. Mar. Micropaleontol. 77, 1–14.

Bonaduce, G., Ciampo, G., and Masoli, M., 1975. Distribution of Ostracoda in the Adriatic Sea. Pubblicazioni della Stazione Zoologica di Napoli, 40, 304 pp.

Bondesan, M., and Simeoni, U., 1983. Dinamica e analisi morfologica statistica dei litorali del delta del Po e alle foci dell'Adige e del Brenta. Memorie di Scienze Geologiche, Padova XXXVI, 1–48.

Bondesan, M., Favero, V., and Vinals, M.J., 1995. New evidence on the evolution of the Podelta coastal plain during the Holocene. Quat. Int. 29–30, 105–110.

Boomer, I., Horne, D. J., and Slipper, J., 2003. The use of ostracods in palaeoenvironmental studies, or what can you do with an ostracod shell? In: Park, L. E. and Smith, A. J. (Eds.), Bridging the gap: Trends in the Ostracode Biological and Geological Sciences. The Paleontological Society Papers 9, 153–179.

Brambati, A., Ciabatti, M., Fanzutti, G.P., Marabini, F. and Marocco, R., 1983. A new sedimentological textural map of the northern and central Adriatic Sea. Boll. Oceanog. Teor. Appl. I, 267– 271.

Breman, E., 1975. The distribution of Ostracodes in the bottom sediments of the Adriatic Sea. PhD thesis, Free University of Amsterdam, the Netherlands.

Bruno, L., Bohacs, K.M., Campo, B., Drexler, T.M., Rossi, V., Sammartino, I., Scarponi, D., Hong, W., and Amorosi, A., 2017. Early Holocene transgressive palaeogeography in the Po coastal plain (northern Italy). Sedimentology 64, 1792–1816.

Cabral, M.C., and Loureiro, I., 2013. Overview of Recent and Holocene ostracods (Crustacea) from brackish and marine environments of Portugal. J. Micropalaeontol., 32, 135–159.

Calabrese, L., Lorito, S. and Perini, L., 2010. Variazione della linea di riva dalla foce del Reno alla foce del Po di Volano. In: Perini, L., Calabrese, L. (Eds.), Il sistema mare-costa dell'Emilia-Romagna. Pendragon, 239 pp.

Campo, B., Amorosi, A., and Vaiani, S. C., 2017. Sequence stratigraphy and late Quaternary paleoenvironmental evolution of the Northern Adriatic coastal plain (Italy), Palaeogeogr. Palaeocl. Palaeoecol., 466, 265–278.

Carboni, M.G., Bergamin, L., Di Bella, L., Iamundo, F., and Pugliese, N., 2002. Palaeoecological evidences from foraminifers and ostracods on Late Quaternary sea-level changes in the Ombrone river plain (central Tyrrhenian coast, Italy). Geobios, 24, https://doi.org/10.1016/S0016-6995(02)00047-5.

Carboni, M. G., Succi, M. C., Bergamin, L., Di Bella, L., Frezza, V., and Landini, B., 2009. Benthic foraminifera from two coastal lakes of southern Latium (Italy). Preliminary evaluation of environmental quality. Mar. Pollut. Bull., 59, 268–280.

Carboni, M.G., Bergamin, L., Di Bella, L., Esu, D., Pisegna Cerone, E., Antonioli, F., and Verrubbi, V., 2010. Palaeoenvironmental reconstruction of late Quaternary foraminifera and molluscs from the ENEA borehole (Versilian plain, Tuscany, Italy). Quaternary Res. 74, 265–276.

Castellarin, A., Eva, C., Giglia, G., Vai, G.B., Rabbi, E., Pini, G.A., and Crestana, G., 1985. Analisi strutturale del Fronte Appenninico Padano. Giornale di Geologia 47, 47–75.

Cattaneo, A., Correggiari, A., Langone, L., and Trincardi, F., 2003. The late-Holocene Gargano subaqueous delta, Adriatic shelf: sediment pathways and supply fluctuations. Mar. Geol. 193, 61–91.

Cearreta, A., Benito, X., Ibáñez, C., Trobajo, R., and Giosan, L., 2016. Holocene palaeoenvironmental evolution of the Ebro Delta (Western Mediterranean Sea): Evidence for an early construction based on the benthic foraminiferal record. The Holocene, 1–19.

Ciabatti, M., 1967. Ricerche sull’evoluzione del Delta Padano. Giornale di Geologia, 34, 381–406.

Cimerman, F., and Langer, M. R., 1991. Mediterranean Foraminifera. Academia Scientiarum et Artium Slovenica, Classis IV, 30, Ljubljana, 118 pp.

Coccioni, R., 2000. Benthic foraminifera as bioindicators of heavy metal pollution – a case study from the Goro Lagoon (Italy). In: Martin, R. E. (Ed.), Environmental micropaleontology: the application of microfossils to environmental geology. Kluwer Academic/Plenum Publishers, New York, 71–103.

Coccioni, R., Frontalini, F., Marsili, A., and Mana, D., 2009. Benthic foraminifera and trace element distribution: A case-study from the heavily polluted lagoon of Venice (Italy), Mar. Pollut. Bull., 59, 257–267.

Colalongo, M.L., 1969. Ricerche sugli Ostracodi nei fondali antistanti il delta del Po. Giornale di Geologia, 36, 335–362.

Correggiari, A., Trincardi, F., Langone, L., and Roveri, M., 2001, Styles of failure in heavily sedimented highstand prodelta wedges on the Adriatic shelf. J. Sediment. Res., 71, 218–236.

Correggiari, A., Cattaneo, A., and Trincardi, F., 2005. Depositional patterns in the Holocene Po Delta system. In: Bhattacharya, J.P., Giosan, L. (Eds.), River Deltas: Concepts, Models and Examples. SEPM Special Publication, 83, 365–392.

Cronin, T.M., De Martino, D.M., Dwyer, G.S., and Rodriguez-Lazaro, J., 1999. Deep-sea ostracode species diversity: response to late Quaternary climate change. Mar. Micropaleontol. 37, 231–249.

D'Onofrio, S., 1969. Ricerche sui Foraminiferi nei fondali antistanti il Delta del Po. Giornale di Geologia, 36, 283–334.

D'Onofrio, S., Marabini, F., and Vivalda, P., 1976. Foraminiferi di alcune lagune del delta del Po. Giornale di Geologia, 40, 267–276.

d'Orbigny, A., 1826. Tableau Methodique de la Classe des Cephalopodes. Ann. Sci. Nat. Zool., 7, 96–314.

Debenay, J.-P., and Guillou, J.-J., 2002. Ecological transitions indicated by foraminiferal assemblages in paralic environments. Estuaries, 25, 1107–1120.

Debenay, J. P., Guillou, J. J., Redois, F., and Geslin, E., 2000. Distribution trends of foraminiferal assemblages in paralic environments: a base for using foraminifera as bioindicators. In: Martin, R. E. (ed.), Environmental micropaleontology: the application of microfossils to environmental geology. Kluwer Academic/Plenum Publishers, New York, 39–67.

Di Bella, L., Bellotti, P., and Milli, S., 2013. The role of foraminifera as indicators of the Late Pleistocene–Holocene palaeoclimatic fluctuations on the deltaic environment: The example of Tiber delta succession (Tyrrhenian margin, Italy). Quatern. Int., 303, 191–209.

Di Bella, L., Frezza, V., Bergamin, L., Carboni, M.G., Falese, F., Martorelli, E., Tarragoni, C., and Chiocci, F.L., 2014. Foraminiferal record and high-resolution seismic stratigraphy of the Late Holocene succession of the submerged Ombrone River delta (Northern Tyrrhenian Sea, Italy). Quatern. Int., 328-329, 287–300.

Doglioni, C., 1993. Some remarks on the origin of foredeeps. Tectonophysics, 228, 1–20.

Donnici, S., and Serandrei Barbero, R., 2002. The benthic foraminiferal communities of the northern Adriatic continental shelf. Mar. Micropaleontol., 44, 93–123.

El Kateb, A., Stalder, C., Neururer, C., Fentimen, R., Spangenberg, J.E., and Spezzaferri, S., 2018. Distribution of benthic foraminiferal assemblages in the transitional environment of the Djerba lagoon (Tunisia). Swiss Journal of Geosciences, https://doi.org/10.1007/s00015-018-0300-0.

Ellis, B. F., and Messina, A. R., 1940. Catalogue of Foraminifera. Micropaleontology Press, New York.

Ellison, R.L., 1984. Foraminifera and meiofauna on an intertidal mudflat, Cornwall, England: Populations; respiration and secondary production; and energy budget. Hydrobiologia 109, 131–148.

Fairbanks, R.G., 1989. A 17,000-year glacio-eustatic sea level record: influence of glacial melting rates on the Younger Dryas event and deep-ocean circulation. Nature, 342, 637–642.

Fanget, A.-S., Bassetti, M.-A., Arnaud, M., Chiffoleau, J.-F., Cossa, D., Goineau, A., Fontanier, C., Buscail, R., Jouet, G., Maillet, G.M., Negri, A., Dennielou, B. and Berné, S., 2013a. Historical evolution and extreme climate events during the last 400 years on the Rhone prodelta (NW Mediterranean). Mar. Geol., 346, 375–391.

Fanget, A.-S., Bassetti, M.-A., Berné, S., and Arnaud, M., 2013b. Epi-bathyal ostracod assemblage in Holocene Rhone deltaic sediments (Gulf of Lions, NW Mediterranean) and their palaeoecological implications. Revue de Paléobiologie, 32, 589–606.

Fanget, A.-S., Bassetti, M.-A., Fontanier, C., Tudryn, A., and Berné, S., 2016. Sedimentary archives of climate and sea-level changes during the Holocene in the Rhône prodelta (NW Mediterranean Sea). Clim. Past, 12, 2161–2179.

Faranda, C., and Gliozzi, E., 2008. The ostracod fauna of the Plio-Pleistocene Monte Mario succession (Roma, Italy). B. Soc. Paleontol. Ital., 47, 215–267.

Ferraro, L., Rubino, F., Belmonte, M., Da Prato, S., Greco, M., and Frontalini, F., 2016. A multidisciplinary approach to study confined marine basins: the holobenthic and merobenthic assemblages in the Mar Piccolo of Taranto (Ionian Sea, Mediterranean). Mar. Biodivers., DOI 10.1007/s12526-016-0523-0.

Fiorini, F., and Vaiani, S. C., 2001. Benthic foraminifers and transgressive–regressive cycles in the Late Quaternary subsurface sediments of the Po Plain near Ravenna (Northern Italy). B. Soc. Paleontol. Ital., 40, 357–403.

Fornasini, C., 1904. Illustrazione di specie orbignyane di foraminiferi istituite nel 1826. Memorie della Reale Accademia delle Scienze dell'Istituto di Bologna, series 6(I).

Frenzel, P., and Boomer, I., 2005. The use of ostracods from marginal marine, brackish waters as bioindicators of modern and Quaternary environmental change. Palaeogeogr. Palaeocl. Palaeoecol., 225, 68–92.

Frenzel, P., Keyser, D., and Viehberg, F. A., 2010. An illustrated key and (palaeo)ecological primer for recent to postglacial Ostracoda (Crustacea) of the Baltic Sea, Boreas, 39, 567–575.

Frezza, V., and Carboni, M.G., 2009. Distribution of recent foraminiferal assemblages near the Ombrone River mouth (Northern Tyrrhenian Sea, Italy). Rev. Micropaléontol., 52, 43–66.

Frezza, V., and Di Bella, L., 2015. Distribution of recent ostracods near the Ombrone River mouth (Northern Tyrrhenian Sea, Italy). Micropaleontology, 61, 101–114.

Frignani, M., Langone, L., Ravaioli, M., Sorgente, D., Alvisi, F., and Albertazzi, S., 2005. Fine-sediment mass balance in the western Adriatic continental shelf over a century time scale. Mar. Geol. 222–223, 113–133.

Frontalini, F., and Coccioni, R., 2011. Benthic foraminifera as bioindicators of pollution: a review of Italian research over the last three decades. Revue de Micropaléontologie, 54, 115–127.

Frontalini, F., Buosi C., Da Pelo, S., Coccioni, R., Cherchi, A., and Bucci C., 2009. Benthic foraminifera as bio-indicators of trace element pollution in the heavily contaminated Santa Gilla lagoon (Cagliari, Italy). Mar. Pollut. Bull., 58, 858–877.

Frontalini, F., Coccioni, R., and Bucci, C., 2010. Benthic foraminiferal assemblages and trace element contents from the lagoons of Orbetello and Lesina. Environ. Monit. Assess. 170, 245–260.

Frontalini, F., Margaritelli, G., Francescangeli, F., Rettori, R., Armynot du Châtelet, E., and Coccioni, R., 2013. Benthic foraminiferal assemblages andb in a coastal lake: the case study of Lake Varano (southern Italy). Acta Protozool., 52, 147–160.

Galloway, W.E., 1975. Process framework for describing themorphologic and stratigraphic evolution of delta depositional systems. In: Broussard, M.L (Ed.), Deltas: Models for Exploration. Houston Geological Society, Houston, 87–98.

Gehrels, W.R., 2007. Sea Level Studies: Microfossil Reconstructions, Encyclopedia of Quaternary Science. Elsevier, Oxford, 3015–3024 pp.

Goineau, A., Fontanier, C., Jorissen, F. J., Lansard, B., Buscail, R., Mouret, A., Kerhervé, P., Zaragosi, S., Ernoult, E., Artéro, C., Anschutz, P., Metzger, E., and Rabouille, C., 2011. Live (stained) benthic foraminifera from the Rhône prodelta (Gulf of Lion, NW Mediterranean): Environmental controls on a river-dominated shelf. J. Sea Res. 65, 58–75.

Goineau, A., Fontanier, C., Jorissen, F. J., Buscail, R., Kerhervé, P., Cathalot, C., Pruski, A. M., Lantoine, F., Bourgeois, S., Metzger, E. , Legrand, E., and Rabouille, C., 2012. Temporal variability of live (stained) benthic foraminiferal faunas in a river-dominated shelf: faunal response to rapid changes of the river influence (Rhône prodelta, NW Mediterranean). Biogeosciences 9, 1367–1388.

Goineau, A., Fontanier, C., Mojtahid, M., Fanget, A.-S., Bassetti, M.-A., Berné, S., and Jorissen F., 2015. Live-dead comparison of benthic foraminiferal faunas from the Rhône prodelta (Gulf of Lions, NW Mediterranean): Development of a proxy for palaeoenvironmental reconstructions. Mar. Micropaleontol., 119, 17–33.

Guélorget, O., and Perthuisot, J.-P., 1983. Le domaine paralique. Expressions géologiques, biologiques et économiques du confinement. Travaux du laboratoire de Géologie. Presses de l'Ecole Normale Supérieure, 16, 1–136.

Hansen, H. J. ,and Lykke-Andersen, A.-L., 1976. Wall structure and classification of fossil and recent elphidiid and nonionid Foraminifera. Fossils and Strata, 10, 1–37.

Harris, C. K., Sherwood, C. R., Signell, R. P., Bever, A. J. and Warner, J. C., 2008. Sediment dispersal in the northwestern Adriatic Sea. J. Geophys. Res. 113, C11S03, doi:10.1029/2006JC003868.

Hayward, B. W., Hollis, C. J., and Grenfell, H. R., 1997. Recent Elphidiidae (Foraminiferida) of the South-west Pacific and fossil Elphidiidae of New Zealand. Institute of Geological & Nuclear Sciences monograph, 16. Lower Hutt, New Zealand, 170 pp.

Henderson, P. A., 1990. Freshwater ostracods. In: Kermack, D. M. and Barnes, R. S. K., (Eds.), Synopses of the British Fauna (New Series), 42. Brill E.J., Leiden, 228 pp.

Hohenegger, J., Piller, W., and Baal, C., 1989. Reasons for spatial microdistributions of foraminifers in an intertidal pool (Northern Adriatic Sea). Marine Ecology 10, 43–78.

Horton, B.P., and Edwards, R.J., 2006. Quantifying Holocene sea-level change using intertidal foraminifera: lessons from the British Isles. Cushman Foundation for Foraminiferal Research, Washington, D.C.

Horton, B.P., Engelhart, S.E., Kemp, A.C., and Sawai, Y., 2013. Microfossils in Tidal Settings as Indicators of Sea-Level Change, Paleoearthquakes, Tsunamis, and Tropical Cyclones. In: Shroder, J., Switzer, A.D., Kennedy, D.M. (Eds.), Treatise on Geomorphology. Academic Press, San Diego, CA, vol. 14, Methods in Geomorphology, 292–314.

Jorissen, F. J., 1987. The distribution of benthic foraminifera in the Adriatic Sea. Mar. Micropaleontol., 12, 21–48.

Jorissen, F. J., 1988. Benthic Foraminifera from the Adriatic Sea; principles of phenotypic variation, Utrecht Micropaleontological Bulletins, 37, 176 pp.

Jorissen, F.J., Nardelli, M.P. , Almogi-Labin, A., Barras, C., Bergamin, L., Bicchi, E., El Kateb, A., Ferraro, L., McGann, M., Morigi, C., Romano, E., Sabbatini, A., Schweizer, M. and Spezzaferri, S., 2018. Developing Foram-AMBI for biomonitoring in the Mediterranean: species assignments to ecological categories. Mar. Micropaleontol., 33–45.

Kemp, A.C., Horton, B.P., and Culver, S.J., 2009. Distribution of modern salt-marsh foraminifera in the Albemarle–Pamlico estuarine system of North Carolina, USA: Implications for sea-level research. Mar. Micropaleontol. 72, 222–238.

Legendre, P., and Gallagher, E.D., 2001. Ecologically meaningful transformations for ordination of species data. Oecologia, 129, 271–280.

Legendre, P., and Legendre, L., 2012. Numerical Ecology. Elsevier, 1006 pp.

Linnaeus, C., 1758. Systema Naturae per Regna Tria Naturae, secundum classes, ordines, genera, species, cum characteribus, differentiis, synonymis, locis. Imprensis Laurentii Salvii, Stockholm.

Marco-Barba, J., Holmes, J. A., Mesquita-Joanes, F., and Miracle, M. R., 2013. The influence of climate and sea-level change on the Holocene evolution of a Mediterranean coastal lagoon: Evidence from ostracod palaeoecology and geochemistry, Geobios, 46, 409–421.

Mare, M.F., 1942. A study of a marine benthic community with special reference to the micro-organisms, J. Mar. Biol. Ass., 25, 517–554.

Martinson, D. G., Pisias, N. G., Hayes, J. D., Imbrie, J., Moore, T. C., and Shackleton, N. J., 1987. Age dating and the orbital theory of the ice ages – Development of a high-resolution 0 to 300,000 year chronostratigraphy. Quaternary Res., 27, 1–29.

Maselli V., Hutton E.W., Kettner A.J., Syvitski J.P.M., and Trincardi F., 2011. High-frequency sea level and sediment supply fluctuations during Termination I: an integrated sequence-stratigraphy and modeling approach from the Adriatic Sea (Central Mediterranean). Mar. Geol., 287, 54–70.

Mazzini, I., Anadón, P., Barbieri, M., Castorina, F., Ferreli, L., Gliozzi, E., Mola, M., and Vittori, E., 1999. Late Quaternary sea-level changes along the Tyrrhenian coast near Orbetello (Tuscany, Central Italy): paleoenvironmental reconstruction using ostracods. Mar. Micropaleontol., 37, 289–311.

McKee, B.A., Aller, R.C., Allison, M.A., Bianchi, T.S., and Kineke, G.C., 2004. Transport and transformation of dissolved and particulate materials on continental margins influenced by major rivers: benthic boundary layer and seabed processes. Cont. Shelf Res., 24, 899–926.

Melis, R., and Covelli, S., 2013. Distribution and morphological abnormalities of recent foraminifera in the Marano and Grado Lagoon (North Adriatic Sea, Italy). Mediterr. Mar. Sci., 14, 432–450.

Mesquita-Joanes, F., Smith, A.J., and Viehberg, F.A., 2012. The ecology of Ostracoda across levels of biological organisation from individual to ecosystem: a review of recent developments and future potential. In: Horne, D. J., Holmes, J. A., Rodriguez-Lazaro, J., Viehberg, F. (Eds.), Ostracoda as proxies for Quaternary climate change. Developments in Quaternary Science, 17, Elsevier, pp. 15–36.

Migani, F., Borghesi, F., and Dinelli, E., 2015. Geochemical characterization of surface sediments from the northern Adriatic wetlands around the Po river delta. Part I: Bulk composition and relation to local background. Journal of Geochemical Exploration, 156, 72–88.

Milker, Y. and Schmiedl, G., 2012. A taxonomic guide to modern benthic shelf foraminifera of the western Mediterranean Sea. Palaeontol. Electron., 15, 134 pp.

Milker, Y., Schmiedl, G., and Betzler, C., 2011. Paleobathymetric history of the Western Mediterranean Sea shelf during the latest glacial period and the Holocene: Quantitative reconstructions based on foraminiferal transfer functions. Palaeogeogr. Palaeocl. Palaeoecol., 307, 324–338.

Milker, Y., Weinkauf, M.F.G., Titschack, J., Freiwald, A., Krüger, S., Jorissen, F.J., and Schmiedl, G., 2017. Testing the applicability of a benthic foraminiferal-based transfer function for the reconstruction of paleowater depth changes in Rhodes (Greece) during the early Pleistocene. PLoS ONE 12(11): e0188447.

Milli, S., D'Ambrogi, C., Bellotti, P., Calderoni, G., Carboni, M.G., Celant, A., Di Bella, L., Di Rita, F., Frezza, V., Magri, D., Pichezzi, R.M., and Ricci, V, 2013. The transition from wave-dominated estuary to wave-dominated delta: The Late Quaternary stratigraphic architecture of Tiber River deltaic succession (Italy). Sediment. Geol., 284-285, 159–180.

Milliman, J.D., Bonaldo, D., and Carniel, S., 2016. Flux and fate of river-discharged sediments to the Adriatic Sea. Adv. Oceanogr. Limnol., 7.

Moodley, L., Van der Zwaan, G.J., Herman, P. M. J., Kempers, L., and van Breugel, P., 1997. Differential response of benthic meiofauna to anoxia with special reference to Foraminifera (Protista: Sarcodina). Mar. Ecol. Prog. Ser., 158, 151–163.

Mojtahid, M., Jorissen, F., Lansard, B., Fontanier, C., Bombled, B., and Rabouille, C., 2009. Spatial distribution of live benthic foraminifera in the Rhône prodelta: Faunal response to a continental–marine organic matter gradient. Mar. Micropaleontol. 70, 177–200.

Molinari, F.C., Boldrini, G., Severi, P., Dugoni, G., Rapti Caputo, D., and Martinelli, G., 2007. Risorse idriche sotterranee della Provincia di Ferrara. In: Dugoni G., Pignone R. (Eds.), Risorse idriche sotterranee della Provincia di Ferrara, 7–61.

Montenegro, M. E., and Pugliese, N., 1996. Autecological remarks on the ostracod distribution in the Marano and Grado Lagoons (Northern Adriatic Sea Italy). B. Soc. Paleontol. Ital., 3, 123–132.

Morigi, C., Jorissen, F.J., Fraticelli, S., Horton, B.P., Principi, M., Sabbatini, A., Capotondi, L., Curzi, P.V. and Negri, A., 2005. Benthic foraminiferal evidence for the formation of the Holocene mud-belt and bathymetrical evolution in the central Adriatic Sea. Mar. Micropaleontol. 57, 25– 49.

Murray, J.W., 1991. Ecology and palaeoecology of benthic foraminifera. Longman Scientific & Technical, London, 397 pp.

Murray, J. W., 2006. Ecology and applications of benthic foraminifera. Cambridge University Press, Cambridge, 426 pp.

Palinkas, C.M., and Nittrouer, C.A., 2007. Modern sediment accumulation on the Po shelf, Adriatic Sea. Cont. Shelf. Res. 27, 489–505.

Paschini, E., Artegiani, A., and Pinardi, N., 1993. The mesoscale eddy field of the middle Adriatic during fall 1988. Deep-Sea Res. Pt. I, 40, 1365–1377.

Perini, L. and Calabrese, L. 2010. Il sistema mare-costa dell'Emilia-Romagna. Pendragon, 239 pp.

Pieri, M.. and Groppi, G., 1981. Subsurface geological structure of the Po Plain, Italy. Pubblicazione del Progetto Finalizzato Geodinamica, 414, 1–23.

Pint, A., and Frenzel, P., 2017. Ostracod fauna associated with Cyprideis torosa – an overview. J. Micropalaeontol., 36, 113–119.

Piovan, S., Mozzi, P., and Zecchin, M., 2012. The interplay between adjacent Adige and Po alluvial systems and deltas in the late Holocene (Northern Italy). Géomorphologie, 18, 427–440.

Poulain, P.-M., 2001. Adriatic Sea surface circulation as derived from drifter data between 1990 and 1999. J. Marine Syst., 29, 3–32.

Pranzini, E. , 2013. Italy. In: Pranzini, E., Williams, A. (Eds.), Coastal erosion and protection in Europe. Routledge, Oxon, 294–323.

Preti, M., De Nigris, N.,Morelli, M., Monti, M., Bonsignore, F., and Aguzzi,M., 2009. State of the Emilia-Romagna Littoral at 2007 and Ten-Years Management Plan. I quaderni dell'ARPA, Bologna.

Rasmussen, T. L., 2005. Systematic paleontology and ecology of benthic foraminifera from the Plio–Pleistocene Kallithea Bay Section, Rhodes, Greece. In: Thomsen, E., (Ed.), Lagoon to deep–water foraminifera and ostracods from the Plio–Pleistocene Kallithea bay section, Rhodes, Greece. Cushman Foundation Special Publication, 39. Washington DC. 53–157

Rasmussen, T.L., and Thomsen, E., 2017. Ecology of deep-sea benthic foraminifera in the North Atlantic during the last glaciation: Food or temperature control. Palaeogeogr. Palaeocl. Palaeoecol., 472, 15–32.

Regione Emilia-Romagna and ENI–AGIP, 1998. Riserve idriche sotterranee della Regione Emilia-Romagna, S.EL.CA, Firenze.

Ricci Lucchi F., Colalongo M.L., Cremonini G., Gasperi G., Iaccarino S., Papani G., Raffi I., and Rio D., 1982. Evoluzione sedimentaria e paleogeografica del margine appenninico. In: Cremonini G., Ricci Lucchi F. (Eds.), Guida alla geologia del margine appenninico-padano. Guide Geologiche Regionali Soc. Geol. Ital., 17–46.

Rodriguez-Lazaro, J., and Ruiz-Muñoz, F., 2012. A General Introduction to ostracods: morphology, distribution, fossil record and applications. In: Horne, D. J., Holmes, J. A., Rodriguez-Lazaro, J., Viehberg, F., (Eds.), Ostracoda as proxies for Quaternary climate change. Developments in Quaternary Science, 17, Elsevier, 1–14.

Rossi, V., 2009. Ostracod assemblages from Holocene subsurface deposits of modern Po Delta: a palaeoenvironmental proxy record. B. Soc. Paleontol. Ital. 48, 95–103.

Rossi, V., and Vaiani, S. C., 2008. Microfaunal response to sediment supply changes and fluvial drainage reorganization in Holocene deposits of the Po Delta, Italy. Mar. Micropaleontol., 69, 106–118.

Rossi, V., and Horton, B. P., 2009. The application of a subtidal foraminiferal-based transfer function to reconstruct the Holocene paleobathymetry of the Po Delta, Northern Adriatic Sea. J. Foramin. Res., 39, 180–190.

Rossi, V., Amorosi, A., Sarti, G., and Mariotti, S., 2017. Late Quaternary multiple incised valley systems: An unusually well-preserved stratigraphic record of two interglacial valleyfill successions from the Arno Plain (northern Tuscany, Italy). Sedimentology, 64, 1901–1928.

Ruiz, F., González-Regalado, M.L., and Muñoz, J.M., 1997. Multivariate analysis applied to total and living fauna: seasonal ecology of recent benthic ostracoda off the North Cádiz Gulf Coast (southwestern Spain). Mar. Micropaleontol., 31, 183–203.

Ruiz, F., González-Regalado, M.L., Menegazzo, L., and Rampazzo, G., 1999. Distribución ecológica de los ostrácodos de la Cuenca de Malamocco (Laguna de Venecia, NE de Italia). Revista Española de Paleontología, 14, 59–65.

Ruiz, F., González-Regalado, M. L., Baceta, J. I., Menegazzo-Vitturi, L., Pistolato, M., Rampazzo, G., and Molinaroli, E., 2000. Los ostrácodos actuales de la laguna de Venecia (NE de Italia). Geobios, 33, 447–454.

Ruiz, F., Abad, M., Galán, E., González, I., Aguilá, I., Olías, M., Gómez Ariza, J.L., and Cantano, M., 2006. The present environmental scenario of El Melah Lagoon (NE Tunisia) and its evolution to a future sabkha. J. Afr. Earth Sci., 44, 289–302.

Salel, T., Bruneton, H., and Lefèvre, D., 2016. Ostracods and environmental variability in lagoons and deltas along the north-western Mediterranean coast (Gulf of Lions, France and Ebro delta, Spain). Revue de Micropaléontologie, 59, 425–444.

Schönfeld, J., 2012. History and development of methods in recent benthic foraminiferal studies. J. Micropalaeontol., 31, 53–72.

Scott, D.B., Medioli, F.S., 1980. Quantitative studies of marsh foraminiferal distributions in Nova Scotia: implications for sea level studies. Cushman Foundation for Foraminiferal Research Special Publication 17.

Scott, D.B., Medioli, F.S., and Schafer, C.T., 2001. Monitoring in coastal environments using Foraminifera and Thecamoebian indicators. Cambridge University Press, 177 pp.

Schönfeld, J., 2012. History and development of methods in recent benthic foraminiferal studies. J. Micropalaeontol., 31, 53 –72.

Serandrei Barbero, R., Albani, A.D., and Bonardi, M., 2004. Ancient and modern salt marshes in the Lagoon of Venice. Palaeogeogr. Palaeocl. Palaeoecol., 202, 229–244.

Sgarrella, F., and Moncharmont Zei, M., 1993. Benthic Foraminifera of the Gulf of Naples (Italy): systematics and autoecology. B. Soc. Paleontol. Ital., 32, 145–264.

Sherman, K.M., and Coull, B.C., 1980. The response of meiofauna to sediment disturbance. J. Exp. Mar. Biol. Ecol., 46, 59–71.

Simeoni, U., and Corbau, C., 2009. A review of the Delta Po evolution (Italy) related to climatic changes and human impacts. Geomorphology, 107, 64–71.

Slack, J. M., Kaesler, R. L., and Kontrovitz, M., 2000. Trend, signal and noise in the ecology of Ostracoda: information from rare species in low-diversity assemblages. Hydrobiologia, 419, 181–189.

Spagnoli, F., Dinelli, E., Giordano, P., Marcaccio, M., Zaffagnini, F., and Frascari, F., 2014. Sedimentological, biogeochemical and mineralogical facies of Northern and Central Western Adriatic Sea. J. Marine Syst., 139, 183–203.

Stefani, M., and Vincenzi, S., 2005. The interplay of eustasy, climate and human activity in the late Quaternary depositional evolution and sedimentary architecture of the Po Delta system. Mar. Geol., 222–223, 19–48.

Storms, J.E.A., Jan Weltje, G., Terra, G.J., Cattaneo, A., and Trincardi, F., 2008. Coastal dynamics under conditions of rapid sea-level rise: Late Pleistocene to Early Holocene evolution of barrier– lagoon systems on the northern Adriatic shelf (Italy). Quaternary Sci. Rev. 27, 1107–1123.

Trincardi, F., Correggiari A., and Roveri, M., 1994. Late Quaternary transgressive erosion and deposition in a modern epicontinental shelf: the Adriatic Semienclosed Basin. Geo-Mar. Lett., 14, 41–51.

Tyler, C.L., and Kowalewski, M., 2014. Utility of marine benthic associations as a multivariate proxy of paleobathymetry: a direct test from recent coastal ecosystems of North Carolina. PLoS One 9 (4), e95711.

Uffenorde, H. 1972. Okologie und jahreszeitliche Verteilung rezenter benthonischer Ostracoden des Limski kanal bei Rovinj (nördliche Adria) [Ecology and seasonal distribution of Recent benthonic Ostracodes from the Limski kanal near Rovinj (northern Adriatic Sea)]. Göttinger Arbeiten zur Geologie und Paläontologie, 13. Göttingen, 136 pp.

Van Der Zwaan, G.J., and Jorissen, F.J., 1991. Biofacial patterns in river-induced shelf anoxia. In: Tyson, R.V., Pearson, T.H., (Eds.), Modern and Ancient Continental Shelf Anoxia. Geological Society Special Publication, 58, 65–82.

Veggiani, A., 1990. Fluttuazioni climatiche e trasformazioni ambientali nel territorio imolese dall'alto medioevo all'età moderna. In: Mancini, F., Gioberti, M., Veggiani, A. (Eds.), Imola nel Medioevo, 41–102.

Verza, E., and Catozzo, L., 2015. Atlante lagunare costiero del Delta del Po. 341 pp.

Weinkauf, M.F.G., and Milker, Y., 2018. The effect of size fraction in analyses of benthic foraminiferal assemblages: a case study comparing assemblages from the >125 and >150 µm size fractions. Front. Earth Sci. 6, 37. doi: 10.3389/feart.2018.00037

Wheatcroft, R. A., Hunt, L., Stevens, A., and Lewis, R., 2006. The large-scale distribution and internal geometry of the fall 2000 Po River flood deposit: evidence from digital X-radiography. Cont. Shelf Res. 26, 499–516.

ACKNOWLEDGEMENTS

I would like to acknowledge all the people that helped me during these three years of Ph.D. and that made this research reality.

First of all, I want to acknowledge my advisor, Dr. Stefano Claudio Vaiani, who taught me what is the meaning of the word “research”. I will not stop saying that I couldn’t have a better advisor.

Many thanks to my co-advisor Dr. Veronica Rossi for the constant support provided since the beginning of this project, for her valuable help with ostracoda and for the beautiful moments we spent together (even struggling with the kayak at Bellocchio).

I want to thank Prof. Benjamin P. Horton who gave me the opportunity to visit Nanyang Technological University in Singapore, opened my eyes through the international world of research and inspired me to explore new methods of data analysis.

Thanks to Prof. Alessandro Amorosi for the access to core material and for his support.

I acknowledge Prof. Fabrizio Frontalini who gave us the possibility to start the “Bellocchio project” and supported me since the first year of Ph.D.

I would like to acknowledge Dr. Maria Roberta Randi and Dr. Giorgio Gasparotto for providing me access to SEM.

Thanks to all the people that I collaborated with during these three years and that improved my knowledge, especially Dr. Daniele Scarponi, Dr. Luigi Bruno and Dr. Bruno Campo.

A special thanks to my colleagues Ilenia Maria D’Angeli and Michele Azzarone, who shared the office with me, and made my academic life brighter even in the winter gloomy days of the Po Plain.

Outside of academia, I want to thank my family and my dear friends. Especially my mum Beatrice for her great support during the dark moments of this project and Alessio, who shared with me ISF, bad and good experiences of our Ph.D. projects and, above all, always made me feel special inside and outside of academia.